Oil & Natural Gas Technology

DOE Award No.: DE-FC26-01NT41099

Characterization and Alteration of Wettability States of Alaskan Reservoirs to Improve Oil Recovery Efficiency (including the within-scope expansion based on Cyclic Water Injection – a pulsed waterflood for Enhanced Oil Recovery)

Submitted by:
Petroleum Development Laboratory
Institute of Northern Engineering
University of Alaska Fairbanks
P.O. Box 755880
Fairbanks, Alaska 99775-5880

Prepared for:
United States Department of Energy
National Energy Technology Laboratory

November 2008

Office of Fossil Energy

Characterization and Alteration of Wettability States of Alaskan Reservoirs to Improve Oil Recovery Efficiency (including the within-scope expansion based on Cyclic Water Injection – a pulsed waterflood for Enhanced Oil Recovery)

Final Report

Submitted to

United States Department of Energy
National Energy Technology Laboratory
3610 Collins Ferry Road
P.O. Box 880
Morgantown, WV 26507-0880
Ph: 304-285-4764, Fax: 304-285-4403

Principal Authors

Abhijit Dandekar

Shirish Patil

Santanu Khataniar

Submitted by

Petroleum Development Laboratory
Institute of Northern Engineering
University of Alaska Fairbanks
P.O. Box 755880, Fairbanks, Alaska 99775-5880
Telephone: (907) 474 – 7734, FAX: (907) 474 – 5912

November 2008

University of Alaska Fairbanks
America's Arctic University

PDL INE

DISCLAIMER

ABSTRACT

Numerous early reports on experimental works relating to the role of wettability in various aspects of oil recovery have been published. Early examples of laboratory waterfloods show oil recovery increasing with increasing water-wetness. This result is consistent with the intuitive notion that strong wetting preference of the rock for water and associated strong capillary-imbibition forces gives the most efficient oil displacement. This report examines the effect of wettability on waterflooding and gasflooding processes respectively. Waterflood oil recoveries were examined for the dual cases of uniform and non-uniform wetting conditions.

Based on the results of the literature review on effect of wettability and oil recovery, coreflooding experiments were designed to examine the effect of changing water chemistry (salinity) on residual oil saturation. Numerous corefloods were conducted on reservoir rock material from representative formations on the Alaska North Slope (ANS). The corefloods consisted of injecting water (reservoir water and ultra low-salinity ANS lake water) of different salinities in secondary as well as tertiary mode. Additionally, complete reservoir condition corefloods were also conducted using live oil. In all the tests, wettability indices, residual oil saturation, and oil recovery were measured. All results consistently lead to one conclusion; that is, a decrease in injection water salinity causes a reduction in residual oil saturation and a slight increase in water-wetness, both of which are comparable with literature observations. These observations have an intuitive appeal in that water easily imbibes into the core and displaces oil. Therefore, low-salinity waterfloods have the potential for improved oil recovery in the secondary recovery process, and ultra low-salinity ANS lake water is an attractive source of injection water or a source for diluting the high-salinity reservoir water.

As part of the within-scope expansion of this project, cyclic water injection tests using high as well as low salinity were also conducted on several representative ANS core samples. These results indicate that less pore volume of water is required to recover the same amount of oil as compared with continuous water injection. Additionally, in cyclic water injection, oil is produced even during the idle time of water injection. It is understood that the injected brine front spreads/smears through the pores and displaces oil out uniformly rather than viscous fingering.

The overall benefits of this project include increased oil production from existing Alaskan reservoirs. This conclusion is based on the performed experiments and results obtained on low-salinity water injection (including ANS lake water), vis-à-vis slightly altering the wetting conditions. Similarly, encouraging cyclic water-injection test results indicate that this method can help achieve residual oil saturation earlier than continuous water injection. If proved in field, this would be of great use, as more oil can be recovered through cyclic water injection for the same amount of water injected.

TABLE OF CONTENTS

LIST OF FIGURES

LIST OF TABLES

ACKNOWLEDGMENTS

The authors are thankful to the U.S. Department of Energy (USDOE) for its financial assistance in support of the presented work.

CHAPTER 1: Introduction

The monotonic and geometric increase in world demand for energy in the face of rapid industrialization requires the production of increasing quantities of crude oil, even with declining production of individual fields, while maintaining acceptable cost levels. Many abandoned and/or matured fields have become the subject of novel enhanced oil recovery (EOR) field trials in order to meet energy demand. Resources have gone into research and development in a bid to better understand ways to manipulate factors at pore scale levels and higher to improve oil recovery.

Oil recovery efficiency is a function of many interacting variables/factors at pore levels as well as macroscopic scales. Some of these interacting factors include the reservoir rock-wetting state, pore geometry, size and distribution, salinity of the connate water and the displacing fluid, recovery/displacement mechanisms, rock mineralogy, and other reservoir rock and fluid properties. Efficient and cost-effective oil recovery requires an in-depth understanding of the nature and, where possible, the *optimal* manipulation of these interacting variables. The study of these variables has been a subject of interest and research in the oil industry for several decades.

Among the many identified factors that affect the pore-scale displacement mechanism, the reservoir-wetting state has been shown to be one of the most important. Information about wettability is fundamental to understanding multiphase flow problems, ranging from oil migration from source rocks through primary production mechanisms to EOR processes. Wettability also determines the nature of fluid distribution observed in the reservoir. Based on research findings over the last six decades on the nature of wettability, the importance of wettability in the oil recovery process has been agreed on by many researchers[1,2,3,4,5].

1.1 Fundamental Concepts of Wettability

Wettability is the tendency of the reservoir rock surface to preferentially contact a particular fluid in a multiphase or two-phase fluid system. Consequently, a water-wet reservoir rock will preferentially contact water; an oil-wet reservoir will preferentially contact oil; and a gas-wet reservoir will preferentially contact gas. However, the concept and the possibility of a truly gas-wet reservoir has been the subject of intense debate among researchers. Experimental reports on wettability effects on recovery in gas condensate reservoirs[6] suggest that wettability in gas-liquid-rock systems can be altered from strong preferential liquid-wetness to preferential neutral gas-wetness by chemical treatment. However, there is currently no acceptable, unified definition of gas wettability and the conditions under which it is achieved. Whether a reservoir rock is strongly water-wet or oil-wet depends on the chemical composition of the fluids, resulting in molecular attraction between the water molecules and the rock and/or the oil molecules and the rock. The degree to which a rock is either water-wet or oil-wet is strongly affected by the following:

(1) Adsorption or desorption of constituents in the oil phase: Usually the presence of large, polar compounds such as asphaltenes in the oil phase enables adsorption onto the solid surface, leaving an oil film which may alter the reservoir rock surface wettability. Where a reservoir neither imbibes the oleic phase nor the water phase, a neutral-wet condition exists.

(2) Reservoir rock mineralogy: In the presence of "pure" paraffinic hydrocarbons, water preferentially wets calcite and silica surfaces. However, variation in the constituents of the crude oil component may result in the observation of other wetting states even for these surfaces.

(3) Film deposition and spreading capability of the oleic phase.

1.2 Measurements of Wettability

Currently, there is no universally accepted method of wettability determination in the petroleum industry. A number of wettability determination methods are available and are divided broadly into two categories: quantitative and qualitative methods. Quantitative methods include (1) contact angles, (2) Amott/Modified Amott (Amott-Harvey), and (3) USBM. Qualitative methods include (1) imbibition rates[7,8], (2) permeability/saturation relationship, (3) nuclear

magnetic resonance, NMR[9], (4) dye absorption, (5) relative permeability curves[10,11], and (6) capillary pressure curves. Of the two methods—qualitative and quantitative—the latter is generally used.

1.2.1 Contact Angle Measurement

The conventional means of measuring the reservoir rock-wetting state is by contact angle (Θ) measurement. The measurement is usually carried out on flat, polished mineral crystals. For a single-phase fluid in contact with a solid surface, the contact angle is defined by the angle between the fluid-solid interface. When two immiscible fluids, such as oil and water, are together in contact with a rock face, the contact angle is defined by the angle measured through the water (**Figure 1.1**). If the reservoir-wetting condition is defined in terms of the contact angle, then when $\Theta < 90$, the reservoir rock is water-wet; when $\Theta > 90$, it is oil-wet; and when $\Theta \cong 90$, a neutral-wet system exists. This is a loose definition of the reservoir-wetting state, as it may further be divided into strongly water-wet, weakly water-wet, strongly oil-wet, and weakly oil-wet.

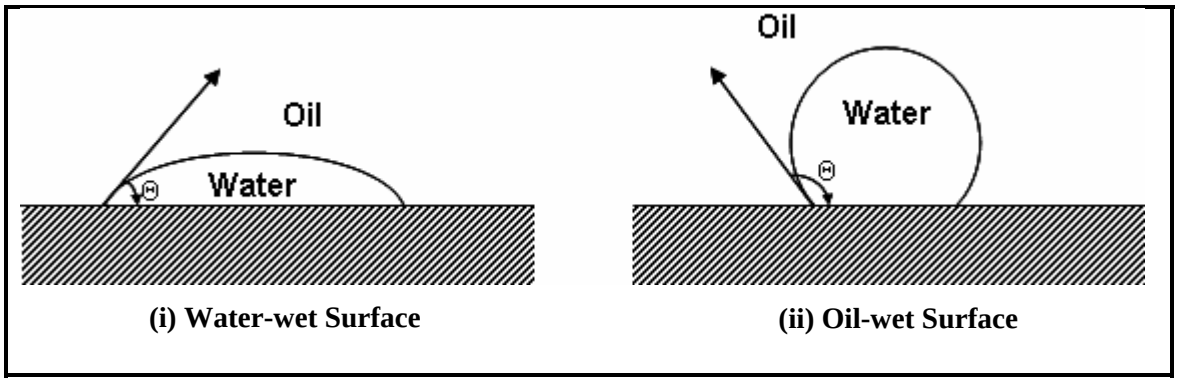

Figure 1.1: Wettability of Oil/Water/Rock System.

Available methods for contact angle measurements include the tilting plate method, capillary rise method, cylinder method, vertical rod method, sessile drops or bubbles, and tensiometric method. Application of these methods to the petroleum industry is limited by the requirement that the fluid used should be pure. The methods generally used in the petroleum industry are the sessile drop method and its modified form[12].

An important phenomenon worthy of note in contact angle measurement is the observed hysteresis of the contact angle. It has been found experimentally that a liquid drop can have many different stable contact angles[12]. Because of reproducibility problems, the contact angles reported in literature are based either on the water-advancing contact angle or the water-receding contact angle. However, in an experiment carried out by Treiber et al.[13], only the water-advancing contact angle was reported to correlate with other wettability indicators.

One of the more obvious limitations of wettability characterization using contact angle measurement is the absence of a standard reference. Consequently, except at the end-value wetting states (i.e., strongly water-wet or strongly oil-wet states), the classification of wetting state from contact angle measurement is arbitrary and subjective. Another important limitation of the contact angle method is that the required length of equilibration time cannot be reproduced in the lab. This may lead to problems such as erroneous classification of wetting state and sometimes lack of reproducibility. A third and equally important limitation is that contact angle measurement does not take into account the rock surface heterogeneity. Contact angle measurements are carried out on a "pure" single mineral crystal, which excludes the many other different mineral constituents present in the reservoir rock. A fourth limitation is that information about the presence or absence of strongly adsorbed organic materials cannot be obtained. This information is particularly important in determining the efficiency of the core-cleaning process when working with restored state cores.

1.2.2 Amott-Harvey Wettability Test

The Amott[14] wettability test is one of the traditional means of characterizing reservoir wettability from displacement studies. It involves a series of forced and spontaneous displacements of oil by water and vice versa. The principle behind this method is that the core sample will spontaneously imbibe a higher volume of the wetting phase than the non-wetting phase. Consequently, the Amott wettability index reflects the ease with which the wetting fluid will displace the non-wetting fluid (spontaneous imbibition), as shown in **Figure 1.2**.

Determination of the wetting condition using the Amott test consists of the determination of two different ratios (1) the displacement-by-water ratio, I_w, which is the ratio of oil volume spontaneously displaced by water (V_{osp}) (**Figure 1.2a**) to the total volume of oil displaced by water, spontaneously and by forced displacement (V_{ofd}),

$$I_w = \frac{V_{osp}}{V_{osp} + V_{ofd}} \qquad \textbf{1.1}$$

and (2) the displacement-by-oil ratio, I_o, which is the ratio of water volume spontaneously displaced by oil (V_{wsp}) (**Figure 1.2b**) to the total volume of water displaced by oil, spontaneously and by forced displacement (V_{wfd}),

$$I_o = \frac{V_{wsp}}{V_{wsp} + V_{wfd}} \qquad \textbf{1.2}$$

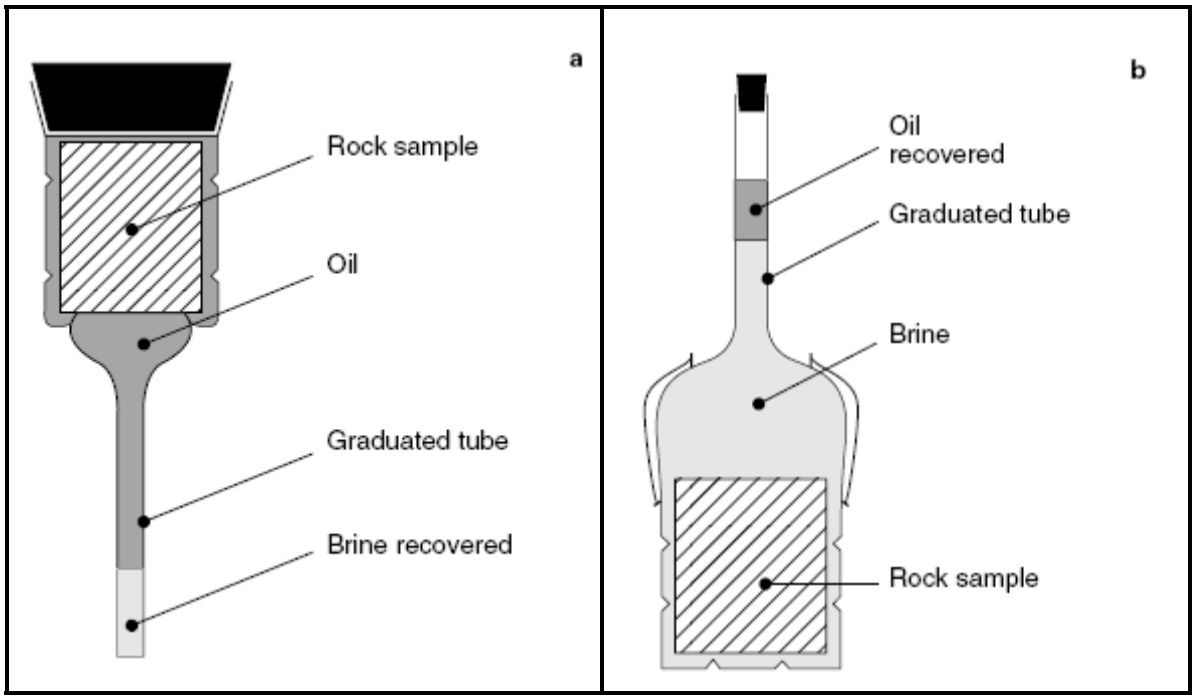

Figure 1.2: Apparatus for Spontaneous Displacement of (a) Brine and (b) Oil[15]

For an extremely water-wet system, I_w will be positive (≅ 1) while I_o will be zero, which indicates that oil is not imbibed spontaneously. Similarly, I_w will be zero for an extremely oil-wet system, while I_o will be positive (≅ 1). For a neutral-wet system, both I_o and I_w will be zero.

A modified Amott test, popularly known as the Amott-Harvey Relative Displacement Index[16], has gained increasing popularity and is now used instead of the original Amott test. The experimental process for both tests is the same except that the modified Amott test has an additional step in core preparation prior to running the test. The additional step involves the saturation of the core sample with water/brine and flooding with (or centrifuging under) oil to reduce the water/brine to some initial water saturation. A further modification of the modified Amott test, called the Amott/IFP method, replaces all the centrifuging steps by injection at a constant rate[17]. The expression for the Amott-Harvey Relative Displacement Index is given by

$$WI_{AMOTT} = I_W - I_O = \frac{V_{osp}}{V_{osp} + V_{ofd}} - \frac{V_{wsp}}{V_{wsp} + V_{wfd}} \qquad \textbf{1.3}$$

Since the maximum and minimum values of I_o and I_w are 1 and 0, respectively, it follows that the Amott-Harvey Relative Displacement Index will take values between +1 and -1. These extremes, respectively, represent the strongly/completely water-wet and oil-wet conditions. Cuiec[18] classified the index between +0.3 and 1 (inclusive) as water-wet, -1 and -0.3 (inclusive) as oil-wet and -0.3 and +0.3 (non-inclusive) as intermediate-wet. This classification of the relative displacement index for different wetting states by Cuiec is arbitrary. Robin[17] reported the values of the Amott-Harvey Relative Displacement Index for two mixed-wet sandstone and carbonate samples as equal to -0.57 and -0.81, respectively.

One of the limitations of the Amott method and its modified form is the insensitivity of the calculated index at near-neutral wetting conditions. The key principle to the Amott test is that the wetting phase will spontaneously imbibe and displace the non-wetting phase from the core. However, it has been discovered[19,20,21] that neither phase will spontaneously imbibe nor displace the other at contact angles roughly between 60° to 120°[12]. Another limitation is the dependence of the value of the limiting contact angle above which spontaneous imbibition will occur on the initial saturation of the core. A third limitation is imposed to a lesser extent by the pore

geometry. In vugular limestone with large, irregular vugs, the wetting index has been observed to vary markedly for core plugs cut from the same core[14].

1.2.3 United State Bureau of Mines (USBM) Wettability Test

The USBM[22] wettability test is derived directly from capillary pressure phenomena. The basis of the USBM method is that the hysteresis of the capillary pressure curve depends on the wetting state of the core/rock sample. The hysteresis of the capillary pressure curve also indicates the amount of work done in displacing a particular fluid phase by another fluid phase. Thus, the USBM test compares the work requirement for the displacement of one fluid by another.

It has been reported[23,24] that the area under the capillary pressure curve is proportional to required work. The work requirement of the wetting fluid phase in displacing the non-wetting fluid is lower than that required by the non-wetting fluid phase in displacing the wetting fluid phase. Consequently, for both water-wet and oil-wet systems, the area under the imbibition curve is smaller than the area under the drainage curve (**Figure 1.3**). Where a neutral wetting condition subsists, the area under the drainage and the imbibition curves are approximately the same (**Figure 1.3**). This sensitivity of the USBM test near the neutral wetting condition is one of the advantages of this wettability measure over the Amott method. For the purpose of this work, imbibition is defined as an increase in wetting-phase saturation (i.e., brine displacing oil in a water-wet system), while drainage refers to a decrease in wetting-phase saturation, (i.e., oil displacing brine in a water-wet system or brine displacing oil in an oil-wet system).

The USBM wettability index is determined from the areas under the capillary pressure curves for the drainage and imbibition processes and is calculated according to **Eq. 1.4**.

$$WI_{USBM} = Log\left(\frac{A_W}{A_O}\right) \qquad \textbf{1.4}$$

From **Eq. 1.4**, A_w is the area under the capillary pressure curve when water/brine is displaced by oil, and A_o is the area under the capillary pressure curve when oil is displaced by water/brine. For an extremely water-wet system, WI_{USBM} is very large and positive; for a neutral-wet condition,

WI_{USBM} lies around zero; and for an extremely oil-wet condition, WI_{USBM} is very large and negative. One limitation of the USBM index is that cores can only be classed as either water-wet (wettability index is greater than 0), oil-wet (wettability index is less than 0) or neutral-wet (wettability index is equal to 0). Another limitation is that the determination of wettability using this approach can only on carried out on core plugs because of the need to load the sample in a centrifuge.

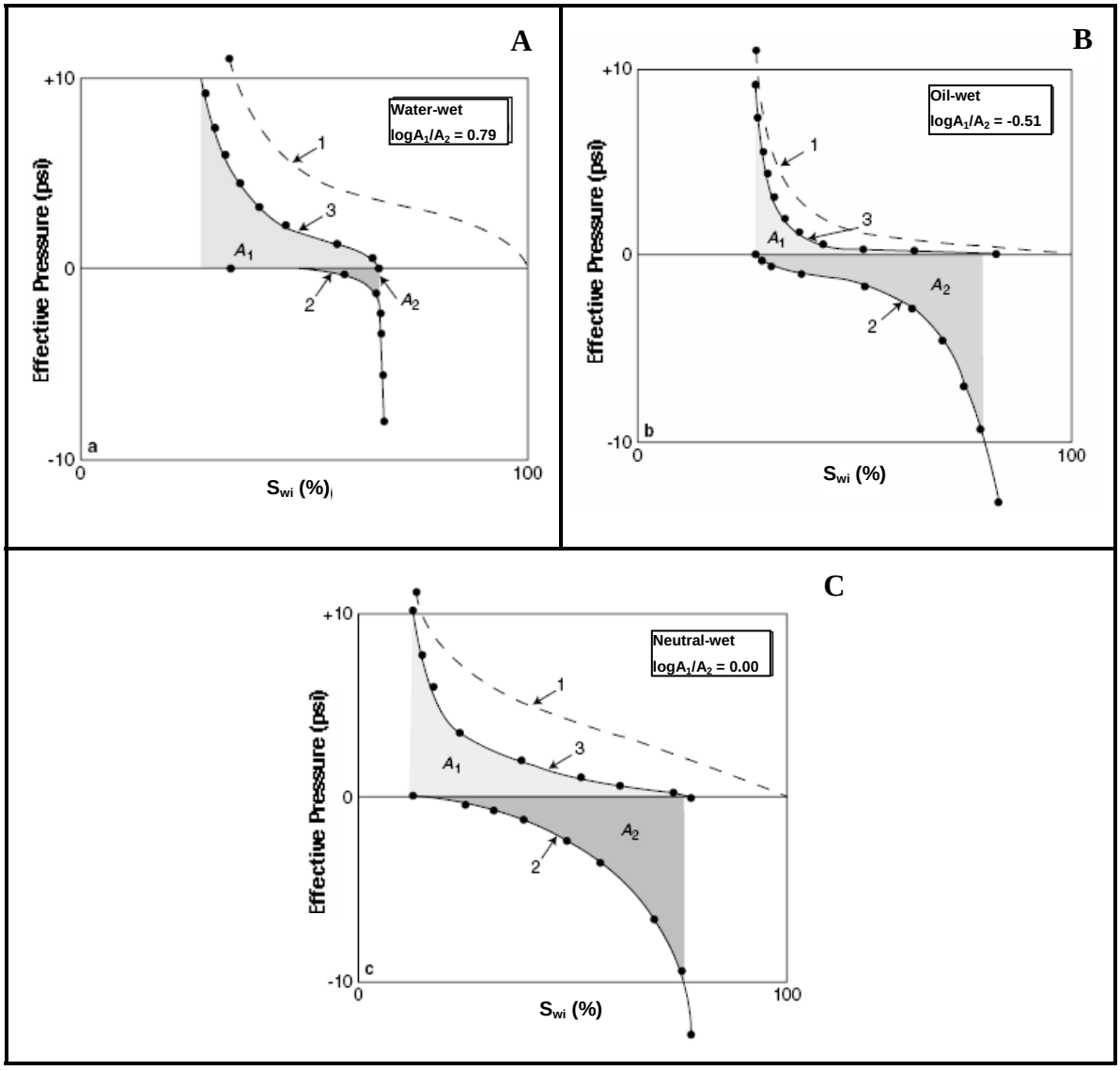

Figure 1.3: USBM Wettability Measurement: (A) Untreated Core; (B) Core Treated with 10% Dri-Film 99; (C) Core Pretreated with Oil for 324 Hours at 140°F; Brine Contains 1,000 PPM Sodium Tripolyphosphate[22]

On a general note, contact angle measurement, Amott/Amott-Harvey indices and the USBM Index are best suited for characterizing wettability where a uniform wetting condition exists. However, the use of the Amott wettability test to distinguish the occurrence of speckled wettability (a form of non-uniform wetting) from uniform wettability and to characterize mixed-wet systems has been reported[17,25]. In both cases, the fact that the displacement-by-water and the displacement-by-oil ratios were both positive was taken to indicate that the system is non-uniformly wetted.

Table 1.1[12] shows the relationship amongst the various quantitative measures of wettability that have been examined.

Table 1.1: Approximate Relationship between Wettability, Contact Angle, USBM, and Amott Wettability Indices[12]

	Water-Wet	**Neutral-Wet**	**Oil-Wet**
Contact angle			
Minimum	0^o	60 to 75^o	105 to 120^o
Maximum	60 to 75^o	105 to 120^o	180^o
USBM Wettability Index	Index near 1	Index near 0	Index near -1
Amott Wettability Index			
Displacement-by-Water Ratio	Positive	Zero	Zero
Displacement-by-Oil Ratio	Zero	Zero	Positive
Amott-Harvey Wettability Index	$0.3 \leq I_{AH} \leq 1.0$	$-0.3 < I_{AH} < 0.3$	$-1.0 \leq I_{AH} \leq -0.3$

1.2.4 Combined USBM/Amott Method

The combined USBM/Amott Method wettability measurement was developed by Sharma and Wunderlich[26] and entails the calculation of both the USBM and Amott indices. The advantages of this approach are (1) the resolution of the USBM method is improved by accounting for the

saturation changes that occur at zero capillary pressure, and the Amott index is also calculated; and (2) it incorporates the advantage of the Amott method in sometimes determining non-uniformly wetted systems.

1.3 Recent Advances in Methods of Wettability Index Determination

Because of the inherent limitations in the currently accepted industry standard for wettability characterization, new methods of wettability determination have been developed. Some of the recently developed methods include (1) Spontaneous Imbibition Measurement[27], (2) Atomic Force Microscopy[28], (3) Chromatographic Method[29], (4) Nuclear Magnetic Resonance (NMR)[30], and (5) Three Phase Wettability Index[31,32].

Spontaneous Imbibition Measurement: This method proposed by Ma et al.[27] addresses specific limitations of the Amott/Harvey and the USBM methods with respect to certain observed capillary pressure effects, namely (1) the inability of the Amott/Harvey index to discriminate between systems that attain residual non-wetting phase saturation without change in sign of the imbibition capillary pressure (usually for strongly wetted system; and (2) the inability of the USBM method to recognize variation in wetting behavior for contact angles ranging from 0° to 55°. Within this range, the area under the forced imbibition curve is zero.

Atomic Force Microscopy[28]: This method is proposed for the characterization of mixed-wet states by direct measurement of the capillary pressure required to rupture brine films on mineral surfaces. This is achieved by measuring the force versus distance curve between crude oil and a mineral surface in brine using an atomic force microscope.

Chromatographic Method[29]: This method is based on the chromatographic separation between the tracer thiocyanate (SCN^-) and the potential determining sulfate ion, SO_4^{2-}, at the water-wet sites on the rock surface. The area between the effluent curves of the tracer and sulfate is directly proportional to the water-wet surface area inside the core. Heptane is used as the reference oil to symbolize a completely water-wet system. This method is reported to be sensitive to small wettability changes, even at close to neutral conditions where the Amott test method is not very sensitive.

Nuclear Magnetic Resonance (NMR)[30]: This method is used to determine in situ wettability of rocks from NMR logs. It is based on the fact that fluids experience additional relaxation when in direct contact with the rock surface. The reduction of oil relaxation time away from its bulk value is generally known as a qualitative measure of wettability. Based on this concept, a quantitative wettability index, I_w, is developed based on detailed modeling of NMR response and is defined by

$$I_w = \frac{Surface\ wetted\ by\ water - Surface\ wetted\ by\ oil}{Total\ Surface} \qquad 1.5$$

It is reported that this new wettability method has been verified extensively on core data against standard wettability tests.

Three Phase Wettability Index[31,32]: This index is based on the evaluation of the relative permeability and capillary pressure at specific wetting-phase saturation using the developed analytical expression given in **Eq 1.6**. The authors proposed that the index is suitable for wettability evaluation for both a gas-liquid-rock system and a liquid-liquid-rock system. The equation is expressed as follows:

$$W_{iw} = \frac{P_c}{\sigma}\sqrt{\left(\frac{\lambda+2}{\lambda}\right)\left(\frac{k}{F\phi}\right)\left(\frac{k_{rw}}{S_w^*}\right)} \qquad 1.6$$

where W_{iw} is the wettability index at a specific wetting-phase saturation; λ is the pore size distribution index; k and ϕ are the absolute permeability and the porosity of the rock; F is the lithology factor; σ is the interfacial tension between the fluids; P_c and S_w^* are the capillary pressure and the normalized saturation of the wetting phase; k_{rw} is the relative permeability of the wetting phase. The value of W_{iw} ranges from -1 to +1.

1.4 Wettability in Reservoirs

Most early analyses on the effect of wettability on oil recovery were based on two simplistic assumptions, which state that (1) most of the reservoirs were strongly water-wet and the

reservoir rock surface was completely "coated" with water[22,33] and that (2) the wetting state was such that a uniform/homogeneous wetting condition existed throughout the reservoir.

The assumption of a strongly water-wet reservoir was informed by the saturation history of the reservoir, wherein the reservoir was completely saturated by water prior to the displacement of the initial volume of water occupying the pore volume (PV) due to migration and trapping of oil. It was believed that there was no alteration of the wetting condition in the reservoir after the migration of oil. This opinion held sway for a long time and guided many research experiments.

While the fact that the pore volume was initially occupied by water is generally not in doubt, it has been shown[13,21,34] that the actual wetting state of the reservoir may depart from the strongly water-wet state to other wetting states. This final wetting state of the reservoir is dependent on a number of factors, including the following:

(1) the presence or absence in the crude oil of (a) polar compounds, (b) film forming components, and (c) high molecular-weight hydrocarbon compounds such as paraffins, porphyrins;

(2) the type and distribution of minerals present;

(3) the reservoir rock type; and

(4) the height of the oil-water contact.

After it became clear that the initial wetting state of the reservoir may possibly depart from the strongly water-wet condition, the assumption of uniform wetting condition was unchallenged. Consequently, initial studies into the relationship between wettability and oil recovery were conducted on samples that were uniformly wetted, that is, strongly water-wet, strongly oil-wet, intermediate/neutral wettability, etc. However, problems connected with observed reservoir production data sparked research interest into a possible departure of the reservoir-wetting state from uniform wettability. Consequently, beginning from the early 1950s, the assumption of uniform wettability for most reservoirs was challenged by many early authors who posited[35,36] that the wetting of the reservoir rock surface is indeed heterogeneous. Further research insights, into the wetting state of reservoir rocks, did suggest[9,37] that heterogeneous wettability may be the

normal condition in reservoirs. The discovery of possible non-uniform wetting conditions in the reservoir opened up new vistas of understanding and research in reservoir rock wettability and led to the definition of other wetting states, besides the gamut covering strongly water-wet to strongly oil-wet conditions. These conditions include

(1) the mixed wetting condition[38] (see **Figure 1.4**), where the reservoir has distinct and separate water-wet and oil-wet surfaces that coexist in a porous medium. Typically, the oil occupies and forms continuous paths through the larger pores, while the water occupies the smaller pores;

(2) the "dalmatian" wetting condition (see **Figure 1.4**), where the reservoir has distinct but discontinuous water-wet and oil-wet surfaces; and

(3) the speckled[25] or spotted wetting condition, where the reservoir has a continuous water-wet surface enclosing regions of discontinuous oil-wet surfaces or vice versa.

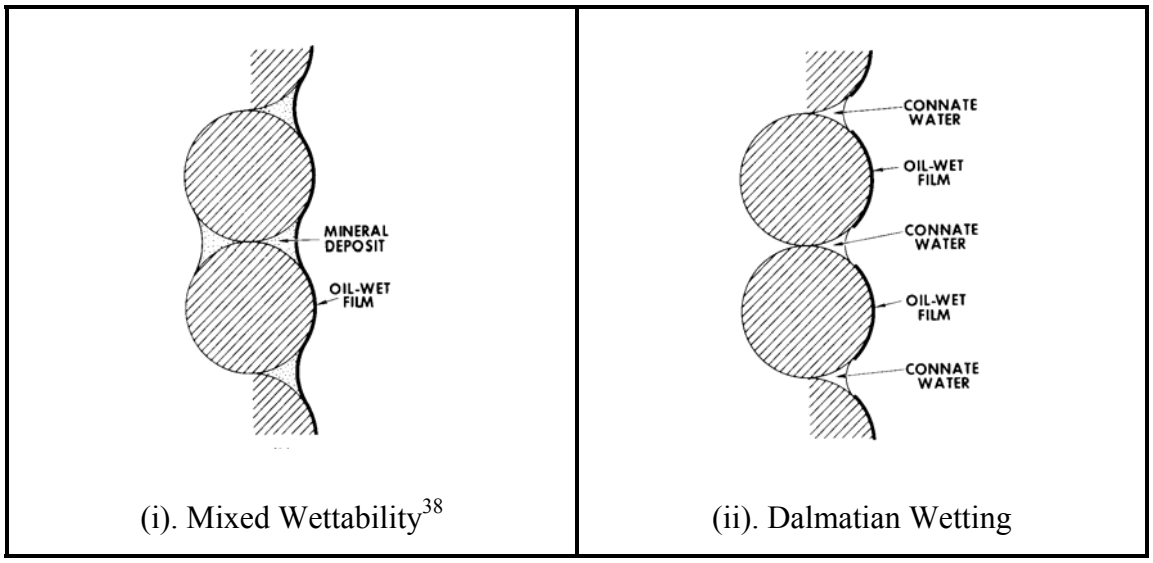

(i). Mixed Wettability[38] (ii). Dalmatian Wetting

Figure 1.4: Effect of Mineralogy on Wetting Condition

From the foregoing, an underlying feature of heterogeneous wettability is the presence of distinguishable zones that respectively exhibit preferentially oil-wet and water-wet characteristics. It is worthy of note that in some literature, the term heterogeneous wettability is divided broadly into fractional wettability and mixed wettability, while in some others, the term

fractional wettability is defined as synonymous to heterogeneous wettability. For this work, the former definition is adopted.

The extent, type, and distribution of wetting heterogeneity are greatly influenced by the chemical variation/distribution of the minerals present in the pores of the reservoir rock. Carbonates are believed to be more oil-wet than clastics. Clean sandstone or quartz has been known to exhibit extremely water-wet conditions, although departure from this general trend has been reported due to the presence of certain minerals. A case in point is the quartz reservoir rock of North Burbank that was observed to exhibit a strongly oil-wet character because of the coating of chamosite [$(Fe_5^{2+}$ $Al)(Si_3Al)O_{10}(OH)_8$] clay, which is reported to cover about 70% of the reservoir rock surface[39]. It is noteworthy that the existence of an extremely water-wet or extremely oil-wet reservoir is rare; only for the gas-liquid system is it generally safe to assume that gas is always in the non-wetting phase.

1.5 Mechanism of Wettability Variation in Reservoirs

It is generally accepted that the initial/"first" wetting state of the reservoirs, particularly for sandstone reservoirs, is a strongly water-wet state, since all reservoirs are initially occupied by water. With the migration of oil into the reservoir, the water is displaced first from the very large pores and then from progressively smaller pores until such a point where the capillary forces holding the water in the very small pores cannot be overcome by the displacing force of the oil. This condition is typically observed at grain contacts and small capillaries. Over a long geologic period and equilibration/stabilization time, certain components from the oil, which include surface active materials, polar compounds, porphyrins, or high molecular paraffinic hydrocarbon, may deposit on or be adsorbed into the rock matrix, altering the wettability of the reservoir. Where film deposition accounts for wettability variation, it has been suggested[40] that the deposited film is identical to the "prune skin" film observed at the oil-brine interface. From the foregoing, it is evident that the crude oil composition is important in wettability variation in the reservoir, a fact that has been demonstrated by several researchers[41,42]. In addition to the composition of the crude oil, the "ability of the oil to contact the reservoir rock surface" is equally as important in the wettability variation process.

Hirasaki[43] observed that variations in wettability are often related to the presence or absence of stable water films between the oil and the reservoir rock surface. He argued that wetting in crude oil/brine/rock (COBR) systems would be determined by thickness of the water film. If stable thick water films separate the oil from the rock, the system will be water-wet. Conversely, unstable films will rupture possibly leaving one to a few molecular layers of water, and the oil comes in close contact with the rock surface. Polar oil components can then adsorb or deposit on the rock surface. Asphaltenes have specifically been considered responsible for wettability alterations because of their polar groups that may interact and bind to the mineral surface.

This concept of water-film stability may be extended to account for the variation of wettability with height above the oil-water contact. The stability of water film depends on the capillary pressure and the value of the critical disjoining pressure. The disjoining pressure is the change in energy per unit area with change in distance that is observed when two interfaces are brought together from a large separation distance to finite thickness[43]. A positive disjoining pressure tends to disjoin or separate two interfaces while a negative disjoining pressure tends to attract two interfaces. The relationship between the disjoining pressure and capillary pressure is expressed by the augmented Young-Laplace equation thusly:

$$p^{\alpha} - p^{\gamma} = \Pi + 2H^{\alpha\gamma} + \sigma^{\alpha\gamma} \qquad \textbf{1.3}$$

where

$p^{\alpha} - p^{\gamma}$ = Laplace pressure or capillary pressure, P_c

Π = disjoining pressure

$H^{\alpha\gamma}$ = mean curvature

$\sigma^{\alpha\gamma}$ = interfacial tension (IFT)

Where the capillary pressure is above the critical disjoining pressure, thin films of water that wet the reservoir rock are ruptured such that the crude oil contacts the reservoir rock and eventually wets it. Consequently, it is expected that the reservoir will get progressively more oil-wet as the capillary pressure increases and the water saturation decreases. This accounts for the variation in wetting condition with increasing height above the oil-water contact.

Kaminsky and Radke[44] have reported, however, that it is possible for the wettability of the reservoir to be altered without rupturing the stable film of water. In their work, it was shown that components having only minute solubility in water are capable of diffusing through the water films at fast enough rates (laboratory scale) and then adsorbing onto the mineral surface. The fact that not all asphaltic oil reservoirs are oil-wet seems to contradict this explanation. In explaining this apparent contradiction, they suggested that in such cases, asphaltene adsorption in the presence of a finite water film is not necessarily strong enough to alter the wetting state.

1.6 Reservoir Wettability and Oil Recovery Efficiency

The fact that wettability affects oil recovery efficiency is widely acknowledged. One of the seminal works on the importance of wettability on waterflooding performance was by Buckley and Leverett[1] in 1941. However, the wetting phase that will result in optimal recovery of oil appears to be the subject of intense research debate. Reported observed cases of optimal oil recovery for water-wet, intermediate-wet/neutral-wet and oil-wet conditions have been published[2,11,14,22]. The reason for this divergence in reports is attributable to a number of modifying factors, which include, among other reasons, the following:

(1) constraint of difficulty in wetting state reproducibility;

(2) lack of a unified standard procedure for coring, core handing, and core storage;

(3) different methods adopted for wetting-state characterization and their inherent limitations; and

(4) the fact that a host of other reservoir rock and fluid properties, in addition to the reservoir wetting condition, also act to influence oil recovery efficiency.

1.7 Wettability Alteration in Cores

Departure from strongly water-wet conditions has been reported to result in either a decrease or an increase in oil recovery efficiency, reflecting the range of possible wettability changes. The difficulty in measuring the in situ reservoir-wetting state necessitates the “surface” determination of reservoir wettability through the use of core plugs or whole length cores. However, the wetting state of the core samples may be altered from their in situ values during cutting,

surfacing, and handling of the core samples. Variation of core wettability from in situ reservoir wettability is due to a number of reasons including the following:

1. Temperature and pressure drop as the core sample is brought to the surface which results in the flashing of the connate water present
2. Drying of the core
3. Invasion of drilling mud during coring
4. Compositional changes resulting in asphaltene deposition or wax precipitation from the crude oil because of reduction in temperature and pressure
5. Oxidation, contamination, and desiccation during handling/storage. The oxidation process may sometimes enhance deposition.

Care must be taken in the handling of the core samples to ensure that the actual wettability is not altered. Usually the wetting state of the core plug may be altered in one of the stages beginning with coring, core handling, core preservation, and wettability measurement in the laboratory. Where the core wetting state has been altered, care should be taken to duplicate/reproduce the reservoir wetting conditions as closely as possible. The subject of preservation of core wettability and the accurate reproduction of altered core wettability is another area of research debate. However, some published reports[7,5,42,45,46,47,48] in this regard have suggested ways of preserving and restoring in situ core wetting state so as to ensure that reservoir rock wettability is accurately measured. In addition, these methods help to ensure that core samples used in the laboratory for determination of oil recovery efficiency and related studies are representative.

1.8 Objectives

The primary aim of this research study is to experimentally ascertain the influence of wettability on oil recovery efficiency in representative Alaskan cores. Analysis of the resulting data from the experimental work will be used to demonstrate how influencing the wettability through injection of fluids with different salinities can be used to improve recovery efficiency in typical EOR processes of interest to ANS exploration.

Several EOR methods have been evaluated for use in Alaska for improved oil recovery (IOR) and these include (1) thermal methods; (2) gasflooding (including water-alternating gas [WAG]); (3) chemical methods for medium to light oils; and (4) microbial methods. Currently only the second option is applied widely at the ANS field for EOR applications, while active research is still ongoing in the applicability of some of the other EOR methods to ANS. Apart from these EOR methods, secondary oil recovery methods such as waterflooding (using formation and/or treated seawater) and gas injection (for pressure maintenance) are also employed in a bid to increase the total volume of oil recovered from ANS. Despite the application of all these EOR and secondary oil recovery methods in Alaska, significant oil volumes remain in place in a typical reservoir after these methods are applied. Industry production data do suggest, however, the possibility of significantly improving EOR operations in ANS fields by developing (1) a better understanding of wettability in general and mixed wettability in particular; and (2) methods to alter wetting states in Alaskan reservoirs. Consequently, characterizing the wetting state of ANS reservoirs, understanding how the injected and resident fluid composition influences wettability and oil recovery, and developing methods that fundamentally improve wettability to achieve higher recovery efficiencies, are crucial to the EOR mission of the Arctic Energy Technology Development Laboratory (AETDL).

In order to realize the EOR mission of AEDTL and improve oil production characteristics in ANS fields, the need exists to (1) experimentally ascertain the influence of wettability on recovery efficiency in representative Alaskan cores; and (2) demonstrate how influencing the reservoir wettability through injection of fluids with different salinities and composition can be used to improve recovery efficiency. The effects of salinity on wettability, oil recovery efficiencies, and residual oil saturation during waterflooding are of particular interest in Alaska, where a unique opportunity exists to develop low-salinity reservoirs (e.g. the Prince Creek formation) to provide injection water for new waterfloods in Western Prudhoe Bay, and new heavy oilfloods at Milne Point and Kuparuk.

Based on the foregoing, the overall aim of this research study entails the determination of the effect of wettability and its variation (because of changes in brine salinity) on oil recovery on representative cores from ANS. Based on this development, the experimental studies were

conducted on core samples: Berea sandstone samples, Kuparuk River unit cores (KR-L01), cores from the archives of the Alaska Department of Natural Resources (DNR), and representative core samples from an ANS operator. Consequently, the specific objectives of this research study are as follows:

1. Observe the effect of variation in the salinity of the injected brine on oil recovery and residual oil saturation.

2. Determine the effect of increasing the temperature of the injected brine on oil recovery efficiency

3. Characterize the wettability changes/alteration, if any, induced by (1) and (2) using the Amott-Harvey wettability index

4. Employ cyclic water injection for EOR (within scope expansion of the project)

EXECUTIVE SUMMARY

Multiphase fluid flow distribution and behavior in petroleum reservoirs is influenced by a myriad of interacting variables like pore geometry, wettability, rock mineralogy, brine salinity, oil composition, brine injection rate, and chemical properties of the brine. Reservoir wettability is known to have very significant influence on pore scale displacement and is a strong determinant of the final residual oil saturation and hence the oil recovery. Studies have indicated the improved oil recovery potential of low-salinity brine injection.

The experimental work and the results covered in this report can aptly be divided into three phases. The first and second phases investigate low-salinity brine injection effect on wettability of the rock and final residual saturation. The third phase evaluates the added benefits of cyclic water injection to the earlier work.

As part of the first phase, extensive literature study was performed on wettability characterization of reservoir rocks and low-salinity brine injection as a means for improved oil recovery. Coreflood studies were carried out on DNR and Berea cores to determine the recovery benefits of low-salinity waterflood over high-salinity waterflood and the role of wettability in any observed recovery benefit. Two sets of coreflood experiments were conducted; the first set examined the EOR potential of low-salinity floods in tertiary oil recovery processes while the second set examined the secondary oil recovery potential of low-salinity floods. Changes in residual oil saturation with variation in wettability and brine salinity were monitored. All the coreflood tests consistently showed an increase in produced oil and water-wetness with decrease in brine salinity and increase in brine temperature.

In the second phase, three sets of coreflood experiments were conducted on representative Alaska North Slope (ANS) core samples. All the sets of experiments examined the effect of brine salinity variation on wettability and residual oil saturation of representative core samples. The core samples used in the first and third set were new (clean) while in the second set core samples were oil aged. For first and second sets laboratory reconstituted 22,000 TDS, 11,000 TDS and 5,500 TDS (total dissolved solids) brines were used while for the third set ANS lake water was used. Oil aging of core decreased the water-wetting state of cores slightly. This observation could be attributed to adsorption of polar compounds of crude oil. The general trend observed in all the coreflood experiment was reduction in S_{or} (up to 20%) and slight increase in the Amott-Harvey wettability index with decrease in salinity of the injected brine at reservoir temperature. Additional coreflooding tests included water injection (high as well as low salinity in tertiary mode) under complete reservoir conditions using live oil. These tests, which were carried out on two core samples, also indicated a reduction in residual oil saturation with decrease in water salinity.

Cyclic flooding is performed by injecting the brine at a lesser flow rate with cyclic pulses of flow period and idle period. This allows the brine to spread well into the pore capillaries and displace the oil effectively. Low-salinity cyclic water injection is an interesting combination that offers the effects of both, with notably high oil recovery and less usage of water. In this third phase of the project work, water-oil flood experiments were conducted on dry sandstone cores from BPXA (some of them used in the second phase) in a core holder apparatus at atmospheric

temperature and overburden pressure conditions. After establishing irreducible water saturation, cyclic waterfloods were conducted to calculate oil recovery from the volume of produced fluids. Pulsed cyclic floods were programmed in the injection pump. Two sets of experiments were repeated with cores of different permeability and lab-reconstituted brines of 21,000, 11,000, and 5,500 TDS salinity and ANS lake water. Results were compared with available data from continuous injection performed on the same cores. In the third set, cyclic floods were tested for two symmetric on-off time intervals. It is observed that residual oil saturation is achieved as early as 3–4 PVs of injected water in cyclic injection as compared to 6–7 PVs in continuous injection. Additional oil recovery is observed in cyclic injection's idle time, when the already flooded water spreads smoothly within the pores to displace oil out of the core. Consistent increase in oil recovery and reduction in residual oil saturation (up to 40%) was observed as brine salinity was lowered. Within cyclic injection, lesser pulse intervals yielded better results.

In terms of "academic products" or "academic accomplishments," the project has produced two Master of Science theses, with another in progress; a journal publication in *Transport in Porous Media;* and three conference publications. The work presented by one of the graduate students that worked on the project won a second place award at the 2006 Society of Petroleum Engineers (SPE) Western Regional Meeting student paper contest, competing against some of the top petroleum engineering schools in the nation. In terms of benefits to the industry, the results from this work are of practical significance to ANS producers and offer significant evidence for executing low-salinity water injection projects on the ANS.

CHAPTER 2: Literature Review – Wettability and Oil Recovery

Waterflooding is a secondary oil recovery process in which water is injected into a reservoir to recover additional quantities of oil that have been left behind after primary recovery. Waterflooding is by far the most widely applied method for improved oil recovery and accounts for more than one-half of U.S. domestic oil production. Similar proportions hold worldwide.

When waterflooding is carried out in a strongly water-wet system, water is imbibed into smaller pores because of favorable capillary forces and oil displaced into the larger pores. The displacement process is such that the water phase maintains a fairly uniform front, and only the oleic phase moves ahead of the front. Because of the preferential wetting of the rock surface by water, the oil is displaced in front of the water, which advances along the walls of the pores. At some point, the neck connecting the oil in the pore with the remaining oil will become unstable and snap off, leaving spherical oil globule trapped in the center of the pore[49] **(Figure 2.1)**. After water passes and traps the oil, almost all the remaining oil is immobile. The disconnected residual oil exists as (1) small, spherical globules in the center of the larger pores; and (2) larger patches of oil extending over many pores that are surrounded by water.

In strongly oil-wet systems, the location of the two fluids is reversed from the water-wet case. Waterflooding in strongly oil-wet system is generally less efficient than in a strongly water-wet case. After the start of waterflooding, the water will form continuous channels or fingers through the centers of the larger pores, pushing oil in front of it (**Figure 2.2**). Oil is then left in the smaller pores and crevices. Typically, in strongly oil-wet reservoirs, the oil remaining is found (1) as continuous film over pore surfaces, (2) in pore throats, and (3) big pockets of oil trapped and surrounded by water (due to formation of continuous fingers and channels of the displacing water in the center of the pore. These fingers may eventually merge trapping the oil in between them).

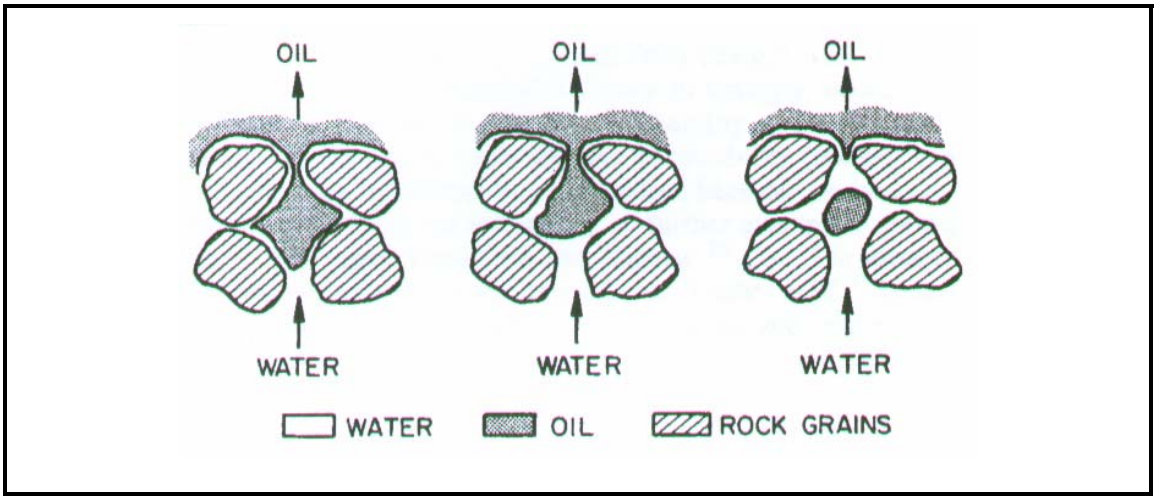

Figure 2.1: Waterflood Oil Displacement in a Strongly Water-Wet Rock. [49]

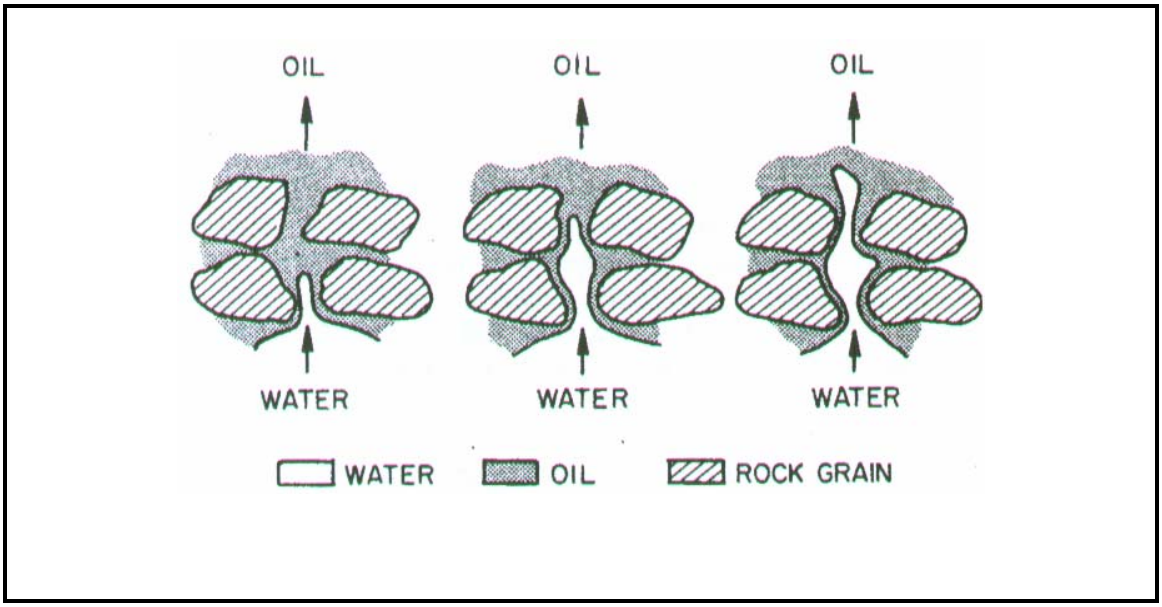

Figure 2.2: Waterflood Oil Displacement in a Strongly Oil-Wet Rock. [49]

2.1 Wettability and Relative Permeability

It has long been known that wettability is a primary determinant of waterflood recovery efficiency[1,2,11,14,22]. Additionally, waterflood recovery is controlled by the oil-water relative permeability, which is an implicit function of wettability. In practice, the most generally accepted method of taking wettability effects into account in waterflooding is through making relative permeability measurements on reservoir core samples using reservoir fluids at reservoir temperature and pressure[50]

2.1.1 Wettability and Relative Permeability in Uniformly Wetted Media

The uniformly wetted medium represents a system where the wettability of the entire surface is uniform; that is, it is either oil-wet, water-wet, or intermediate-wet. Depending on the way the relative permeability curve is normalized, the shape of the relative permeability curve may differ for similar fluid combinations under the same condition as wettability changes. Normalization of the relative permeability curve is achieved either by using the absolute permeability of the rock to brine/air or the effective permeability of the rock to oil at interstitial water saturation (IWS). In this work, the terms interstitial water saturation, connate water saturation and irreducible water saturation are assumed to mean the same thing and are thus used interchangeably. It has been reported that the effective permeability to oil at IWS decreases as the core becomes more oil wet[11]. It has also been shown that as the core becomes more oil-wet, relative permeability curves normalized with the absolute permeability result in the decline in relative (effective) oil permeability at initial water saturation[51]. Where the relative permeability curve is normalized with the effective oil permeability, the wettability effect observed in the former case (absolute permeability normalization) is factored out such that the curves start at the same point irrespective of wettability changes[52].

Figure 2.3A and **Figure 2.3B** illustrate the dependence of the oil-water relative permeability on wettability. They show the imbibition relative permeability (on a semilog scale) for oil and water in a fired Torpedo sandstone core[11].

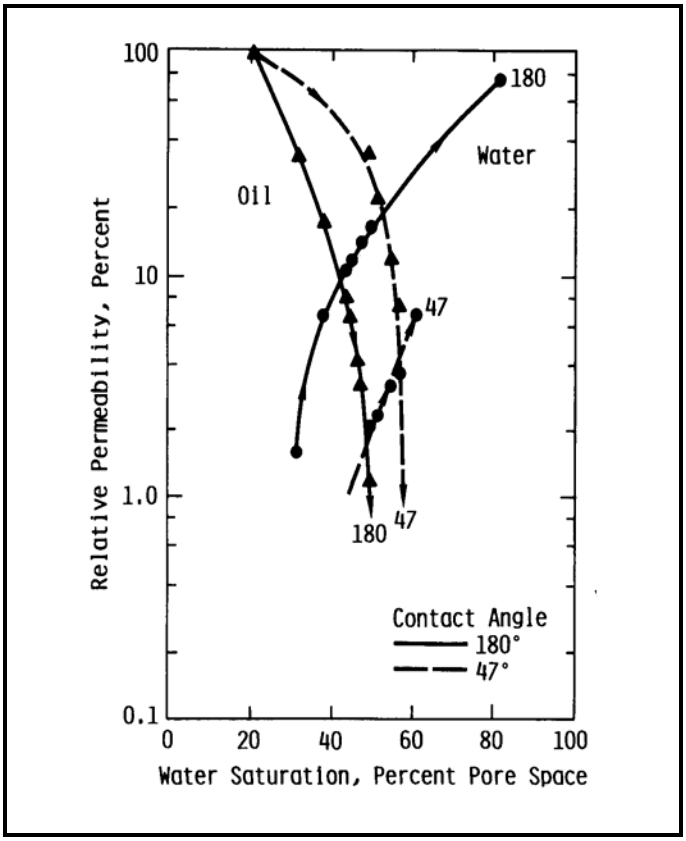

Figure 2.3A[11]: Relative Permeabilities for Two Wetting Conditions.

In the experiment, uniform rock surface was created through firing the core. Oil wettability was induced by the use of an oil-soluble surfactant in the oil. Contact angle measurement was used to characterize the wetting state of the core. Base permeabilities for both figures were determined as the effective permeabilities of the rock to the oil at connate water saturation. From **Figure 2.3A**, the relative permeability to oil is higher in the slightly water-wet case ($\Theta = 47^o$) than in the strongly oil-wet case ($\Theta = 180^o$). This observed hysteresis of the relative permeability curves agrees with the understanding of saturation distribution obtainable for the different wetting states. Because of the fact that oil is strongly held in the pore throats (for $\Theta = 180^o$) by strong capillary forces, it is easier to displace water than the oleic phase in this case. The converse situation is also observed for a strongly water-wet system.

The trend in relative permeability relationship to wettability observed in **Figure 2.3A** is also illustrated in **Figure 2.3B**. It is observed that for all values of water saturation above the connate

water saturation, the relative permeability to water decreases with increasing water-wetness. When the water saturation is 60%, the relative permeability of the rock to water is 4% while that to oil is 11% for the strongly water-wet case (contact angle equal to 0^o). For the strongly oil-wet case, with contact angle equal to 180^o, the relative permeability to water at the same saturation increases a factor of 10 to a value of 40% while that to oil decreases to a value almost equal to zero. The implication is that at higher values of contact angle (where the reservoir rock becomes progressively more oil-wet), the transmissibility of the reservoir rock to water is higher than to oil and as such the recovery of oil should be less efficient in a strongly oil-wet case than in a water-wet case.

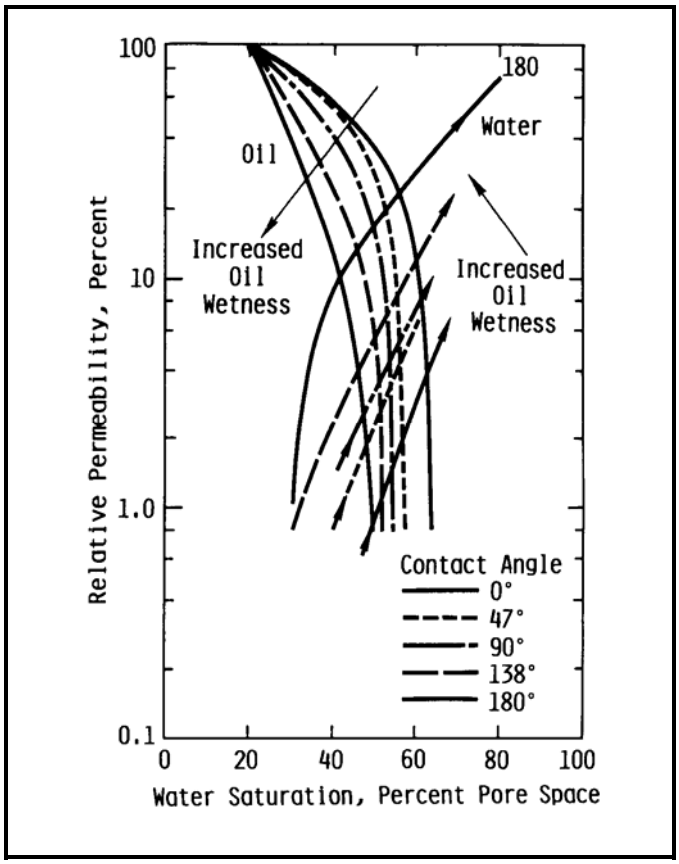

Figure 2.3B[11]: Relative Permeabilities for a Range of Wetting Conditions.

Morrow et al.[4] studied the effect of wettability variation on steady-state relative permeability with water and mineral oil. Their studies were conducted under water-wet, neutral-wet, and oil-wet conditions. Wettability changes were achieved by the use of varying concentrations of

octanoic acid in the oil. They observed that the water relative permeability increased as the system became more oil-wet, while the oil relative permeability decreased. They also observed that the crossover point occurred at lower water saturations as oil-wetness of the system increased.

Mungan[53] measured the unsteady state relative permeability in Teflon cores and reported that the relative permeability ratio (displacing to the displaced phase) is nearly vertical and extends over a short saturation interval when the wetting fluid displaces the non-wetting fluid. He further observed that the converse situation is obtained when the non-wetting fluid displaces the wetting phase. In this case, the relative permeability ratio is comparatively higher at a given ratio and extends over a greater saturation range.

The reported dependence of the relative permeability curve on wettability changes/variation has been validated by many researchers[53,54,55]. However, McCaffery et al.[55] reported that relative permeability is not affected by wettability changes at strongly wetted conditions and that large changes occurred only when the system's wettability is near neutral. Similar observations were reported by Morrow et al.[56,57] on changes in capillary pressure curves with variation in wettability. However, the reported observation by Owen and Archer[11] disagreed with this finding as they only observed changes in relative permeability curves for the wettability range between the contact angles of 0° and 47°.

Trend observations of the relative permeability behavior (**Figure 2.3**) suggest the possibility of developing some generic correlation relating relative permeability to wettability for uniform wetness and for homogeneous wettability. Development of this correlation will aid in inferring wettability from relative permeability curves. However, no functional correlation has been developed even though guidelines for evaluating wetting conditions have been proposed.

Before concluding this section, it is pertinent to present Craig's *Rule of Thumb*[48] for determining wettability from relative permeability curves for strongly wetted systems. The rule of thumb is presented in **Table 2.1**. Note, however, that other factors such as pore geometry, initial water saturation, pore size distribution, and pore connectivity also influence the shape of the relative permeability curve. Morgan and Gordon[58] demonstrated this fact when they measured relative permeabilities in cleaned water-wet cores and reported pronounced differences between the cores

that have large, well-connected pores and ones that have smaller, less-well-interconnected pores. Caudle et al.[59] reported that relative permeability curves measured on water-wet sandstone were dependent on initial water saturation. Changes in the initial water saturation will result in a change in shape and location of the curves. Consequently interpretation of rock wettability using Craig's *Rule of Thumb* [48] should be supplemented where possible with other measures of wettability less susceptible to "noise" (i.e., other factors which also influence the shape of the relative permeability curve as already described above).

Table 2.1: Craig's *Rules of Thumb* for Determining Wettability from Relative Permeability Curves[48]

	Water-Wet	**Oil-Wet**
Interstitial water saturation	Usually greater than 20% to 25% PV.	Generally less than 15% PV. Frequently less than 10%
Saturation at which water and oil relative permeabilities are equal	Greater than 50% water saturation	Less than 50% water saturation
Relative permeability to water at the maximum water saturation (i.e., floodout); Based on the effective oil permeability at interstitial water saturation	Generally less than 30%	Greater than 50% and approaching 100%

2.1.2 Wettability and Relative Permeability in a Non-uniformly Wetted Media.

For a mixed-wet case, water and oil may be spontaneously imbibed respectively at high oil and water saturations. The peculiar characteristic of a mixed-wet reservoir is that parts of the rock surfaces (usually the large pore spaces) are preferentially oil-wet with the oil film being continuous, while the remaining parts (fine pores and grain contacts, pore throats) are preferentially water-wet. For mixed-wet systems, the relative permeability to oil is reasonably

high even at low oil saturations. **Figure 2.4**[60] shows the relative permeability data for Berea core material before and after treatment with Dri-film.

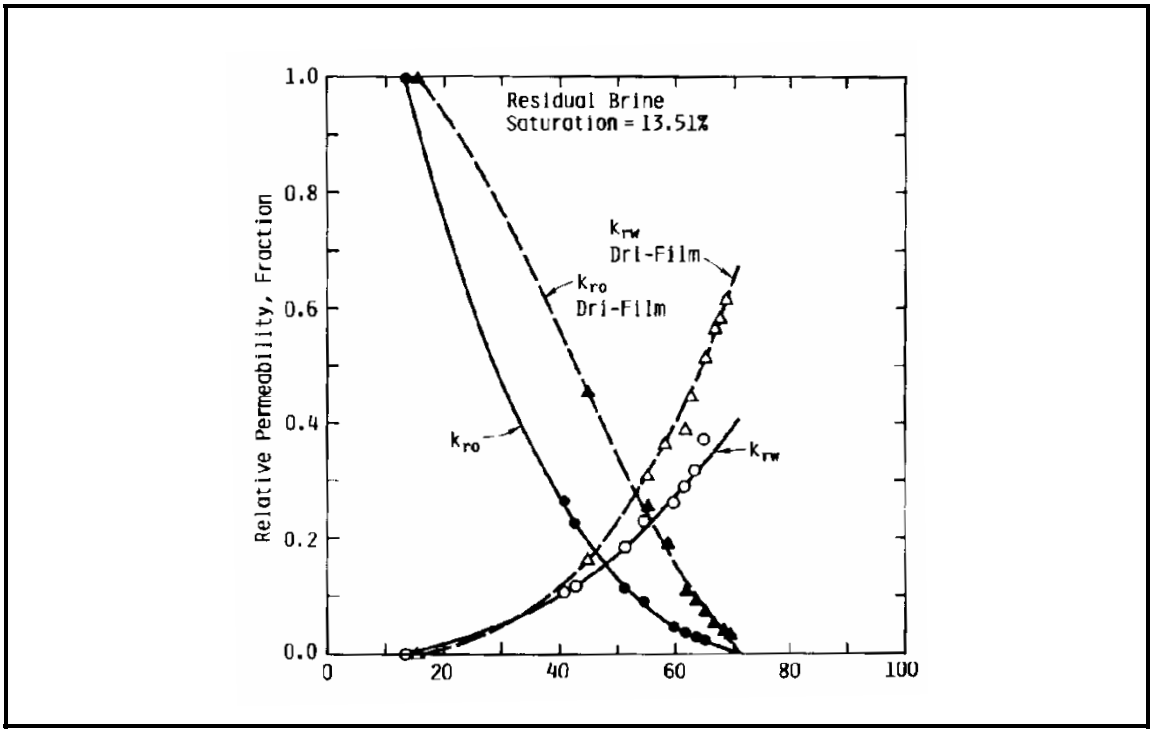

Figure 2.4: Relative Permeability Curves for Berea Sandstone before and after Dri-Film Treatment. [60]

Dri-Film is a silicon polymer used to decrease water wettability of the rocks as well as attain the desired mixed-wet behavior. It is suspected that the use of silicon polymers to alter wettability will result in non-uniform wetting because of preferentially biased adsorption/deposition of the chemical on the mineral rock.

Both sets of curves in **Figure 2.4** were obtained with the unsteady-state method for relative permeability determination. From the figure, it is seen that at fixed-water saturation, oil permeability increased more than water relative permeability as water wetness decreased (because of treatment with Dri-Film, which made the core water-wet). This is contrary to what is obtained in systems of uniform wetness, where the relative permeability to oil decreases when there is an increase in oil wetness.

Wang et al.[61] examined the effect of wettability alteration on water-oil relative permeability using two Berea and Loudon cores. The Loudon cores were initially mixed-wet and were made water-wet by Dean Stark's extraction, while the mixed wetting state was achieved in the water-wet Berea core by aging in Loudon crude. Measurement of the steady-state relative permeability was done using the principle described by Braun and Blackwell[62]. They compared the imbibition relative permeabilities of the Berea before and after aging, and discovered significant differences at high-water saturations >50%. They reported that the aged Berea had a residual oil saturation of 17% while the natural Berea showed a value as high as 47%. The endpoint water relative permeability was 35% in the aged Berea and 3.4% in the natural Berea. For water saturation lower than 50%, the relative permeability characteristics were similar. Similar observations were made with the Loudon cores where the endpoint water relative permeability reduced from 20% for the mixed-wet state to 7.8% for the water-wet case. Similar reduction in endpoint oil relative permeability from 82% to 63% was observed.

Richardson et al.[63] studied the behavior of the relative permeability ratio on native-state and cleaned East Texas Woodbine cores by measuring the unsteady-state oil-water relative permeabilities on the cores. They observed that as the core was rendered more water-wet through cleaning, the behavior differed from that observed in uniformly and fractionally wetted systems. For uniformly and fractionally wetted systems, the relative permeability ratio (wetting phase displacing non-wetting phase) at a given water saturation was lowest for a strongly water-wet system, and the more oil-wet curves were located to the left of the strongly water-wet curve. That is, there was a higher relative permeability ratio at similar water saturation. However, they observed that the water-wet curve was positioned to the left of the native-state curve. Flooding of the native-state core resulted in very low ROS, ranging from 2% PV to 12% PV, while that of the extracted (water-wet) core resulted in average residual oil saturation (ROS) of 30% PV. This observation was attributed to the mixed-wet condition of the native-state cores.

Other researchers[64,65] have measured the relative permeability ratio (k_w/k_o) in fractionally wetted systems, using either treated/untreated sandpacks or glass/Teflon beads to simulate fractional wetting condition. The general observation is that the changes in the relative permeability ratio as the oil-wet fraction is increased from 0 to 1 (or decreased from 1 to 0) is similar to the

trend/changes observed when the wettability of a uniformly wetted core is changed from water-wet to oil-wet (or from oil-wet to water-wet).

2.2 Wettability and Fractional Flow of Water during Waterflooding

As has already been noted, oil typically occupies the larger pore spaces in water-wet reservoirs, while the water is held/trapped in the much smaller pores and/or pore throats. The pressure gradient required to displace water from the reservoir is thus higher than that of the oleic phase because of high capillary forces. Consequently, increase in water-wetness is reflected in an increase in oil effective permeability and a decrease in water effective permeability. From the foregoing, if other rock and fluid parameters/properties are kept constant, oil recovered at any given time interval will be higher in a water-wet reservoir than an oil-wet reservoir.

A pragmatic approach to the assessment of waterflood displacement efficiency is through the analysis of the fractional flow curve. While the highly idealized nature of the fractional flow equation is recognized, it does provide, within the limits of its inherent assumptions, an insight into saturation distributions in waterflood displacement studies as well as the observed effects of the wetting state on the shape and position of the curve. The expression for fractional flow curve, f_w, is given by **Eq. 2.1.**

$$f_w = \left[\frac{1}{1 + \left(\frac{k_{ro}}{k_{rw}} \right) \left(\frac{\mu_w}{\mu_o} \right)} \right]_{Sw} \qquad \textbf{2.1}$$

where

f_w = fractional flow of water,
k_{ro}, k_{rw} = oil and water relative permeability respectively (or effective permeability, in md),
μ_o, μ_w = oil and water viscosities, respectively, cp
S_w = water saturation of interest.

In its most simplistic form, the fractional flow equation is an indication of the amount of water that is produced along with the oil at any point in time. **Eq. 2.1** shows that this depends on

viscosity and relative permeability relationship. Since relative permeability is an implicit function of wettability and an explicit function of saturation, it follows that the breakthrough water-saturation value depends also on the wetting state of the reservoir. Consequently, at constant values of the oil-water viscosity ratio, the fractional flow value depends implicitly on the observed wetting state in the reservoir. **Figure 2.5**[60] shows this relationship between the fractional flow curve and wettability. The wetting state was determined using the contact angle measurement, and the oil-water viscosity ratio was kept constant at a value of 25.

The fractional flow curve for the oil-wet case is much steeper and has a longer tail compared to the water-wet case. Consequently, the flood front/breakthrough saturation and the average saturation behind the front at breakthrough is much higher for the slightly water-wet system ($\Theta = 47^{o}$) than the strongly oil-wet system ($\Theta = 180^{o}$). The implication is that more oil will be produced at breakthrough in a slightly water-wet system compared to a strongly oil-wet system. Another important deduction that may be made from **Figure 2.5**[60] is that, though the ultimate recovery of both wetting systems will ultimately be the same, recovery for the strongly oil-wetted case after breakthrough will be at the expense of large volumes of produced water because of the long tail. Ultimately, the unfavorable economics will prevent the attainment of the ultimate recovery.

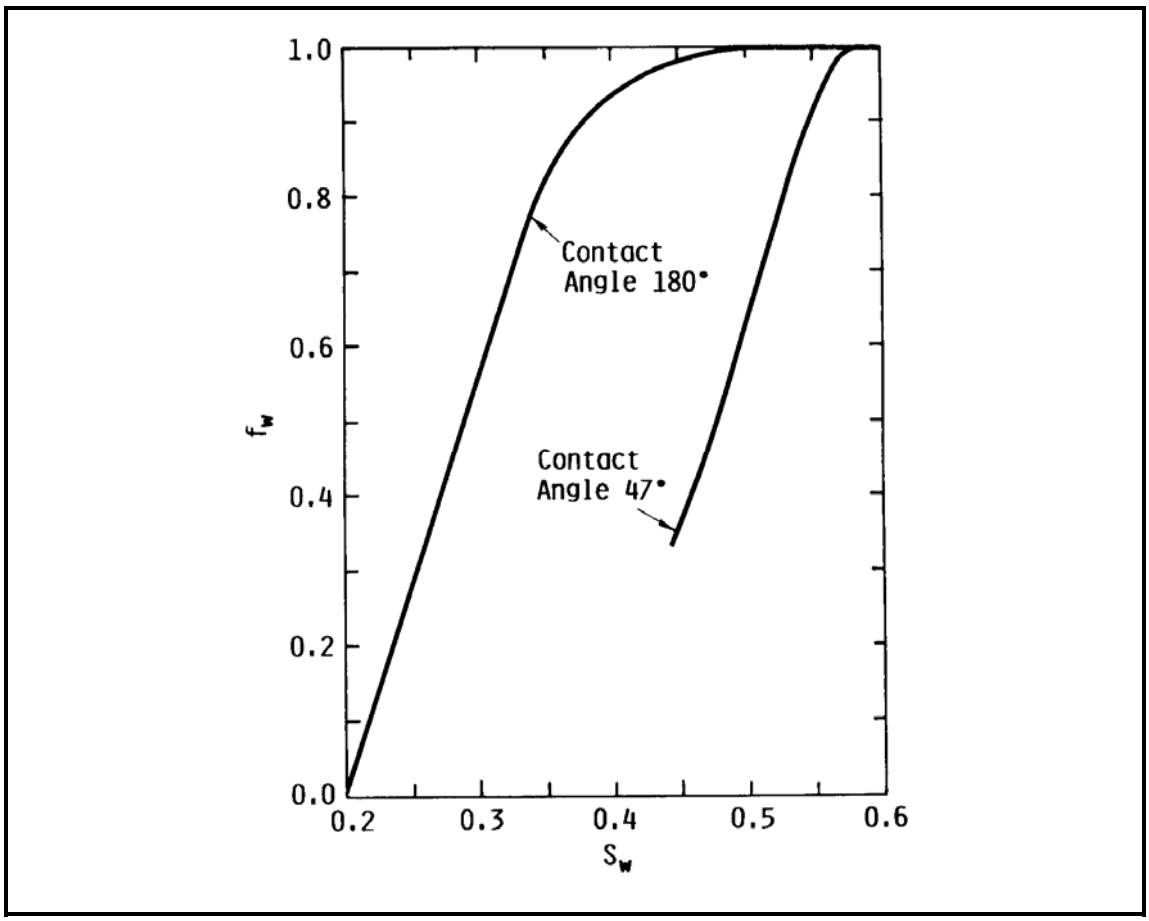

Figure 2.5: Fractional Flow Curves for Waterfloods of Water- and Oil-Wet Rocks at an Oil/Water Viscosity Ratio of 25.[60]

If we define the average water saturation behind the breakthrough front as $\overline{S}_{wBT}$ and the connate water saturation as S_{iw}, then the displaced hydrocarbon saturation at breakthrough is defined by $\overline{S}_{wBT} - S_{wi}$. Consequently, the cumulative oil displaced (or produced due to linear displacement by water) is

$$N_p = V_p\left(\overline{S}_{wBT} - S_{wi}\right) \qquad \textbf{2.2}$$

where V_{p} defines the reservoir pore volume. It is noteworthy that in deriving **Eq. 2.2**, a fundamental assumption is that at the start of waterflooding program, water is at the connate/immobile saturation. From **Figure 2.5**, $\overline{S}_{wBT}$ is ≅ 0.55 for the slightly water-wet and

$\overline{S}_{wBT}$ is ≅ 0.39 for the strongly oil-wet case. The connate water saturation is assumed constant at 0.2. Thus the cumulative oil N_p displaced at water breakthrough for both cases is respectively given by:

$N_p(\Theta = 47^o) = 0.35PV$ [i.e., 35% of the reservoir pore volume]

$N_p(\Theta = 180^o) = 0.19PV$ [i.e., 19% of the reservoir pore volume]

Thus for the system represented by **Figure 2.5**, at breakthrough of the water, the slightly water-wet case will produce/displace about twice the volume of oil that would otherwise be produced if the system is strongly oil-wet. **Figure 2.6**[60] further illustrates this observation. In **Figure 2.6** a comparison is made, for the same system, of oil produced (y-axis) as a function of waterflood pore volumes injected (x-axis).

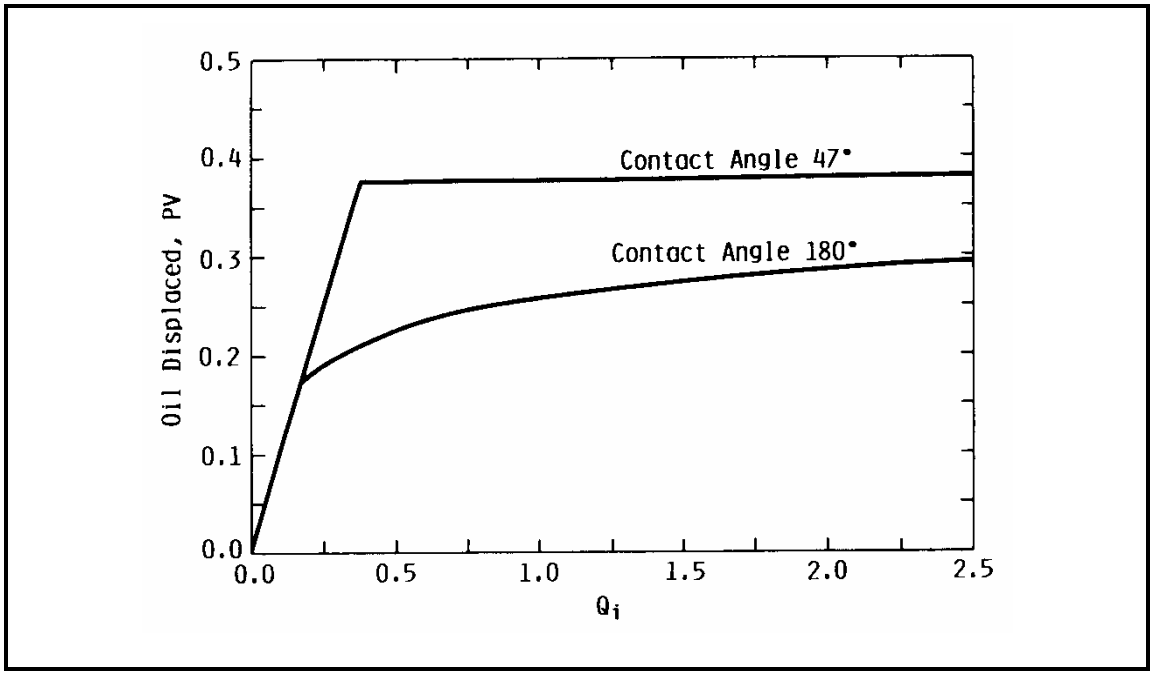

Figure 2.6: Effect of Wettability on Oil Displacement by Water Injection.[60]

Figure 2.6 shows a consistently observed trend in waterflood displacement and perhaps reflects what may be defined as a waterflood oil-recovery norm. The following important points are

worthy of note: (1) there is no further (significant) oil recovery after breakthrough, for the slightly water-wet (to strongly water-wet) system; (2) water breakthrough occurred at less than 1 PV of injected water. Typical field observations range from 1 to 1.5 PVs; and (3) for volumes above 1 PV of injected water, the strongly oil-wet system is a weak function of injected PVs.

2.3 Wettability Effects on Oil Recovery Efficiency

2.3.1 Uniformly Wetted Media

A number of laboratory studies and research have been performed in a bid to understand the effect of uniform wettability on oil recovery and recovery efficiencies. One of the early works on the effect of oil-wet and water-wet systems on oil recovery in waterflood displacement studies was by Donaldson and Thomas[51]. They utilized micromodels (double-layered sand between two flat microscopic specimen slides) to observe the effect of uniform wettability on oil recovery. Results from the micromodel studies were validated by sandstone coreflood studies. Wetting state for the micromodels were determined from visual observation while that of the sandstone cores were characterized using the USBM index. Wettability alteration of the core samples was achieved by treating with GE Dri-Film No. 144. Brine used was reconstituted brine (0.10 NaCl). The coreflood test was conducted at constant differential pressure of 50 psi. From their experiment, they reported that more oil is recovered from a water-wet system than from either the intermediate-wet or the oil-wet system. Low oil recoveries in oil-wet systems were attributed to the very fast formation of brine fingers resulting in simultaneous brine breakthrough with the first oil produced. However, production of oil still continued for a long time even after this breakthrough. After production of oil ceased, large oil pockets (extending from 20 to 30 grain diameters of space) were still trapped in the system and extended from the inlet to the outlet. For the water-wet case, similar trapped oil pockets were observed. However, the oil pockets extended for only short distances (usually 3 to 4 grain diameters of space), and further migration of these trapped oil pockets was reported possible at very high injection rates.

Contrary to the Donaldson and Thomas report[51] on the relatively poor displacement efficiency and oil recovery under intermediate wetting conditions compared to strongly water-wet case, other researchers[66,67,68,69] had indicated that recovery from the strongly water-wet or oil-wet cores is actually lower than recovery from cores that are at some intermediate wettability. Some

plausible explanations for this apparent discrepancy in observed experimental outcome may lie in (1) the varying definition of intermediate wettability as well as the method of wettability characterization; (2) The influence of waterflood injection rate on recovery (some research studies neglect this effect). The lack of standardized definition for this wetting state is such that different authors have different, subjective, definitions. Some of the observed wetting states that have been classified under intermediate wettability by different authors include (1) neutral wetting state; (2) weakly water-wet to weakly oil-wet state; and (3) mixed wetting state (a combination of strong water-wet and strong oil-wet regions). The wetting characteristics of each of these wetting states have been shown to have varying effects on oil recovery and displacement efficiencies.

Jadhunandan and Morrow[69] investigated the relationship between wettability and oil recovery by waterflooding and the dominant variables that control wettability in COBR systems using Berea sandstone. Wettability alteration of the core from water-wet to oil-wet was achieved by aging for 10 days at temperatures between 26°C and 80°C inclusive. Blends of Soltrol 130 and paraffin oil were prepared to give refined oils with the desired viscosities and were subsequently referred to as Moutray and ST-86 crude oil. Water injection was carried out at room temperature, and rates ranged from 2 to 100 ft/day (to determine the effect of flood rate on oil recovery) with most between 3.5 to 7 ft/day (to characterize wettability effects on oil recovery). The wetting index was determined using the modified Amott method. A spontaneous imbibition time of 3 weeks was adopted after observing the trend of imbibition-versus-time curves. A pressure drop of ≤ 35 psi was used in the study because of core damage at pressure gradients above 50 psi. Results of their work reported that aging temperature, initial water saturation, brine composition, and crude oil were all factors in determining the wettability of COBR systems. The authors further reported that in determining the effect of wettability on oil recovery, data that showed obvious end effects and viscous fingering were discarded.

Figure 2.7[69] and **Figure 2.8**[69] show the observed effect of wettability on oil recovery at breakthrough, 1 PV, 3 PVs, 5 PVs, and 20 PVs of injected brine. From **Figure 2.7**[69], the maximum recovery of oil is attained at wettability close to the water-wet side of neutral ($I_{w\text{-}o} \approx 0.2$). A similar trend is observed in **Figure 2.8**[69]**,** which shows the corresponding result for

residual oil saturation. In both cases the maximum oil recovery and minimum oil saturation values were reported to become "*better defined*" with continued flooding. The curves show that

(1) a strongly water-wet system ($I_{w\text{-}o} \approx 1.0$) is independent of the number of PVs of water injected;

(2) oil-wet systems ($I_{w\text{-}o} \approx -0.5$) are weakly dependent on injected PVs with the weak dependence getting stronger as the wetting states tend toward some intermediate state; and

(3) if we define the value of the modified Amott-Harvey index as being equal to zero ($I_{w\text{-}o} \approx 0$) at neutral wetting state then the optimum oil recovery/waterflood residual oil saturation is obtained at this wetting state.

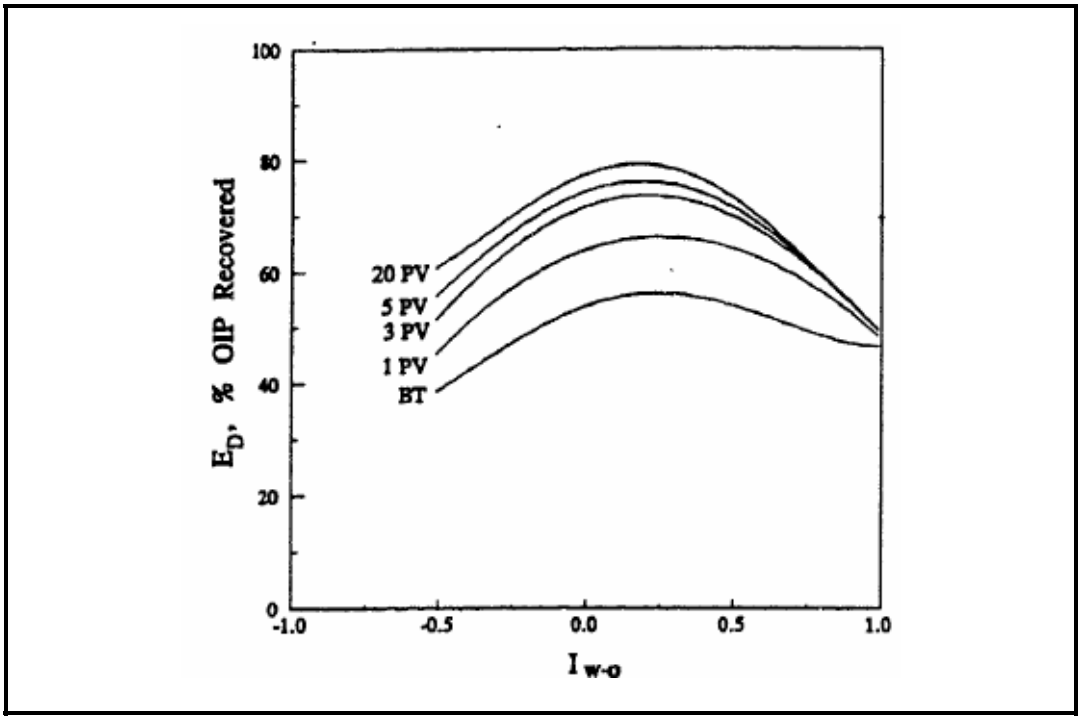

Figure 2.7: Oil Recovery vs. Amott-Harvey Index at Different Injected PVs.[69]

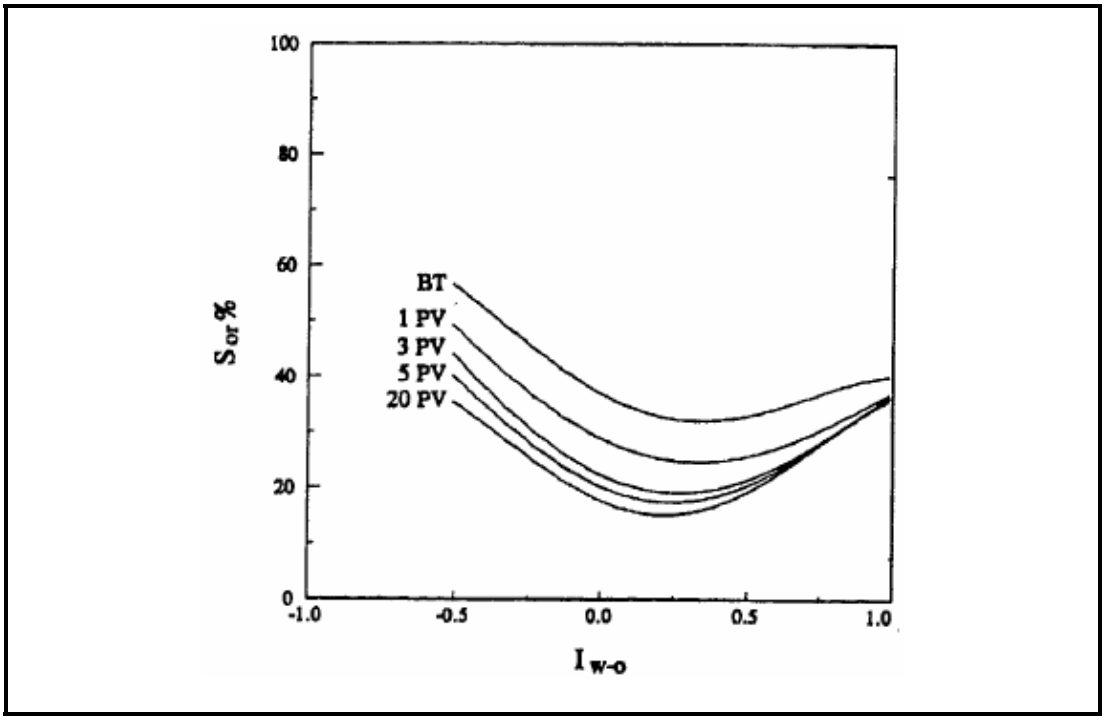

Figure 2.8: Residual Oil Saturation vs. Amott-Harvey Index at Different PVs.[69]

However, care must be taken in interpreting the observed optimal recovery at the neutral-wet condition given by the Amott-Harvey index since it has been shown[19,20,21] that this index is relatively insensitive to neutral wettability at contact angles between 60^o and 120^o.

Tweheyo et al.[70] examined production characteristics in water-wet, neutral-wet, and mixed-wet cores using two different North Sea sandstones and three different fluid systems composed of NaCl-brine and pure n-decane, or n-decane with additives. Wettability modification was achieved by addition of small amounts of organic acid or organic base to the oil. They reported that the water-wet cores had the highest recoveries at water breakthrough and the non-water-wet systems had tail production of oil. The highest ultimate oil recoveries were obtained for the neutral-wet systems and the lowest recoveries were given by the oil-wet systems. The core-wetting states were characterized using the combined Amott/USBM method.

Many other authors[71,72,73,74,75] have also compared waterflood oil recoveries in water-wet and oil-wet cores and reported greater recoveries in water-wet cores for uniformly wetted media.

Contrary to the wetting condition observed in sandstone reservoirs, 90% of carbonate reservoirs are characterized as neutral to preferentially oil-wet. For carbonate oil reservoirs, the water-wetting nature increases with temperature. It is believed that the acid number, AN, may be a crucial factor in dictating the reservoir wetting state since it has been observed that water wetness decreases as AN increases. The AN is defined as the milligrams of KOH required in tests to neutralize all the acidic constituents present in a 1 gram sample of petroleum product. Acid number is an indirect function of reservoir temperature, since decarboxylation occurs as temperature increases. Consequently, the AN in the crude oil decreases as temperature increases. Zhang and Austad[76] experimentally decoupled the effects of temperature and AN as wetting parameters of chalk formations and determined that the wettability of a carbonate reservoir is mainly dictated by the AN of the crude oil and not the reservoir temperature.

Tang and Firoozabadi[77] studied the effect of wettability and initial water saturation on water injection performance on a Kansas chalk outcrop sample. Since Kansas chalk is strongly water-wet, wettability alteration from this condition was achieved by use of stearic acid. The Amott index to water (I_w) and rate of spontaneous imbibition were used to characterize wettability. Water injection was carried out at different rates and pressure gradients. They reported that initial water saturation has a very pronounced effect on waterflood oil recoveries in intermediate-wet chalk and much less pronounced effect in strongly water-wet chalk; for a strongly water-wet condition, oil recovery decreased mildly with increase in initial water saturation, while for weakly water-wet and intermediate-wet conditions, oil recovery increased significantly with an increase in initial saturation. They further reported that oil recovery efficiency is susceptible to viscous forces when the chalk is intermediate and/or weakly water-wet. There was no effect on endpoint recovery when the chalk was strongly water-wet. When the viscous force was high (Δp = 13.5 psi/cm), the intermediate-wet state (I_w = 0.09) gave the best waterflood performance and the strongly water-wet state the worst performance. However, at low viscous force, (Δp = 0.96 psi/cm) the strongly water-wet gave the best performance.

Høgnesen et al.[78] examined the improvement of oil recovery efficiency in oil-wet carbonates by spontaneous water imbibition through wettability modification to water-wetting condition. Spontaneous imbibition tests were performed on chalk outcrops and reservoir limestone samples at different temperature ranges (70°C–130°C) using modified seawater with various

concentrations of sulfate. They reported favorable results at elevated temperatures, more so with increase in the sulfate concentration in the seawater. At lower temperatures, increased spontaneous imbibition was achieved by the addition of cationic surfactant to the imbibing fluid. Limitations to the use of sulfate as a potential determining ion include (1) the problem of souring and scale formation and (2) initial brine salinity and temperature.

The work by Zhang and Austad[79] further validated the reported observations by Høgnesen et al[78]. They correlated the waterflood oil recovery in chalk formation in terms of a "new" wettability index (based on the chromatographic method defined by Strand[29]) and the brine composition (similar to the work done by Høgnesen et al.). They noted that spontaneous imbibition will only occur in chalk formation if the water-wet fraction of the chalk surface is > 0.6.

Al-Hadhrami and Blunt[80] examined the effect of hot-water injection on oil recovery from naturally fractured oil-wet carbonate reservoirs. They reported that conventional recovery from an Omani field having extensive fractures was only 2% after 20 years. Water injection in such fields will be inefficient because of significant bypass issues. However, use of hot water/steam resulted in a thermally induced wettability reversal/shift to a water-wet state, which allows imbibition of the hot water into the rock matrix leading to improved oil recovery.

Graue and Bognø[81] examined the oil recovery mechanism in fractured chalks at different wettability conditions by iterative comparison between experimental work (coreflood studies) and numerical simulation. For all the chalk blocks used, the authors reported two vertical and three horizontal fractures. The first and second vertical fractures were at 4 cm and 13 cm, respectively, from the inlet end, and the horizontal fractures were at the center line of the block and at the inlet and outlet ends to provide hydraulic contact from inlet to outlet. Wettability was characterized using the Amott-Harvey Index, and wettability measurements were reported to have been verified for stability and reproducibility. They observed that, though water movement was significantly affected by the presence of fractures for strongly water-wet conditions and less so for less water-wet conditions in "closed" fractures, fracturing of the chalk did not significantly improve oil recovery for both strongly water-wet chalk and moderately water-wet chalk. It is pertinent to note that the chalk permeability increased by a factor of 50 after fracturing.

2.3.2 Non-Uniformly-Wetted Systems

The understanding that heterogeneous wettability may be the normal wetting state of a reservoir is supported by the observation that many reservoirs have heterogeneous wettability. Whether it is possible to have reservoirs that can be characterized strictly as uniformly wetted is in question, as some form of variation in wetting state over the entire area of the reservoir is expected. In this work, a uniformly wetted surface refers to that surface which is preferentially wetted by either water or oil over the entire area. Using this baseline definition, we define the non-uniformly-wetted system as one that has distinct and identifiable wetted areas, within the same system, that clearly can be characterized as either oil-wet or water-wet regions.

Two types of non-uniformly-wetted systems are of interest in the petroleum industry: (1) the mixed-wet system and (2) the fractionally-wet system. The mixed-wet system is one that has continuous oil-wet paths in the larger pores and water-wet paths in the smaller pores/pore throats. It is important to state at this point that this definition has been extended to include the observed presence of intermediate-wet sites within the rock also. In fractionally wet systems, the individual water-wet and oil-wet surfaces have sizes on the order of a single pore, and specific locations of the oil-wet or water-wet surfaces are not necessarily defined. **Figures 2.9 and 2.10** are schematic models of mixed-wet and fractionally-wet systems as proposed by Dixit et al.[82].

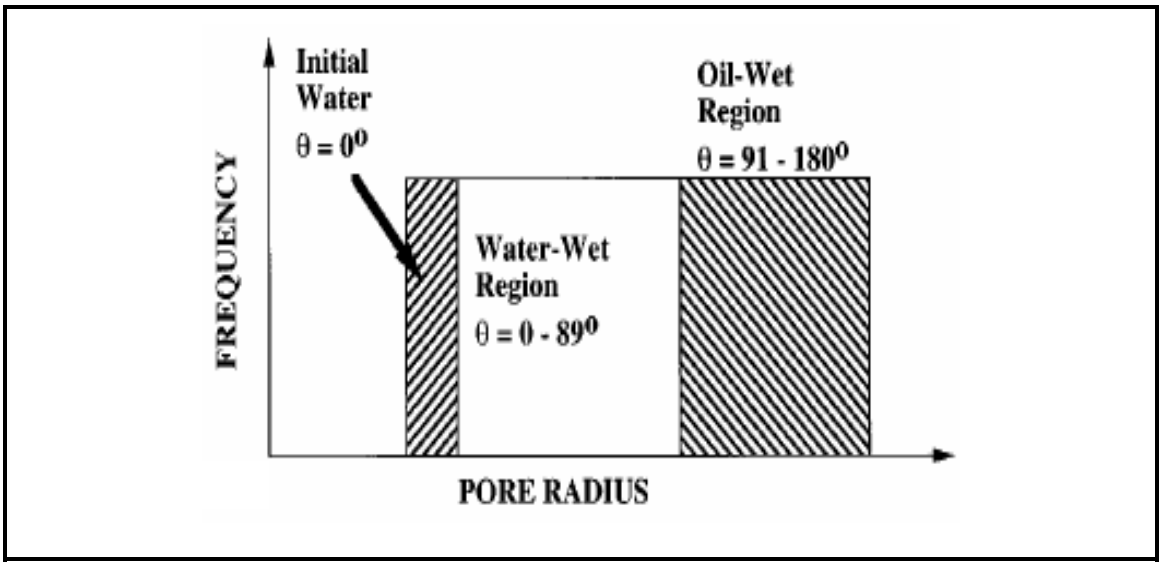

Figure 2.9: Schematic Representation of a Mixed-Wet System.[82]

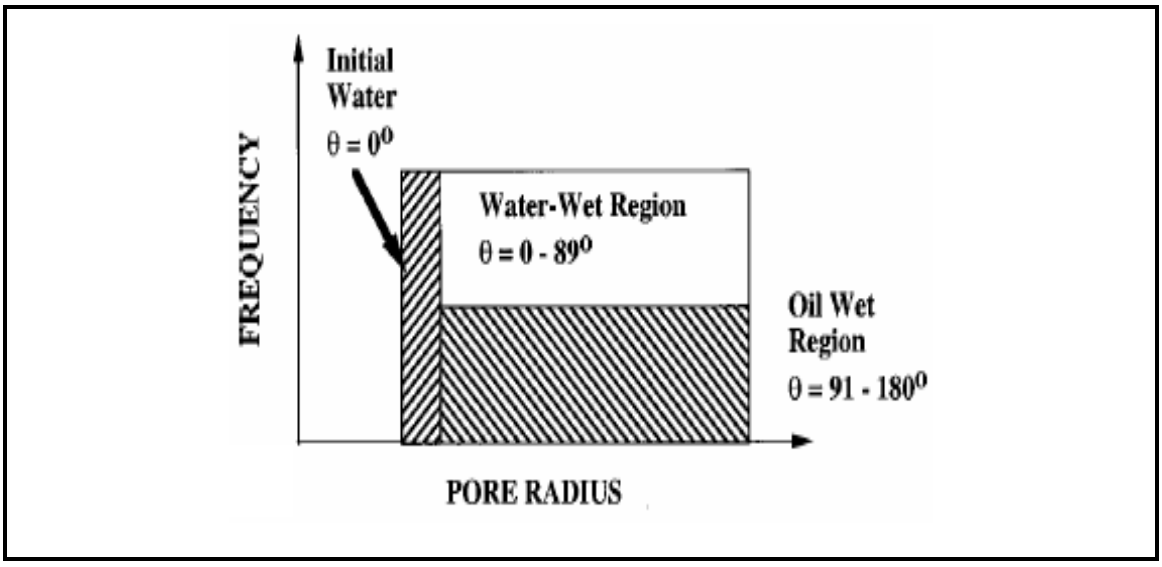

Figure 2.10: Schematic Representation of a Fractionally-Wet System.[82]

2.3.2.1 Mixed-Wet Systems

It has been shown that waterflood residual oil saturation in mixed wettability reservoirs is often a strong function of pore volumes injected[38, 83]. The effect of the number of pore volumes injected has been shown for different oil fields with mixed-wet reservoirs, for example, the East Texas Woodbine reservoir[38] and the Endicott Field Alaska[83]. Further decrease in the waterflood residual oil saturation is possible in a mixed-wet reservoir where there is surface film drainage. Surface film drainage does not act in all mixed-wet reservoirs, but has been shown to be particularly active in mixed-wet reservoirs having high vertical permeability. Lower residual oil saturation has been reported[38] for mixed-wet reservoirs undergoing surface film drainage compared to reservoirs without this drainage mechanism.

The Endicott Field in Alaska is an example of a mixed-wet reservoir with surface drainage effects[83]. In a preserved reservoir-condition coreflood experiment, it was observed that the waterflood residual oil saturation, S_{orw}, was 40% after 1 PV injection, 22% after 500 PVs, and 12% at infinite PVs. Centrifuge flooding was used to observe the effect of surface film drainage on residual oil saturation and thus isolate oil recovery efficiency due to the waterflood. Higher oil recoveries for the mixed-wet condition over the water-wet condition were reported. Oil

recovery from the mixed-wet core was a strong function of the number of pore volumes, while for the water-wet core, oil saturation declined until water breakthrough (≈ 1 PV injection) after which no significant increase in oil recovery was observed.

Similar studies[38] on Boise East Texas reservoir core samples revealed that oil saturation continued to decline as long as water was injected in the mixed-wet cores, while oil saturation quickly reached a constant value (after breakthrough) in the water-wet core irrespective of PVs injected (**Figure 2.11**). Oil viscosity also influenced the endpoint waterflood oil saturation with the low viscosity oils giving much lower S_{orw}. It was also shown that the mineral content of the reservoir rock has limited effect on S_{orw} for the same wetting condition (**Figure 2.12**).

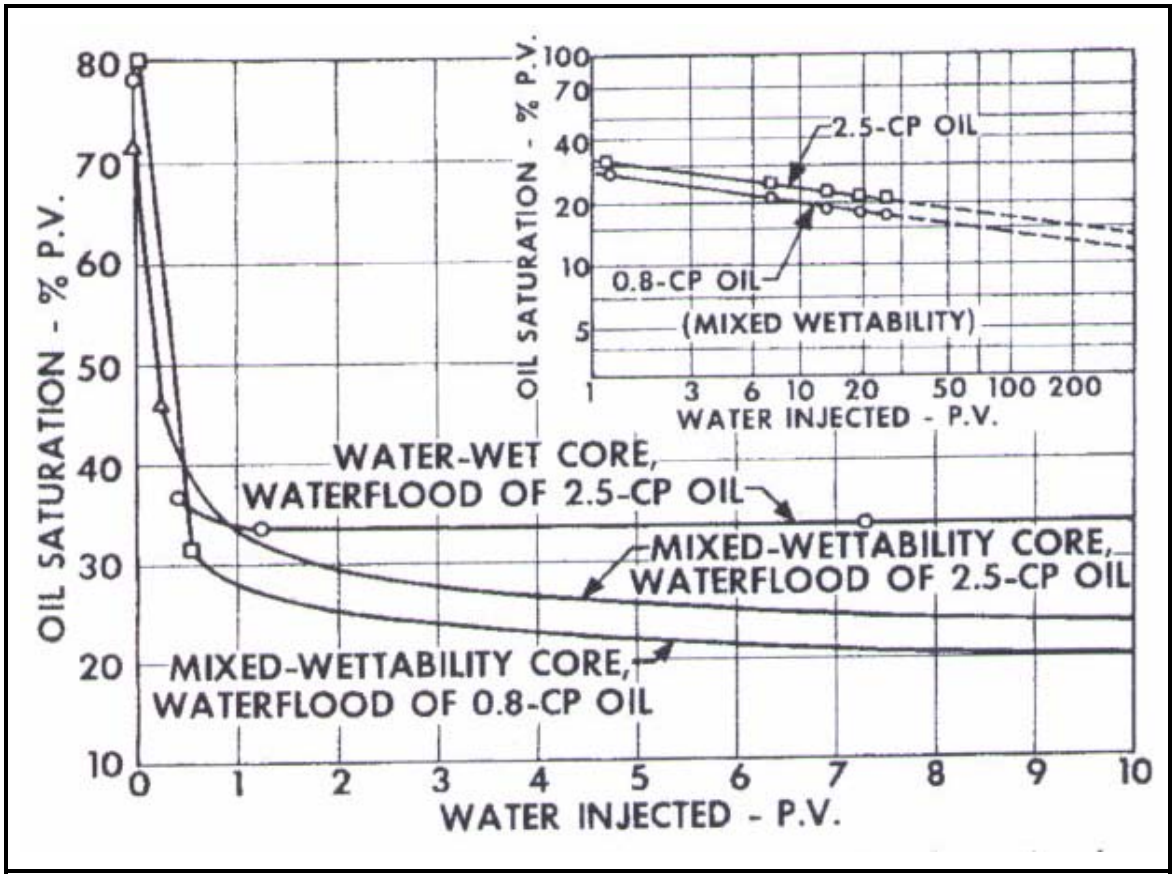

Figure 2.11[38]: Comparison of Waterflood Behavior for Mixed-wet and Water-wet Cores from East Texas Field.

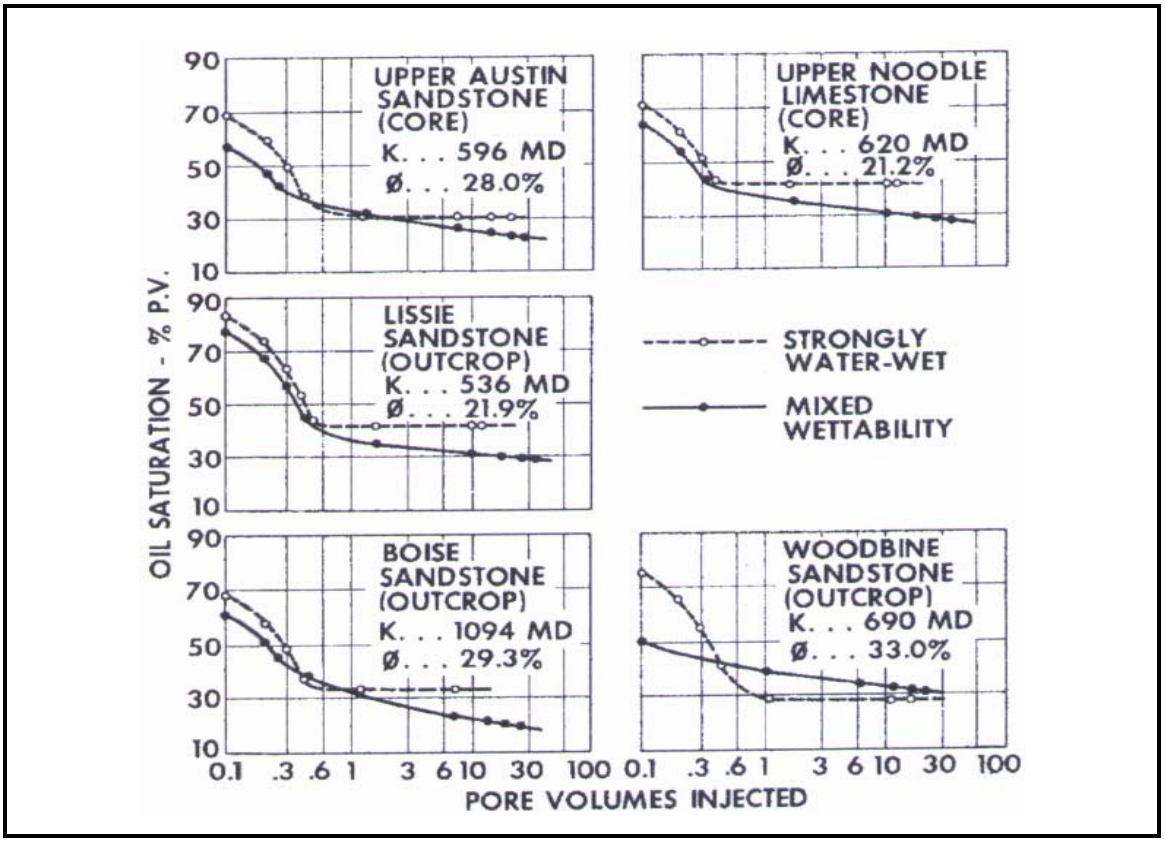

Figure 2.12[38]: Comparison of Waterfloods under Different Wetting Conditions in Several Porous Rocks.

Morrow et al.[25] altered the wettability of a strongly water-wet core to some heterogeneous -wet state through aging in brine and Moutray crude oil and observing oil recoveries for both wetting states. Analogous displacements were also run in glass micromodels to make direct observations of the effect of wetting state and wetting alteration on displacement efficiency and the recovery mechanism. They observed that even though breakthrough characteristics were the same for all cases (as oil recovery was complete within 1.5 PVs of injected water), a much lower S_{orw} was observed in the aged cores compared to the strongly water-wet core. They further reported that even though variation in oil viscosity affected the S_{orw} for the strongly water-wet condition (lower oil viscosity resulted in lower S_{orw}), the microscopic displacement efficiency was relatively constant, because it was observed that reducing the oil viscosity resulted in a corresponding reduction in the initial oil saturation. The microscopic displacement efficiency is defined as the ratio of the change in oil saturation ΔS_o to the value of the initial oil saturation S_{oi}, that is, $\left[\left(S_{oi} - S_{orw}\right)/S_{oi}\right]$. It is worthy of mention that the authors' opinion of the actual nature of

the altered wetting state was largely speculative, so for the purpose of their work, they defined it as speckled-wetting.

Wang [61] studied the effect of changes in wettability from water-wet to mixed-wet states (and vice versa) on flowable versus bypassed crude oil saturations using Berea and Loudon cores. He observed that strongly water-wet core ceased to produce oil at first breakthrough, while a mixed wettability core continuously produced oil for many pore volumes resulting in very low residual-oil saturation (this observation is consistent with the characteristic behavior of mixed-wettability reservoirs as reported by Salathiel[38] and Wood et. al.[83]). He further reported higher flowable oil saturation in two-phase flow for the mixed-wet cores compared to the water-wet cores. This observed phenomenon is explained by the fact that in a mixed-wet core, the oil-wet surface forms a continuous film throughout the pores, while the smaller pores are occupied by water. Thus, the fraction of oil isolated by water films during the two-phase flow was smaller in a mixed-wet core than in a water-wet core. They also observed that the flowable water saturation is not a function of the core wettability. The bypassed water saturations were small in all cases irrespective of the wettability change from water-wet to mixed-wet and vice versa.

Huang et al. [84] also compared the waterflood oil recoveries between the mixed-wet and the water-wet systems with similar conclusions as described above[38,61,83]. Their research focused on sedimentary clastic rock reservoirs at the laminaset scale. They described the observed mixed-wetting characteristic of the reservoir as *Het-Wet State*, an acronym for a heterogeneous-wet system.

2.3.2.2 Fractionally-Wetted Systems

Behavior of systems that are fractionally-wetted is similar to that described for uniformly-wetted systems. Increase in residual oil saturation was observed as the fraction of oil-wetted surface increased[37,64,65,85]. Reported waterflood performance lies between the performance curves for 100% water-wet and 100% oil-wet sand packs[5].

2.4 Effect of Brine Salinity and Valency on Wettability and Oil Recovery

It has been shown that brine mediates adsorption from crude oil onto a mineral surface[86]. Further research[87,88] also revealed that brine properties such as pH, ionic species and salinity affect crude oil/brine/rock interaction and hence wettability. Consequently, the properties of the connate brine and injection water brine should affect the rock- characteristics as well as oil recovery efficiency.

Tang and Morrow[89] investigated the effect of brine composition on microscopic displacement efficiency of oil by waterflooding and spontaneous imbibition. Their investigation, conducted at reservoir temperature, utilized synthetic reservoir brine as the connate water. Berea sandstone plugs were used, and the brines used were prepared from chloride salts of different cation valency, that is, NaCl, $CaCl_2$, and $AlCl_3$. They reported that waterflood recovery increased and imbibition rate decreased with increase in cation valency for 1% solutions of NaCl, $CaCl_2$, and $AlCl_3$. They further reported that, with the exception of $AlCl_3$, oil recovery generally increased (8% to 13% of the OOIP) with decrease in salinity. This anomalous observation with the trivalent salt was ascribed to the effect of pH. Furthermore, decrease in salinity of the injected brine resulted in wettability transition toward water-wetness. They also observed incremental oil recovered when the injection brine was switched at high water cut from high-salinity brine to dilute brine. However, injection of dilute brine at the outset results in both increased breakthrough and final oil recovered.

Tang and Morrow[90] investigated the effect of temperature on oil recovery and wettability. They also evaluated the effect of changing the salinity of the invading and connate brine on oil recovery and compared the recovery with that obtained when the reservoir brine was used as the invading brine. Their study was based on displacement tests in Berea sandstones with three crude oils and three reservoir brines. They reported that oil recovery increased over that for the reservoir brine with dilution of both initial (connate) and invading brine or dilution of either. The mechanism of the recovery was not explained. For the three crude oils used, oil recovery and water wetness increased with increase in displacement temperatures.

Sharma[91] and Filoco and Sharma[92] examined the waterflood recovery for Berea sandstones from imbibition of brines of different salinities. They observed that decrease in imbibition brine salinity resulted in increased oil recovery only if the invading brine and the connate brine have

similar salinity. They reported that no increased oil recovery was observed with decrease in salinity when the connate brine salinity was kept constant. However, decrease in connate brine salinity results in increased recovery irrespective of the invading brine salinity. These observations are contrary to those reported by Tang and Morrow[90]. The reasons for this discrepancy are unclear yet. Sharma speculated that the increased oil recovery observed at low connate water salinity may be due to wettability change to a mixed-wet state.

Based on the observed impact of the benefits of low salinity in EOR, several field trials have been carried out[93,94]. Four sets of single well chemical tracer tests (SWCTT) performed in Alaska showed similar outcome as laboratory experiments[93]. The SWCTT results showed substantial reduction in waterflood residual oil saturation by low-salinity water injection. The reported low salinity EOR benefits ranged from 6% to 12% OOIP resulting in an increase in waterflood recovery of 8% to 19%. Similar conclusions were also reached in the Middle East[94] where a Log-inject-Log test was conducted to evaluate the low-salinity benefits. The result showed a reduction in waterflood residual oil saturation of 25% to 50%. The authors reported that these successful field trials have led to serious evaluation of full-scale implementation of low-salinity waterfloods.

In a related study, Webb et al. [95] carried out coreflood studies to evaluate the secondary and tertiary oil recovery potential of low-salinity brine injection under reservoir conditions. All the core samples used for the test were restored-state cores. The core samples were first cleaned and aged in live crude oil to restore wettability, prior to performing waterfloods. The initial water saturations of the cores were acquired in such a way that they matched the height above the oil-water contact of the samples in the reservoirs. The corefloods were performed both in secondary mode (low-salinity brine injected from initial water saturation) and tertiary mode (low-salinity brine injected after high-salinity waterflood). The tertiary mode was designed to simulate typical (field) application to a mature waterflood. They evaluated the waterflood recovery benefits by (1) observing the produced oil volume as a function of produced water and (2) micro-visualization of the residual oil saturation at the end of the corefloods. They reported that for all the corefloods, they consistently observed improved production of oil with reduction in brine salinity. However, they reported no recovery benefit in injecting seawater even where the salinity of the seawater is less than the formation brine salinity. The reason for this observation was not

explained. **Figure 2.13**[95] shows the observed recovery profile when the low- and high-salinity brine corefloods were both started at the same initial condition (core at initial water saturation). From the plot, it is seen that no water was produced with the oil until the breakthrough of water occurred. Water breakthrough is seen to occur at less than 1 PV of injected brine. After the breakthrough of water, little or no production of oil is observed. **Figure 2.14**[95] is a pictographic representation of the reported micro-visualizations of residual oil saturation (ROS) after high-salinity and low-salinity waterfloods of identical pieces of a North Sea Reservoir rock, which had the same initial water saturation and the same throughput of water flooded through them. The figure shows that the low-salinity waterflood results in a much lower ROS compared to the much higher salinity waterflood (50,000 ppm against 1,000 ppm). In the figure, the blue color represents oil, while the orange color represents water.

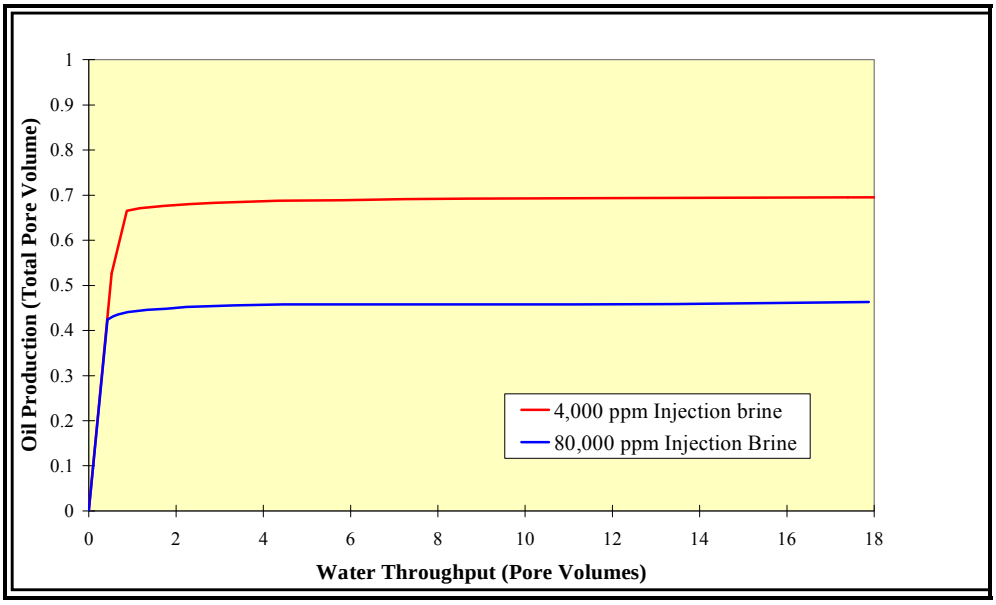

Figure 2.13[95]**: Comparison of Reservoir Condition Secondary Waterflood Characteristics (Low-Salinity vs. High-Salinity Brine Floods).**

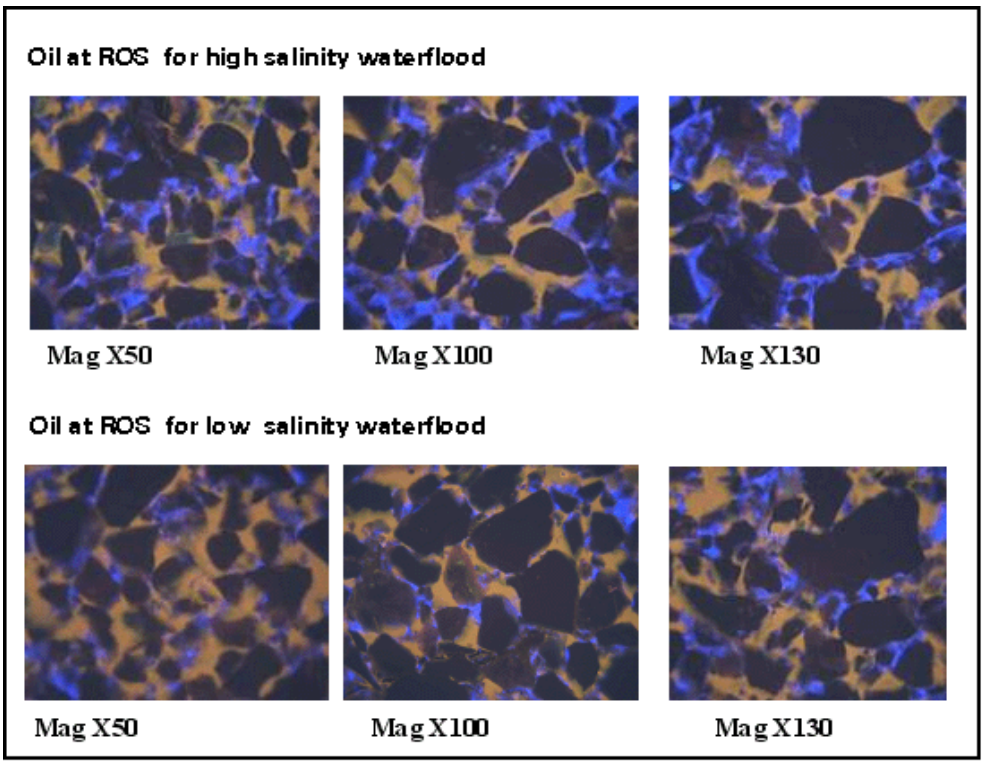

Figure 2.14[95]: Micro-Visualization of ROS Post High- and Low-Salinity Waterflood.

CHAPTER 3: Experimental Setup

As was stated earlier, the primary objective of this work is to evaluate, on the core scale the effect on oil recovery of changes in brine salinity, temperature and core wettability. Lab scale evaluation of these variables and their effect on oil recovery is possible only by conducting coreflood experiments. Consequently, a reservoir-condition coreflood rig was fabricated indigenously. Discussion of the main design philosophies involved in the choice of tubing sizes, lengths of flowlines, pressure ratings of the equipment, etc., is presented in this chapter. Also presented in this chapter are (1) some of the individual operating constraints in using some of the equipment that made up the coreflood rig; (2) some of the observed equipment parameter conflicts which arose because of interfacing various equipment from different manufacturers and how these conflicts were resolved; and (3) the principle of operation of all the equipment used in fabricating the coreflood rig. The design of the (reservoir condition) coreflood rig is such that it is easily adapted for fast-track coreflooding using dead oil at ambient pressure and ambient temperature or above.

3.1 Overview of Equipment Setup

Figure 3.1 is a schematic of the coreflood rig set up for the fast track and live corefloods, which also shows the principal equipment of the set-up. Fluid displacement within the system is achieved by operating the ISCO pump at constant rate and constant-pressure conditions. Separation between the pump fluid (de-ionized water) and the coreflood fluids (brine and oil) is achieved by using floating piston accumulators. Inlet and outlet valves (2-way ball valves) leading respectively into and away from the accumulators help isolate the brine and oil accumulators during the operation of the coreflood rig. When injecting the brine, the oil accumulator valves are closed and when injecting oil, the brine accumulator valves are closed. A 3-way check valve after the accumulator valves provides means for fluid bypass when required. This bypass is planned for periodic recalibration of the PFS and bleedoff of line pressure where needed.

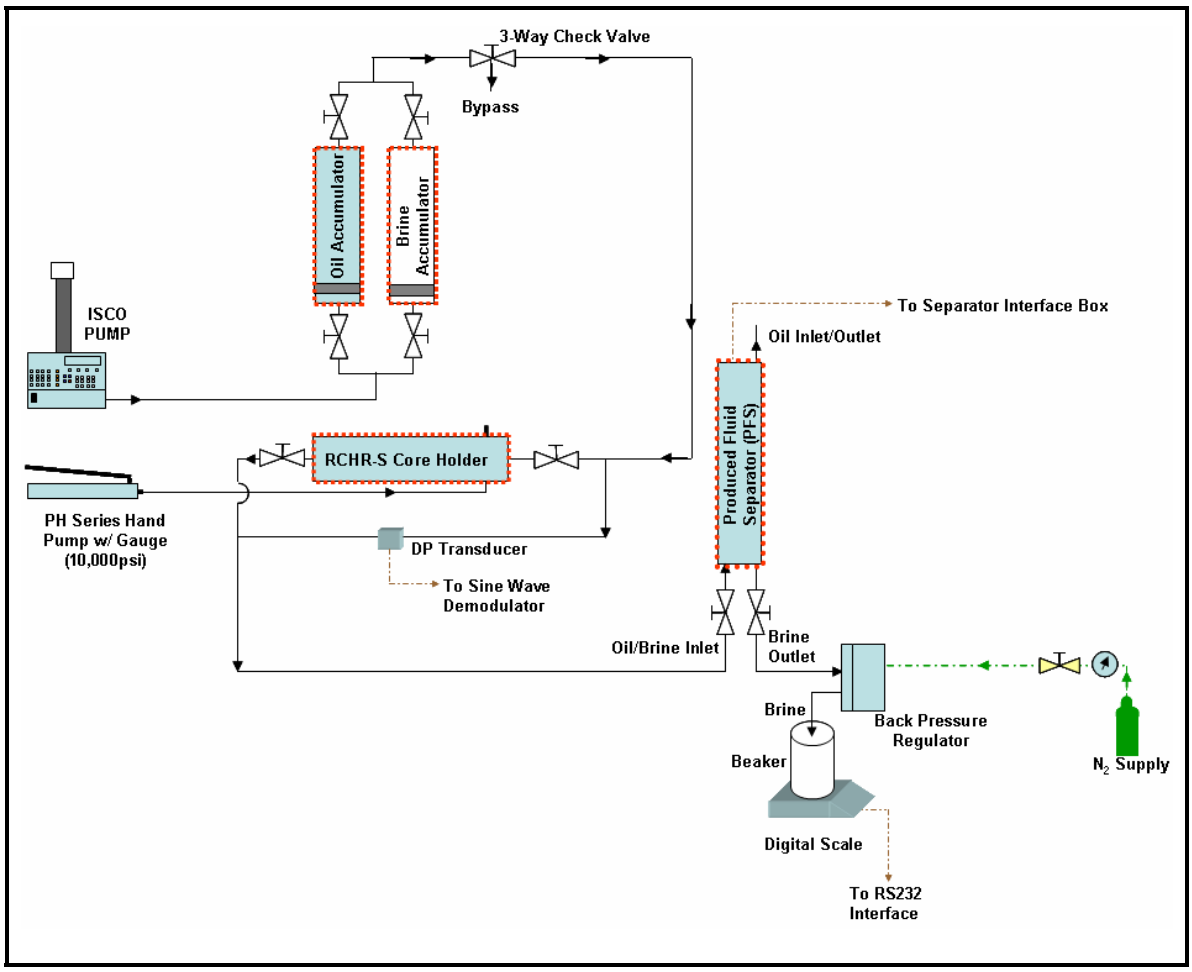

Figure 3.1: Schematic Representation of the Coreflooding Setup.

Fluid leaving the accumulators flows to the injection face of the core plugs in the core holder. The core holder has inlet and outlet isolation valves for pressure isolation within the lines when it is necessary to change the core plugs. Radial pressure in the core holder is maintained through the use of a hand pump rated at a maximum working pressure (MAWP) of 10,000 psi. The radial pressure simulates the reservoir overburden pressure. A differential pressure transducer is connected to the inlet and outlet ends of the core holder to measure the pressure drop across the core during waterflooding or during fluids injection.

Produced fluid leaving the core holder flows into the Produced Fluid Separator (PFS) where the produced oil is separated from the brine and the volume of recovered oil is measured and recorded. For reservoir condition corefloods, backpressure equal to the reservoir pressure is

maintained within the system through a backpressure regulator connected to the outlet line of the PFS. Backpressure is maintained by compressed nitrogen. Use of the backpressure regulator also ensures that the solution gas remains in solution. Reservoir temperature is achieved by the use of thermal blankets capable of supplying heat within an inclusive temperature range of 75°F and 425°F.

3.2 Fluid Circulation and Pressure Maintenance Pump

The Teledyne ISCO D-Series pump (model 100DM) was utilized for the circulation of fluid through the experimental system and for constant pressure maintenance through the entire system. The 100DM model is a positive displacement pump that is capable of pressures up to a maximum of 10,000 psi and flow rates range from 0.01µl/min up to 20ml/min. The pump is capable of displacing fluid volumes up to 500 ml. De-ionized (DI) water is used as the displacing fluid within the pump, thus preventing buildup of scale on the cylinder walls as well as the development of rust.

The pump has four basic modes of operation: constant pressure, constant flow, refill, and programmed gradient modes. These modes may be classified broadly into two groups: (1) three delivery modes and (2) one refill mode. The constant-pressure mode maintains fluid delivery at a constant pressure by varying the flow rate. Consequently, the desired pressure is achieved by either positive or negative displacement of the piston. For the constant flow mode, the converse to the constant-pressure mode holds. In this case, the pump delivers the displacing fluid at a constant flow rate during the pumping operation while the delivery pressure is varied, thus ensuring that a constant delivery rate is maintained. The refill mode allows for the (automatic) refilling of the pump cylinder with the displacing fluid. This is achieved in either of two ways: (1) manually setting the refill rate at any point desired during the pumping operation or (2) setting the pump to refill automatically when a certain volume has been reached. For this work, it was expedient to use option (1) because of the nature of the experiment. In the programmed gradient mode, the pump is capable of providing three types of gradients: (1) two-pump concentration gradients, (2) single-pump linear pressure gradients, and (3) single-pump flow programs. Only the three delivery modes were used in carrying out the experiment.

ISCO pump 100DM also has the added functionality of remote manipulation of the pump through the RS232 interface. A single RS232 interface can control up to four pumps. Apart from remote control of the pump from a computer interface, the pump can also be queried for data through the RS232 interface. This functionality can only be used either by writing specialized programs using the Labview Programming Language Toolkit or the already packaged Teledyne DASNET Application. This establishes a two-way information exchange, between the computer and the pump, for data collection.

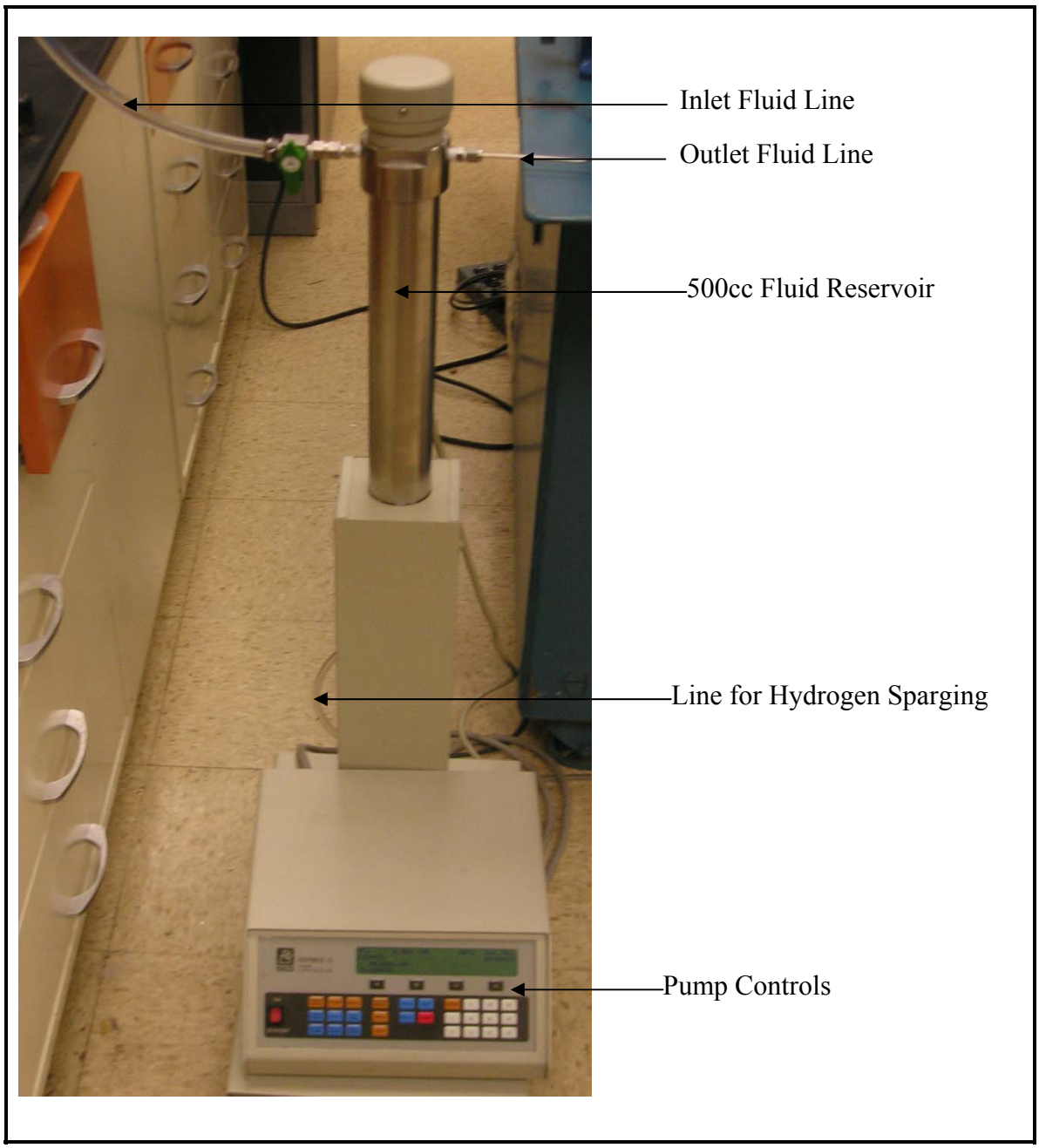

Figure 3.2: Photographic Representation of the Teledyne ISCO D-Series Pump (Model 100DM).

3.3 Floating Piston Fluid Accumulator

An accumulator is a transfer vessel used for displacing fluids through corefloods and similar displacement tests. Accumulators serve a number of purposes, which include: (1) Isolating corrosive fluids from pumping systems; (2) Dampening pulsations from pumps (3) Recombining

fluids and gases; and (4) Displacement of fluids or gases. Depending on the specific function/application desired, the design and type of accumulator utilized will differ.

For this work, two (Model CFR-100-50) floating piston accumulators, manufactured by TEMCO, were utilized. The restrictions imposed by using the model CFR-100-50 accumulators are (1) they are rated at an operating pressure of 10,000 psi each; (2) each of the accumulators have a capacity of 500ml each; and (3) they can only be subjected to temperatures up to 350^{o}F (176.67^{o}C).

The model CFR-100-50 accumulators have the following features:

(1) **end caps**: These are made of bronze, which helps prevent galling while screwing on the end caps to the accumulators, by acting as lubricants. One limitation of the bronze end caps is that they do not provide a metal-to-metal seal and are thus not capable of preventing fluid loss under high pressure. This limitation is compensated for by the presence of viton seals on the end plugs.

(2) **stainless steel cylindrical cell**: This is essentially a hollow cylindrical piece of metal with external threads at both ends onto which the end caps are screwed. When the piston is installed, the cylindrical cell serves as a liquid/fluid container. Both ends of the cylinder have internal shoulders which serve as “seats” for the end plugs when the end caps are fully screwed in.

(3) **end plugs**: There are two end plugs that fit though the holes in the end caps and are held in place by the snap rings. One end of the plug extends beyond the surface of the end cap and is threaded internally with 1/8 in. snap-tite thread taps. The other end fits into the cylindrical cell and “bottoms-out” on the internal shoulder of the cell. The end that fits into the cell is grooved to allow the installation of one viton seal in each of the plugs. These seals ensure that the fluid in the vessel does not bleed out through the thread connection between the end caps and the cylindrical cell when the system is subjected to high pressures;

(4) **snap rings**: There are two snap rings installed in the grooves located at the top of each of the end plugs. These have two basic functions: to hold the end plug in place in the end cap, and to aid in the removal of the end plugs;

(5) **Teflon piston**: The piston separates the displacing fluid from the displacement fluid. The piston is also grooved which allows the installation of viton seals which aid in pressure isolation. The viton seals maintain the separation integrity even under high pressure up to 10,000psi for the CFR-100-50 model. The piston also displaces the cell fluid from the cell to the coreflood rig. The piston is made of Teflon material allowing easier movement of the piston inside the cylinder.

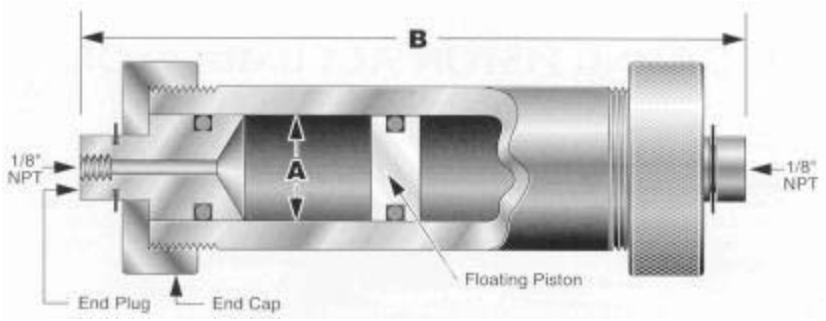

Figure 3.3[96]: Cross-Sectional View of the Fluid Accumulator.

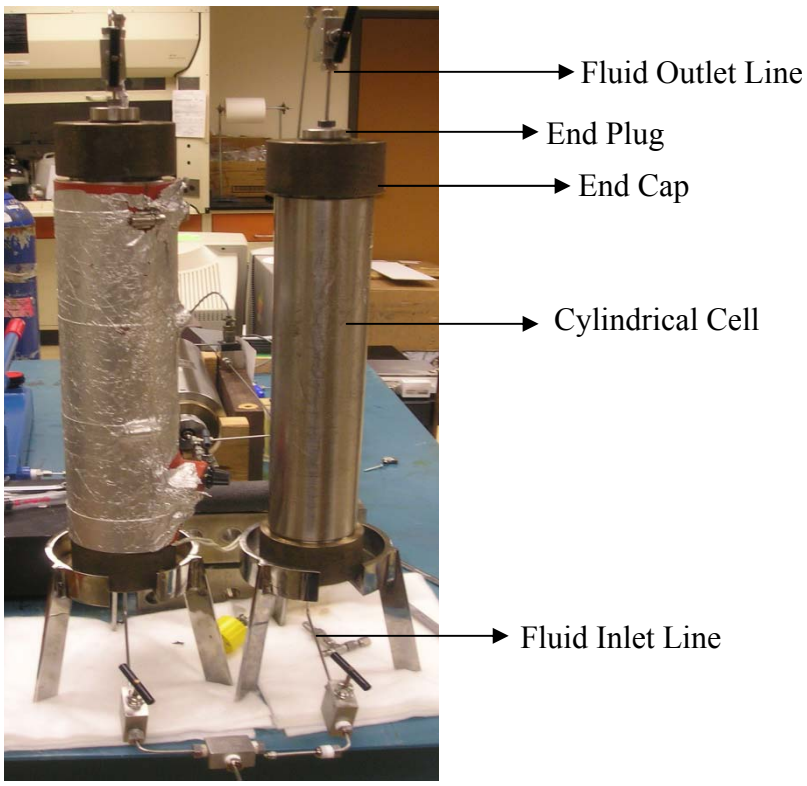

Figure 3.4: Photographic Representation of the Temco Model CFR-100-50 Fluid Accumulators.

3.4 Core Holder

The core holder houses the core plug and is used for a number of coreflood studies depending on the design and type. It consists essentially of a hollow cylindrical cell with inlet and outlet ports (for the overburden pressure fluids) drilled in the housing. Both ports are located respectively at opposite ends of the cylindrical housing and are vertically opposite. While injecting the fluid for maintaining the overburden pressure, the cylindrical cell is positioned such that the (fluid-entry) inlet port is positioned vertically downwards, while the outlet port is positioned vertically upwards and is left open to vent air. The outlet port is plugged after filling, and the pressure of the hand pump is increased until the desired value of the overburden pressure is reached. The outlet port may be opened slightly after the target overburden pressure is reached to release any trapped air bubbles, after which it is closed and the pump pressure increased again to the target overburden pressure. Typically, hydraulic oil is the preferred fluid for maintaining the

overburden pressure because of its anti-corrosive properties. The cylindrical cell houses a rubber sleeve which serves the triple purpose of (1) holding the core plug in place, (2) transmitting the overburden pressure to the core plug, and (3) separating the annulus fluid from the displacement fluid (oil and/or brine). Each end of the cylindrical cell housing is threaded internally, and the ferrule assembly is made up to the internal threads. The ferrule assembly comprises the end cap and a ferrule. The ferrule, held onto the end cap by a set of (three) Allen screws, has a seal and seal spacer which keep the overburden fluid isolated during the experiment when the overburden pressure is applied. The final piece of the core holder is the distribution plug/retainer pair, which ensures that the injected fluid from the lines is distributed uniformly on the injection and exit faces of the core plug. Uniform distribution of the fluid on the face of the core plug is achieved by means of the engraved network of circular and radial grooves on the face of the distribution plug. The distribution plugs are held in place by the retainer, which also ensures that the faces of the distribution plugs rest firmly on the ends of the core plug thus minimizing the occurrence of the capillary end effects.

The core holder used for this experiment is the TEMCO RCHR-series Hassler-type core holder (**Figure 3.5**). Hassler core holders allow the application of overburden pressure only in the radial direction. The core sample is held within the sleeve, and the radial confining pressure simulates the overburden pressure. Two sizes of core plugs may be used with the TEMCO RCHR-series core holder: 1 in. diameter and 1½ in. diameter cores. The maximum useable core length is 6 in. The equipment is rated at a maximum working pressure of 7,500 psi and temperature of 350°F. Changing of the core plug is done by releasing the confining pressure, unscrewing the retainer, removing the distribution plug, and taking out the core plug.

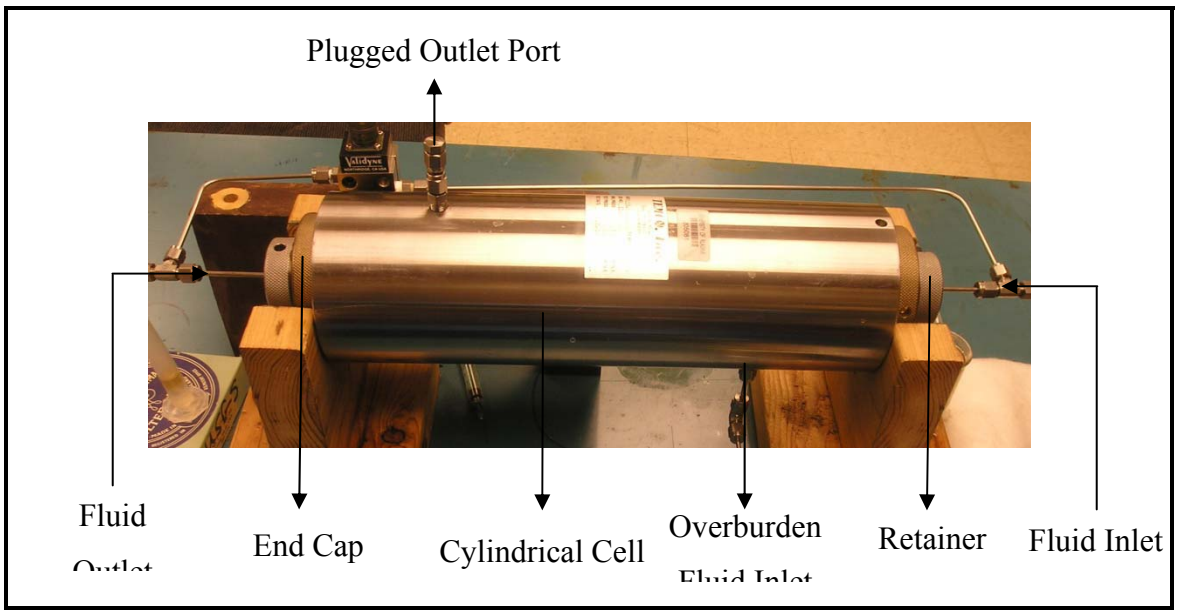

Figure 3.5: Photographic Representation of the Temco RCHR-Series Core Holder.

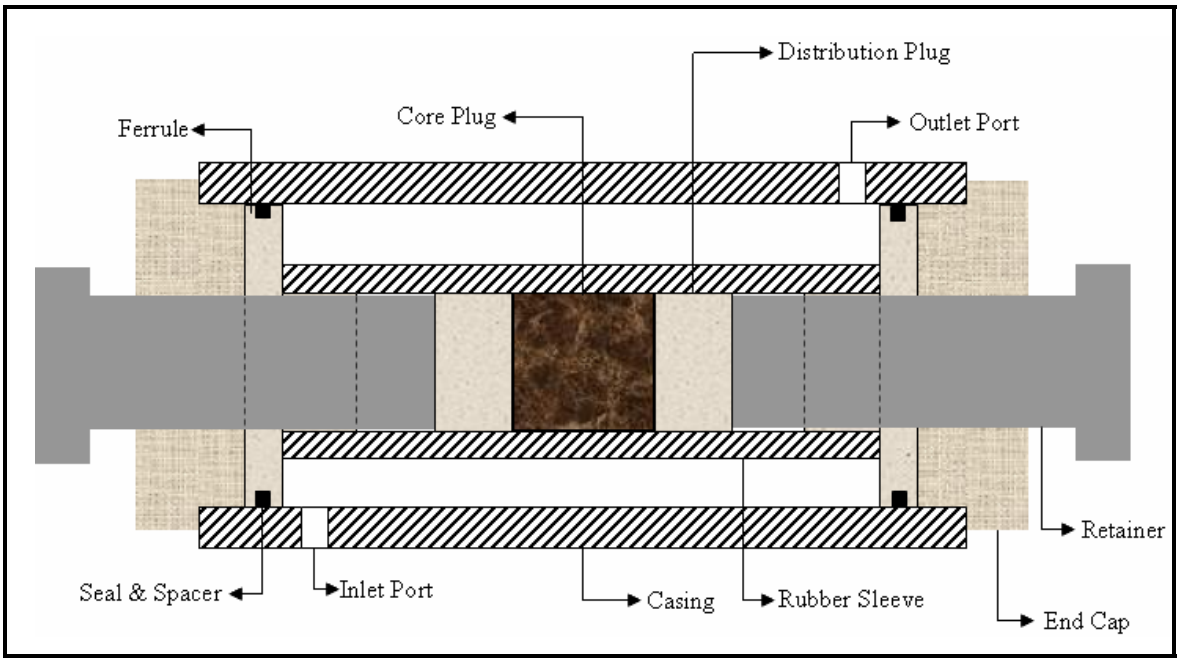

Figure 3.6: Schematic Representation of the RCHR-Series Hassler-Type Core Holder.

3.5 Overburden Pressure Pump

The radial load necessary for simulating the reservoir overburden pressure was applied using the PH-Series (Model PH1) hand pump. The pump is rated to a maximum working pressure of 10,000 psi and has a capacity of 70 $in.^3$ (1147 cm^3) The hand pump is operated by filling the fluid reservoir/chamber with required overburden fluid (typically hydraulic oil) and engaging the non-return valve (NRV), by clockwise rotation of the valve screw, to ensure unidirectional flow of fluid from the pump to core holder annulus. This allows the buildup of the required overburden pressure within the core holder as desired. Actual fluid delivery into the annulus of the core holder is achieved through the up-and-down stroking movement of the 18 in. lever arm. The lever arm, which is attached to a ½ in. diameter piston, creates suction with its upward stroke sucking the fluid into a containment chamber behind the NRV. The downward stroke of the piston forcefully opens the NRV, and fluid is delivered to the system. Each stroke of the piston delivers a fluid volume equal to 0.29 in^3 (4.75 cm^3). The overburden fluid is delivered to the core holder through the pump 3/8 in. diameter outlet port. A 3/8 in. x 1/8 in. reducing union was utilized to allow connection between the outlet port of the hand pump to the 1/8 in. diameter overburden fluid inlet port of the core holder.

The pump outlet is connected to the core holder inlet port. The outlet port of the core holder is placed vertically upwards allowing the escape of air during the filling process. When the annulus of the core holder is completely filled, the outlet port is sealed, allowing a buildup of pressure within the system to the predetermined value. Pressure bleedoff/reduction from the core holder annulus is achieved by releasing the manually operated pressure release valve. This action disengages the NRV and allows fluid flow back into the pump fluid reservoir.

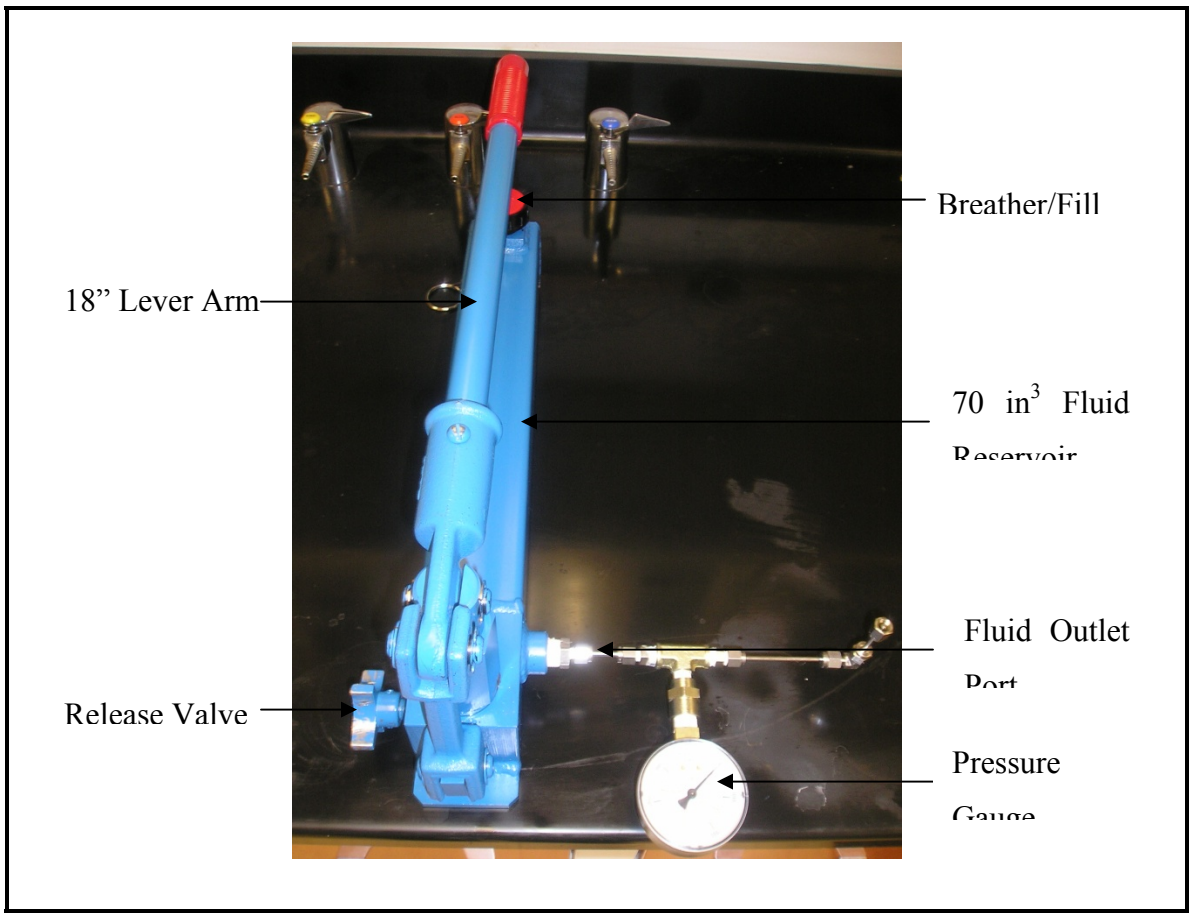

Figure 3.7: Photographic Representation of the PH-Series (Model PH1) Hand Pump.

3.6 Differential Pressure Transducer

Pressure drop across the core plugs was measured using the Model DP-360 differential pressure transducer manufactured by Validyne Engineering. The DP-360 model is designed to measure small differential pressures at extremely high static line pressures or extremely high gage or differential pressure. Because of the anticipated high pressure drop in the lines when the experiment is carried out under live condition, care was taken to select a transducer that can measure differential pressures up to 1250 psid. The downside to selecting a transducer that is sensitive to high differential pressure is that sensitivity is compromised when the pressure drop is low. However, this disadvantage is mitigated by the available option of changing the diaphragm inside the transducer to one that is more sensitive at lower pressures. The observed pressure drop for this work was lower than anticipated. Consequently, another pressure transducer, the DP-15 pressure transducer, was used in addition to the DP-360 transducer. The diaphragm used with the

DP-15 transducer had a maximum pressure differential rating of 125 psi, and this ensured higher sensitivity at very low pressure drops.

The differential pressure transducer consists essentially of the transducer body, the (pressure) diaphragm, “electrical” connection at the top, a set of bleed screws, and the positive and negative ports (**Figure 3.8**). The body of the transducer, made from stainless steel material, consists of two halves held together by a set of four Allen screws. The diaphragm is held firmly between both halves of the transducer body. The desired transducer sensitivity for the measured differential pressure is achieved by exchanging the diaphragm for another with the correct “dash” number depending on the expected maximum differential pressure. In changing the diaphragm, care must be taken to ensure that the right torque is applied to all four Allen screws, or measurement using the transducer will be inaccurate. There is a direct proportional relationship between the thickness of the diaphragm and the expected maximum differential pressure. Depending on the application, the diaphragm may be stainless steel, nickel-plated, or gold-plated. The diaphragms are designed with a safety factor of 1.25 above the maximum expected differential pressure load. This ensures that the diaphragm does not deform permanently, should a differential pressure slightly above the stated maximum be applied erroneously. However, care should be taken not to exceed the maximum allowable working pressure differential value to avoid permanent deformation of the transducer.

Each half of the transducer body is internally threaded for 1/8 in. NPT fittings, which allows connection with the coreflood rig flowlines through a 1.8 in. tubing x 1/8 in. NPT fitting. One fitting is made up to the positive port on the first half and the other fitting to the negative port on the second half. The upstream pressure line is connected to the positive port while the downstream pressure line is connected to the negative port of the transducer. Connecting the ports to the right pressure lines is essential to the transducer performing as expected. Fluids entering these ports are channeled to the corresponding inlet/outlet “face” of the diaphragm. Both faces of the diaphragm are grooved to accommodate two o-rings. Again, depending on the nature of application and choice of the user, the o-rings may be made of any of the following: (1) BUNA-N, (2) Ethylene Propylene, (3) Viton A, (4) Silicone, or (5) Teflon. The o-rings serve two primary functions; (1) isolate and confine fluids (upstream and downstream) to their respective sides of the diaphragm and (2) prevent fluid leakage from the diaphragm.

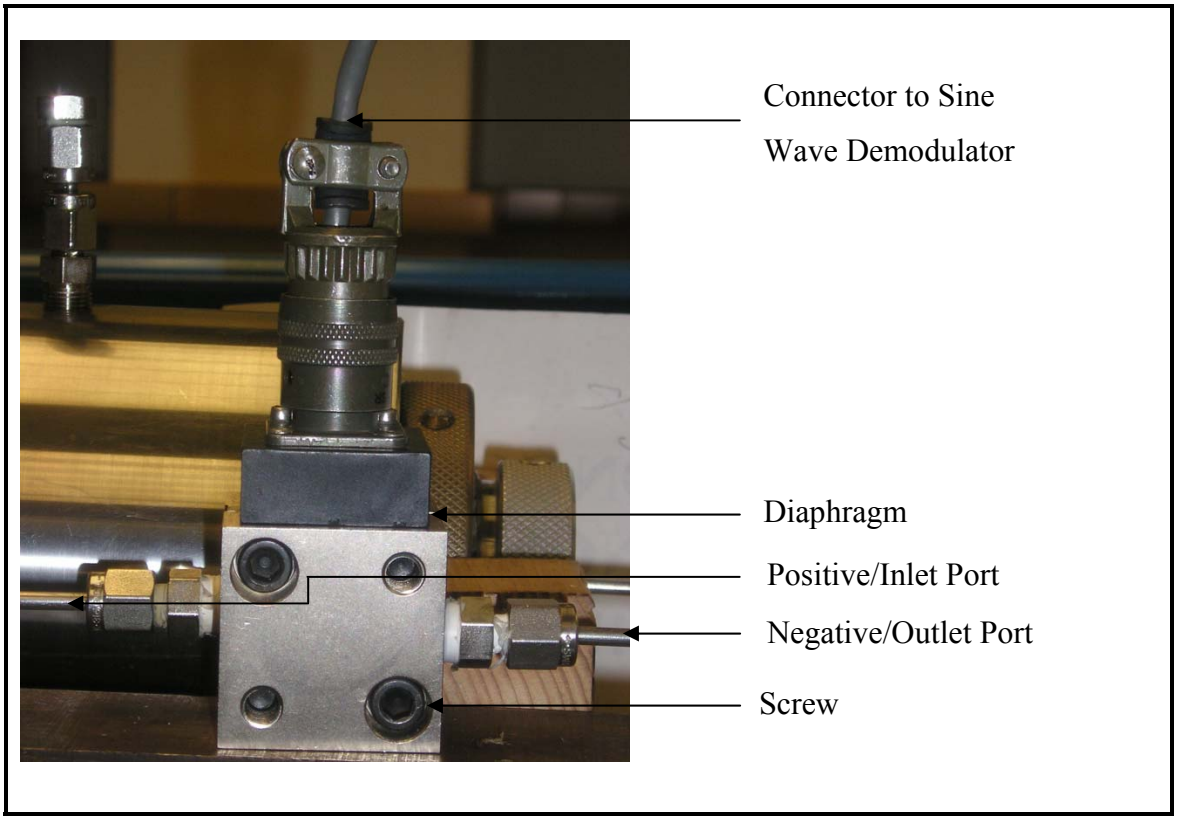

Figure 3.8: Photographic Representation of the Model DP-360 Differential Pressure Transducer.

The diaphragm undergoes some form of "elastic deformation" proportional to the value of the net pressure (upstream pressure less downstream pressure) acting on the diaphragm. This proportional deformation of the diaphragm triggers a corresponding voltage change, which is transmitted through the electrical connection at the top. The electrical connection consists of six pins labeled A–F, out of which pins A, B and D are the active/"live" pins. The output voltage can be preset to a maximum/minimum voltage corresponding to any of ±2 vdc, ±5 vdc, or ±10 vdc. The output voltage is transmitted through an electrical connection (WK-5-32S) to either a digital indicator or a demodulator. For this experimental setup, the output voltage was sent to a sine-wave carrier demodulator (**Figure 3.9**).

The sine wave demodulator has a zero and span dial, a power on/off switch and two voltage outlets. The zero dial is used to calibrate the zero pressure/voltage setting and the span dial sets the desired maximum output voltage/pressure. Both dials have major divisions that number from

1 to 10 and minor divisions that number from 1 to 99. Simultaneous adjustments of both dials during calibration ensure that the correct output voltage/pressure are achieved.

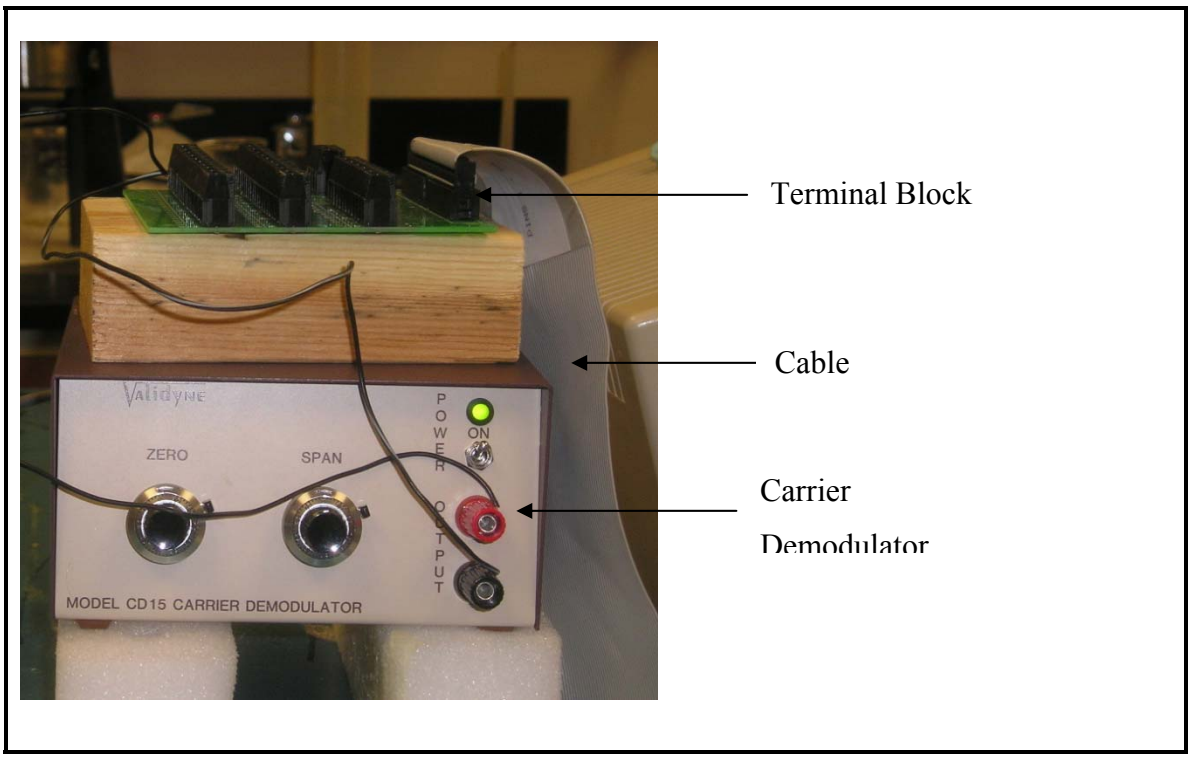

Figure 3.9: Photographic Representation of the Model CD-15 Carrier Demodulator.

The sine-wave carrier demodulator is interfaced to a computer via a terminal block and cable (**Figure 3.9**) to enable continuous data collection. To complete the interface, the MFC214 card which is installed in the computer is used as the voltage input A/D card. The MFC214 card accepts DC voltage inputs from any source, not just the Validyne transducer. Data on the output pressure differential can be collected in its "raw" voltage form or scaled to record actual pressure data via the SC5 strip chart (**Figure 3.10**). Before this can be done, the InstaCal software must be calibrated such that communication between the computer and the MFC214 A/D card is established.

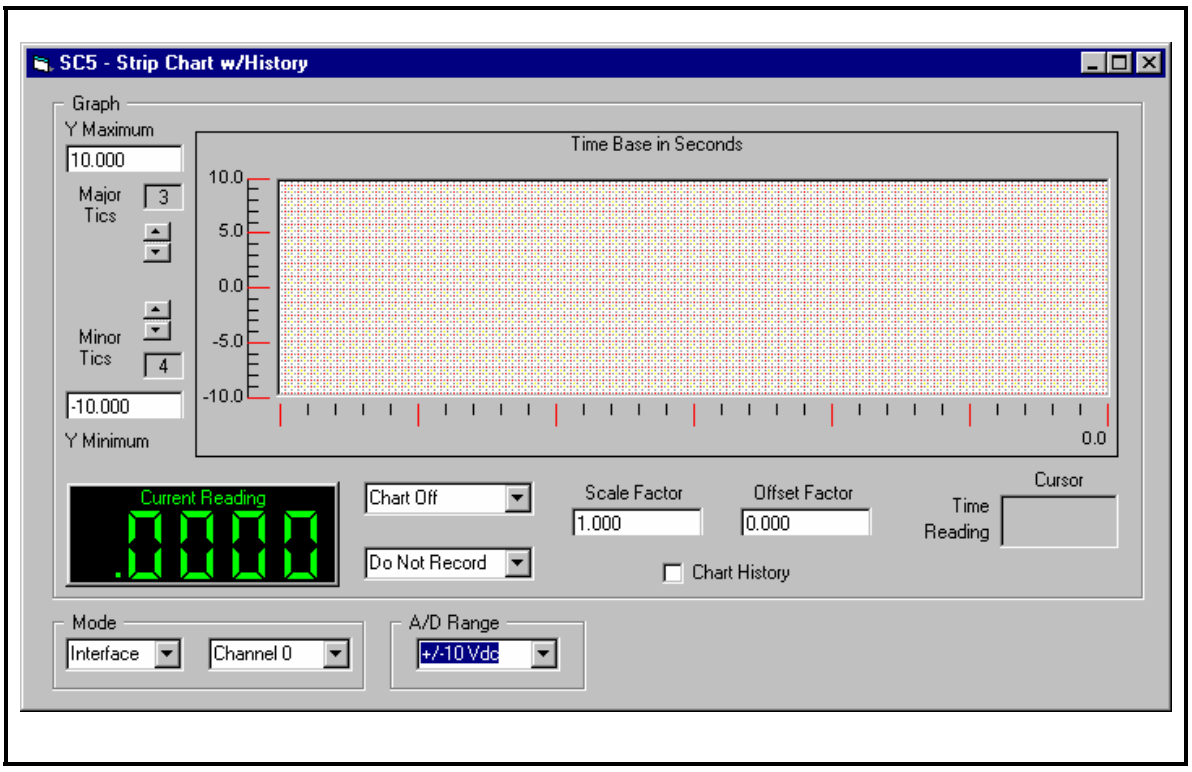

Figure 3.10: Photographic Representation of the SC5 Strip Chart with History.

The Y Maximum and Y Minimum options set the maximum and minimum scale for the y-axis. The Major and Minor Tics option determines the major and minor intervals on the y-axis. The "Do Not Record" drop down box has options for logging data to the SCData text file. Data logging is activated when both the "Do Not Record" and "Chart Off" options are simultaneously changed to "Record" and "Chart On" options. The "Scale Factor" option changes the recorded output value from output voltage to output pressure by appropriate scaling. The A/D Range is maximum voltage output from the pressure transducer. The SC5 strip chart logs data at a frequency of 10 Hertz. However, it was observed while logging data during the experiment that the CPU could not log data at this frequency. The lag was removed by normalizing the logged data with the actual logging time obtained by using a stopwatch. For example if the total data logging time determined by using the stop watch is 90 minutes and the actual time logged by the computer is 60 minutes, then there is a lag by a factor of 0.666667. The timing of all logged data is then multiplied by this lag factor.

3.7 Produced Fluid Separator

The produced fluid separator (PFS) was not used in this experiment because of some technical difficulties encountered during the calibration of the equipment that resulted in its being sent back to the manufacturer for further diagnostic work. The separator, manufactured by Coretest Systems Inc., is normally used to measure the accumulation of produced oil in a brine-displacing-oil test (waterflood). The PFS is basically a hollow cylindrical piece of steel that houses a PVC glass tube holder. Two glass tubes are installed in the glass tube holder: one primary separation tube and a measurement tube. The measurement glass tube is differentiated from the separation tube by the stainless steel coiled spring wrapped around the measurement tube. The spring is gold plated at the top. Gold is used because of its higher electrical conductivity compared to steel. The separator has one oil/gas inlet/outlet tubing at the top and two ports (one an outlet port and the other an inlet) at the bottom for the conductive fluid. The fluid inlet steel tubing is connected to the port leading to the measurement glass tube (and should extend inside the tube at least ¾ of an inch) while the fluid outlet tubing is connected to the port leading to the separation glass tube. To allow the fluid interface level to be equal in both of the tubes, both separation tubes are in contact at the top and bottom of the vessel in some form of u-tube formation (**Figure 3.11**).

The PFS works on the principle of capacitance change based on the change in the level of the oil-brine interface or the gas-brine interface. Data are collected from the PFS through a special interface board that monitors the change in capacitance. The interface board is connected to the computer, and data are logged using the supplied software. To ensure accuracy in measurement, the TDS in the conductive fluid (brine) should be $\geq$ 1,000 PPM. The change in capacitance changes primarily with the volume of the conductive fluid in the tube in a linear manner. The PFS is capable of measuring the capacitance change up to 500 pico-farads.

Calibration of the separator involves plugging the bottom ports and applying vacuum to the separator through the top port. While under vacuum, both glass tubes and their annuli are allowed to self-fill from the top of the separator with the appropriate oleic phase (in our case crude oil or decane). Alternatively, oil can be pumped from the bottom of the separator and air displaced from the top. The glass tubes have a total volume of 200 cc, but are also available in

other volume sizes. After filling under vacuum, the separator is pressured to the desired pressure, the slope is set to 1.0 in the configuration window (**Figure 3.12**), and the pump volume is set to zero. Note that at this point, the separator software will display the signal value, in counts, and not the actual volume. If the experiment is at ambient condition, the separator need not be pressured. Brine injection into the separator is started at a rate no faster than 5 cc/min. The volume and graphic displays are then monitored for any sudden changes in the volume reading. Typically, it may take from 5 to 30 cc of brine injected before the separator electronics first detect a volume change.

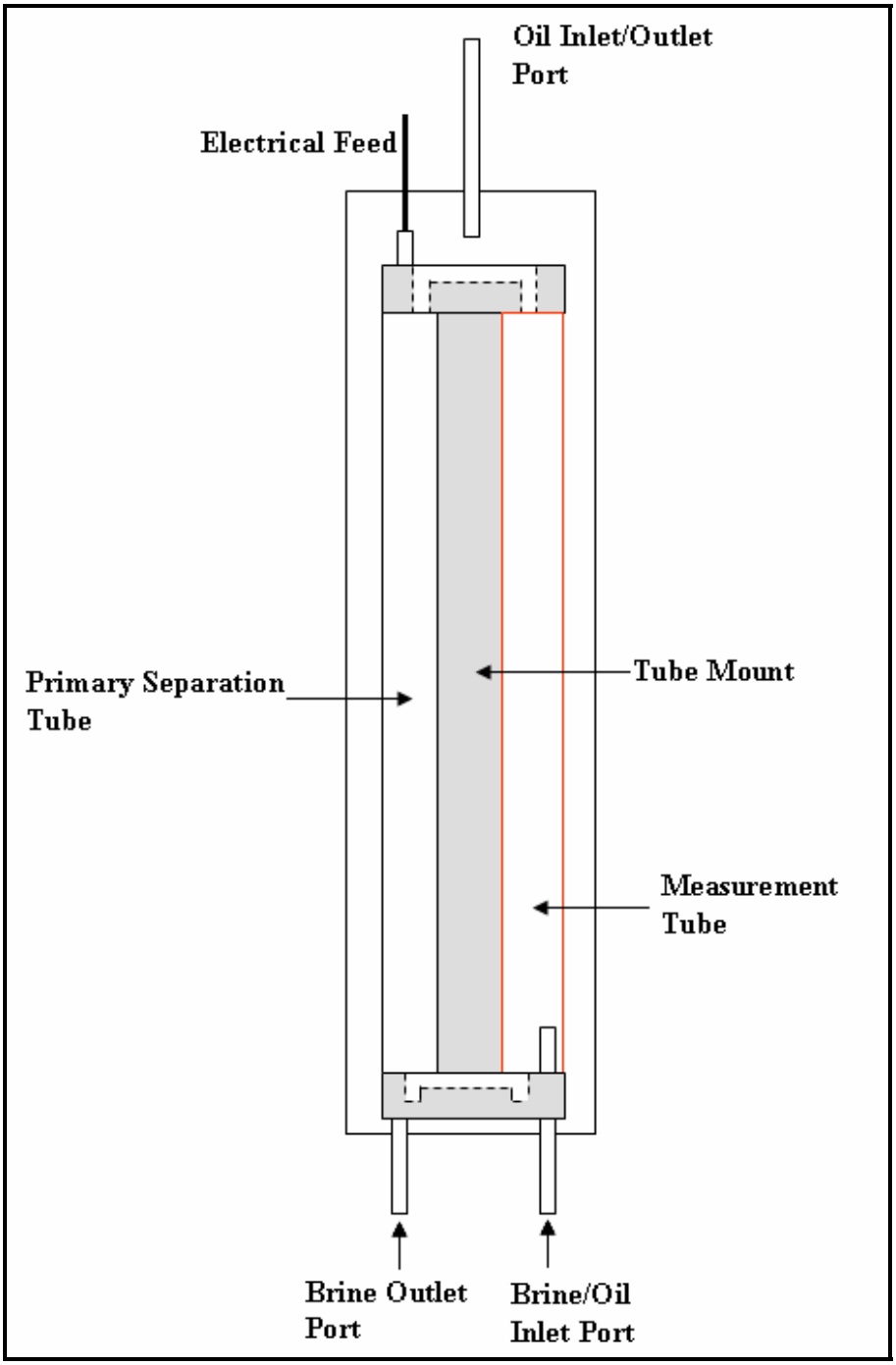

Figure 3.11: Schematic Representation of the Produced Fluid Separator.

When the change is detected, the brine injection rate is reduced to a rate ≤ 1 cc/min and data logging is then initiated. The injection rate should not be changed while data logging is on. After enough volume of brine has been injected, a plot of the logged data (V_{rel} in counts) and the

injected brine volume (in cm^3) is made in Microsoft Excel and the slope noted. The slope option in the configuration window (**Figure 3.12**) is then changed from 1.0 to the calculated slope. The accuracy of the calibration is validated by injecting more brine, followed by displacing some of the brine by oil such that the movement of the oil-brine interface in both the upwards and downwards direction is monitored and the volume of the injected and displaced brine logged. Ideally, the injected and displaced brine volume should correspond to the logged V_{rel} value. It is reported by the manufacturers that the accuracy of the calibration coefficient of counts to volume has a correlation factor of better than 99.9%. However, the accuracy of this correlation factor was discovered to be << 99.9%, and a reasonable match between the injected brine volume and the value of the logged volume based on the change in capacitance was not achieved.

During the troubleshooting process, it was suspected that the chemical composition of the refinery blend crude oil used in the calibration process might be interfering with the calibration process. Use of kerosene was suggested in lieu of the crude oil. However, other reported similar complaints by other PFS users resulted in the redesign of the separator interface box by the manufacturer, Coretest Systems Inc. Another problem encountered in using the separator is the breaking of the glass tubes while installing them in their housing. Subsequent diagnosis showed that some of the glass tubes were actually longer than the tube housing, resulting in glass breakage when the glass tube bottom plate is torqued in place. Currently, the PFS and its accessories have been sent back to CoreTest for complete diagnosis of the problems.

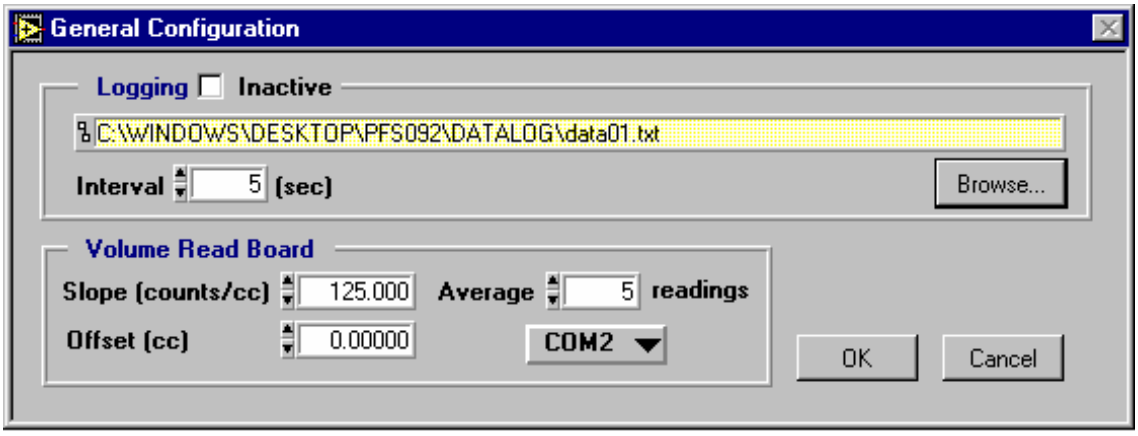

Figure 3.12: Photographic Representation of the PFS Configuration Window.

3.8 Backpressure Regulator

A backpressure regulator is used to maintain a certain desired level of constant pressure in the system. The regulator is manufactured by Temco Inc., and there are many different models available depending on the proposed application with respect to the experimental condition. The regulator is made of two composite parts held together by a set of high-strength cap screws. Between the two parts sits a diaphragm that is made from either Teflon elastomer or Buta-N rubber depending on the type of application. For this work, the BP-series backpressure regulator was utilized and has a maximum working pressure of 10,000 psi and temperature of 350°F. The diaphragm type within the transducer is Teflon elastomer.

The transducer works on the principle of balanced pressure. Gas is charged into the dome side of the transducer and pressure allowed to build up to a maximum of 500 psi after which flow is established downstream of the transducer to build up the downstream pressure to approximately 500 psi. The gas pressure is then increased by the same maximum pressure, and this pressure is equalized by establishing flow downstream of the separator. The stage-wise pressurization is very important to prevent damage to the diaphragm. The design of the diaphragm is such that the area exposed to the flowing pressure is smaller than the area exposed to the dome-side gas. Consequently, the flowing pressure will always be higher than the dome side pressure. It is pertinent to emphasize that only gas may be used to maintain the dome side pressure; use of liquids is not advisable. For this work, nitrogen gas was used to maintain the backpressure. For this experiment, the backpressure regulator is located downstream to the coreholder. This ensures that the design pressure is maintained within the system. The application of the pressure regulator for this experiment is to maintain/simulate the actual reservoir pressure with a view to keeping the gas in solution when live crude oil is used. In addition, it is used to keep the superheated steam in its liquid state during hot waterflooding, by maintaining a backpressure that is greater than the saturated liquid pressure of the superheated steam.

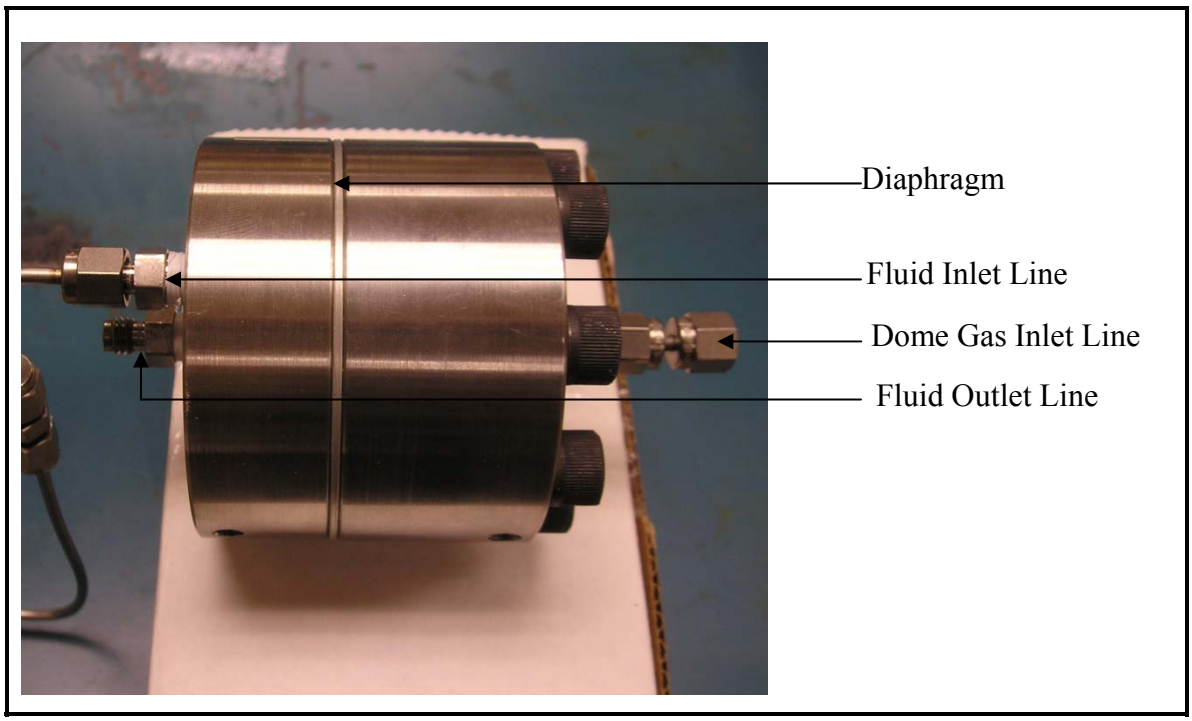

Figure 3.13: Photographic Representation of the Backpressure Regulator.

3.9 Digital Scale

The Sartorius digital scale was used in this work for gravimetric analyses. The scale is interfaced with the computer via the RS-232 port. Data logging is made possible by the use of the proprietary software SartoConnect. The use of the SartoConnect has one major drawback: The software takes complete control of the computer when it is running, such that multitasking on the computer is impossible; that is, while mass data are being logged, one cannot observe the data logging of other equipment that is interfaced with the computer. Consequently, the SartoConnect software was not used and the "AND" WinCT was utilized to log data from the Sartorius scale. Another observed constraint is the 0.1 g sensitivity of the scale. Where very sensitive measurements are required, such as when the DNR cores (1 in. dia. x 1.5 in. long) were used in the experiment, accuracy may be compromised by use of the scale. To overcome this constraint, the "AND" scale (model GF-4000) which is accurate up to 0.01 g was utilized.

3.10 Laminated Silicone Rubber Heater Blankets

Heating of the fluids, crude oil, and brine is achieved by the use of rectangular/square heater blankets. The heater blankets consist essentially of heating coils sandwiched between two outer rubber layers. There are several available options, such as adhesive vs. no-adhesive and fixed temperature vs. adjustable thermostat. For this work, the "*no-adhesive*" and adjustable thermostat options were chosen. The adjustable thermostat has a dial setting with numbers ranging from 1 to 10. The dial setting of "1" corresponds to the minimum temperature of 75°F and the dial setting of 10 corresponds to the maximum temperature of 425°F. **Table 3.1** shows the available dial settings and the corresponding temperature value. Though it is reported that the blankets have a thermostat tolerance of ± 5°F much larger fluctuations up to ± 10°F have been observed while running the experiment. To prevent heat loss to the atmosphere from the heater blankets, the blankets are covered with materials having low heat conductivity. The experimental design allows for the use of four heater blankets for the following equipment: (1) oil accumulator, (2) brine accumulator, (3) core holder, and (4) PFS. The heater blankets are held in place on the equipment by adjustable ring clamps. **Figure 3.14** is a photographic representation of one of the heater blankets wrapped around the brine accumulator for heating the brine.

Table 3.1: Heater Blanket Dial Settings and the Corresponding Temperature.

Dial Setting	Temperature	
	°F	°C
1.00	75.00	21.11
1.50	89.74	32.07
2.00	109.44	43.02
2.50	129.17	53.98
3.00	148.89	64.94
3.50	168.61	75.90
4.00	188.33	86.85
4.50	208.06	97.81
5.00	227.78	108.77
5.50	247.50	119.72
6.00	267.22	130.68
6.50	286.94	141.64
7.00	306.67	152.59
7.50	326.39	163.55
8.00	346.11	174.51
8.50	365.83	185.46
9.00	385.56	196.42
9.50	405.28	207.38
10.00	425.00	218.33

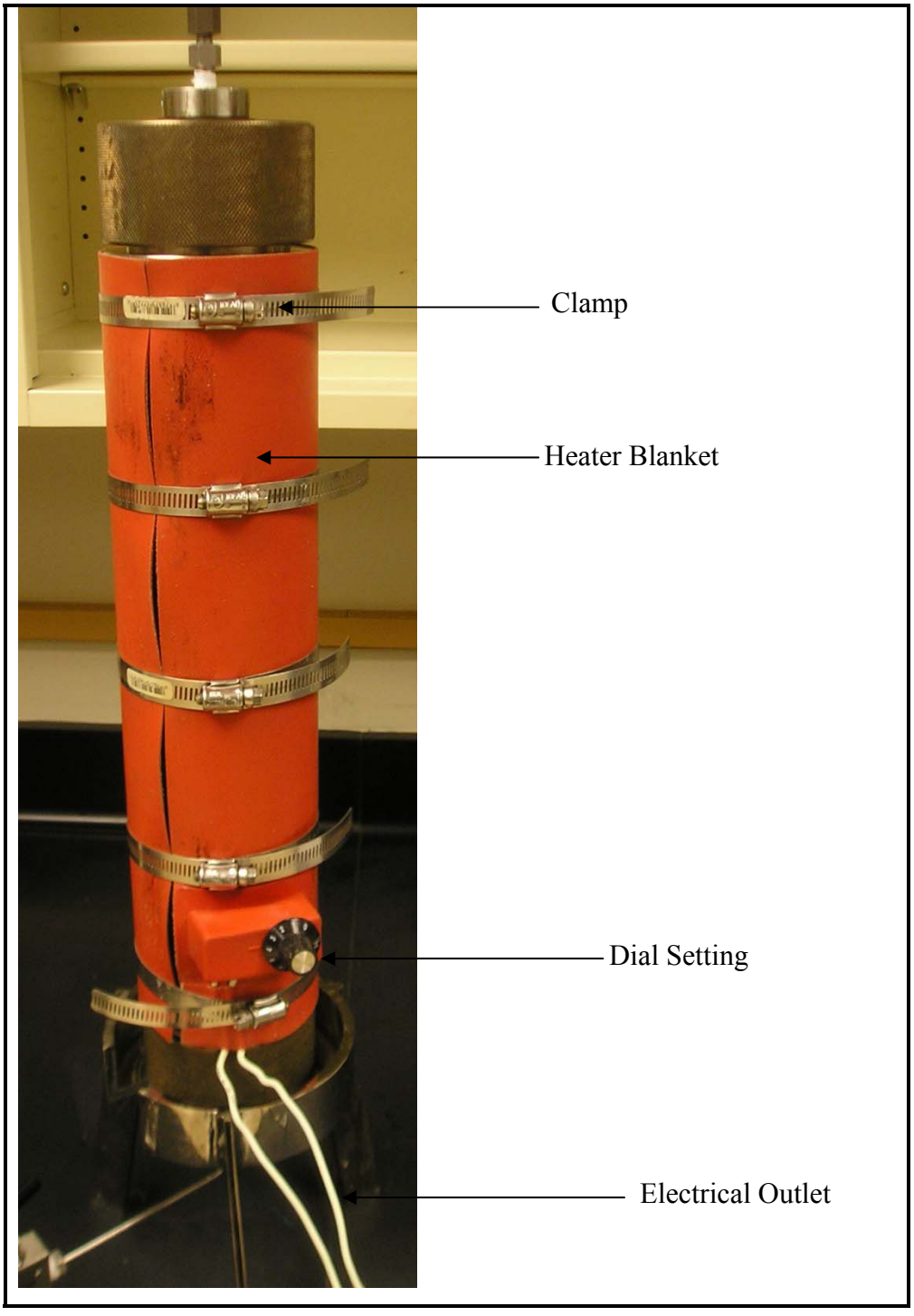

Figure 3.14: Photographic Representation of the Laminated Silicon Rubber Heater Blanket (Wrapped Around One of the Pieces of Equipment).

3.11 Gas Supply and Regulator

The gas supply to the backpressure regulator and for the calibration of the pressure transducer is by means of pressurized nitrogen cylinders (2,263 psi). Nitrogen is the preferred option because of its relatively inert nature. Before these pressurized gas cylinders are put to use, a pressure regulator is installed to ensure controlled pressure supply and buildup. The two types of available regulators are the single- and the double-stage pressure regulators. The single-stage pressure regulator reduces the cylinder gas pressure to the required delivery pressure in one step, while the double-stage pressure regulator does the same in two steps. The single-stage regulator is a preferred option if slight variations in delivery pressure are not detrimental to the application.

3.12 Fluid Lines and Fittings

The design of the experiment is such that all fluid lines are 1/8 in. tubing supplied by Swagelok Company. The design choice of 1/8 in. tubing is based on the need to minimize dead volume within the tubing during the coreflooding process. Using a larger tubing size will result in a higher value of dead volume within the tubing. All the tubing fittings (union connector, elbow connector, tee connector, etc.) were supplied by Swagelok. Both the tubing and the fittings are rated at a maximum working pressure of 10,000 psi. The only constraint to using the 1/8 in. tubing is that it crimps easily compared with tubing of larger diameters. Because of the expected high-pressure requirement when “live oil” is used, the “HiP” valves were utilized. These valves are two-way on/off valves capable of withstanding pressures up to 10,000 psi.

CHAPTER 4: Experimental Description and Procedure

4.1 Experimental Description – DNR and Berea Cores

The experiments, carried out as part of this research work, were designed to examine the effect of salinity change and hot water injection on improved oil recovery and to determine if wettability alteration is a possible mechanism for this recovery. Two sets of experiments were carried out. The first set of experiments explored (1) the EOR potential of decrease in brine salinity and (2) the effect of temperature on waterflood residual oil saturation. The second set of experiments, in addition to determining the effects of the second option above, evaluated the potential of low-salinity brine for secondary oil recovery and the associated wettability change, if any. Reduction in salinity was achieved by reduction in the quantity of total dissolved solids (TDS) in the brine. Berea sandstone core plugs were used in the first set of experiments. The core plugs for the second set of experiments were loaned from the archives of the Alaska Department of Natural Resources (DNR).

Flood rates for the first set of experiments were between 20–50 cc/hr inclusive, while the rate for the second set of experiments was constant at 20 cc/hr. Generated pore pressures were directly proportional to flow rates used. A 1,500 psi overburden was used for the first set of experiments. The overburden pressures used for the second set of experiments were between 1,000 psi and 1,800 psi. This pressure range was necessitated by high pressure drop (1,700 psi) across some of the core samples at the prevailing flow rate and the constraint imposed by the core holder operating condition (the applied radial pressure should be several hundred psi above the flowline pressure in order to avoid fluid leakage to the core holder annulus). It was observed that for some of the DNR core plugs, a flow rate of 20 cc/hr resulted in pressure drops as high as 1,700 psi.

Wettability variation was not examined in the first set of experiments. However, wettability characterization for the second set of experiments was done using the Amott-Harvey wettability index. The choice of the Amott-Harvey wettability determination method was based on its relative ease of application as compared with the other conventional wettability determination methods—the USBM and contact angle methods.

The first step in the experiment was the preparation of the samples. The brine was reconstituted and the core plugs prepared for use by preflushing (with toluene, followed by acetone and then water) and/or heating. The Berea sandstone cores were only heated, while the DNR cores were pre-flushed and heated. Preflushing of the DNR cores was necessary since the states of the cores were unknown. The preflushing and heating treatment was followed by the determination of the rock and fluid properties. The determined fluid properties were the viscosity and density of the brine and the oils, while the rock properties determined were the porosities and absolute permeabilities of the core plugs.

The core was then flooded to interstitial/initial water saturation and, for only the DNR cores, the initial wettability of the all the cores was determined using the Amott-Harvey test. The core sample was then waterflooded with brines of different salinity (at ambient and elevated temperatures) and the waterflood oil recovery noted. The wettability change, if any, was monitored at every stage of the experiment for the DNR cores when the brine salinity and/or brine temperature were changed.

4.1.1 Core Samples

Berea sandstones were used for the first set of experiments, while cores from DNR archives were used for the second set of experiments. Though the design of the experiment was for preserved samples from the ANS fields, absence of these samples necessitated the use of these alternative samples.

The DNR core plugs were from Milne Point, Kuparuk River Unit L-01. The cores, which were all ≈ 1 in. in diameter and 1.5 in. in length, were cut from core taken from depths between 7,170 ft and 9,016 ft. Petrophysical details and storage state of the DNR cores could not be obtained from DNR. However, the drilling schedule was obtained from the AOGCC website. The Kuparuk River L-01 well was drilled to a total depth of 9,500 ft, completed in April 1984, and plugged and abandoned in May 2003. Consequently, it is conceivable that the cores from Kuparuk River L-01 have been on the DNR shelf between 15 to 20 years. Porosity values determined in the lab for these cores ranged from 16% to 26%, while the permeability values were between 0.93 and 194 md. Porosity was determined using the saturation method as

described in Section 4.2.3 of this work. Core permeability was calculated from Darcy's law, based on the observed pressure drop across the brine-saturated core after steady state was achieved when injecting brine (4% salinity) through the core sample. It is suspected that the observed wide variation in permeability value and porosity values was due to (1) the visual observation of shale stringers in the core plugs (particularly with increasing depths) and (2) greater compaction of the sand grains with increasing depth.

All the Berea sandstone core plugs had 1.5 in. diameters and lengths of ≈ 3.5 in. The measured values of the absolute permeability were between 100 and 300 md, while the porosities were between 18% and 20%. **Table 4.1** and **Table 4.2** give the calculated dimensions and some petrophysical properties of the core plugs used in the experiment, while **Figure 4.1** and **Figure 4.2** are plots of the same data

Table 4.1: Berea Sandstone Core Properties

Core #	Porosity (fraction)	Absolute Permeability (md)
1	0.1857	289.84
2	0.1992	212.55
3	0.1905	119.33
4	0.1906	92.43
5	0.1851	110.88
6	0.2017	114.30

Table 4.2: Core Properties from Milne Point Kuparuk River Unit L-01

Core #	Porosity (fraction)	Absolute Permeability (md)	Cored Depth (ft)
1	0.1581	0.93	9200
2	0.2045	5.00	8600
3	0.2579	193.62	7100
4	0.2460	53.74	7101
5	0.2181	14.74	7104

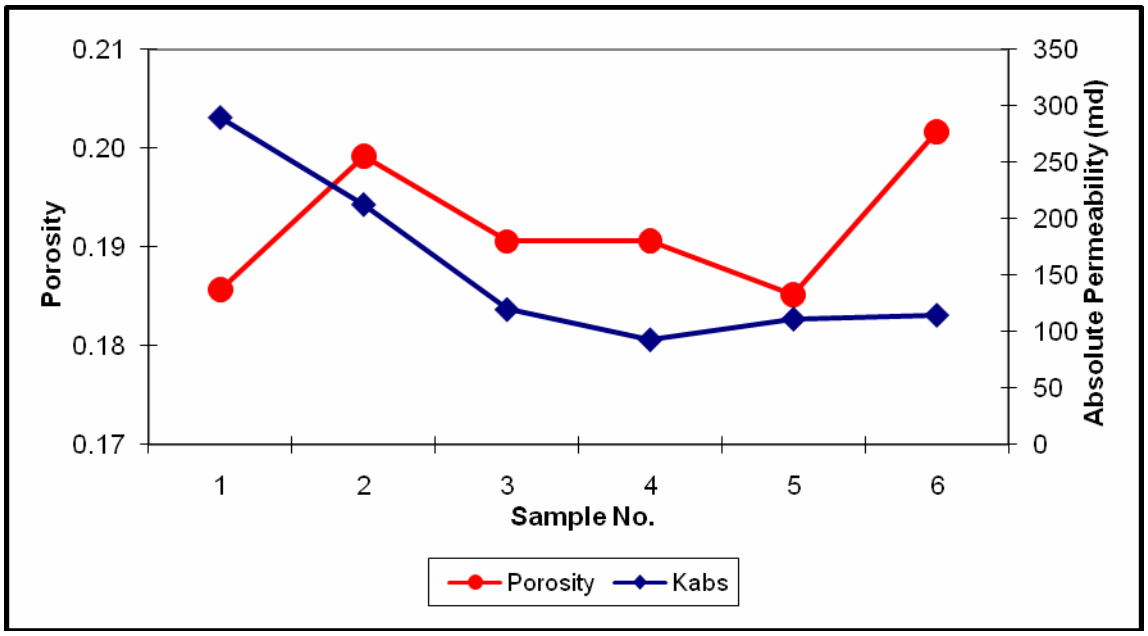

Figure 4.1: Absolute Permeability and Porosity Values of the Berea Core Plugs.

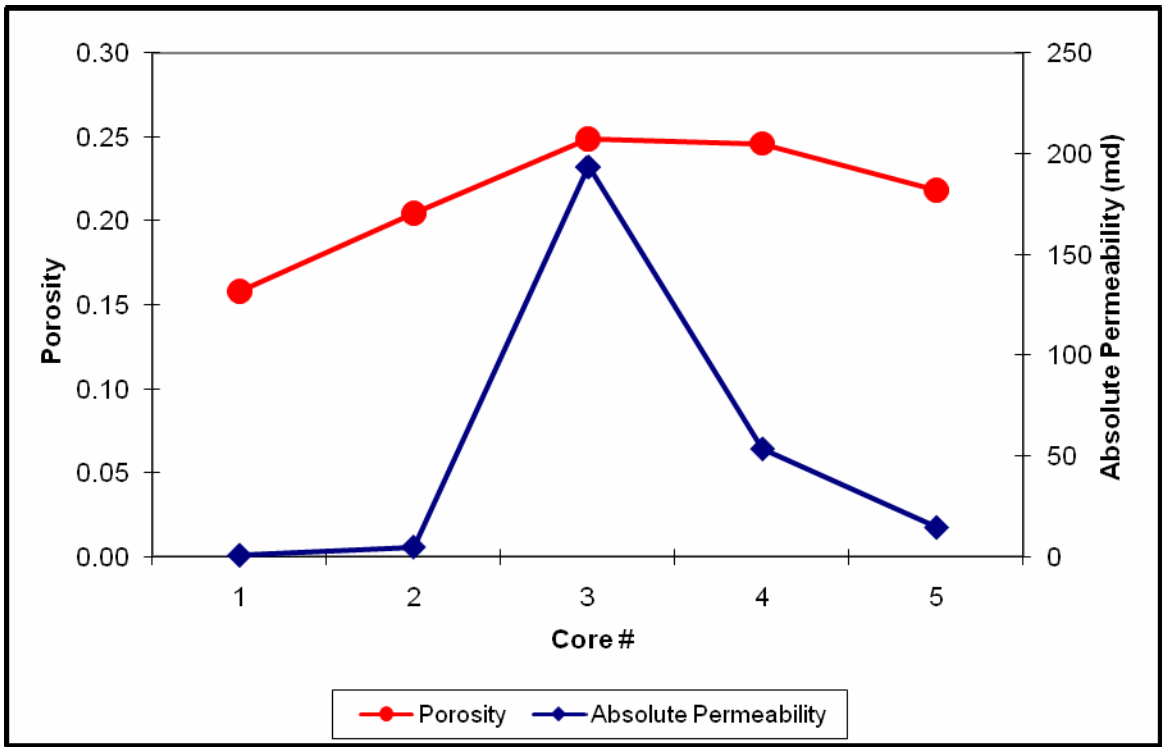

Figure 4.2: Absolute Permeability and Porosity Values of the DNR Cores.

4.1.2 Brine

Synthetic brine was used in the experiments. It was prepared by dissolving NaCl in distilled water (for the Berea cores) and DI water (for the DNR cores). Salinity of brine was varied by changing the concentration of the base brine (4% salinity) by factors of 0.5 and 0.25 to give brines having salinities of 2% and 1%, respectively. To prepare the base brine to a salinity of 4% the mixing ratio of brine and distilled water was determined gravimetrically. The adopted approach is given as follows:

1. Tare the balance scale with the empty measuring beaker on it
2. Fill the beaker with distilled/DI water and take the mass of distilled/DI water, M_{water}.
3. Based on the determined mass, calculate the mass of salt which when mixed with the distilled water gives 4% salinity brine using the expressions given by **Eq. 4.1** to **Eq. 4.3**

$$\frac{M_{NaCl}}{M_{NaCl} + M_{H_20}} = 0.04 \qquad \textbf{4.1}$$

$$M_{NaCl} = 0.04\left(M_{NaCl} + M_{H_20}\right) \qquad \textbf{4.2}$$

$$M_{NaCl} = 0.041667 M_{H_20} \qquad \textbf{4.3}$$

4. Weigh the calculated mass of salt, M_{NaCl}, and mix with the distilled/DI water. Continue stirring until all the salt dissolves in the water.

Densities of the brines were determined using the Anton-Paar Density Meter; measured brine density was 1.0249 g/cc at room temperature (23°C). Variations in the density of the brine with salinity were minor. The viscosity of the brine was also determined using the Canon-Fenske viscometer. It was difficult to determine the brine viscosity using the Brookfield viscometer as the brine appeared to react with the cone plate. The measured brine viscosity using the Canon-Fenske Viscometer was 1.12 cp at room temperature (23°C).

4.1.3 Crude Oils

Two kinds of oils were used in this experiment: (1) a pipeline blend of various crude oils from the ANS, that is, a flashed oil sample from TAPS collected at North Pole, designated in this work as TAPS blend, and (2) refined oil (decane) spiked with crude oil designated as spiked decane. The decane was spiked to differentiate visually the brine from the oil during the displacement studies. Densities of both oils were determined by using the Anton-Paar density meter. The measured density of TAPS blend was 0.8533 g/cc, while that of decane was 0.7260 g/cc. Both densities were determined at room temperature of 23^{o}C. Viscosities were determined using the Brookfield viscometer, and the viscosities of TAPS blend and spiked decane are respectively 8.24 cp and ≈ 0.9 cp.

4.2 Experimental Description – ANS Representative Cores

The present research study was carried out on representative core samples from the Alaska North Slope. Three sets of experiments were carried out in this research study: One set was the observation of the effect of variation in the brine salinity on residual oil saturation and wettability of new (clean) cores. The second set was the study of the effect of oil aging on the core samples and consequent observation of the effect of variation in the brine salinity on residual oil saturation and wettability of these oil aged cores. Reduction in salinity is achieved by reduction in the quantity of TDS in the brine. Furthermore, instead of reducing quantity of TDS in the brine, the option of using the representative low salinity ANS lake water was also investigated. ANS lake water served the purpose of reduced salinity brine in the coreflood studies. Hence, representative ANS lake water was also used in the experiments. Thus, the third set of coreflood experiments were conducted using ANS lake water to evaluate its potential for secondary oil recovery and the associated wettability change, if any.

Flood rate for all the sets of experiments was kept at 30 cc/hr. A reservoir temperature of 220°F was maintained, and 500 psi overburden was used in the experiments. Wettability characterization for all sets of experiments was done using the Amott-Harvey wettability index.

For the first two sets of experiments, the brine was reconstituted in the lab, while ANS lake water was used for the third set of experiments. The first step in all the experiments is the preparation of the core samples. The core plugs were prepared for use by preflushing (with toluene, followed by acetone and then water) and/or heating. Subsequently porosities and absolute permeabilities of all the core samples were determined.

In all three sets of experiments, the core is then flooded to interstitial/initial water saturation and the initial wettability of the cores was determined using the Amott-Harvey test. The core sample is then waterflooded with brines of different salinity (at reservoir temperatures and ambient outlet pressure) and the waterflood oil recovery was noted. The wettability change, if any, is monitored at every stage of the experiment, (i.e., when the brine salinity is changed).

Core Samples

Ten representative ANS core samples were used for the present experimental research study. The cores were approximately 0.8 in. in length and 1.5 in. in diameter. Porosity and absolute permeability values were determined in the lab for all the core samples. Porosity values ranged from 19% to 32% while the permeability values were between 38 mD and 97 mD. Porosity was determined using the saturation method. Core permeability was calculated from Darcy's law based on the observed pressure drop across the brine-saturated core after a steady state was achieved when injecting brine (22,000 TDS salinity) through the core sample.

Porosity and permeability values of all the ten core samples are shown in the following **Figure 4.3**.

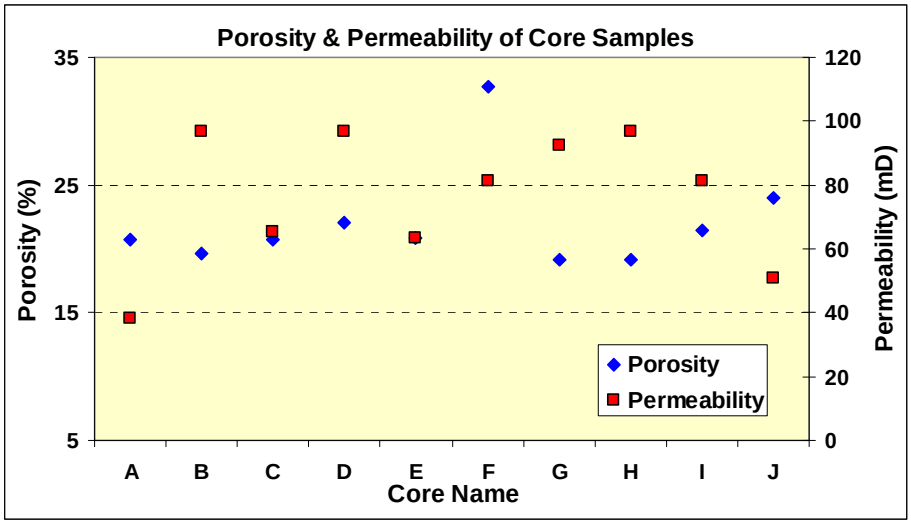

Figure 4.3 Porosity and Permeability Measurement of Tested Core Samples.

Brine Sample

In order to simulate the representative ANS formation water composition of the reservoir, brine was reconstituted in the lab by dissolving different salts that included Sodium Bicarbonate ($NaHCO_3$), Sodium Sulfate (Na_2SO_4), Sodium Chloride (NaCl), Potassium Chloride (KCl), Calcium Chloride ($CaCl_2$), Strontium Chloride ($SrCl_2$), Magnesium Chloride ($MgCl_2$) in de-ionized water in proper proportion. Total dissolved solids (TDS) of the representative ANS formation water was based on the data reported by McGuire et al.[93]. Based on the composition (see **Table 4.3**), three different salinity brines viz. 22,000 TDS, 11,000 TDS and 5,500 TDS were prepared. For the first two sets of the coreflood experiments, lab-reconstituted brine was used, For the third set of experiments, actual ANS lake water and 22,000 TDS brines were used for coreflooding comparisons. The following procedure was followed to reconstitute the brine in lab:

1. Tare the balance scale with the empty measuring beaker on it.
2. Fill the beaker with distilled/DI water and write down liters of distilled/DI water (L).
3. Based on the determined mass, calculate the mass (grams) of salt which when mixed with the distilled water gives 22,000 TDS salinity brine using the expressions given by Eq. 4.4.
4. Required mass of each salt (W) = $(M * Mol.\ Wt * L * \rho)/ 10^6$ **(4.4)**

   where M= Moles of salt

Mol. Wt= Molecular weight of salt

L= Liters of solution (brine) to be prepared

ρ = Density of solution (brine) to be prepared.

The density of formation water at standard conditions can be estimated from the following correlation (McCain, 1991):

$$\text{Density} = 62.368 + 0.438603S + 0.00160074S^2 \quad \textbf{(4.5)}$$

where *S* is the weight percent of total dissolved solids.

5. Weigh the calculated mass of salt; *W*, and mix with the distilled/DI water. Continue stirring until all the salt dissolves in the water.

The densities of different brines at ambient (77°F) and reservoir temperature (220°F) are tabulated in **Table 4.4**. Viscosity of the brine was measured using Brookfield Viscometer. At reservoir temperature, viscosity observed was 1.10 cP.

Table 4.3: Composition of ANS Reservoir Water from McGuire et al.[93]

Species (ppm)	Prudhoe Bay (PB) Aquifer
Barium	5
Bicarbonate	2060
Calcium	159
Chloride	11300
Iron	3
Magnesium	25
Potassium	78
Sodium	7860
Strontium	10
Sulfate	62
Total Dissolved Solids=	21,562

Table 4.4: Densities of Different Brines Used in the Experiment

Brine Salinity	22,000 TDS	11,000 TDS	5,500 TDS	ANS Lake Water
ρ at 77°F (g/cc)	1.0139	1.0065	1.0028	1.0002
ρ at 220°F (g/cc)	0.9590	0.9506	0.9471	0.9342

Crude Oil

Representative ANS crude oil (dead oil) was used for the present coreflood experiments. The density of the crude oil sample was measured using Anton-Paar Density Meter. The density was observed to be 0.8839 g/cc at the reservoir temperature (approximately 220°F).

4.3 Experimental Procedure – DNR and Berea Cores

4.3.1 Core Sample Preparation

All the DNR cores for the experiment were cleaned before use because the storage state and conditions since they were cored are not known. The cleaning process involved flushing the cores with toluene followed by acetone; the toluene was used to clean out/dissolve any hydrocarbon-based substance that might still have been in the core, while the acetone dissolved the toluene and/or water present in the core. The Berea sandstones were not cleaned but were dried along with the DNR cores.

The core plugs were dried in an air oven at 150^{o}C for at least 2 days. Prior to drying, the mass of all the core plugs were determined. After the first day of drying, the cores were weighed and drying continued until constant weight was achieved for all the cores, which indicated that all the pore fluids have been removed.

4.3.2 Core Saturation

The dried core samples were weighed on a balance. The samples were then placed under vacuum for an hour, after which they were saturated with brine of 4% salinity. The saturating brine was deaerated, and the cores were left in the brine under vacuum for at least 5 days to allow

equilibration time during which it was expected that the brine would achieve ionic equilibrium with the rock (core sample).

4.3.3 Pore Volume and Porosity Determination

The porosity of the core plugs was calculated by the saturation method. The saturation method of determining porosity consists of saturating a clean dry sample with fluid of known density and determining the pore volume from the gain in weight of the sample. The pore volume, *PV*, is calculated from the expression

$$PV = \frac{M_{wet} - M_{dry}}{\rho_{brine}} \qquad \textbf{4.6}$$

where M_{dry} is the weight of dry core, M_{wet} is the weight of core after saturating with brine of known density, ρ_b.

Porosity is then calculated as a percentage of the following expression:

$$\phi = \frac{PV}{BV} \times 100 \qquad \textbf{4.7}$$

where *BV* is the bulk volume calculated as follows:

$$BV = \frac{\pi D^2 L}{4} \qquad \textbf{4.8}$$

The dimensions of the core (length, *L* and diameter, *D*) are the average of 4 measurements using a vernier caliper.

In order to check the "accuracy" of the calculated porosity from the saturation method (for the DNR cores), the masses of the core plugs were taken after the brine floods for permeability calculation/determination. Typically, before injecting brine at constant flow rate, the brine-saturated flood was begun at high injection pressure to ensure that all the pores were saturated with brine and that no air bubbles are trapped in the pores of the cores.

Differences in porosities of the core samples, calculated using the two methods, ranged from 0.25% to about 6%. Though the reason for this variation is not clear yet, it is suspected that this may be because of the presence or absence, as it were, of "extra" droplets of water on the body of the core during the weighing process. No consistent trend in the variation of the core sample porosities between methods was observed. The measured porosities of the cores were higher in three of the cores and lower in two of the cores after the high-pressure brine injection (i.e., displacement method) compared to the calculated porosities after complete brine saturation under vacuum. **Table 4.5** shows the measured porosity from saturation and displacement methods and the percentage variation between the two approaches. The values of porosity that are selected for this work are those obtained from the displacement method.

Table 4.5: Core Porosities Measured from Saturation and Displacement Methods – DNR Core Samples

Core #	Porosity		Percentage Variation
	From Displacement	From Saturation	
1	0.1581	0.1492	5.94%
2	0.2045	0.1941	5.38%
3	0.2487	0.2514	1.07%
4	0.2460	0.2423	1.56%
5	0.2181	0.2186	0.25%

4.3.4 Establishing Initial Water Saturation

The cores were first saturated with deaerated brine (4% salinity) and equilibrated in the brine, at room temperature, for at least 5 days. The absolute permeability of the core was then determined by brine flooding after which the core plug was weighed and the porosity of the core calculated again. As has been explained, this served as a check on the initially calculated core porosity after saturating under vacuum. The core plugs were then flooded with crude oil to establish the initial water saturation. Displacement of water by oil continued until no more water was produced. For the DNR cores, the forced displacement of brine was conducted at constant-pressure drop while the forced displacement of brine for the Berea sandstone plugs was at constant injection rate. The

difference between the two approaches was a result of the type of pump used. The DB-Robinson positive displacement pump was used for displacement with the Berea plugs while the ISCO-pump was used with the DNR core plugs. The constant-pressure option on the DBR pump was not functional, resulting in the use of the only functional option—constant displacement rate. Rates as high as 1,800 cc/hr were used. The established initial water saturations are taken to be the interstitial saturation, S_{iw} (or connate water saturation, S_{wc}) which are shown in **Figure 4.4** and **Figure 4.5,** respectively, for the two different types of core samples.

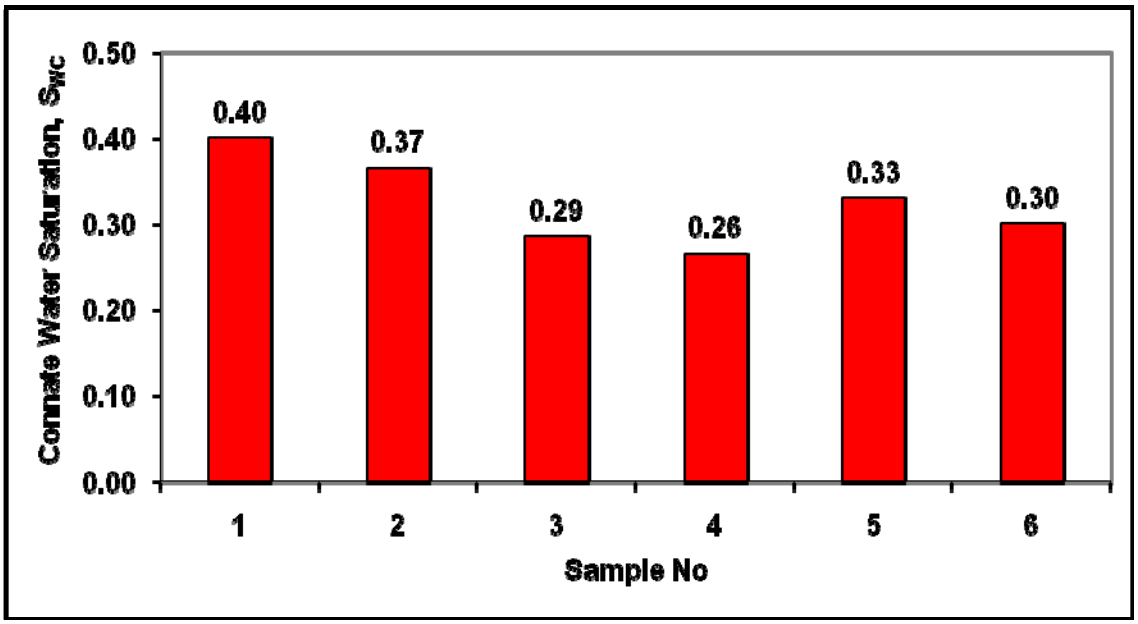

Figure 4.4: Interstitial Water Saturation in the Berea Cores after Forced Brine Displacement.

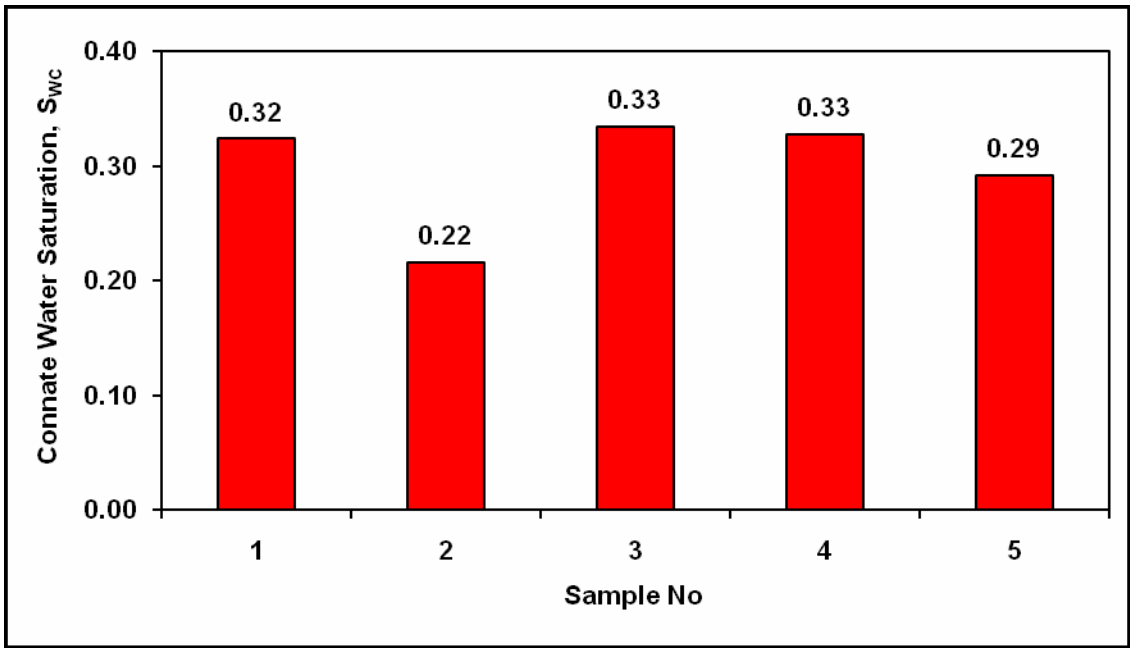

Figure 4.5: Interstitial Water Saturation in the DNR Cores after Forced Brine Displacement.

4.3.5. Absolute Permeability Determination

Determination of the absolute permeability was carried out with the coreflood apparatus. A differential pressure transducer was connected to inlet and outlet ends of the core holder to measure the pressure drop across the core plug. The transducer was configured to take ten (10) measurements every second. Though such rapid measurement is not critical to the determination of the absolute permeabilities of the core plugs, a frequency of 10 Hz was used because no lower measurement frequency is possible with the transducer used. The injection rate varied between 180 cc/hr and 300 cc/hr, depending on the core plug being flooded. Accurate determination of the absolute permeability depends on whether a steady-state condition was achieved within the core sample. Steady-state condition is attained when the pressure drop across the core does not change with time. **Figure 4.6** shows a plot of pressure drop vs. number of injected PVs for one of the DNR core plugs.

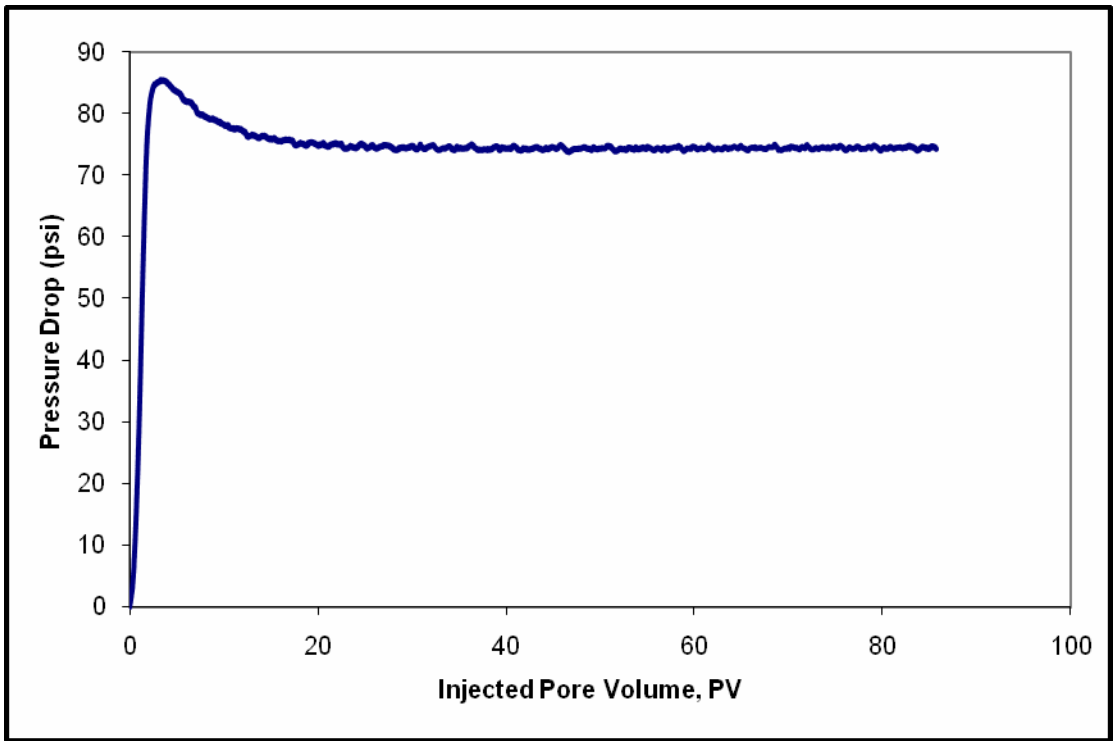

Figure 4.6: Typical Pressure Drop Profile for Absolute Permeability Determination.

Calculation of the absolute permeability of the core was achieved by the application of Darcy's expression for linear flow through porous media given by **Eq. 4.9:**

$$k = \frac{qL\mu}{A\Delta p} \qquad \textbf{4.9}$$

where:

k = absolute permeability, Darcies

A = cross-sectional area, cm^2

Δp = pressure differential, atm

L = length, cm

q = flowrate, cm^3/sec

μ = viscosity, cp

4.3.6 Coreflooding

The saturated core was loaded into the Hassler-type core holder and overburden pressure in applied in the radial direction. The system was left standing for some minutes to allow the sleeve to adjust to the applied radial pressure. An overburden pressure of 1,500 psi was applied on the Berea plugs while an overburden pressure range of 1,000 psi to 1,800 psi, depending on the cored depth, was applied on the DNR cores. The procedure for determining the overburden pressure is given below. Where the overburden pressure is not known, a gross overburden pressure of 1 psia/ft is usually assumed for the ANS.

The core holder sleeve pressure is calculated as follows:

Gross Overburden = ***Depth*** (ft) x 1.0 (psia/ft) = ***Depth*** (psia)

Reservoir Pressure = p_{res} (psia)

Net Overburden = ***Depth*** (psia) - p_{res} (psia) = p_{ovb} (psia)

Sleeve Pressure = p_{ovb} (psia) x 0.62

The sleeve pressure calculated for the DNR cores using the above approach resulted in complete fracture of some of the cores. Consequently the calculated sleeve pressure was further reduced to the already stated pressure ranges. This allowed the coreflooding to continue without fracturing the cores.

After allowing some time for radial uniformity of the sleeve's *grip* on the core plug, the interstitial water saturation was established by flooding with oil. For the DNR cores, this was followed by wettability determination by Amott-Harvey wettability method. It is pertinent to note that the Amott-Harvey wettability test was carried out only for the DNR cores. After the test, the core was loaded into the core holder and flooded again to initial water saturation.

The core was then waterflooded by brine of 4% salinity and the recovery recorded as a function of time at a constant rate of 20 cc/hr. After injecting 10 PVs of brine, the brine accumulator was heated to a temperature of ≈ 200°F. While heating the brine, the core plug was flooded again with oil to establish initial water saturation for 4% hot brine injection. The core plug was then flooded with 4% hot brine until 10 PVs of hot brine have been injected and oil production was monitored as a function of time. The wettability of the core plug was determined after this flood.

This procedure was repeated for 2% brine (ambient and elevated temperature) and 1% brine (ambient and elevated temperature). The wettability of the core plug was also evaluated after the change in brine salinity and/or brine temperature. For the DNR corefloods, the injection rate was maintained at ≈ 1.5 ft/D, while for the Berea sandstone cores, flooding rates were between 1.5 ft/D and 3.0 ft/D. Typical waterflood field rates are between 1 ft/D and 2 ft/D. At every stage of the coreflood process, the mass of the core was taken. The mass was used to calculate the amount of produced oil after a waterflood or the amount of displaced brine after an oilflood. This calculated volume is compared with the actual volume of oil or water produced. The calculation process was based on mass balance and is presented below:

Before waterflood, the mass of the core at initial/interstitial water saturation is given by:

$$M_{bw} = \underbrace{\rho_o V_{o1}}_{Oil\ Mass} + \underbrace{\rho_w V_{w1}}_{Water\ Mass} + \underbrace{\rho_g V_g}_{Grain\ Mass} \quad \textbf{4.10}$$

After waterflood, the mass of the core at waterflood residual oil saturation is given by

$$M_{aw} = \rho_o V_{o2} + \rho_w V_{w2} + \rho_g V_g \quad \textbf{4.11}$$

But

$$V_{w2} = V_{w1} + V_{poil} \quad \textbf{4.12}$$

and

$$V_{o2} = V_{o1} - V_{poil} \quad \textbf{4.13}$$

Substitute **Eq. 4.12** and **Eq. 4.13** into **Eq. 4.11,**

$$M_{aw} = \rho_o V_{o1} + (\rho_w - \rho_o) V_{poil} + \rho_w V_{w1} + \rho_g V_g \quad \textbf{4.14}$$

Subtracting **Eq. 4.10** from **Eq. 4.14** and rearranging algebraically,

$$V_{poil} = \frac{M_{aw} - M_{Bw}}{(\rho_w - \rho_o)} \quad \textbf{4.15}$$

Using a similar approach, the volume of displaced water under forced displacement is given by

$$V_{pwater} = \frac{M_{bo} - M_{ao}}{(\rho_o - \rho_w)} \qquad \textbf{4.16}$$

where

V_{poil} and V_{pwater}	= volume of produced oil and water from mass balance
M_{bw} and M_{aw}	= mass of core plug before and after waterflood
M_{bo} and M_{ao}	= mass of core plug before and after oilflood
ρ	= density
o and w	= subscripts for oil and water
1 and 2	= subscripts before and after waterflood (or oilflood as the case may be)

4.3.7 Imbibition and Wettability Index Determination

Characterization of wettability was achieved in this work by the modified Amott-Harvey method in which the forced displacement was obtained by fluid injection at constant pressure instead of by fluid injection at a constant rate[17] or by centrifuging[14]. The method consists of starting with the core sample at irreducible water-saturation. The core was then weighed and submerged in brine for 20 hours. A time period of 20 hours was chosen in line with the work reported by Amott[14]. During this period, the brine spontaneously displaces oil. The volume of oil spontaneously displaced by brine, V_{osd}, depends on the wettability of the core. For a completely oil-wet system, brine cannot displace oil spontaneously. However, for a completely water-wet system, if the core is immersed in brine for long-enough period, brine can displace oil spontaneously to waterflood residual oil saturation (S_{or}).

After the 20-hour-immersion period, the core was weighed and inserted into the Hassler-Type core-holder for forced displacement of oil by brine. The forced displacement was performed at constant-pressure drop at ambient temperature. The pressure drop ranged from ≈ 500 psi to ≈ 1,700 psi depending on the permeability of the core. Injection of brine was continued until no-more oil was produced (S_{or}). The volume of oil forcefully displaced by brine, V_{ofd}, was measured in a metering cylinder.

The core sample was then removed from the core holder, and the third step involved the immersion of the core in oil for 20 hours after taking the weight of the core sample. The volume of brine spontaneously displaced by oil, V_{wsd}, was measured and the weight of the core taken after the 20-hour immersion period. The volume of brine spontaneously displaced by oil is also a function of the core wettability. As has been stated, for a completely water-wet system, oil cannot displace brine spontaneously. However, for a completely oil-wet system, if the core is left in the oil for long-enough periods, oil can displace brine spontaneously to interstitial water saturation (IWS).

After the 20-hour spontaneous displacement of brine by oil was over, the core sample was then loaded in the coreholder and the brine was forcefully displaced by injecting oil at constant pressure. Oil injection was continued until no more water was produced (IWS). The volume of brine forcefully displaced, V_{wfd}, was noted and the mass of the core was taken after the forced displacement.

Amott defined two indices, which represent the fraction of displaceable fluid that is spontaneously displaced; I_w is the fraction of oil spontaneously displaced by water and I_o is the fraction of displaceable water spontaneously displaced by oil. From the foregoing

$$I_o = V_{wsd}/(V_{wsd} + V_{wfd}) \qquad \textbf{4.17}$$

$$I_w = V_{osd}/(V_{osd} + V_{ofd}) \qquad \textbf{4.18}$$

The wettability index, WI, is shown here as **Eq. 4.19** for convenience:

$$\text{WI} = I_w - I_o \qquad \textbf{4.19}$$

4.4 Experimental Procedure – ANS Representative Cores

Core Cleaning

All the core samples for the experiment were cleaned before use. The cleaning process involved flushing the cores with toluene followed by acetone; the toluene was used to clean out/dissolve any hydrocarbon-based substance that may still be in the core while the acetone dissolved the toluene and/or water present in the core. Then the core plugs were dried in an air oven at 176^{o}F for at least 2 -3 days. After drying, the core samples were weighed to determine if they achieved a steady reading, indicating the removal of all native fluids.

Core Saturation

The dried core samples were weighed on a balance. The samples were then placed under vacuum for 5–7 days in 22,000 TDS salinity to allow equilibration time during which it is expected that the brine will achieve ionic equilibrium with the core sample.

Waterflooding

The next step in the present experiment was to carry out waterflooding on the core sample at reservoir temperature. After carrying out Amott-Harvey index measurement, the core was waterflooded by 22,000 TDS salinity brine and the recovery recorded as a function of time at a constant rate of 30 cc/hr. After injecting 10 PVs of 22,000 TDS brine, residual oil saturation (S_{or}) value was calculated. The wettability of the core plug is determined after this flood. This waterflooding procedure was repeated by using 11,000 TDS brine (reservoir temperature) and 5,500 TDS brine (reservoir temperature) and the respective S_{or} values were calculated. After every waterflood, the Amott-Harvey wettability index was determined. Using this procedure, the first set of experiment was carried out on 7 clean core samples.

Steps Followed in the Second Set of Experiments

The aim of the second set of experiments was to study the effect of oil aging on the core samples and consequently observe the effect of variation in the brine salinity on the residual oil saturation and wettability of these oil aged cores. Hence, after finishing the first set of experiments, the

same core samples were used for second set of experiments. The first step in this set of experiments was to establish initial water saturation.

Oil Aging

After establishing initial water saturation, the core samples were removed from the core holder, immersed in steel tin containing ANS crude oil, and aged at 80°C to 90°C for 21 days. The tin was covered with a lid and aluminum foil to preclude the oxidation of oil during the aging period. After aging, cores were allowed to cool for a couple of hours.

Waterflooding

After oil aging for 21 days, the core samples were taken out from the tin and were brought for waterflooding experiments. In this set of experiments, the same reconstituted brines viz. 22,000 TDS, 11,000 TDS and 5,500 TDS were used. The steps followed in this case are the same steps followed in the new (clean) core samples. S_{or} values and the Amott-Harvey wettability index were calculated after every waterflood.

Steps Followed in the Third Set of Experiments

In the previous two experiments, the brine used for the corefloods was synthetically prepared/reconstituted brine in the laboratory. However, in this set of experiments the option of using the representative low-salinity ANS lake water was investigated. Michael Lilly and Amanda Blackburn (Geo-Watersheds Scientific) helped to procure the ANS lake water. Based on personal communication with Amanda, it was learned that rainwater and melting ice are the main contributors to water accumulation in ANS lakes. Thus, it is believed that ANS lake water is much less saline. Total dissolved solids quantity in the water samples obtained from the ANS was approximately 50–60 TDS. As ANS lake water is much less saline, the option of using ANS lake water as low-saline brine was explored in the third set of experiments.

The steps followed in this set of experiments are the same as in the previous two cases. First, porosity and permeability of the core sample was determined. Then initial water saturation was established in the core sample followed by 22,000 TDS brine waterflood. However, afterwards in the next steps of the experiments, instead of using 11,000 TDS and 5,500 TDS brine, ANS lake

water was used for waterflooding. Thus, ANS lake water serves the purpose of reduced salinity brine in these coreflood studies. S_{or} values and the Amott-Harvey wettability index were calculated after every waterflood.

CHAPTER 5: Salinity Influence on Oil-Water Interfacial Area, Wettability, and Oil Recovery Work Performed by PNNL

Wettability, or the tendency of surfaces to be preferentially wet by one fluid phase, has a strong influence on the distribution and flow of immiscible fluids in oil reservoirs. The efficiency of oil recovery processes and the displacement and production of oil by fluids injected into the reservoir depend on the wetting properties of the rock surfaces. In strongly water-wet rocks, the oil resides in the larger pores and flows with relative ease. However, large quantities of oil are left, trapped in the pore space because it no longer forms a continuous pathway for flow (a sample spanning cluster, in percolation terminology). In oil-wet rock, on the other hand, oil is present in the small pores and its relative permeability is small. However, it can form continuous pathways for oil flow even at small oil saturations, resulting in low trapped oil saturations. In mixed-wet rocks, relatively low residual oil saturations may be obtained if a continuous pathway for oil flow is available. The existence of such continuous pathways depends largely on the fraction of rock surface rendered oil-wet, that is, on the pore level mechanisms of wettability alteration. Therefore, understanding and characterizing reservoir wettability is crucial to estimating relative permeabilities and ultimate oil recovery. It was indicated that the residual oil saturation may be reduced significantly by flooding with low-salinity water instead of seawater or brine. This study investigated the influence of salinity on the oil-water interfacial area, soil wettability, and oil recovery.

5.1 Material and Methods

Two sets of 8 coreflooding column experiments have been completed, using decane and ANS crude oil. Unconsolidated sand packs were used as representative porous media. Oil removal was conducted by flushing columns at residual oil saturation using water with salinity ranging from 0% to 8% wt of NaCl. Oil saturation was determined based on mass balance of the columns, and the oil-water interfacial area (a_{nw}, cm^{-1}) was measured using tracers. Sodium dodecyl benzene sulfonate (SDBS) was used as an interfacial partitioning tracer, and pentafluoro benzoic acid (PFBA) was used as a non-reactive and non-partitioning tracer. Oil was imbibed into an initially water-saturated column, using positive displacement methods. Oil was then flushed out using water at certain salinity. When a column attained residual oil saturation after each water flushing

displacement, the partitioning and conservative tracer experiments were conducted separately to characterize the specific oil-water interfacial areas, and the wettability status. Water with 8%, 4%, 2%, and 0% wt NaCl salinity was used to displace oil from the sand column sequentially. The interfacial tension (IFT) between the salinity water and the ANS oil was measured.

Column Test Procedures

1. Pack a column with clean Accusand using vibration and a dry sand pack. Record the weight of the empty column and, after packing the column, the weight of the column and sand. Make sure that the density is 1.7 g/cm^3 or better.
2. Saturate the column with DI water in an up-flow mode (to drive the air out) at a rate of 30 ml/hr (0.5 ml/min). Record the weight of the water-saturated column. Also monitor the volume and weight of water injected into the column (record the weight and volume of water reservoir before and after injection).
3. Replace the DIW in column with 8% NaCl solution (upward-flow) at 50 ml/hr (0.833 ml/min) flow rate.
4. Run a baseline tracer with 100 ppm PFBA (prepared using 8% NaCl solution) at a pumping rate of 12 ml/hr (0.2 ml/min) in a down-flow mode. Allow the tracer to pump 1.08 hours (for a total of 13.0 ml, or ~0.25 PV), depending on the column's calculated pore volume. Collect samples every 15 minutes. These conditions will be used for all subsequent tracer studies. After the PFBA tracer test, conduct the same test with 100 ppm SDBS (prepared using 8% NaCl solution).
5. Load the column with decane/ANS oil (upward flow) at flow rate of 30 ml/hr (0.50 ml/min). Record the volume of decane/ANS oil added and the weight of the column.
6. Flood the column with 8% NaCl solution (upward flow) at flow rate of 50 ml/hr (0.833 ml/min).
7. Collect column effluent in a graduated cylinder so accurate volumes of water and decane/ANS oil can be measured. Continue to flood the column until no visible decane/ANS oil is collected.
8. Record the amount of decane/ANS oil recovered and the weight of the column after waterflooding. Determine the amount of decane/ANS oil remaining in the column.

9. Perform tracer studies using PFBA and then SDBS (down-flow) prepared with 8% NaCl) solution at flow rate of 12 ml/hr (0.2 ml/min).
10. Analyze the tracer samples by UV and generate a breakthrough curve by plotting C/Co as a function of pore volume.
11. Flood the column with 4% NaCl solution (up-flow) at flow rate of 50 ml/hr (0.833 ml/min).
12. Collect the solution and decane/ANS oil that is flushed out of the column. When decane/ANS oil is no longer visibly coming off the column, record the column weight and the amount of decane/ANS oil recovered.
13. Repeat the PFBA and SDBS tracers using 4% NaCl solutions at flow rate of 12 ml/hr (0.2 ml/min).
14. Repeat the flooding and tracer studies using 2% and 0% salinities using the same pulse, flow rates and flow direction.

5.2 Results

Results from Tests Using Decane

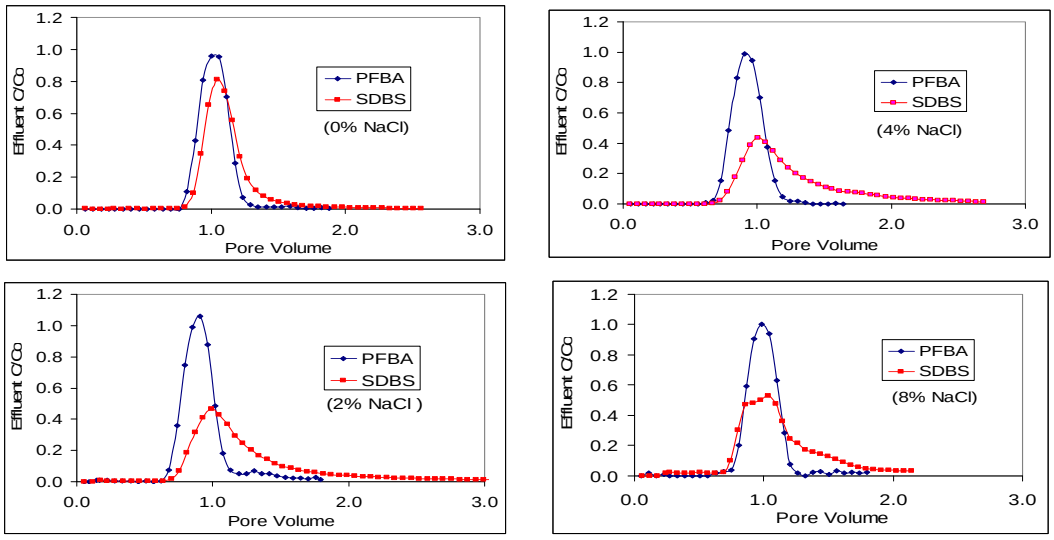

Figure 5.1: Effluent Tracer Curves from Decane-containing Columns after Flushing with Water at Different Salinities.

Analysis of the interfacial tracer breakthrough experimental data for interfacial area and wettability changes from the set of drainage experiments completed earlier, using decane as the non-wetting phase is shown in **Figure 5.1** and **Table 5.1**. Analysis of results so far indicates that

the oil-water interfacial area (a_{nw}, cm^{-1}) does not show a monotonic dependence on salinity; instead, a_{nw} shows an increasing trend with increasing salinity in the lower salinity range, and the opposite trend at high-salinity values (**Figure 5.2**). This trend appears to be consistent with a similar nonlinear dependence of interfacial tension on salinity[104]. Earlier, it was established that interfacial areas are strong, inverse functions of interfacial areas[1,105].

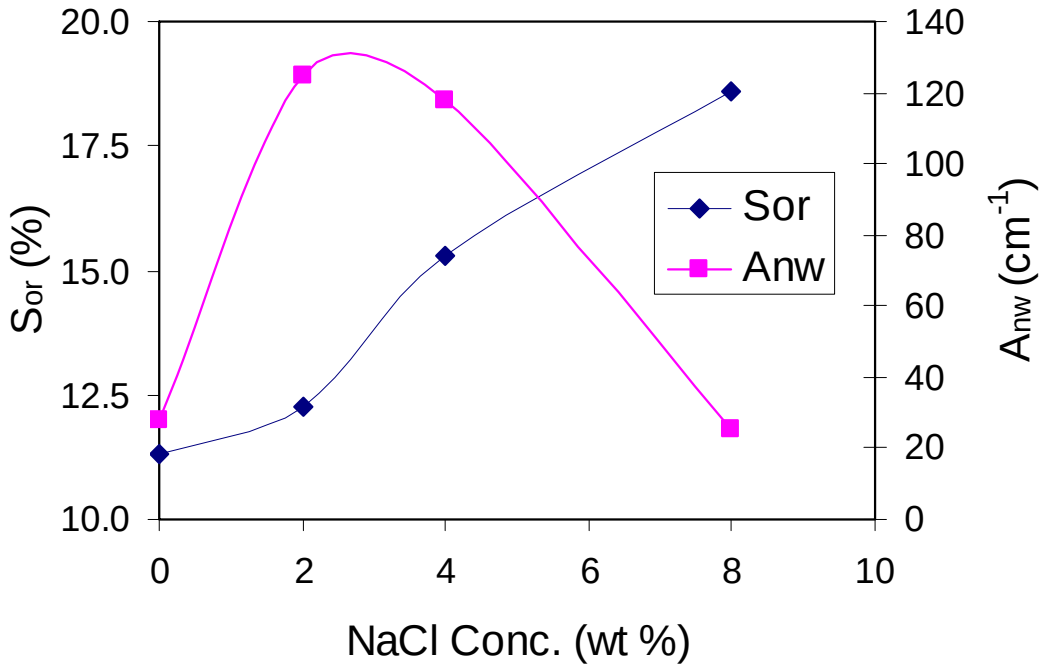

Figure 5.2: Decane Residual Saturation, S_{or}, and Oil/Water-specific Interfacial Area, a_{nw}, vs. Salinity. S_{or} Decreased with Decreasing Salinity, While the a_{nw} Reached a Maximum at Salinity of ~2%.

Table 5.1: Parameters for decane-containing columns tests.

Column Test Stage	**Trapped Decane Vol (ml)**	**PFBA recovery (%)**	**SDBS recovery (%)**	S_{or} **(%)**	**Kd of SDBS**	a_{nw} **(cm^{-1})**
Flushed with decane	40.73	NA	NA	NA	NA	NA
Flushed with 8% NaCl	9.11	113.2	114.6	18.61	1.13	25.12
Flushed with 4% NaCl	7.73	105.8	95.7	15.31	1.47	117.8
Flushed with 2% NaCl	6.19	117.0	102.0	12.26	1.55	124.9
Flushed with 0% NaCl	5.70	102.0	98.0	11.29	1.11	28.07

Results from Tests Using ANS Crude Oil

Interfacial tracer test results for the ANS crude oil experiments are shown in **Figure 5.3**.

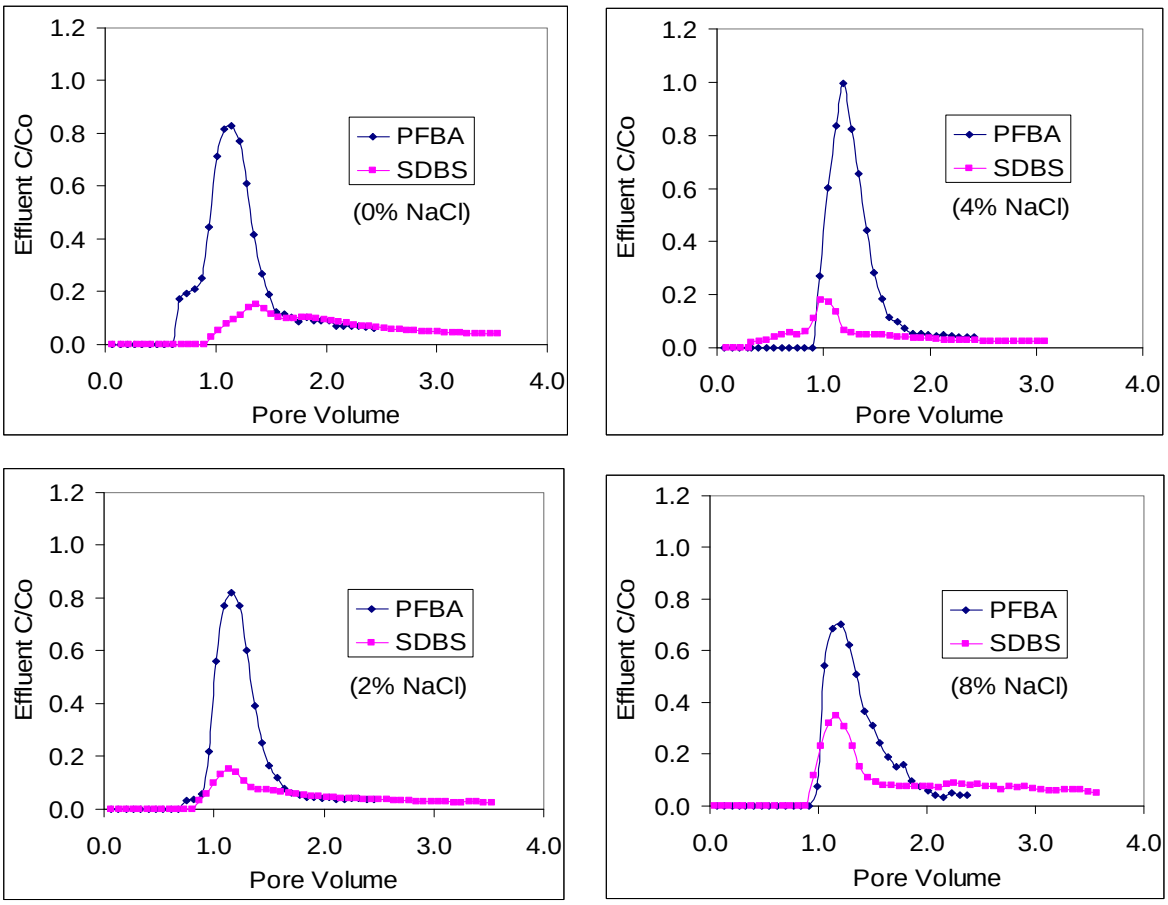

Figure 5.3: Effluent Tracer Curves from ANS Oil-containing Columns after Flushing with Water at Different Salinities.

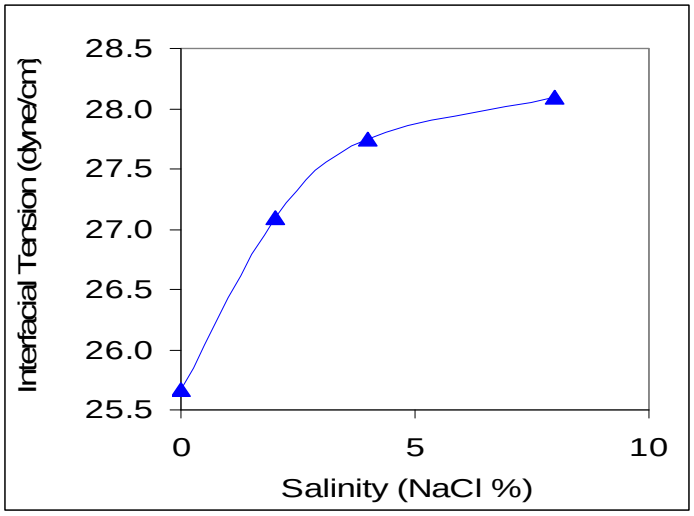

Figure 5.4: Interfacial Tension (IFT) between ANS Oil and Water vs. Water Salinity.

Interfacial tension between ANS oil and Brine were measured using pendant drop method. Interfacial tension decreased as a function of salinity (Figure 5.4). Natural surfactants present in ANS oil are likely to aggregate at a closer packing (area per molecule) with decreasing salinity. This observation is critical to defining an optimal salinity window for ANS oil recovery.

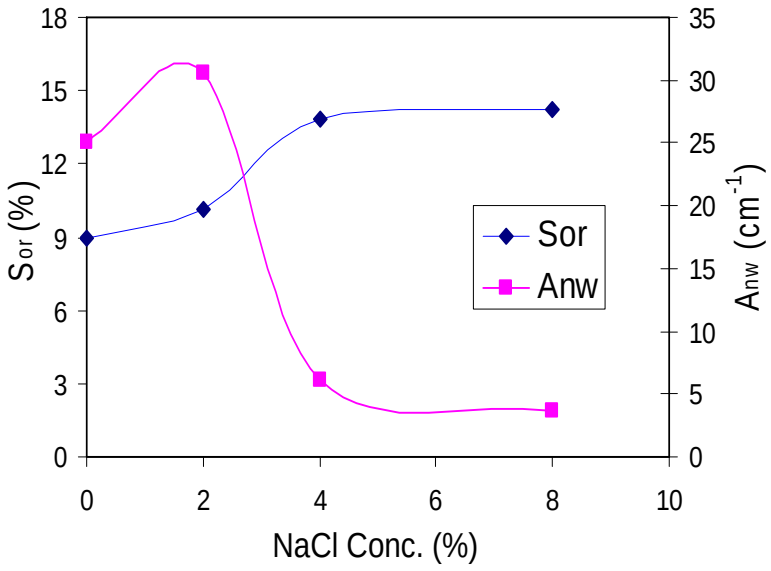

Figure 5.5: ANS Oil Residual Saturation, S_{or}, and Oil/Water-specific Interfacial Area, a_{nw}, vs. Water Salinity.

The S_{or} remaining obtained from the 4 coreflood tests are shown in **Figure 5.5**. Larger recovery was seen with decreasing salinity. This trend has a correlation with the trends found for interfacial tension with salinity, while the a_{nw} reached a maximum at salinity of ~2%.

5.3 Analysis of Results

- The residual oil saturations indicated that the fraction of oil retained in the column increased after water flushing as the salinity in the displacing water increased from 0 to 8%, clearly confirming the earlier findings that lower salinity may cause additional oil to be released.
- The oil-water interfacial area, a_{nw}, does not show a monotonic dependence on salinity; instead, a_{nw} shows an increasing trend with increasing salinity in the lower salinity range, and the opposite trend at high-salinity values. Maximum a_{nw} was obtained in systems flushed with 2% salinity water. This trend appears to be consistent with a similar nonlinear dependence of interfacial tension on salinity, and might be an indication of wettability alternation.
- The observation of this research sheds light on the optimum operation in oil removal. The IFT change between oil and the salinity water might be attributed to EOR.

It is well known that oil present at the same saturation can have vastly different IFA. Information from S_{or} and a_{nw} can be combined into a single oil morphology index, $I=a_{nw}/\theta S_{or}$, where θ is the porosity of the porous medium. This index can be used to characterize the wettability of the porous medium.

CHAPTER 6: Advanced Coreflooding Tests at Reservoir Conditions

The experiments conducted so far were on dead-oil-saturated cores that partially replicate the original reservoir conditions. In real-time reservoir conditions, however, there might be gas caps and solution gas present that affect oil production and recovery. Thus, it is necessary to mimic original reservoir conditions with elevated temperature and pressure conditions. Prudhoe Bay reservoirs contain light oil with high gas-oil ratios. It is necessary to recombine the dead-oil sample with gas and continue the waterflooding experiments with brines of different salinities.

6.1 Materials Used

Two new cores from ANS were used for flooding. Brines of 2 different salinities—22,000 and 11,000 TDS—were used for waterflooding. Conventional continuous injection of water was practiced. Dead oil from Prudhoe Bay was recombined with methane gas at high pressure and temperature to form a representative live-oil sample.

6.2 Modified Setup

The previous experiments were all conducted at atmospheric conditions. Since recombined oil remains as a solution only above bubblepoint pressure and temperature, these runs were conducted above bubblepoint conditions. The original setup was modified by adding a backpressure regulator at the outlet of the core holder to maintain differential pressure. Additional pressure gauges and valves were fitted at the ends of accumulator and core holder to monitor and regulate the pressure. The outlet of the backpressure regulator was connected to a gas flow meter and a measuring cylinder to get the volumes of gas and oil respectively.

6.3 Experimental Procedure

For recombination of gas-oil, methane gas was used as a representative since most of the gas produced in the reservoir contains methane in higher proportions. Details of the Prudhoe Bay well from which the dead-oil sample was acquired were obtained from the well data archives of the Alaska Oil and Gas Conservation Commission (AOGCC). The gas-oil ratio was 1,080

SCF/STB on an average. The solution gas-oil ratio was calculated, and the methane and dead-oil mixture was recombined in a rocker apparatus at 90°C and 2,400 psi for 48 hours.

The new cores were saturated under vacuum in 22,000 ppm salinity brine for about 5 days. After calculating the porosity values, the cores were waterflooded at high flow rates to find the differential pressure and thus absolute permeability. Live oilfloods were conducted to establish irreducible water saturation. Backpressure was maintained to prevent flashing and conduct the experiment at reservoir conditions. Increased overburden pressure of 2,500 psi was maintained to keep the core in place. Continuous injection of water (22,000 ppm salinity) was performed to produce oil and gas (at surface conditions). When no more oil was produced by this injection, 11,000 ppm salinity brine was continually injected to recover any additional oil, if present.

6.4 Results

Low-salinity waterflooding of recombined oil-saturated cores caused significant oil recovery and decrease in residual oil saturation, though not as high as the dead-oil-saturated cores. These results are summarized in **Table 6.1** and **Figure 6.1** and **6.2,** respectively, which are consistent with the partial reservoir conditions corefloods.

Table 6.1: Oil/Gas Recovery and Residual Oil Saturation

Core #	Pore Vol. (cc)	Recombined Oil Present in the core at Reservoir conditions (cc)	Brine Salinity (ppm)	Recovery at surface conditions (cc)		Dead Oil Recovery % (Final)	Initial : Residual Oil Saturation (Final) %
				Oil	Gas		
49	4.8	1.7	22k (Secondary)	0.5	89	29.41	35.41 : 20.83
			11k (Tertiary)	+0.2	-	41.17	
145	5.2	2	22k (Secondary)	0.5	89	25	38.46 : 23.07
			11k (Tertiary)	+0.3	-	40	

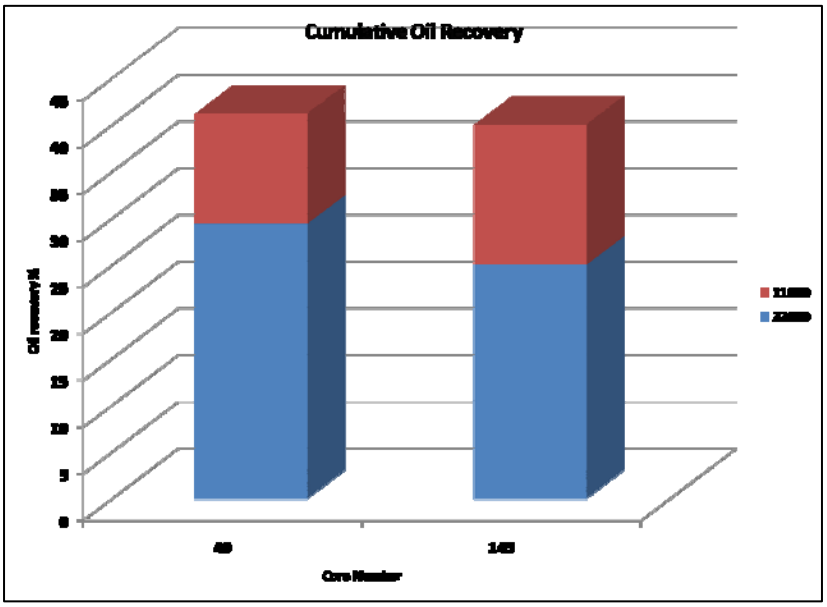

Figure 6.1: Cumulative Oil Recovery (Recombined Oil Floods).

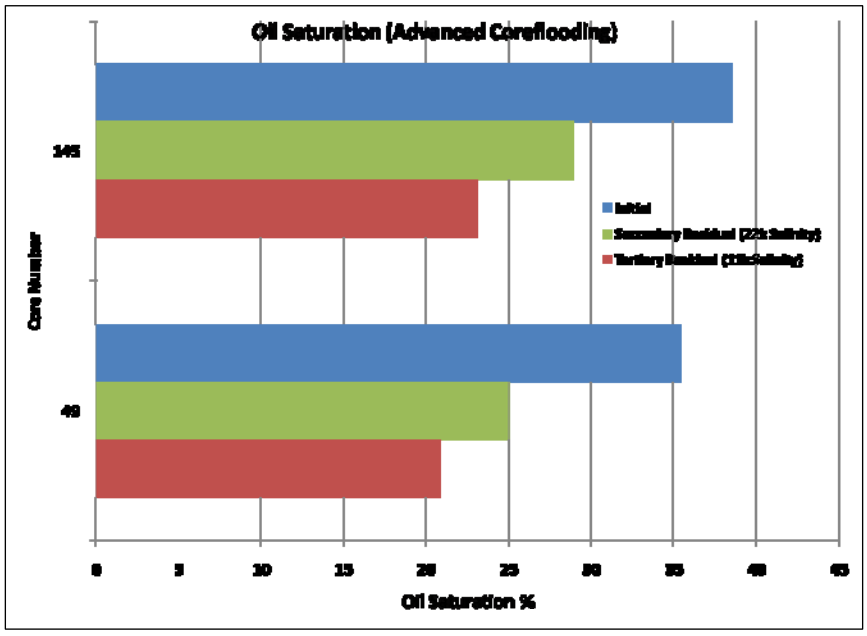

Figure 6.2: Oil Saturation (Recombined Oil Floods).

CHAPTER 7: Results and Discussion – DNR and Berea Cores

The current industry practice, in designing most waterflood processes, requires the use of formation water/brine, or filtered (and treated) seawater or a mixture of both (produced) formation water and seawater. Salinity of seawater is normally between 3% and 3.5% (in terms of the total dissolved solids). The salinity of the reservoir brine on the other hand has been reported to be up to four times higher than that of seawater[95]. Consequently, most waterfloods are carried out using high-salinity brine. Hot-water flooding is typically used for heavy oil recovery and usually results in improved oil production over conventional (primary) or secondary recovery techniques. However, problems of extensive heat loss through the tubing and to the formation, cost of heating, cost of insulation, etc., make this a very expensive and energy intensive option.

This work compares the oil recovery benefits achieved by injecting brine having different salinities. It also evaluates the impact of wettability variation, as a result of varying the brine salinity, on oil recovery efficiency and residual oil saturation. In this work, high-salinity waterflood refers to the injection of brine having a salinity of 4% while low-salinity waterflood refers to the injection of brine having salinities of 2% and 1% respectively.

Two sets of fast-track coreflood experiments were designed to achieve the objectives of this work. Both sets experiments were conducted at ambient pressure and temperature and ambient pressure and elevated temperature conditions. The aim of the first set of experiments was to examine and validate published reports on the EOR potential of low-salinity brine. The impact of injecting brine at elevated temperature on reduction in residual oil saturation was also examined. This first set of experiments involved changing the salinity of the injected brine (to a lower salinity) at high water cut (typically when no more oil is being produced by injecting brine of higher salinity) and observing for the incremental volume of produced oil. Due to the design of this experiment, the initial salinity of the connate water could not be kept constant. Consequently, the initial salinity of the connate water for each waterflood (of a specific salinity) was a function of the brine salinity of the preceding flood. For example, the initial connate water salinity for the 2% salinity waterflood was 4% because the 2% salinity flood was immediately preceded by a 4% salinity flood. However, the “initial” connate water salinity at the start of the

1% salinity waterflood was expected to be somewhere between 2% and 4% salinity because of dilution of the (initial) connate water salinity (of about 4%) by the injection of lower salinity brine (in this case 2%). However, what is important in this case and indeed worthy of note is the fact that the salinity of the connate water is always higher than the salinity of the injected brine. This distinction is important because it is necessary to isolate the *variable* that was instrumental to the incremental recovery of oil.

Sharma and Filoco[91] have reported that variation in connate water salinity influences oil recovery. They observed that more oil is recovered where the connate water salinity is less than the injected brine salinity compared to the converse case. They further reported no improved oil recovery was seen when the connate water salinity was kept constant and the injected brine salinity varied. Based on these observations they opined, contrary to the observations made by other researchers[89,90,95] in similar studies, that the salinity of the connate water appeared to be more important than the injected brine salinity in the observed increase in the value of the recovered oil. In the present study, it is believed that by maintaining higher connate water salinity compared to the salinity of the injected brine, the observed impact of the variation of connate water salinity on oil recovery as reported by Sharma and Filoco is minimized. Thus, any observed increase in oil recovery will be a result of reduction in the salinity of the injected brine. It is pertinent to note that the effect of wettability/wettability variation on oil recovery was not considered in the first set of experiments.

The second set of experiments examined the potential of the low-salinity brine injection in secondary oil recovery. For this set of experiments, care was taken to ensure that all the coreflood experiments commenced at the same initial condition; that is, the cores were at initial oil saturation (S_{oi}) and interstitial water saturation (S_{iw}). An attempt is also made to explain any observed increase in recovered oil volume and reduction in residual oil saturation (S_{or}) in terms of change in wettability using the Amott-Harvey wetting index. The connate water salinity of the second set of experiments was kept constant at a “high” salinity of 4%. This ensured that the same kind of scenario that might be encountered in a real field scenario was also simulated. It is expected that if low-salinity flood is carried out in most reservoirs, the reservoir brine salinity will be (much) higher than the salinity of the injected brine. As has already been mentioned, the

formation water salinity in some cases can be as high as 80,000 ppm total dissolved solids (TDS) of the brine[95].

7.1 EOR Potential of Low-Salinity Brine

Figure 7.1 and **Figure 7.3** compare the recovery of oil from Berea sandstone cores using brines of different salinities (4%, 2%, and 1%) at ambient conditions. In this experiment, the 4% brine is taken to simulate the nature of the high-salinity brine typically used in conventional waterflood processes. Both figures show the results of the experiment where the waterflood process was started by the injection of the 4% salinity brine, followed by 2% salinity brine and finally the 1% salinity brine. For all the cases, a minimum of 10 PVs of brine were injected. The observation of a plateau in the oil production profile indicates that no incremental oil could be recovered using the same brine salinity.

One consistent trend observed in both plots is the increase in oil recovery with decrease in the salinity of the injected brine. More oil is recovered when brine of lower salinity is injected. However, this recovery is at the expense of increased production of water. For the 4% salinity brine, when waterflooding commences, oil is produced without additional production of water until water breakthrough occurs. It is also observed from the plots that water breakthrough occurred at less than 1 PV of injected water. This is consistent with observations which have been reported in literature for water-wet systems. After the initial water breakthrough, no further oil production was observed for the case of the 4% brine. The observed clean breakthrough of water in this case is indicative of the water-wetting condition of the Berea sandstone. The sandstone was made water-wet from the initial heat treatment during the preparation of the core samples. **Figure 7.2** and **Figure 7.4** also show the reduction in residual oil saturation with decreasing brine salinity. The least oil saturation is observed after injecting brine of 1% salinity. In **Figure 7.2**, a reduction in S_{or} from 35.54% (4% brine) to 30.0% (2% salinity) to about 22.93% (1% salinity) is observed. The same consistent trend is observed in **Figure 7.4**. Similar observation of lower S_{or} has also been reported from the result of experimental work conducted at BP Exploration laboratory at Sunbury[95]. In their work, the microvisualisation of residual oil saturation after high- and low-salinity waterflood clearly showed that low-salinity waterflood

achieves much lower remaining oil saturation than the waterflood performed using a much higher salinity injection brine.

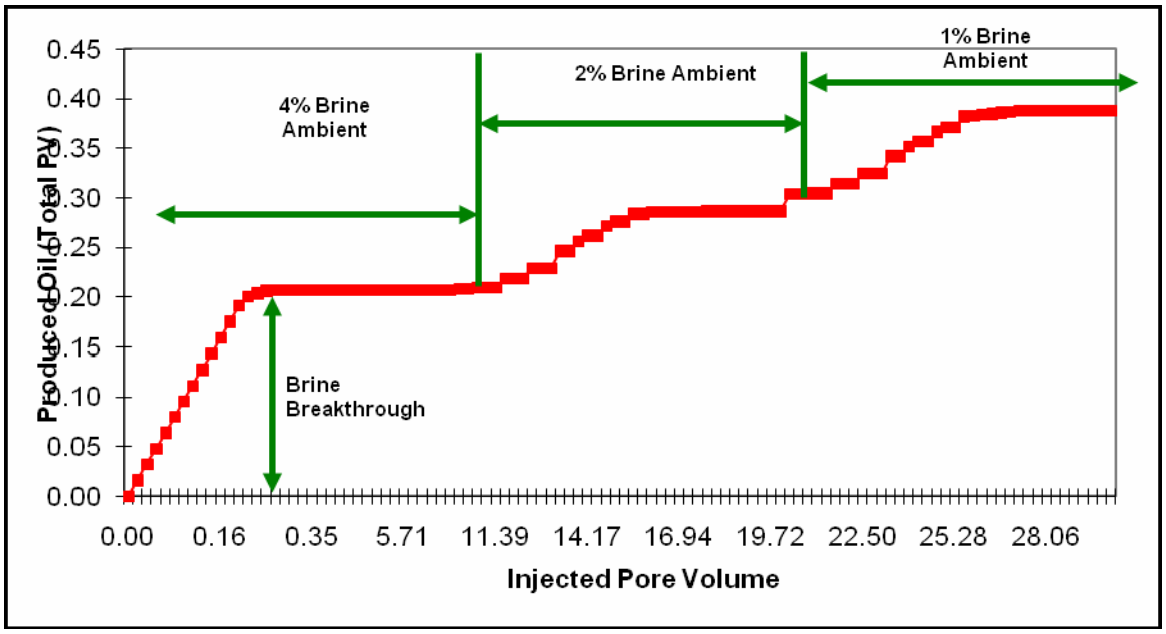

Figure 7.1: Effect of Low-Salinity Flooding on Oil Recovery – Core Sample #3 (Berea/Crude Oil System).

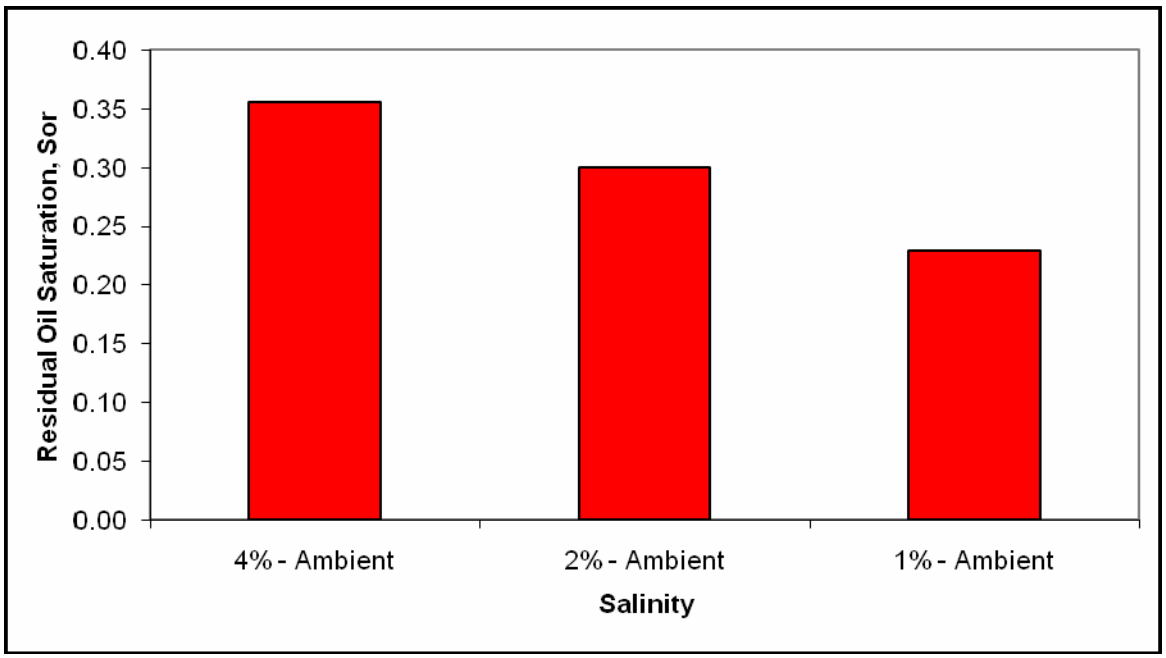

Figure 7.2: Effect of Variation in Brine Salinity on Residual Oil Saturation – Core Sample #3 (Berea/Crude Oil System).

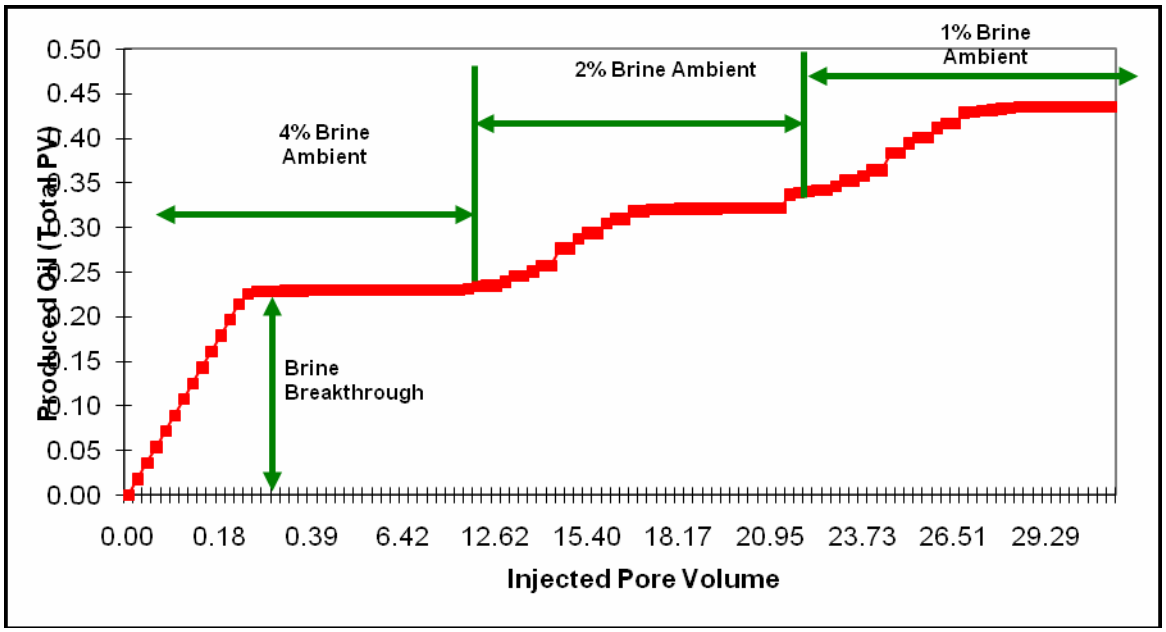

Figure 7.3: Effect of Low-Salinity Flooding on Oil Recovery – Core Sample #6 (Berea/Crude Oil System).

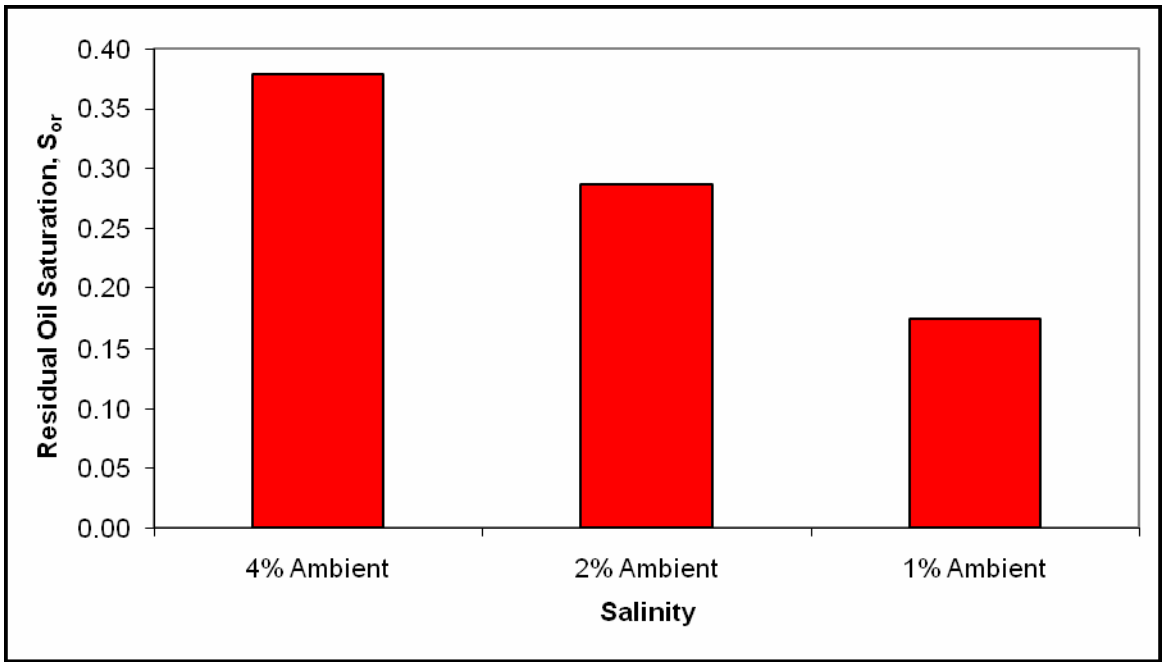

Figure 7.4: Effect of Variation in Injection Brine Salinity on S_{or} – Core Sample #6 (Berea/Crude Oil System).

7.2. EOR Potential of Injecting Hot High-Salinity Brine Followed by Low-Salinity Brine

Figure 7.5 and **Figure 7.7** compare the oil recovery profile in terms of the total pore volume of produced oil from the injection of high-salinity brine at ambient and elevated temperatures followed, respectively, by the injection of 2% and 1% low-salinity brine. The experiment was conducted by injecting high-salinity brine at ambient condition until no more oil was produced. The high-salinity brine was then heated and the hot brine injected into the core holder. Production of more oil from the core plugs was observed and the injection of hot brine was continued until oil production ceased. The hot brine injection was followed by the injection of 2% low-salinity brine in one case (**Figure 7.5**) and 1% low-salinity brine in the other case (**Figure 7.7**). It was observed that injecting high-salinity brine at elevated temperature instead of at room temperature resulted in incremental oil recovery. Further oil recovery was observed when the injection of hot brine is replaced with low-salinity brine injection. **Figure 7.6** and **Figure 7.8** show the corresponding reduction in residual oil saturation for the cases presented in **Figure 7.5** and **Figure 7.7**. It is observed from **Figure 7.6** that increasing the temperature of high-salinity brine results in a reduction in S_{or} by 13.55%, while the subsequent reduction in the brine salinity (i.e., injection of 2% low-salinity brine) results in a further reduction of S_{or} by 28.36%.

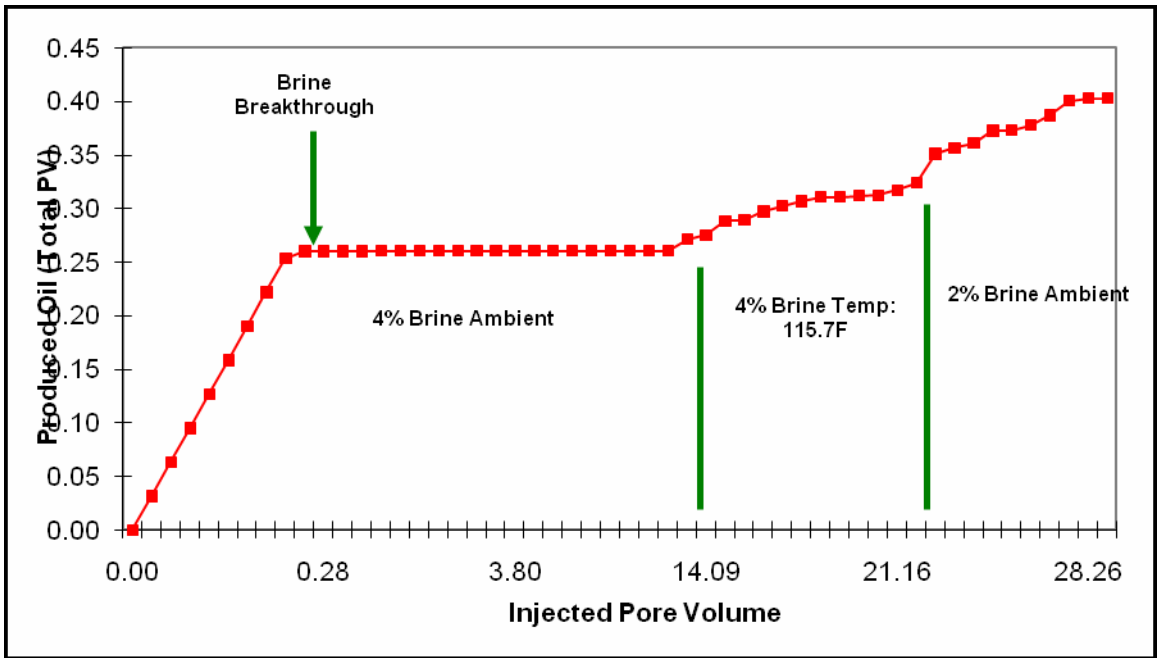

Figure 7.5: Effect of Brine Temperature and Salinity on Oil Recovery – Core Sample #2 (Berea/Crude Oil System).

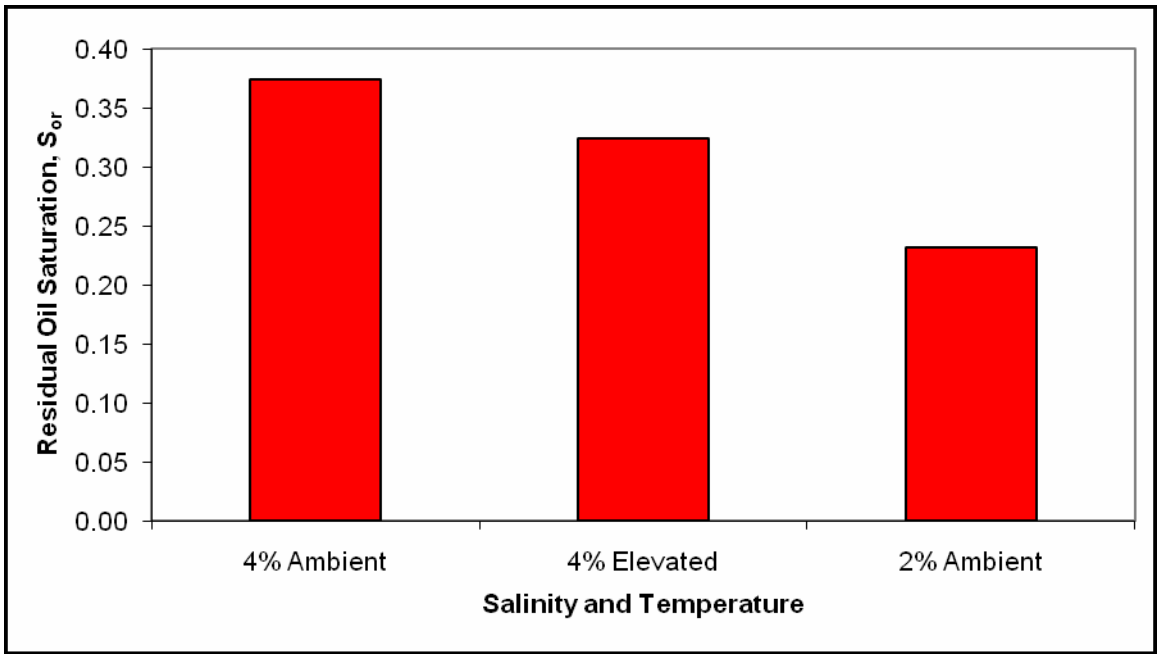

Figure 7.6: Effect of Brine Temperature and Brine Salinity on S_{or} – Core Sample #2 (Berea/Crude Oil System).

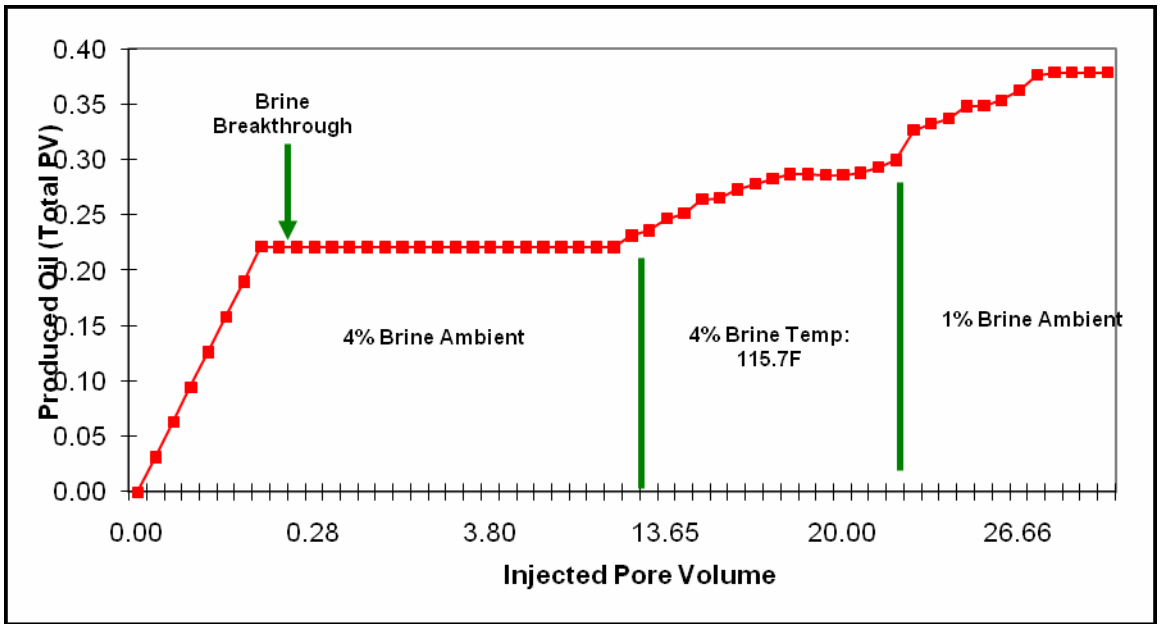

Figure 7.7: Effect of Brine Temperature and Salinity on Oil Recovery – Core Sample #1 (Berea/Crude Oil System).

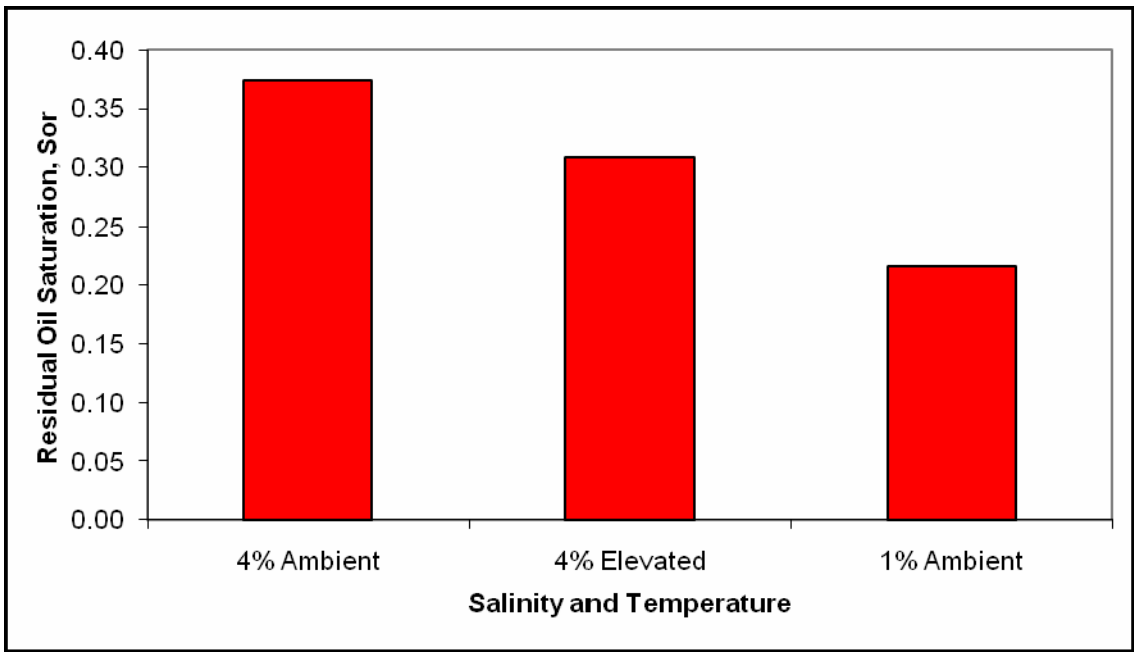

Figure 7.8: Effect of Brine Temperature and Salinity on S_{or} – Core Sample #1 (Berea/Crude Oil System).

7.3 EOR Potential of Injecting Low-Salinity Brine at Ambient and Elevated Temperature

The first set of experiments also determined the EOR potential of injecting brine of different salinities at ambient and elevated temperatures. The observed oil recovery profile for this scenario is shown in **Figure 7.9** and **Figure 7.11**. Both plots show an increase in the number of PVs of produced oil with decrease in brine salinity and increase in the temperature of the injected brine. **Figure 7.9** shows a very significant increase in the produced oil when hot brine of 2% salinity is injected. It is suspected that this significant increase is the combined effects of increase in temperature and viscous forces. It was observed while running the experiment that the pressure drop was significantly higher across the core plug due to forced fluid flow when the brine accumulator valve was opened, as a result of pressure buildup in the accumulator while heating the brine. This undue influence of the viscous force was removed in the next experiment (by venting the steam and allowing the injection of hot brine at a constant flow rate) and the result is plotted in **Figure 7.11**. However, irrespective of the additional viscous effect, it is observed that further injection of low-salinity brine at ambient and elevated temperatures resulted in the production of incremental oil. The observed increase in oil recovery is presented in another form in **Figure 7.10** and **Figure 7.12** which show the reduction in residual oil saturation with injection of low-salinity brine at ambient and elevated temperatures. One set of experiments (**Figure 7.10**) resulted in a decrease in residual oil saturation from 36.84% after injecting 4% brine at ambient condition to 9.87% after injecting low-salinity brine (1% salinity) at elevated temperature. The other set of experiments shows a reduction in S_{or} from 38.91% (high-salinity brine flood at room temperature) to 15.10% (low-salinity brine injection at elevated temperature).

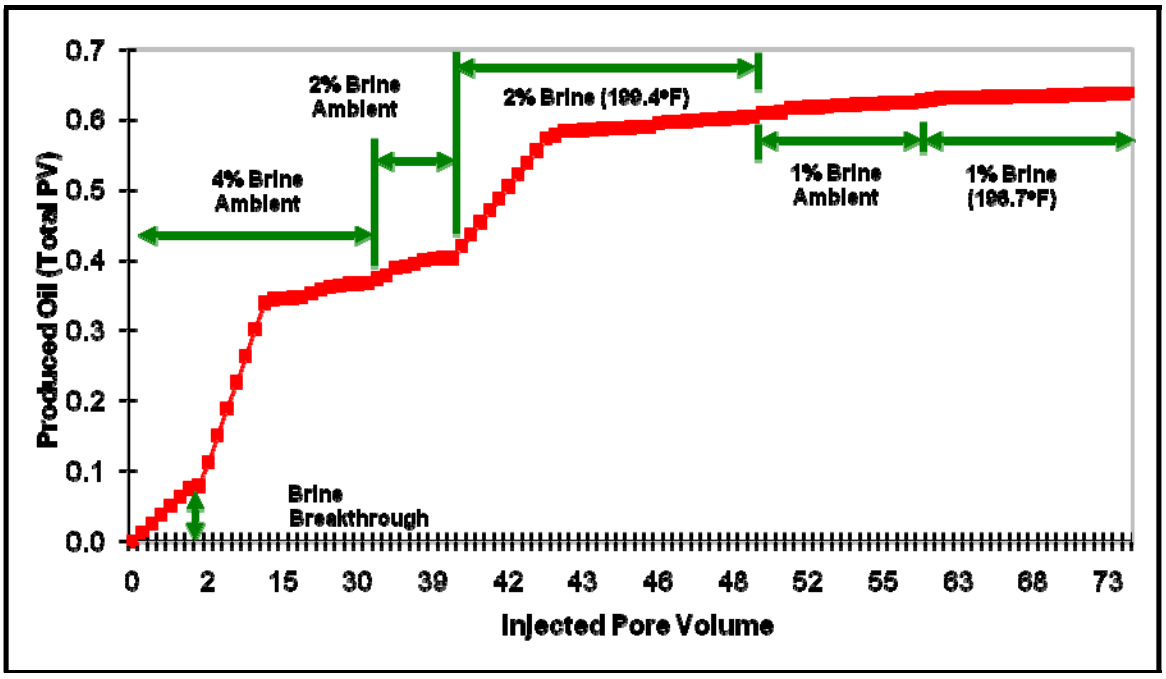

Figure 7.9: Effect of Brine Temperature and Salinity on Oil Recovery – Core Sample #4 (Berea/Crude Oil System).

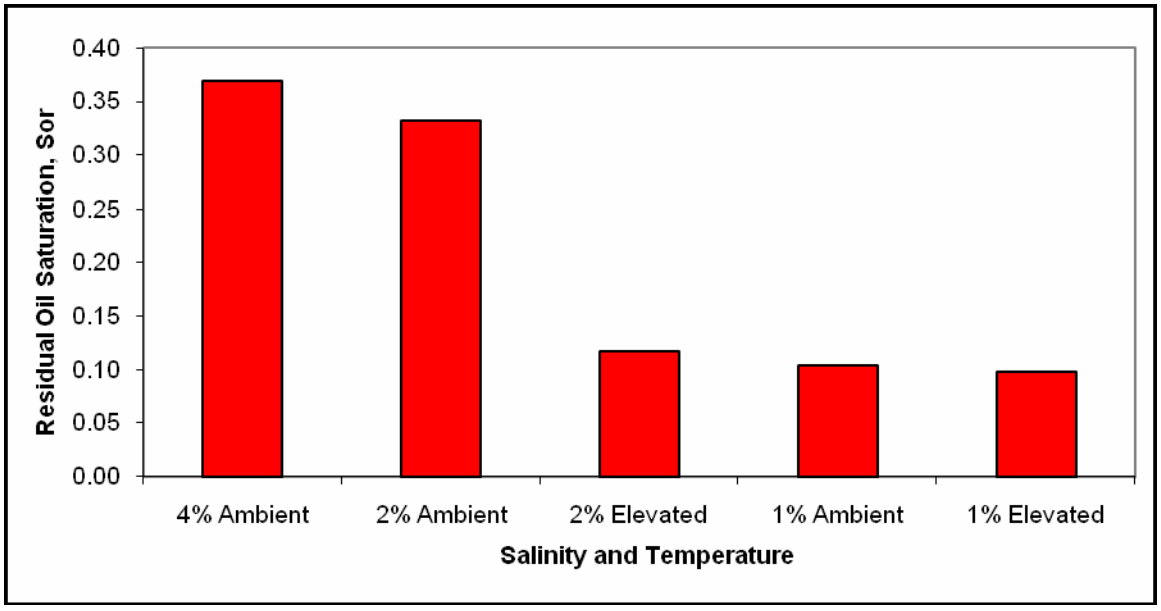

Figure 7.10: Effect of Brine Temperature and Salinity on S_{or} – Core Sample #4 (Berea/Crude Oil System).

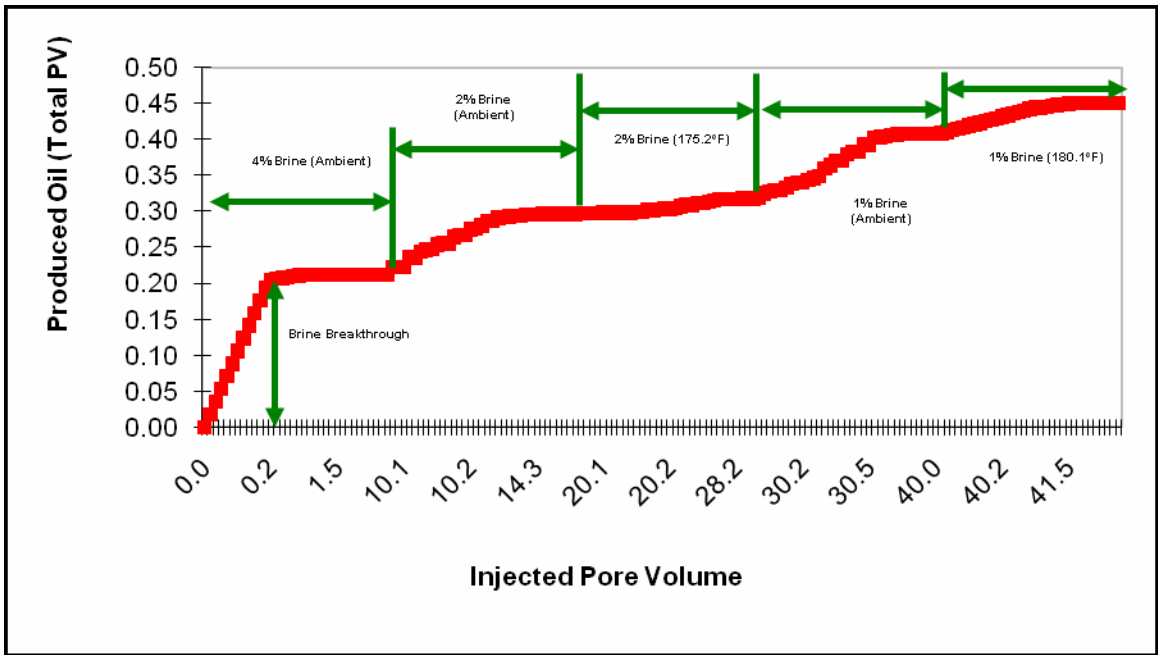

Figure 7.11: Effect of Brine Temperature and Salinity on Oil Recovery – Core Sample #5 (Berea/Crude Oil System).

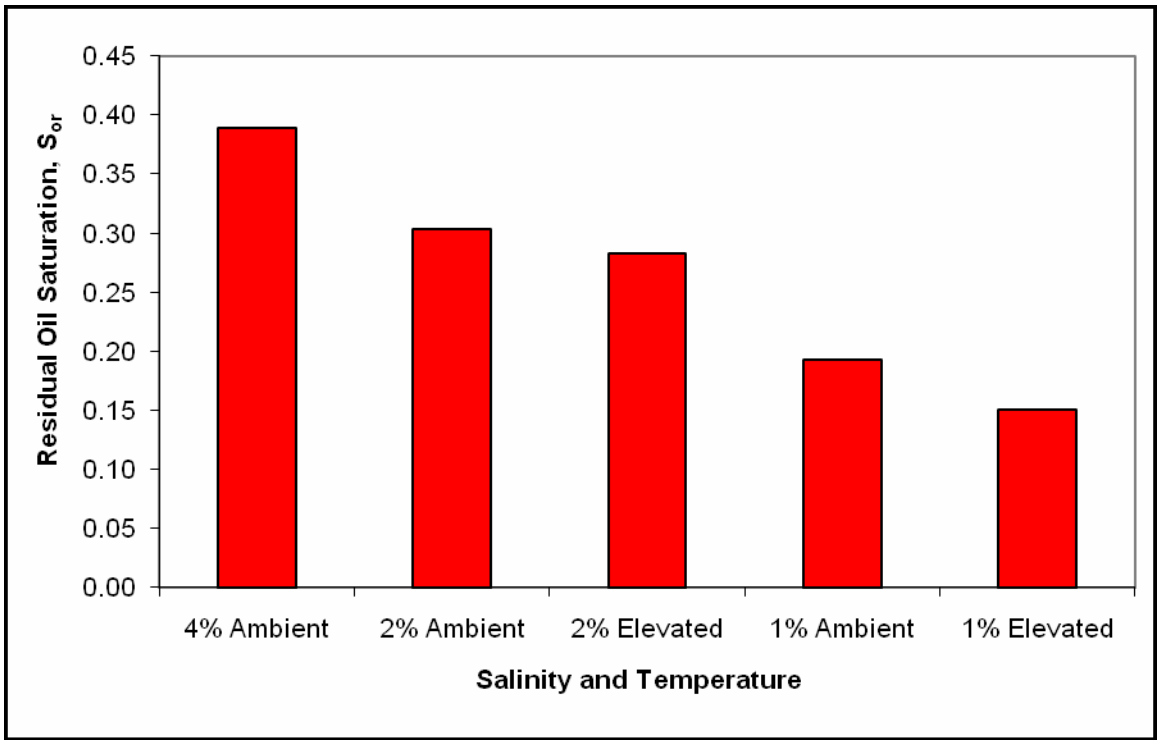

Figure 7.12: Effect of Brine Temperature and Salinity on S_{or} – Core Sample #5 (Berea/Crude Oil System).

Numerous research studies[89,90,91] have indicated that the performance of waterfloods is strongly affected by a number of variables which include the composition of the crude oil and its ability to wet the rock surfaces, the salinities of the connate water in the reservoir and the injected water from waterflood, the height above the oil/water contact, OWC (typically the reservoir rock becomes more oil-wet with increasing height above the OWC). For this first set of experiments, it is speculated that some form of wettability alteration to a mixed-wet state occurred because of the composition of the crude oil and the composition and salinity of the brine. Based on a static asphaltene deposition test conducted at UAF, it has been observed that the crude oil sample used in this first experimental study contains asphaltenes and it has been shown that the deposition of asphaltene onto the rock results in the alteration of wettability state of the reservoir rock. Before asphaltenes can be deposited on the rock surface, the thin stable films of water (brine) coating the water-wet rock grains have to be ruptured. The ability of the oil to rupture this film and thus deposit asphaltene compound on the rock surface depends on the value of the critical disjoining pressure of the water film bounded by mineral-water and the oil-water interfaces.

It is reported that in sandstone reservoirs, diffuse electrical double layer exists at the oil/brine and mineral/brine interfaces[97]. The rationale behind the formation of diffuse electrical double layers is explained hereafter (after Hall et al.[98]). Typically, at an interface, a charged layer may be formed by dissociation of ionogenic groups or by the adsorption of ions. Screening of the resulting ions is restricted to two dimensions and very high electrostatic-potential gradients are then established in the interfacial region. In an aqueous phase, such potentials are compensated by a distribution of counterions usually described as an electrical double layer[99]. It has been noted that in many cases, the diffuse electrical double layers will be quite similar with respect to electric charge and potential.

Consequently, extremely thin aqueous wetting films separating such interfaces are stabilized by electrostatic repulsive force acting between the double layers as a result of osmotic forces within the film. It has been recognized that for these thin films, the effect of osmotic or electrostatic forces is modified by the existence of both dispersion (or van der Waals) forces and hydration (or adsorption) forces. Whereas the very short range hydration forces tend to also stabilize aqueous wetting films, the dispersion forces tend to destabilize the film in question. The dispersion forces are attractive forces while the hydration and electrostatic forces are repulsive forces. For the

formation of stable films, the necessary condition is that the net effect of the force balance should be repulsive. Where stability of the water film is observed, the water-wet condition is promoted.

From the foregoing, it follows that increase in the salinity of the thin film of water will generate more ions resulting in a decrease in electrostatic repulsion because of screening of the surface charges. However, experimental observations[28,88] seem to indicate more stable brine films at higher salinities. Sharma and Filoco[91] attributed this "anomalous" observation to changes in hydrophobic/hydration forces with salinity. They opined that these forces become more repulsive as the salinity increases. It has also been shown (by direct measurement of the critical disjoining pressure, Π_{crit}) that Π_{crit} increases with salinity in some oil[91]. From the foregoing, that is, higher salinity brine resulting in higher film stability, it may be said that lowering the salinity of the brine will result in unstable brine film (which in turn lowers the value of the critical disjoining pressure) resulting in the rupture of the brine film. The value of the critical disjoining pressure depends on a number of other variables that include the mean radius of curvature of the rock grain. Consequently not all the rock grains will "dewet" leading to selective dewetting of the rock matrix and the formation of mixed-wet condition within the core. Research studies[38,83] have shown that the formation of a mixed-wet condition leads to lower residual oil saturation and higher oil recoveries. This may most likely explain the mechanism of the improved recoveries observed with reducing the brine salinity for this first set of experiments.

The observed increase in recovery with increase in temperature may be due additionally to reduction in the viscosity of the crude oil. Experimental studies[100] carried out in Petroleum Development Laboratory, University of Alaska Fairbanks (UAF) have reported the viscosity dependence of similar samples of crude oil on temperature. **Figure 7.13** shows the result of one such experiment[100] carried out at UAF on TAPS blend of crude oil. From the plot it is seen that increasing the temperature of the crude oil from room temperature (22°C) to an elevated temperature value of 50°C results in a viscosity reduction of the oil by 70%.

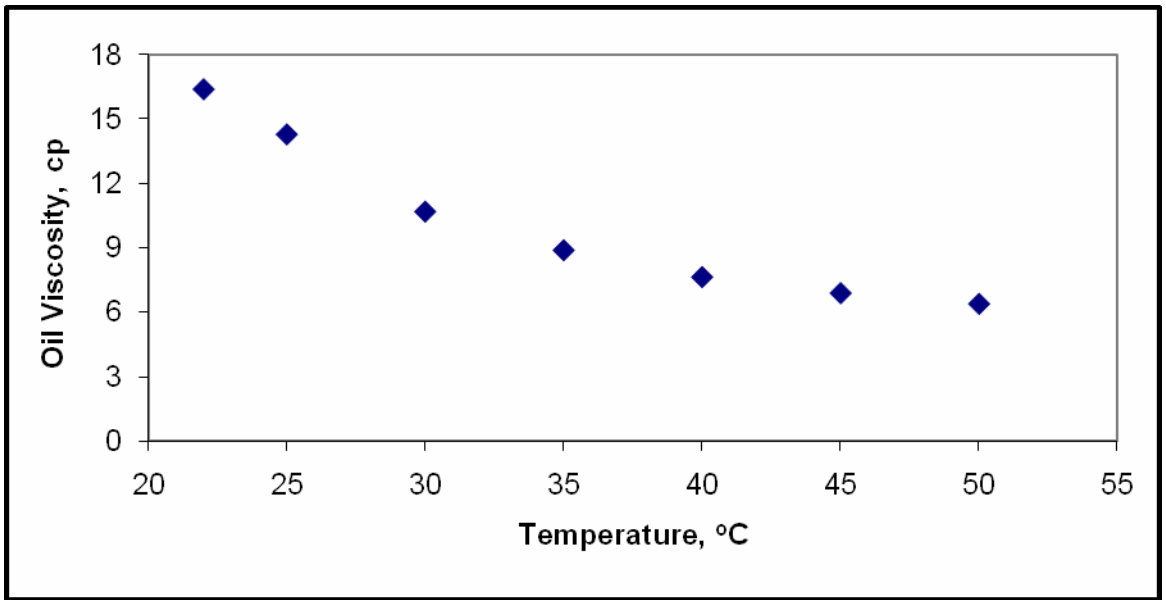

Figure 7.13: Viscosity Dependence of TAPS Crude Oil Blend on Temperature[100].

Laboratory studies have also indicated that some residual oil held in place by capillary forces can be displaced if favorable changes in viscous forces are made. Moore and Slobod[66] presented the effect of change in viscous forces on mobilization of trapped oil for Torpedo and Berea sandstones. They reduced the oil/water viscosity ratio (μ_o/μ_w) from 1.0 to 0.055 while leaving the flowrate constant at the typical waterflood rate of 2 ft/D. They observed additional oil recovery equal to 1.41% of the core pore volume for the Berea sandstone core. They also showed that the impact of viscosity reduction on oil recovery efficiency is more pronounced when trapping of the oil has not yet occurred.

7.4 Secondary Oil Recovery Potential of Low-Salinity Waterflood at Ambient and Elevated Temperature

The second set of experiments examined the impact of wettability alteration on reduction in the core residual oil saturation, S_{or} and the secondary oil recovery potential of low-salinity brine injection at ambient and elevated temperatures. In the initial design of the second set of experiments, it was desirable to carry out similar experimental studies as in the first set of experiments and thus validate the suspected alteration of wettability to a mixed-wet condition. However, several factors militated against this initial design. These factors included

1. The need to determine the wetting state of the core at the end of each coreflood (based on varying the waterflood salinity and temperature) required that different core samples be used for each test. Alternatively, the same core plug could be used but reconditioned to the same initial condition at the start of each experiment.

2. The lack of "fresh" Berea core samples meant that alternative core samples had to be obtained.

3. The high viscosity of the TAPS crude oil (8.24 cp) interfered with the accurate measurement of wettability using the Amott-Harvey Method. The observed interference included (1) "surface coating" of the core plug by oil (during spontaneous displacement of water by oil) which gives erroneous mass measurement when calculating for the volume of brine spontaneously displaced; (2) formation of crude oil "bubbles", by the spontaneously displaced oil, on the surface of the core (during spontaneous displacement of oil by water). Adoption of the approach described Morrow (immersing the core in oil and then back in the brine) resulted in "surface coating" of the core plug which appeared to aggravate the problem of formation of crude oil "bubbles".

Based on the forgoing the initial experimental design of the second set of experiments was modified. The crude oil blend from TAPS was replaced with refined oil (decane). The problem with using decane was in differentiating produced oil from produced water since both fluids are colorless. This problem was solved by spiking decane with some TAPS oil. Initial trials at spiking the decane with oil showed the settling of some substance, suspected to be some of the heavier components of the TAPS blend, after the spiked decane was left standing for some time. A further problem was observed when the spiked decane was injected through the core, which acted as a filter resulting in the formation of a residual filter-cake of the heavier components on the injection face of the core plug. This resulted in unexpected and erratic increase in pressure drop across the core plug. It was initially suspected that mixing the decane with the TAPS crude oil resulted in some form of asphaltene precipitation. However, a static asphaltene precipitation test using decane showed no asphaltene precipitation with decane. Subsequent reduction in the ratio of TAPS oil to decane by a trial-and-error process resulted in a significant reduction of this problem.

To solve the problem of the lack of "fresh" Berea sandstone samples, alternative core plugs were obtained from the archives of the Alaska Department of Natural Resources (DNR). As has been mentioned, these core plugs were from Conoco (BP) Milne Point Unit KR L-01. The incentive for using these plugs was that they were from ANS. However, the size of the core plugs (1"diameter x 1.5" length) was of major concern, in terms of the resultant impact on the experimental outcome. The option of stacking the two or three core plugs together was considered but was not used because of the anticipated complication during the wettability characterization phase. It was anticipated that errors would be introduced during the spontaneous displacement phase of the Amott-Harvey index characterization, because additional fluids would imbibe and/or be displaced from the individual faces of the composite cores. In addition measurement of the absolute permeability would be influenced by how well-meshed the adjoining faces of the stacked cores were during the brine displacement through the stacked core plugs.

Each of these floods was started at the same initial condition (oil-saturated core at irreducible water saturation). This allowed the measurement of the core wettability at the end of every coreflood. Similar values of the irreducible water saturation were obtained for all the floods. In order to normalize the effect of varying initial water saturation, if any, the oil recovery is shown as percentage of oil initially in place. **Figure 7.14**, **Figure 7.15**, **Figure 7.16**, **Figure 7.17** and **Figure 7.18** show the effects of brine temperature and salinity on the waterflood oil recovery profile. For all cases, the production of only decane was observed until water breakthrough, after which no further oil production was observed. This phenomenon is due to the initial core treatment, which is believed to have rendered the core "strongly" water-wet; the initial wettability indices (I_{AH}) of all the cores were between 0.77 and 0.90. One notable characteristic of water-wet systems is the absence of further oil production after water breakthrough because of piston-like displacement of oil by the water.

Waterflood displacement in a water-wet system is assumed to be piston-like as a result of favorable capillary pressure effect. As has been stated, in water-wet cores stable films of water are found around the sand grains. Consequently, the oil phase occupies the pore spaces in between the water films, that is, the large pore spaces. When water is injected at one end of the core, it easily imbibes into the large as well as the very small pores displacing the oil from the

small pores into the very large pores. The fact that water can imbibe easily into the very small pores (as well as the large pores) results in very efficient displacement since bypassing of the oil is minimized. This concept may be developed further by considering what happens when a water-wet core at connate water saturation is immersed in water. Upon immersion, water will spontaneously imbibe into the core plug because of favorable capillary forces at play. If the core is immersed long enough, water will spontaneously displace the oil to residual oil saturation.

A simplistic one-dimensional representation of the waterflood displacement of oil from a water-wet rock is obtained by combining the Buckley-Leverett frontal advance model and the solution to the fractional flow equation. It is shown that upon injection of water only oil is produced until water breakthrough, when the additional volume of produced oil is at the expense of increasing water-cut/water-oil ratio (WOR). An observation of the production characteristics shown in **Figure 7.14**, **Figure 7.15**, **Figure 7.16**, **Figure 7.17** and **Figure 7.18** shows continuous production of oil until water breakthrough. The observed situation where little or no oil is produced after breakthrough of water may be explained by understanding the trapping mechanism in water-wet systems.

Many models[60,101,102,103] have been proposed to explain the isolation and trapping of oil in water-wet pores. One such model, the Jamin Effect, has been discussed by several authors[101] and presents oil trapping in a single capillary as a result of variation in pore size, contact angles, and interfacial tension (IFT) between the wetting and non-wetting phase. While this model does not have the complexity of actual reservoir rock, it does provide a basis for analyzing the model of interest in this work for explaining the observed absence of further oil production after breakthrough—the pore-doublet model[60,103]. The analyses of the pore-doublet model presented in this work are summarized from Willhite[60].

The pore-doublet model tries to represent the complexity of the porous media by considering fluid flow in two connected parallel capillaries having different radii, r_1 and r_2. One of the capillaries has a smaller radius, and for the purpose of this work, r_1 will be assumed to be smaller than r_2. Even though the pore-doublet model still lacks the complexity of actual variation of the reservoir rock pore network, size and distribution it illustrates the concept of a varying pore size network through which fluids can flow (i.e., concept of differential flow channels). The initial

conditions of the pore doublet are (1) both pores are considered water-wet and (2) both pores (and the pore-doublet outlet header) are completely saturated with oil. The pore doublet is connected to common inlet and outlet headers.

To illustrate the waterflood process, water is injected into the inlet header/pipe and oil is displaced simultaneously from both pores. This is a simplified representation of what happens when water is injected in a water-wet core and imbibes into the small and large pore spaces respectively displacing oil from these pore spaces. For ease of analysis, the viscosities and densities of the oil and water phases are assumed equal. For oil to be trapped in any of the pores in this displacement process, it is expected that (1) the displacement of oil will proceed faster in one of the pores than the other and (2) there is insufficient pressure gradient to displace the trapped oil drop from the pore having the lower displacement rate. It has been shown[60] that for a typical displacement condition, the displacement rate proceeds faster in the smaller pore and the oil is trapped in the larger pore once the oil is completely displaced from the smaller pore. Before complete displacement of oil from the smaller pore, pressure drop across the pore doublet is a combination of pressure drop because of capillary forces and pressure drop due to viscous forces.

After the oil is completely displaced from the smaller pore, the pressure at the outlet end decreases (because of the absence of capillary forces in the smaller pore) such that the inlet pressure is now larger. At this point, the oil in pore two is cut off/isolated by the water flowing through the smaller pore and thus exists as an isolated globule of oil. If a constant velocity of flow is maintained in the smaller pore, the pressure drop because of friction pressure loss in smaller pore is now available to force the trapped/isolated oil drop in the larger pore. This will cause some movement of the oil phase, which in turn will result in the variation of the advancing versus receding contact angles. Such variation in the contact angles results in the trapping of oil as a result of the *Jamin Effect*. Though the pore-doublet model is not an exact representation of a porous medium it does incorporate the mechanism of competing flows in parallel flow channels that exist in the reservoir rocks. As has been indicated the isolation of oil in larger pores (where water is the wetting phase) is a result of non-uniform flow because of capillary forces. The trapped/isolated oil phase is strongly held in place by capillary forces that cannot be overcome by the relatively small viscous force which is available. Once the oil is isolated, it becomes

trapped by capillary forces such that once water breakthrough occurs, little or no oil production is observed.

Examination of the plots from the experiments shows that incremental oil is recovered with a decrease in brine salinity and/or an increase in temperature of the displacing brine. This increase is not very significant, however, in comparison with the observed recovery with the Berea sandstone cores. It is suspected that this observation may be due to the very small size of the cores used in this second-set of experiments; all the cores have diameters ≈ 1 in. and lengths ≈ 1.5 in. The trapping of oil in a porous medium, and thus its overall recovery, has been shown to be a function of pore size and pore-size distribution. Consequently, the reduced length of the core sample used in this experiment is believed to have impacted oil recovery because of reduction in complexity of the pore distribution and the *multiplier effect* (on any error) due to the small core size. This concept can be illustrated by considering the presence of two (or more) discontinuous streaks of shale, laterally displaced, of lengths 0.6 in. and 0.8 in., respectively, in any of the core samples. The impact of the shale streaks on the observed production characteristics will be more pronounced in a 1-in. diameter core with a length of 1.5 in., compared with a second core either having the same diameter as the first core but much longer length (about 4 in.) or having a larger diameter (1.5 in.) and a slightly longer length (2.5 in. or more). As was reported, the presence of shale streaks was observed in the cores sourced from DNR archives.

Blown-up inserts are included in all the plots (**Figure 7.14**, **Figure 7.15**, **Figure 7.16**, **Figure 7.17** and **Figure 7.18)** to aid in the visual observation of the recovery profile. The general trend observed in all experiments is that injection of low-salinity waterfloods (2% and 1% salinities) results in higher volume of recovered oil compared to the high-salinity waterfloods (4% salinity); additionally, increasing the temperature of the injected water results in increased recoveries for the high-salinity and low-salinity brines.

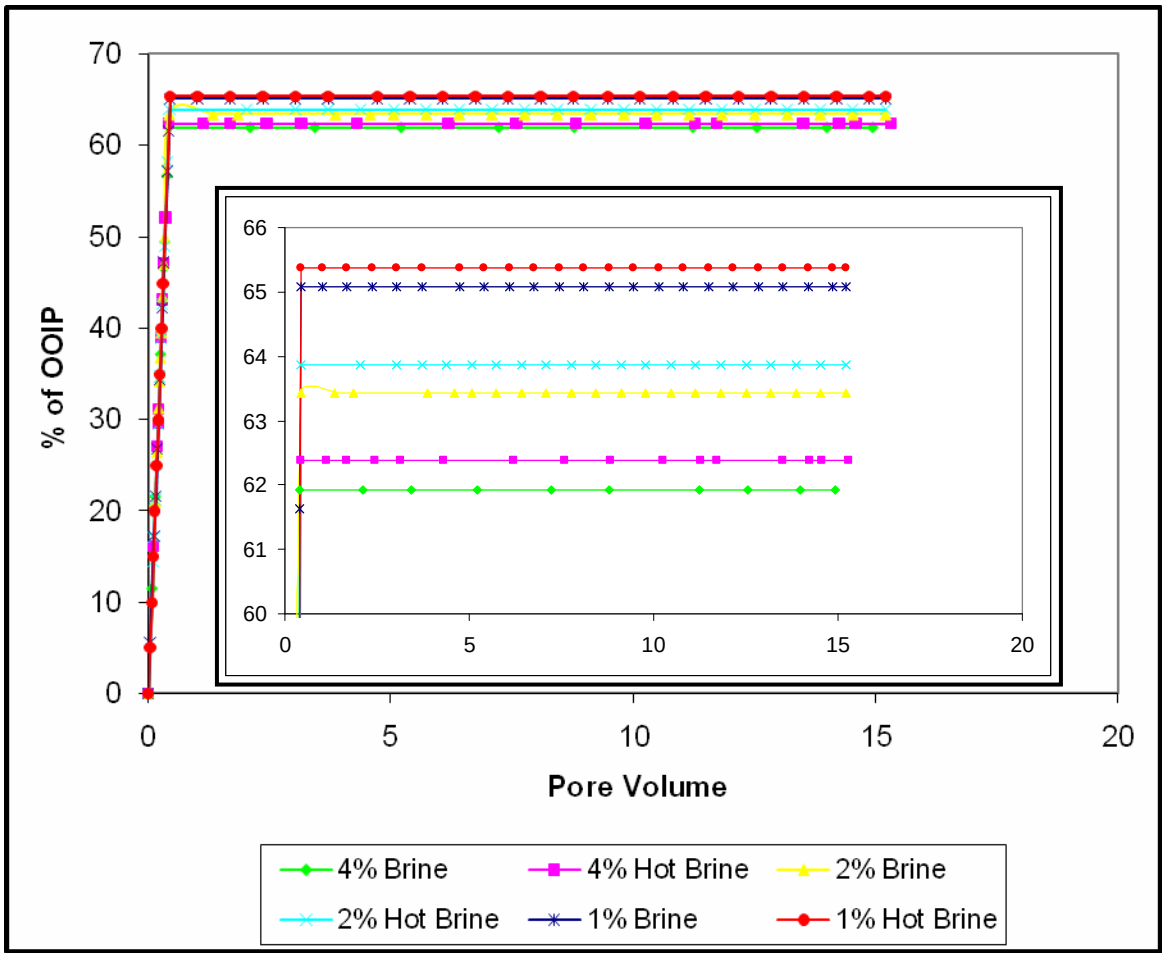

Figure 7.14: Oil Recovery Profile - Temperature and Salinity Effects, Core Sample #1 (DNR Cores/Decane System).

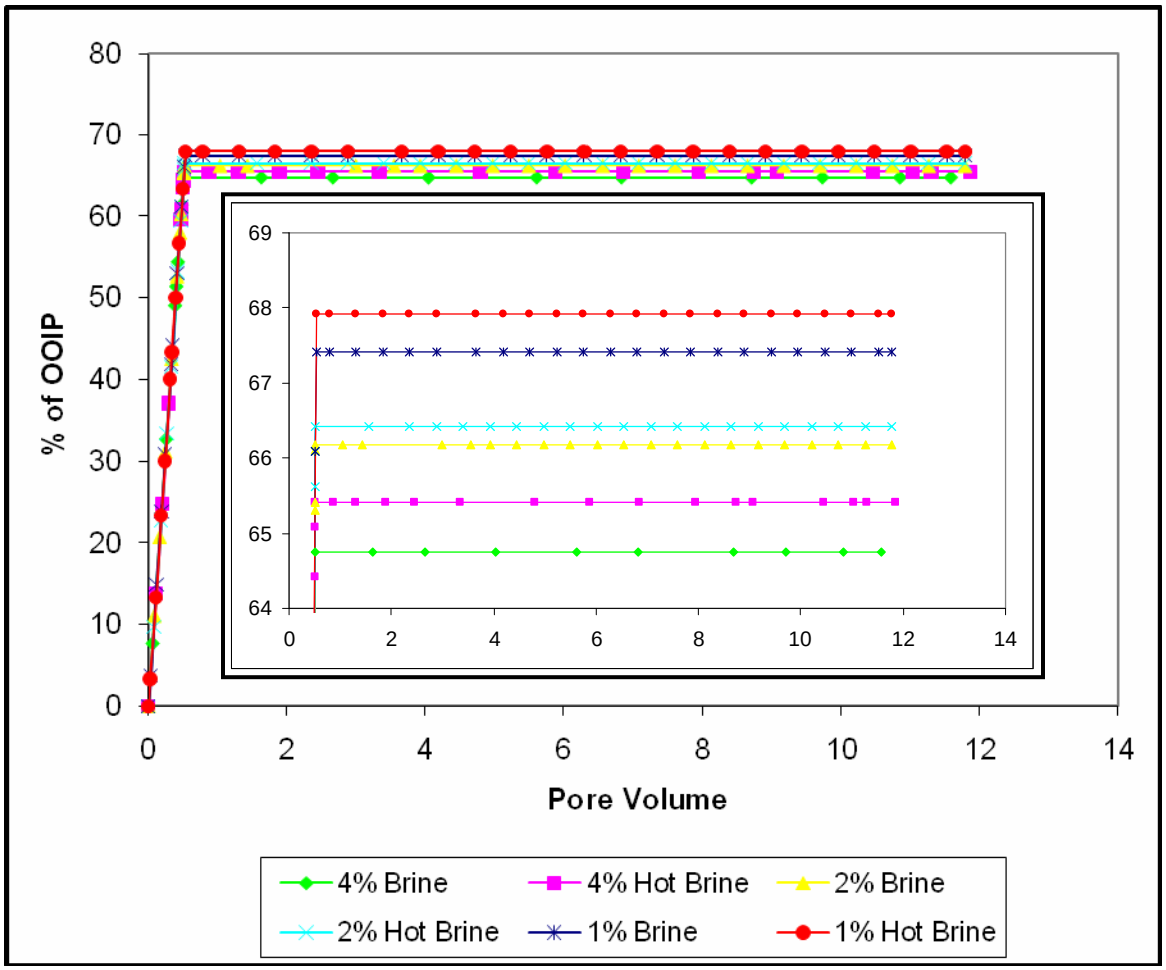

Figure 7.15: Oil Recovery Profile - Temperature and Salinity Effects, Core Sample #2 (DNR Core/Decane System).

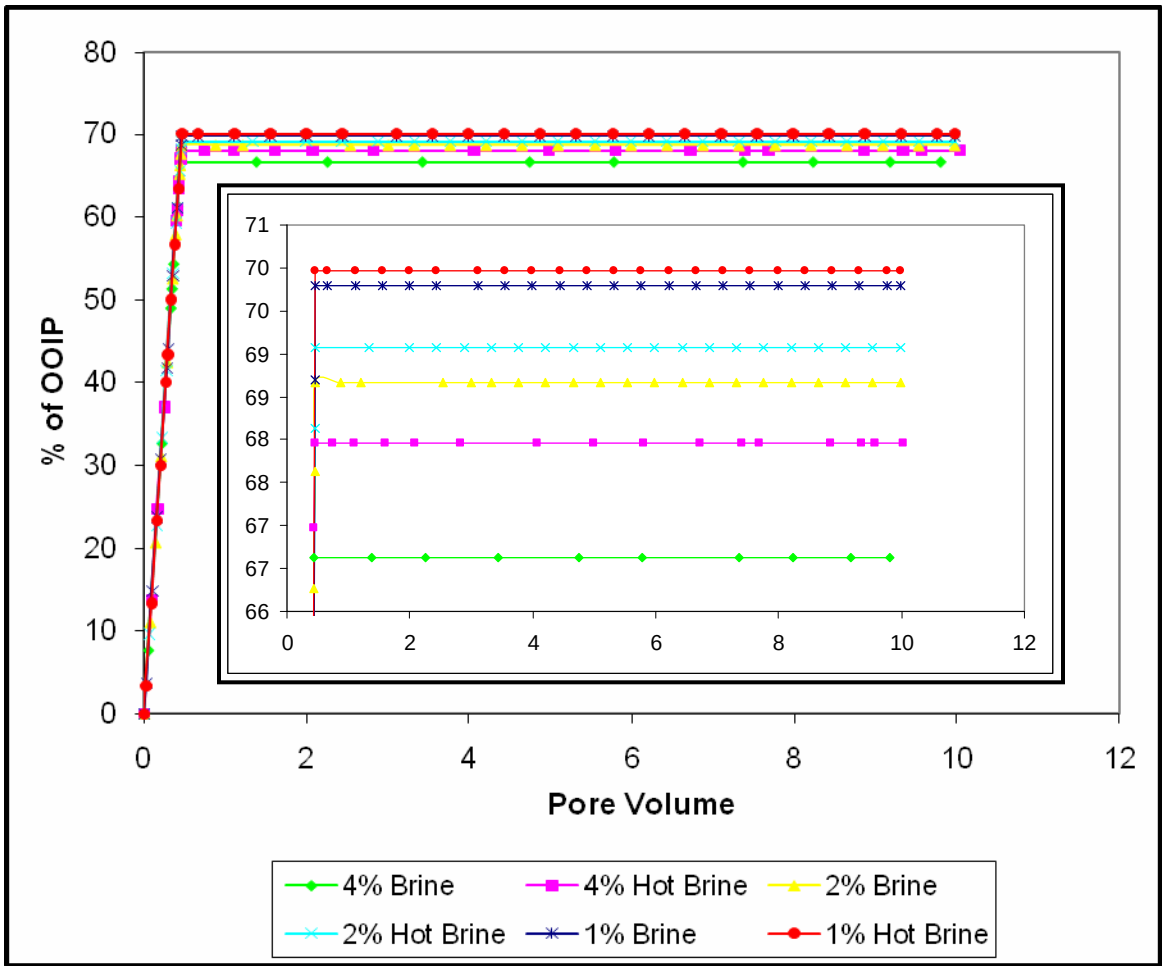

Figure 7.16: Oil Recovery Profile - Temperature and Salinity Effects, Core Sample #3 (DNR Core/Decane System).

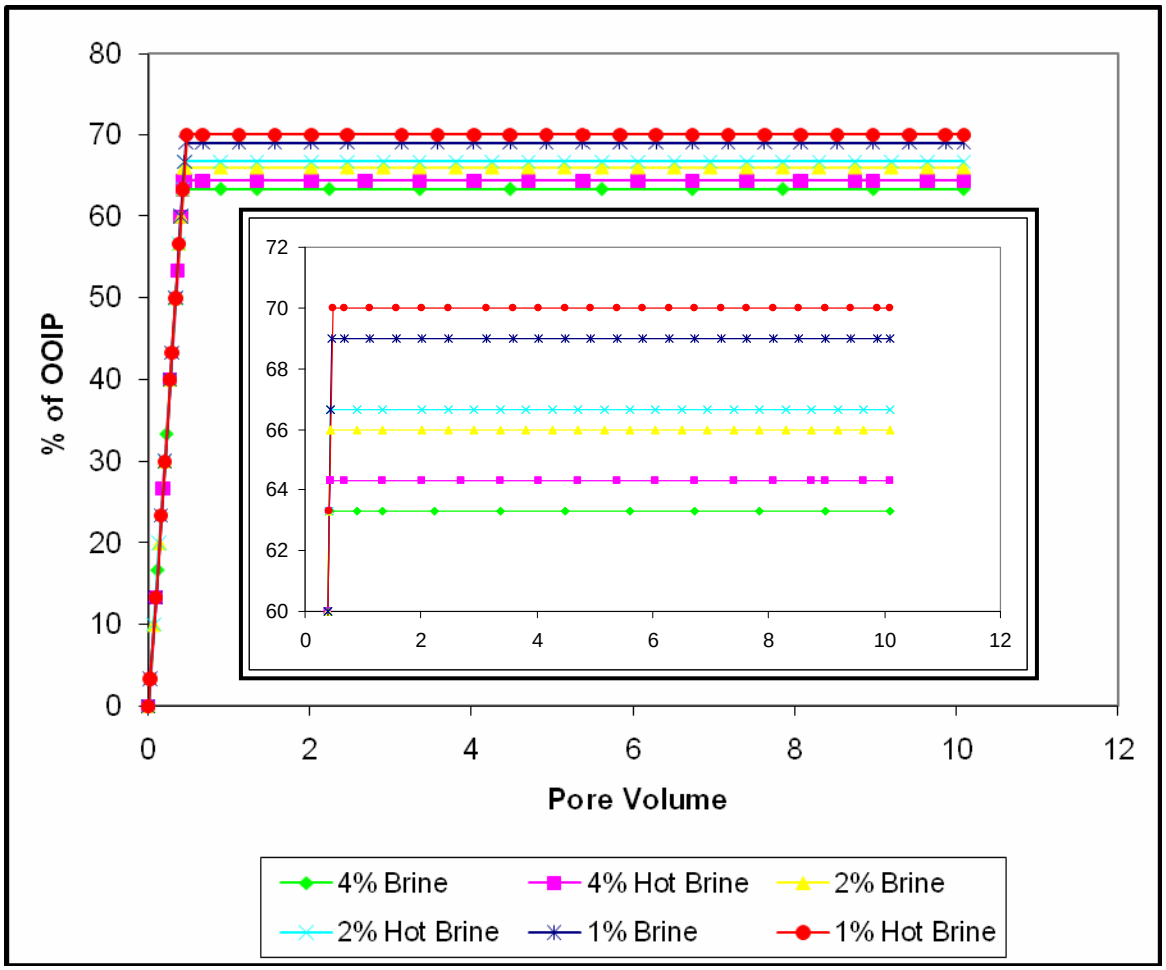

Figure 7.17: Oil Recovery Profile - Temperature and Salinity Effects, Core Sample #4 (DNR Core/Decane System).

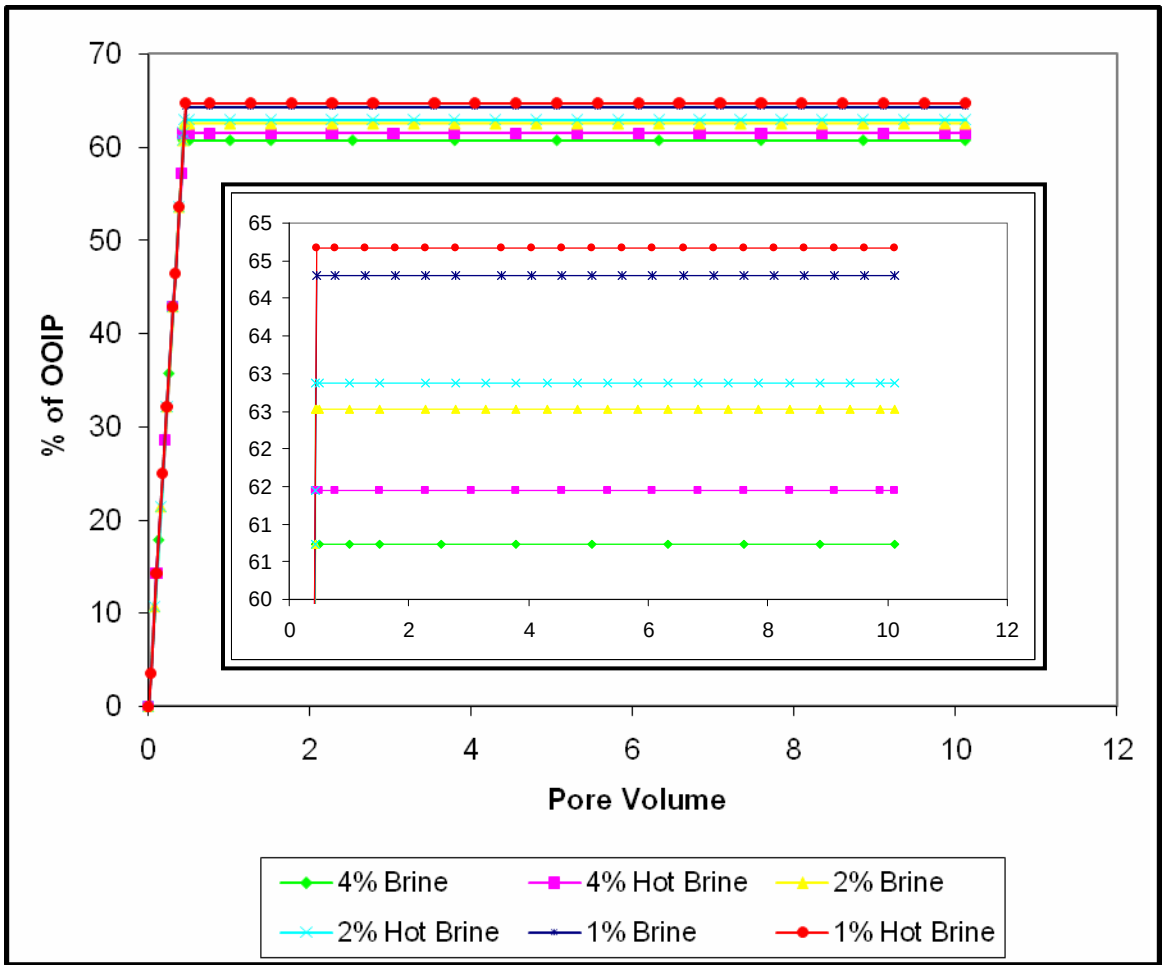

Figure 7.18: Oil Recovery Profile - Temperature and Salinity Effects, Core Sample #5 (DNR Core/Decane System).

7.5 Impact of Low-Salinity Waterflood (Ambient and Elevated Temperatures) and/or Variation in Wettability on Residual Oil Saturation

Other studies on observed waterflood recoveries have reported increases in recovered oil volume and/or recovery efficiency for various wetting conditions, which include (1) a shift towards the strongly water-wet condition[51]; (2) a shift towards intermediate/neutral wettability[66,67,68,69], and (3) the mixed-wet condition[38]. Consequently, it is believed that the observed incremental oil recovered and thus reduced S_{or} may be due to some changes in wettability. To confirm this dependence of oil recovery efficiency on wettability and wettability variation, the wetting states of all the core samples were determined after each run using the Amott-Harvey wetting index.

Figure 7.19 to **Figure 7.23** show the variations in the values of the Amott-Harvey wettability index and the residual oil saturation with changes in brine salinity and temperature.

The general observed trend is a reduction in S_{or} and an increase in the Amott-Harvey wetting index with decrease in salinity of the injected brine and increase in the brine temperature. A deviation in the initial wettability index trend was observed in one of the experiments and the result is presented in **Figure 7.22,** which shows a decrease in the wetting index after high-salinity waterflood at elevated temperature. Though the immediate reason for this deviation is unclear, it is suspected that it may have been because of some measurement noise/error introduced by the very small size of the core. However, the general trend after this deviation corresponds to the observed trends in the other similar experiments in this work.

The observed results seem to indicate that for this set of experiments, the decrease in residual oil saturation corresponds to an increase in water-wetness. Similar observations of an increase in the water-wetting nature of the core sample with a decrease in brine salinity have been reported[89,90]. Tang and Morrow[89] carried out exploratory studies to determine the effect of cation valency and salinity on core wettability and oil recovery for selected crude oil/brine/rock (COBR) systems. All the waterflood studies showed improved oil recovery with decrease in brine salinity for monovalent (NaCl) and divalent ($CaCl_2$) brine systems. For both systems, they observed that the increase in oil recovery with reduction in brine salinity corresponded with an increase in the wettability of the cores towards increased water-wetness. The reason for this trend is not clear (it was anticipated that an increase in oil recovery would be a result of a decrease in the water-wetting nature of the core sample) and attempts to explain this trend using the Derjaguin, Landau, Verwey, and Overbeek (DLVO) theory has limited success. Tang and Morrow[87] hypothesized that the increase in recovery they observed in their experiment was related to the transfer of a fraction of the fine particles from the rock walls to the oil-water interface during the course of displacement.

As has already been indicated in this work, wettability alteration in COBR systems depends on the composition of the crude oil in addition to the salinity and pH of the brine. The importance of the oil composition lies in the fact that the wetting-state modifying components such as asphaltenes, high molecular-weight paraffins, porphyrins, acids, and bases (which determine the

system pH) are constituents of the crude oil. The role of brine in mediating adsorption from the crude oil has already been explained. The oil phase used in the second set of experiments is refined oil (decane spiked with a very small quantity of TAPS crude oil blend). Consequently, it is not anticipated that wettability alteration will be by the adsorption onto the core surface of any heavy fraction from the crude oil. Though the pH of the system was not measured, it is suspected that the pH will be close to neutral. Ionization of the NaCl brine in solution does not affect the pH of the system since the ions do not react with the water to form weak acids or weak bases. The decane does not contain any acidic or basic components, and it is expected that the low mixing ratio (TAPS oil to decane) will minimize the effect of any acidic or basic constituent in the TAPS oil.

Consequently, it is conceivable that, in this case, the variation in wettability and reduction in ROS is not a result of the aforementioned mechanisms/variables. Unfortunately, none of the published results where similar trends on wettability change towards increasing water-wetness with reduction in injected brine salinity have been able to explain the reason for this observed trend. It is suspected that the observed increase in water-wettability may be a result of minute production of fines that may have been oil-wet sites. This will result in an increased volume of water that will spontaneously imbibe into the core and/or a reduction in the total volume of water that will be displaced spontaneously by oil. The outcome of this is an increase in the value of the Amott-Harvey wettability index.

Another observation made on the wettability variation shows that the variation in the wettability index is not very significant. The observation made by Tang and Morrow[89] on the variation in wettability towards increasing water-wetness also showed similar cluster of the endpoint wetting-state value using the spontaneous imbibition measurement of wettability discussed by Ma et al.[27]. It is pertinent to note that there may be no basis for comparing the two results, in terms of the endpoint cluster of the wetting indices for the different cores, as the wettability determination methods used are based on two different approaches. In addition, the experimental conditions were different as were the fluid and core systems for the two experiments. It is possible, though unsubstantiated, that the brine salinity may have influenced the extent of wettability variation in both cases.

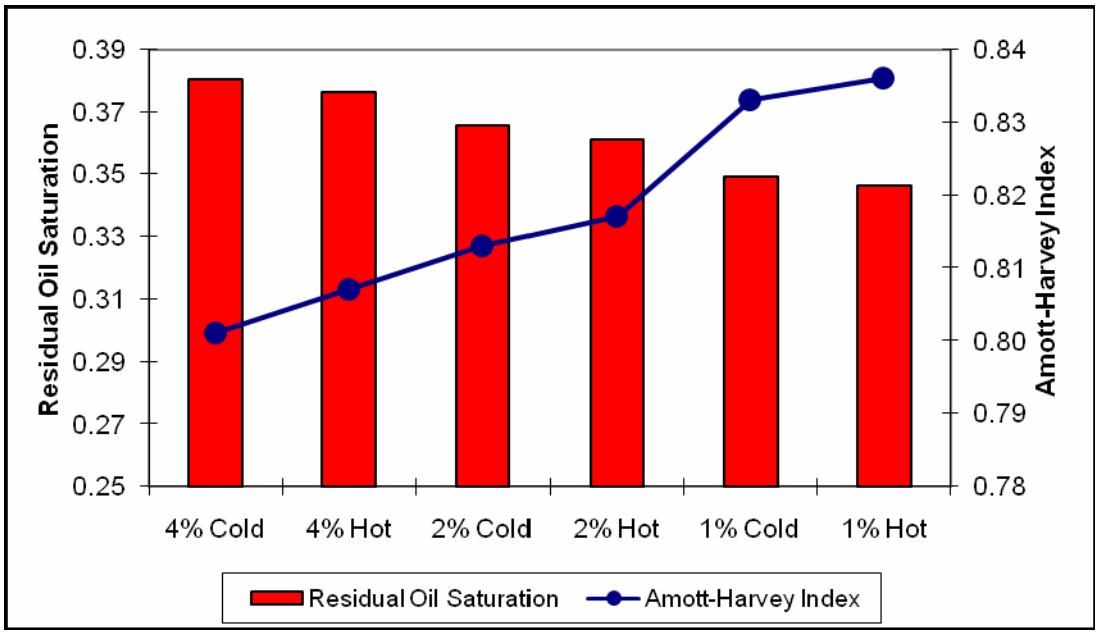

Figure 7.19: ROS - Temperature and Salinity Effects on Wettability, Core Sample #1 (DNR Cores/Decane System).

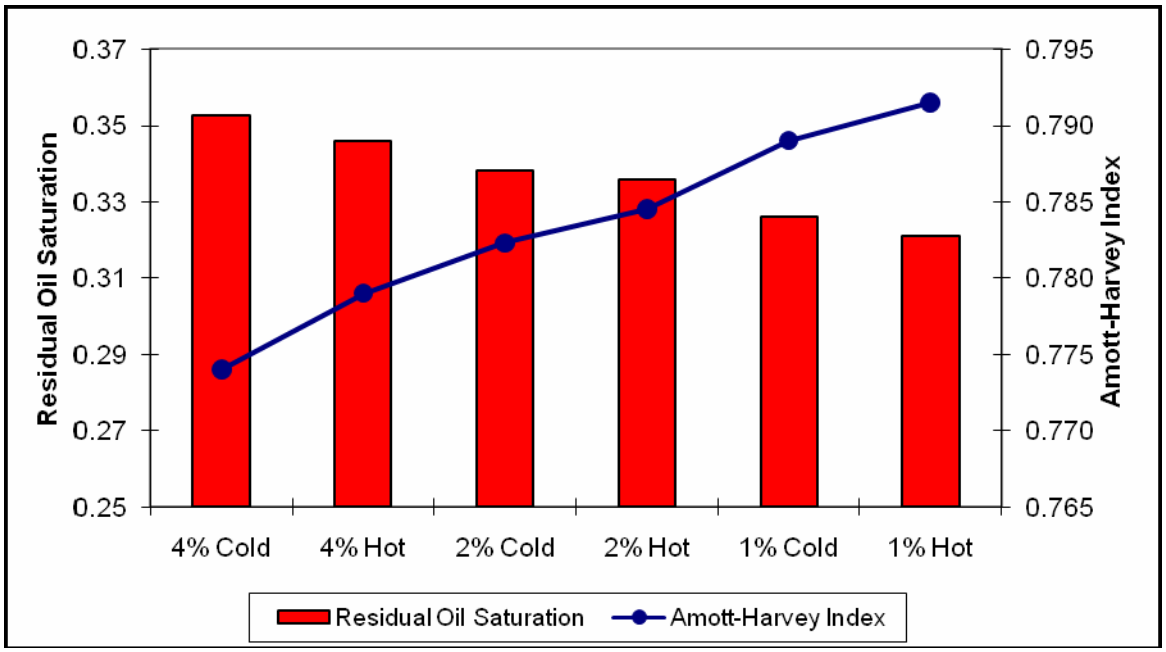

Figure 7.20: ROS - Temperature and Salinity Effects on Wettability, Core Sample #2 (DNR Cores/Decane System).

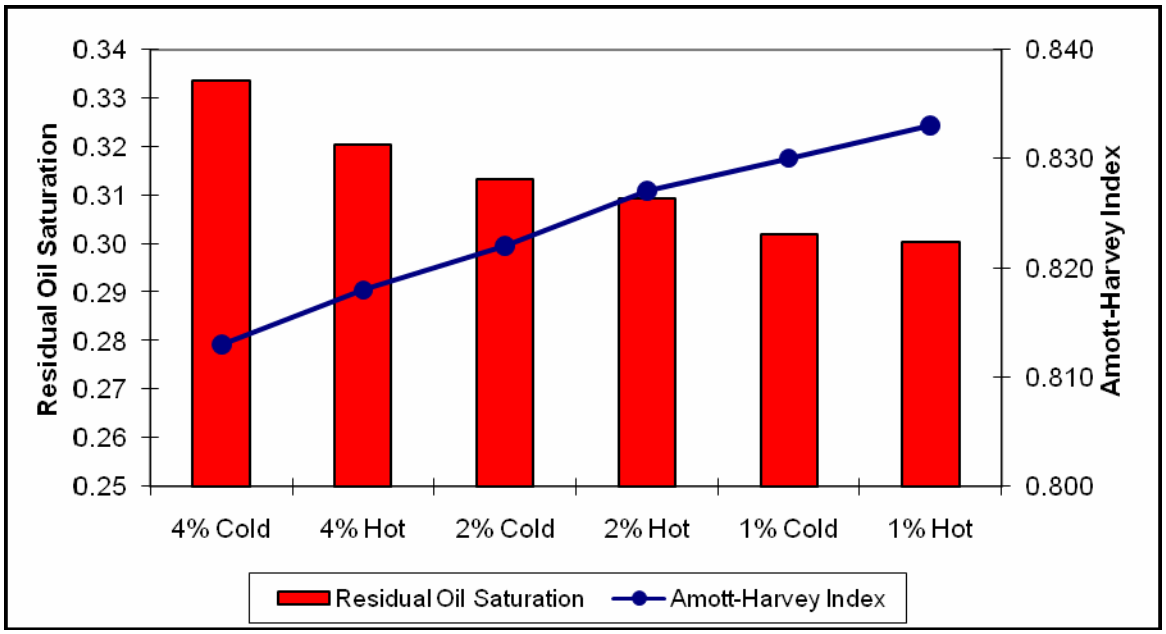

Figure 7.21: ROS - Temperature and Salinity Effects on Wettability, Core Sample #3 (DNR Cores/Decane System).

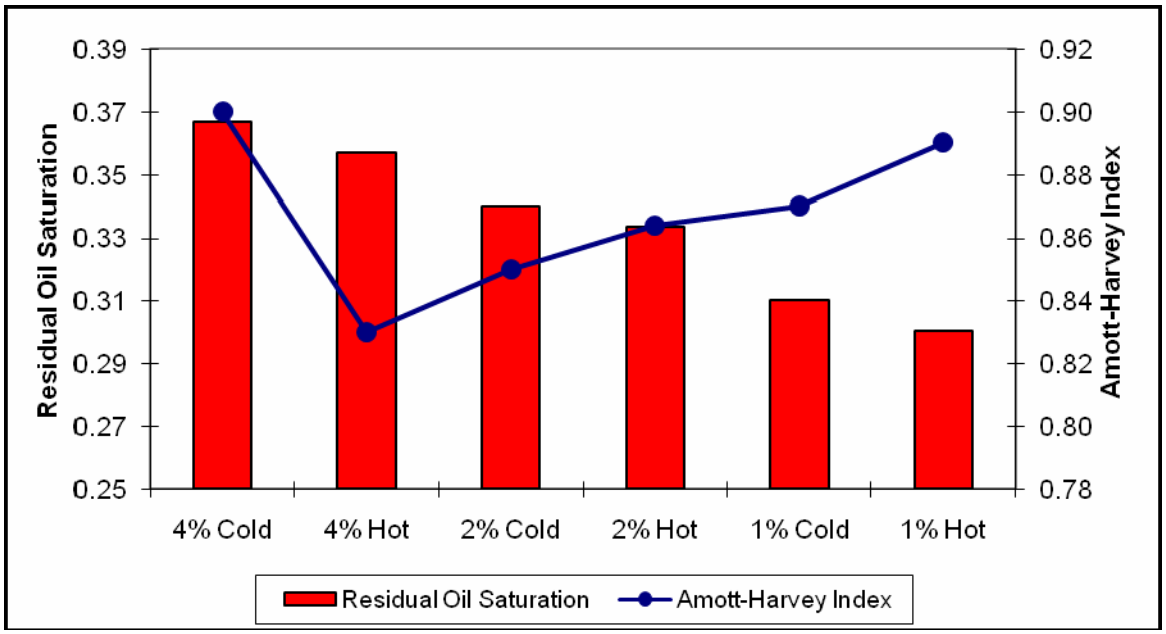

Figure 7.22: ROS - Temperature and Salinity Effects on Wettability, Core Sample #4 (DNR Cores/Decane System).

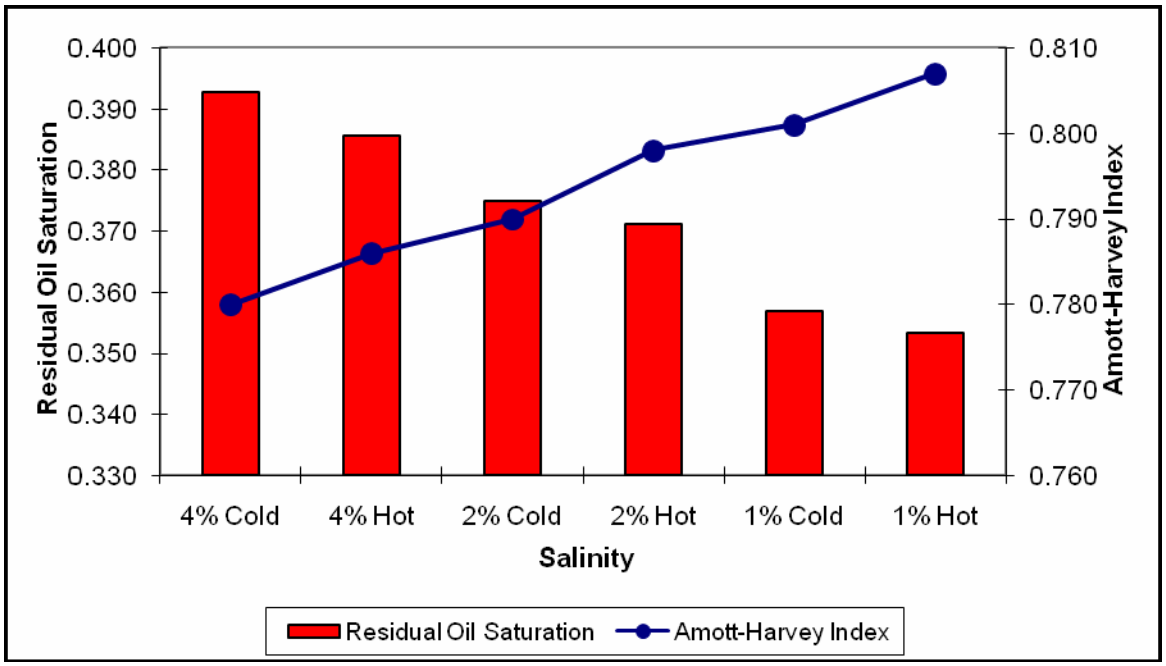

Figure 7.23: ROS - Temperature and Salinity Effects on Wettability, Core Sample #5 (DNR Cores/Decane System).

CHAPTER 8: Results and Discussion – Representative Cores

In all the three sets of experiments, the potential of the low-salinity brine injection in secondary oil recovery was examined. For all three sets, an attempt was made to commence all the coreflood experiments at the similar initial condition; that is, the cores were at initial oil saturation (S_{oi}) and interstitial/connate water saturation (S_{wi}). An attempt is also made to explain any observed increase in recovered oil volume and reduction in residual oil saturation (S_{or}) in terms of change in wettability using the Amott-Harvey wettability index. The connate water salinity of the all the set of experiments was kept constant at a "high" salinity of 22,000 TDS in order to mimic the reservoir saturation conditions.

In most of the experiments, it is observed that there was an increase in oil recovery with a decrease in the salinity of the injected brine. Thus, more oil is recovered when brine of a lower salinity is injected. It is encouraging to observe, in most of the experiments, a more or less consistent trend.

For the first sets of experiments, (i.e., on new [clean] cores), waterfloods were carried out using all the three brines viz. 22,000 TDS, 11,000 TDS and 5,500 TDS. After every waterflood, the Amott-Harvey wettability index and residual oil saturation value were calculated. For the second set of experiments, the cores used were the same cores on which previously the first set of experiments had been carried out. But before using these cores for the second set of experiments, these cores were oil aged for 21 days. Similar to the first set of experiments, waterfloods were carried out on these oil aged cores using all the three brines viz. 22,000 TDS, 11,000 TDS and 5,500 TDS. After every waterflood, the Amott-Harvey wettability index and residual oil saturation value were calculated.

For the third set, experiments were carried out on new (clean) core samples. As stated earlier, waterfloodings were carried out using 22,000 TDS salinity brine and ANS lake water. Similar to the first two sets of experiments, after every waterflood the Amott-Harvey wettability index and residual oil saturation value were calculated.

8.1 Experiment on New (Clean) Cores

Figure 8.1 shows that when new (clean) Core E was waterflooded with 22,000 TDS brine the Amott-Harvey wettability index (I_{AH}) was observed to be 0.320. As the brine salinity decreased to 11,000 TDS, I_{AH} value increased to 0.330. Finally, I_{AH} value increased to 0.350 when waterflooding was done with 5,500 TDS brine.

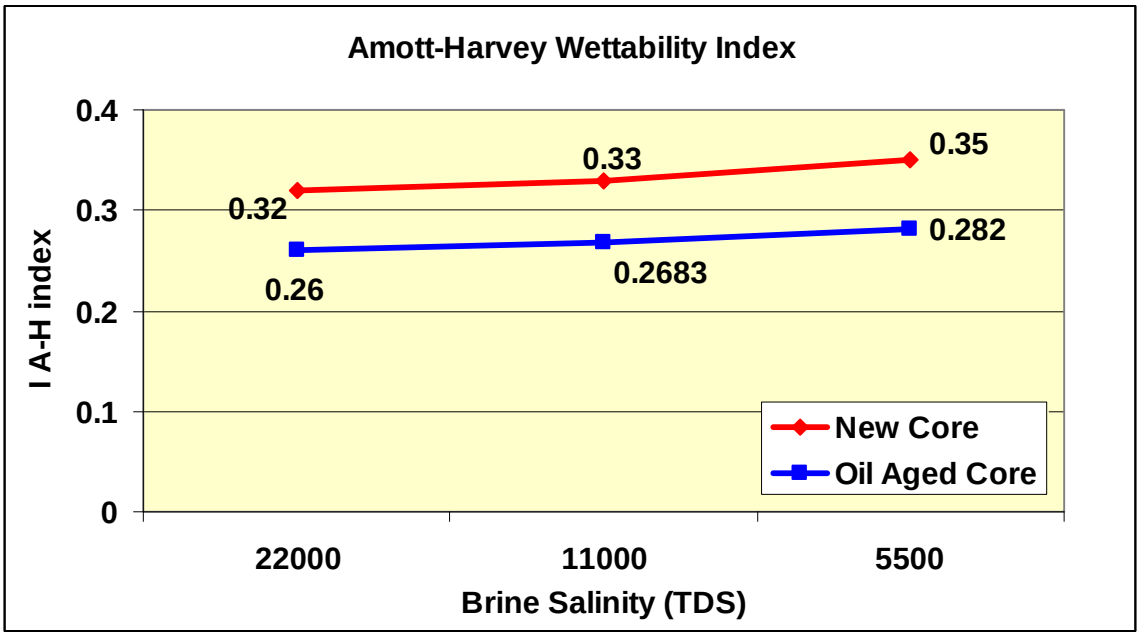

Figure 8.1: Effect of Brine Salinity on Wettability (Core E).

The Amott-Harvey wettability index (I_{AH}) is used to characterize the wettability of the cores. From **Figure 8.1**, it is observed that water-wetness of the core increased slightly when it was flooded with less saline brine. However, the change in I_{AH} appears to be very marginal.

The residual oil saturation (S_{or}) value indicates how much oil is left behind in the pore space of the rock/core sample. When cores were flooded with different salinity brines, each waterflood resulted in a particular value of S_{or}. In case of the new (clean) Core E, when it was waterflooded with 22,000 TDS brine, it resulted in (S_{or}) value of 0.4077. But when brine salinity decreased from 22,000 TDS to 11,000 TDS to 5,500 TDS, the (S_{or}) value decreased from 0.4077 to 0.3837 to finally 0.3218, respectively (see **Figure 8.2**). It implies that when the core was flooded with

22,000 TDS brine, the recovery was 36% of the original oil in place (OOIP), but when flooded with 11,000 TDS brine, the recovery was 37% of OOIP. Finally, recovery rose to 50% of the OOIP when the core was waterflooded with 5,500 TDS brine.

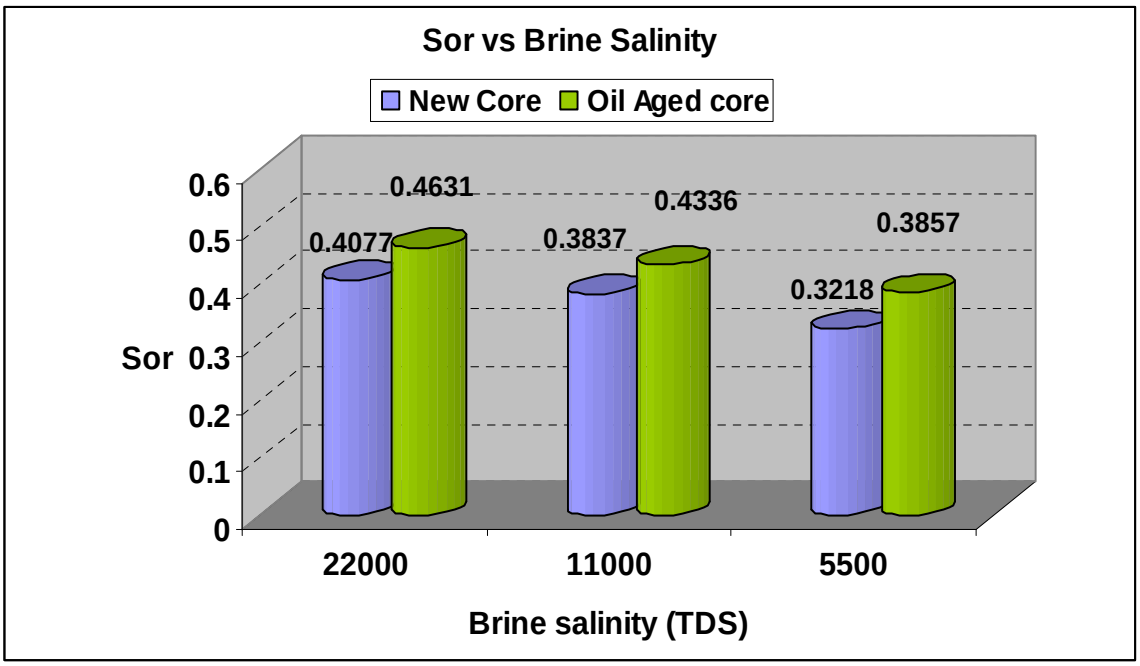

Figure 8.2: Effect of Brine Salinity on Residual Oil Saturation (Core E).

Thus, it is observed that there was an increase in oil recovery with a decrease in the salinity of the injected brine. Consequently, more pore volumes of oil are recovered when brine of lower salinity is injected (see **Figure 8.3**).

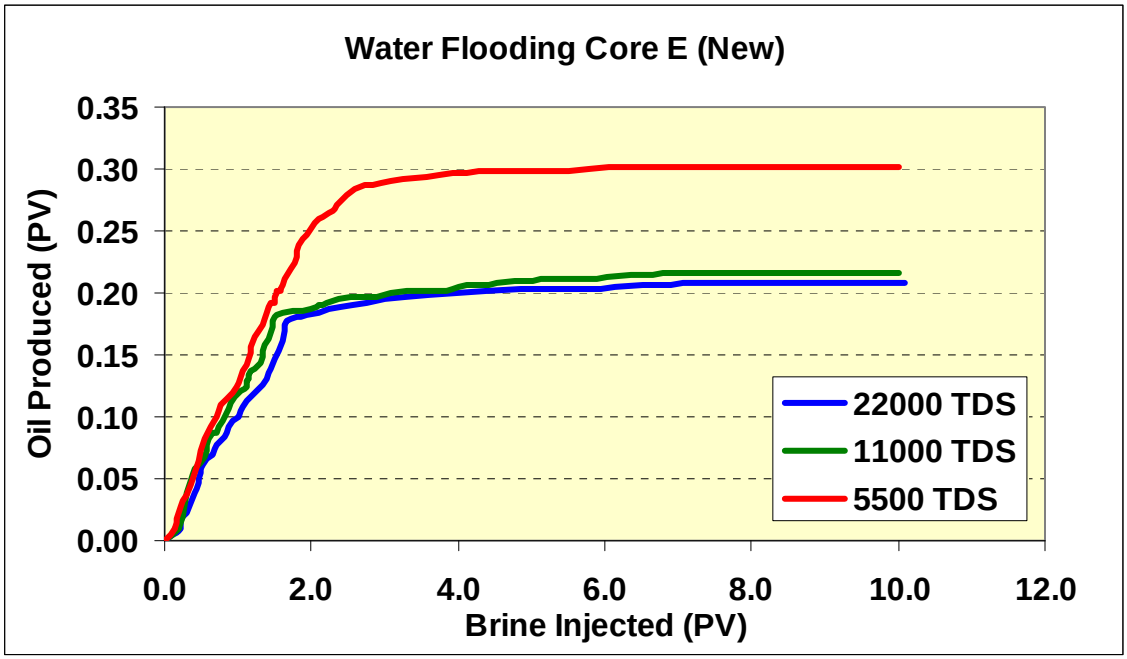

Figure 8.3: Oil Recovery Profile for New Core E.

8.2 Experiment on Oil Aged Cores

When the same Core E was oil aged, Amott-Harvey index (I_{AH}) values decreased compared to its previous values when the core was new (clean). However, it is interesting to note that I_{AH} value increased from 0.260 to 0.268 to 0.282 when flooded with 22,000 TDS, 11,000 TDS and 5,500 TDS brine, respectively. It shows that when the cores were flooded with less saline brine, it resulted in a slight increase in the water-wetting state of the cores. However, this change in the I_{AH} appears to be marginal (see **Figure 8.1**).

It is also interesting to observe that when Core E was oil aged, there was an increase in the values of residual saturation compared to its residual saturation values when core was new (clean). However, it is also observed that as brine salinity decreased, the residual oil saturation value also decreased. When Core E was waterflooded with 22,000 TDS brine, it resulted in (S_{or}) value of 0.4631, but when brine salinity decreased from 22,000 TDS to 11,000 TDS to 5,500 TDS, the (S_{or}) value decreased from 0.4631 to 0.4336 to finally 0.3857, respectively (see **Figure 8.2**).

This implies that when the core was flooded with 22,000 TDS brine, the recovery was 31% of the OOIP. But when flooded with 11,000 TDS brine, the recovery was 34% OOIP and, finally, recovery rose to 42% of the OOIP when the core was waterflooded with 5,500 TDS brine. As a consequence, more pore volumes of oil are recovered when brine of lower salinity is injected (see **Figure 8.4**).

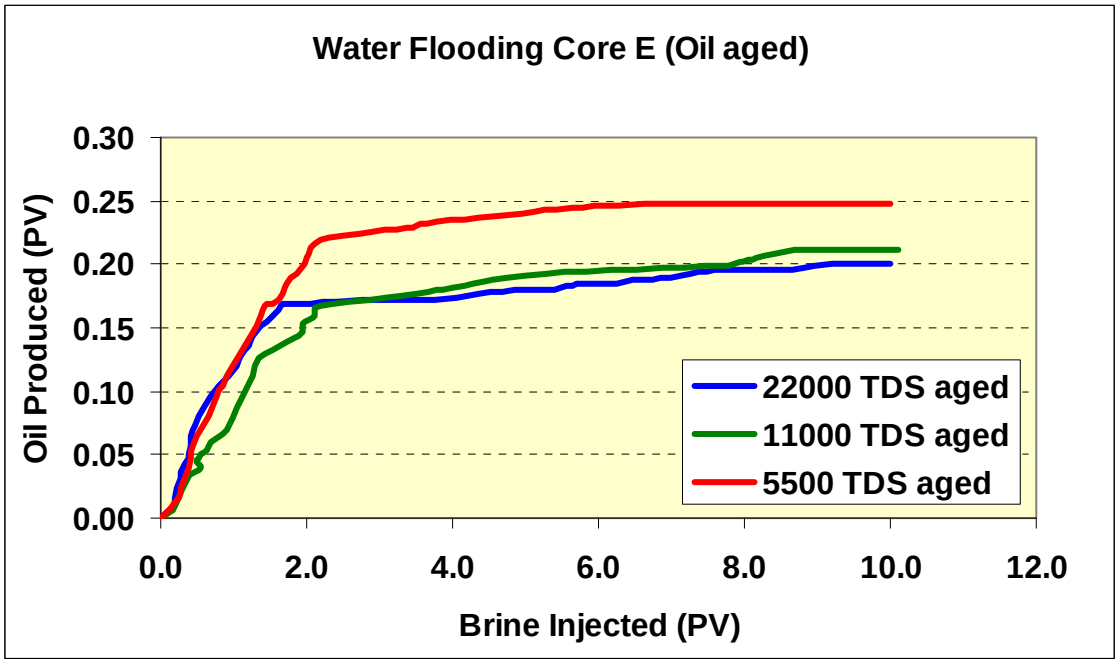

Figure 8.4: Oil Recovery Profile for Oil Aged Core E.

Thus when waterflood experiments were conducted on oil aged core, it was observed that the wettability state of the core shifted from a strongly water-wet (I_{AH} = +0.3 to +1.0) to a slightly water-wet (I_{AH} = +0.1 to +0.3) wetting state. The above-stated observations for oil aged Core E can be attributed to the adsorption of polar compounds and/or the deposition of organic matter that was originally in the crude oil. Surface-active compounds in the crude oil are generally believed to be polar compounds that contain oxygen, nitrogen, and sulfur. These compounds are most prevalent in the heavier fractions of crude oil. It is believed that these compounds are responsible for altering the wetting state of the rock metrics/core surface.

Many researchers have proposed that the shifting of the wettability state towards a water-wet state has given increase in oil recovery. Many have also proposed that shift towards oil-wet state

or intermediate-wet state gives increased oil recovery. Consequently, it is believed that the observed incremental oil recovered and thus reduced S_{or} may be due to subtle alterations in wettability.

In the present study, for new (clean) and oil aged cores, the wettability of all the core samples is determined after each run using the Amott-Harvey wettability index. The measurements/characterization of wettability at every stage of run was done to validate the dependency of oil recovery efficiency on wettability and wettability variation.

As stated earlier, the general observed trend is a reduction in S_{or} and an increase in the Amott-Harvey wettability index with a decrease in the salinity of the injected brine at reservoir temperature. Plots show the variations in the values of the Amott-Harvey wettability index and the residual oil saturation with changes in brine salinity. From the graphs, it can be understood that the shift towards a water-wetting state resulted in a decrease of residual oil saturation.

Donaldson and Thomas[51] reported that more oil is recovered from a water-wet system than from either the intermediate-wet or the oil-wet system. While Amott[14], Rathmell et al.[2], Morrow et al.[25], and Salathiel[38] showed that that the alteration in wetting from strongly to weakly water-wet resulted in reduced S_{or}. Conversely, in the present study it is observed that as the Amott-Harvey wettability index increased—that is, as water-wetness increased—the residual oil saturation S_{or} value decreased. These observations are consistent with observations made in the literature by Tang and Morrow[89] and Sharma and Filoco[91]. The reason for this trend is not clear, but as stated earlier; Tang and Morrow[89] supposed that the detachment of mixed-wet clay particles from pores mobilized previously retained oil droplets attached to these clays, allowing an increase in oil recovery.

8.3 Experiment Using ANS Lake Water

In the previous two experiments, the brine used for the corefloods was synthetically prepared/reconstituted brine in the laboratory. As the ANS lake water has much less salinity (approximately 50–60 TDS), in this set of coreflooding experiments the representative low-

salinity ANS lake water was used as an alternative to low-saline brines viz. 11,000 TDS and 5,500 TDS brine. Results of specimen Core H will be discussed in this section.

Plots from these experiments show that incremental oil is recovered with a decrease in brine salinity of the displacing brine. **Figure 8.5** shows that when new (clean) Core H was waterflooded with 22,000 TDS brine, the Amott-Harvey wettability index (I_{AH}) was observed to be 0.26. When the less saline ANS lake water was used, I_{AH} value increased to 0.29. However, the I_{AH} change appears to be marginal and takes place within the window of slightly water-wet characteristics when the core was flooded with less saline brine.

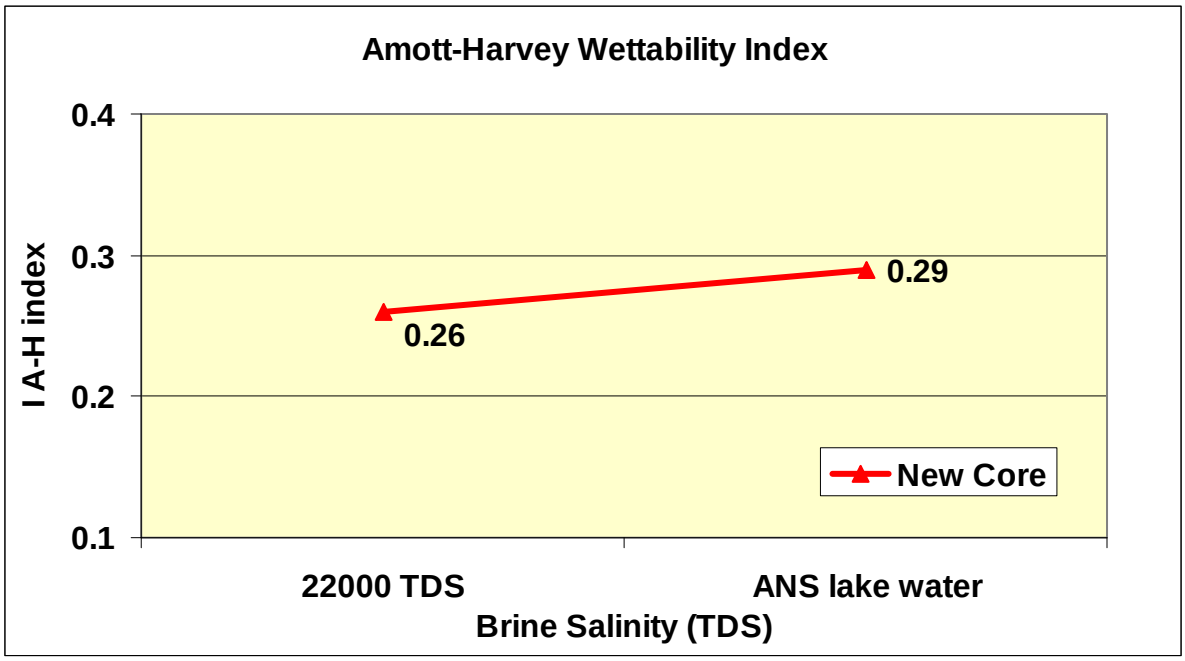

Figure 8.5: Effect of Brine Salinity on Wettability (Core H).

When the new (clean) core H, was waterflooded with 22,000 TDS brine, it resulted in (S_{or}) value of 0.3971. But when brine salinity decreased, that is, when the less saline ANS lake water was used, the (S_{or}) value decreased from 0.3971 to 0.2052 (see **Figure 8.6**).

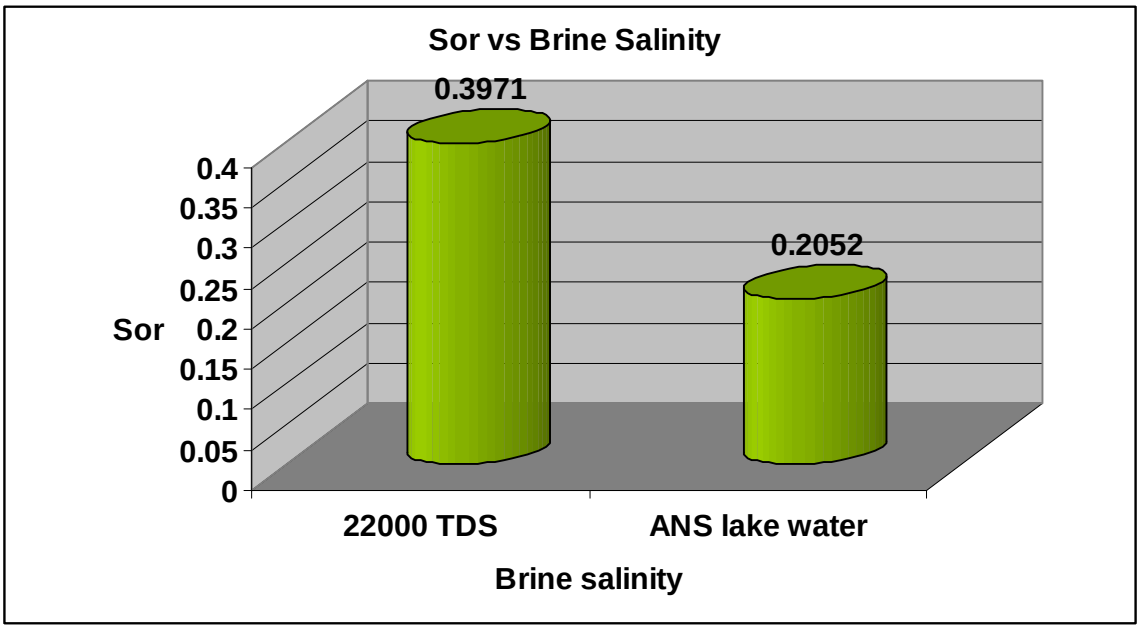

Figure 8.6: Effect of Brine Salinity on Residual Oil Saturation (Core H).

This means that when the core was flooded with 22,000 TDS brine, the recovery was 40%, but when flooded with ANS lake water, the recovery was 68%. Thus, more pore volumes of oil are recovered when brine of lower salinity is injected (see **Figure 8.7**).

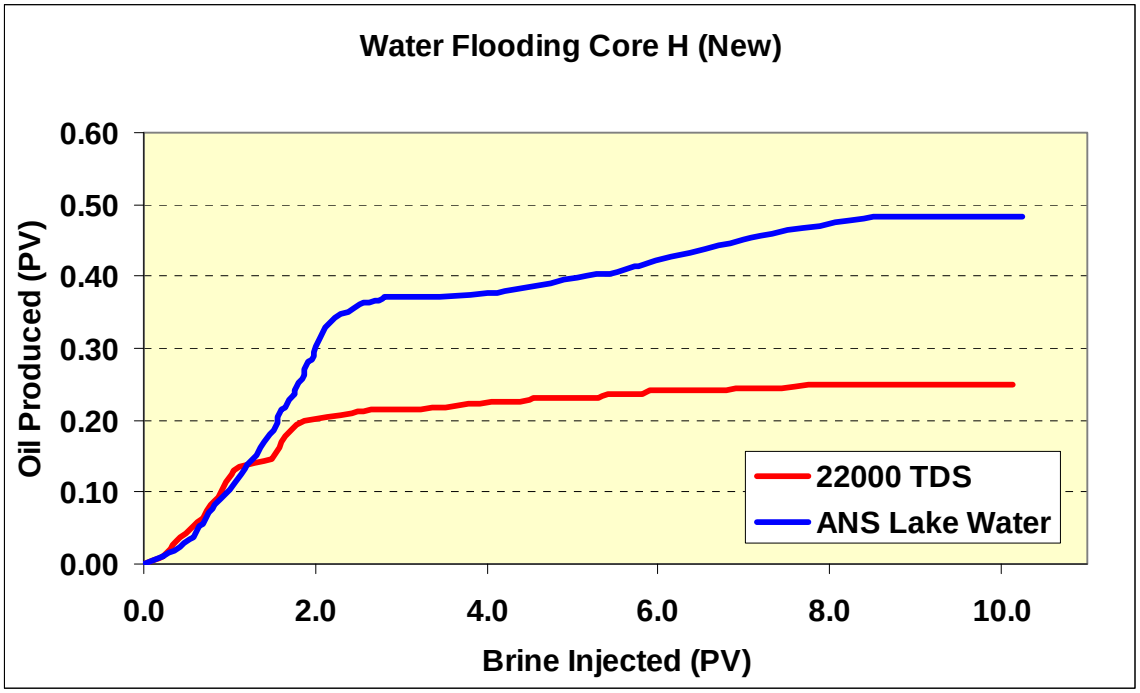

Figure 8.7: Oil Recovery Profile (Core H).

The first and second types of experiments were performed on seven ANS core samples. All of them have shown result trends similar to Core E (i.e., a slight increase in Amott-Harvey wettability index (I_{AH}) and a substantial decrease in residual oil saturation (S_{or}) as the salinity of the brine used for waterflooding is decreased). The third type of experiment was performed on three ANS core samples. It was interesting to observe that all of them showed result trends similar to Core H (i.e., an increase in the Amott-Harvey wettability index and a decrease in residual oil saturation, as the salinity of the brine used for waterflooding is decreased to that of ANS lake water).

The results obtained using ANS lake water are similar to some of the field or reservoir condition low-salinity waterflood experiments done by other researchers. In laboratory tests of secondary recovery by injection of low-salinity brine, Webb et al.[95] reported that injection of 4,000 ppm brine into a reservoir core gave recoveries of up to 40% (~23% PV) higher than given by injection of 8,000 ppm brine. Whereas, in the present study, the injection of ANS lake water (50–

60 TDS) into ANS core gave recoveries of up to 68%, which is 28% higher than given by injection of 22,000 TDS brine.

McGuire et al.[93] conducted the SWCTT (Single Well Chemical Tracer Tests) two in the Ivishak sandstone, one each in the Kuparuk and Kekiktuk sandstones. The results from the tests showed that waterflood residual-oil saturation (S_{or}) was substantially reduced by low-salinity water injection. The low-salinity EOR (LoSal$^{TM;}$ owned by BP) benefits ranged from 6% to 12% OOIP, resulting in an increase in waterflood recovery of 8% to 19%. Based on these encouraging results, low-salinity oil recovery is being actively evaluated for North Slope reservoirs.

Formation water is one of the main sources for waterflooding process at ANS. Sometimes seawater is also considered for waterflooding process. Seawater salinity is typically 30,000–35,000 ppm, while formation waters can vary from almost fresh water to ~250,000 ppm, that is, almost salt saturated[95]. If the high-saline water is diluted with less saline water then the resulting water would be of salinity which is higher than less saline water but would obviously be less than high-salinity water. Thus in order to achieve low-salinity water for waterflooding at ANS, diluting the formation water or seawater with less salinity water sources like ANS lake waters looks to be a promising option.

In **Figure 8.8**, results from different studies (McGuire et al.[93]; Webb et al.[95] and present work) are plotted to see how reduction in brine salinity results in a decrease of residual oil saturation or in other words how a decrease in brine salinity helps to increase the oil recovery. **Figure 8.8** shows that as brine salinity decreased there is always a reduction in residual oil saturation, that is, an increase in oil recovery. It is observed that when reduction in brine salinity is more than 80%, there is a significant increase in oil recovery.

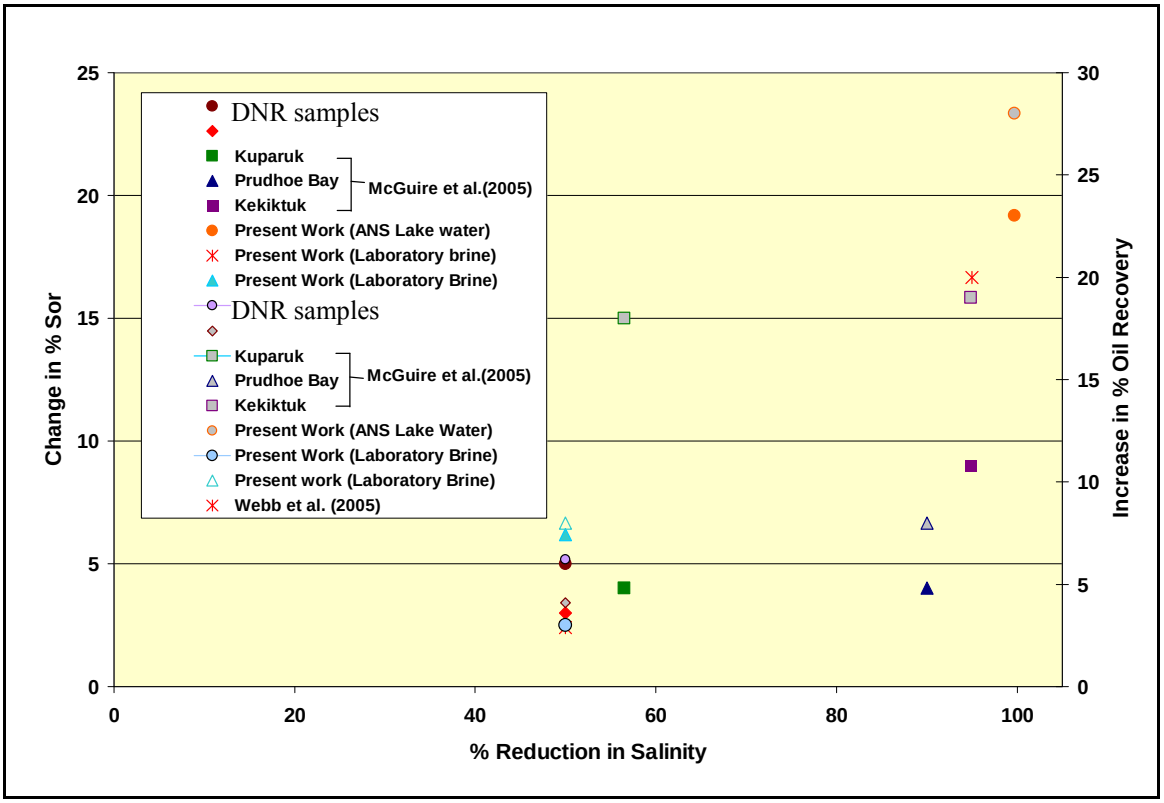

Figure 8.8: Increase in % Oil Recovery/Change in % S_{or} With Reduction of Brine Salinity for Different Studies (McGuire et al.[93]; Webb et al.[95]; present work is using ANS representative core samples).

The results of the remaining core samples of the present study are shown graphically and summarized in Table 8.1.

Table 8.1: Results of Core Samples (A through G) Using Laboratory Brine

Core Name	Unaged (New) Core Experiment Results			Aged Core Experiment Results		
	22000 TDS	11000 TDS	5500 TDS	22000 TDS	11000 TDS	5500 TDS
A						
S_{or}	0.3959	0.2033	0.1986	0.4456	0.4239	0.4131
I_{AH}	0.4483	0.45	0.4545	0.375	0.3684	0.381
B						
S_{or}	0.3751	0.3011	0.297	Core got damaged		
I_{AH}	0.35	0.36	0.38	Hence no results		
C						
S_{or}	0.3862	0.3646	0.2775	0.401	0.3878	0.3246
I_{AH}	0.45	0.455	0.46	0.375	0.381	0.409
D						
S_{or}	0.443	0.4125	0.4112	0.4548	0.449	0.429
I_{AH}	0.28	0.2857	0.31	0.26	0.26	0.28
E						
S_{or}	0.4077	0.3837	0.3218	0.4631	0.4336	0.3857
I_{AH}	0.32	0.33	0.35	0.26	0.2683	0.282
F						
S_{or}	0.3606	0.3517	0.3185	0.3634	0.3388	0.327
I_{AH}	0.25	0.3	0.31	0.22	0.23	0.24
G						
S_{or}	0.4193	0.3968	0.3685	0.4717	0.454	0.4211
I_{AH}	0.35	0.37	0.38	0.33	0.33	0.34

Table 8.2: Results of Core Samples (H through J) Using ANS Lake Water

Core Name	22000 TDS	ANS lake Water
H		
S_{or}	0.3971	0.2052
I_{AH}	0.26	0.29
I		
S_{or}	0.3535	0.2216
I_{AH}	0.25	0.27
J		
S_{or}	0.3765	0.2115
I_{AH}	0.24	0.277

1) Core A

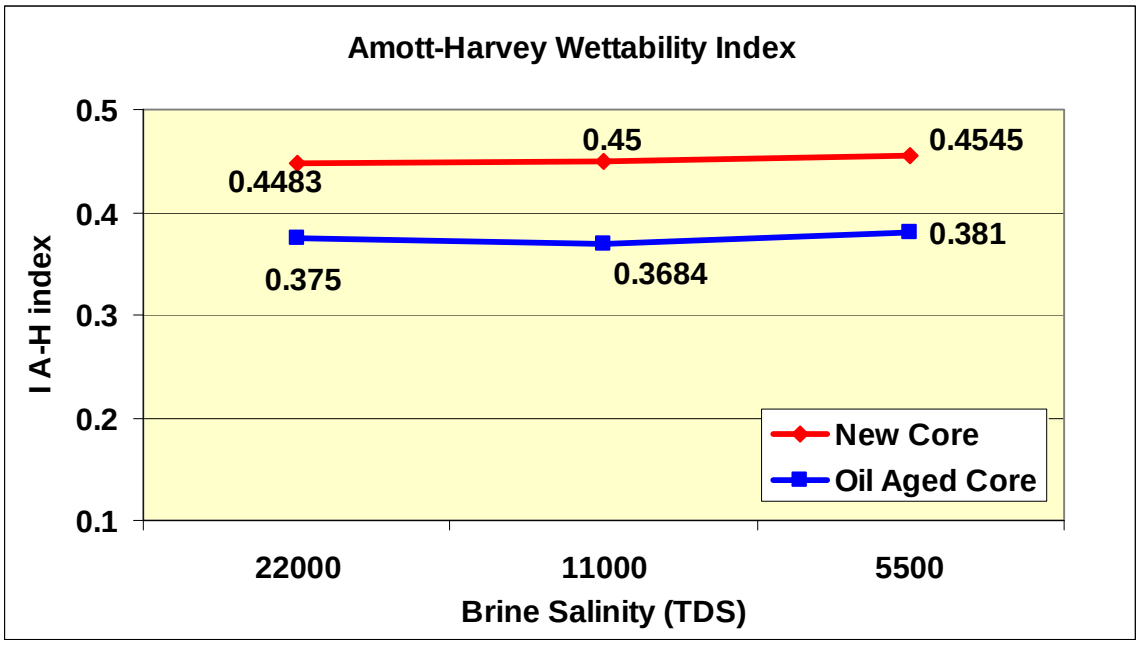

Figure 8.9: Effect of Brine Salinity on Wettability (Core A).

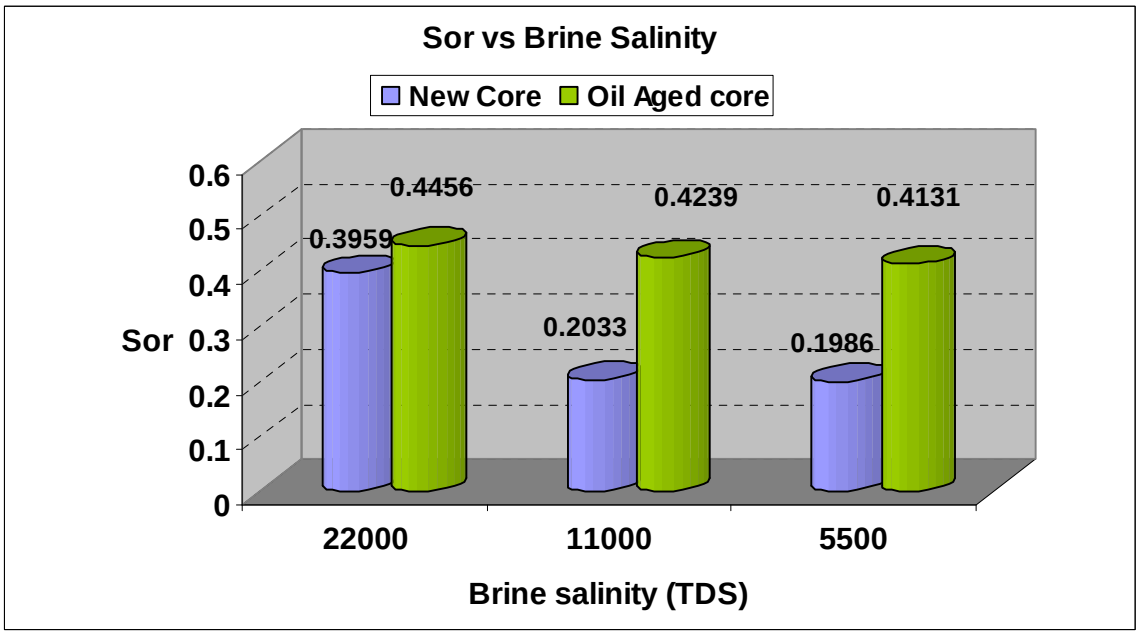

Figure 8.10: Effect of Brine Salinity on Residual Oil Saturation (Core A).

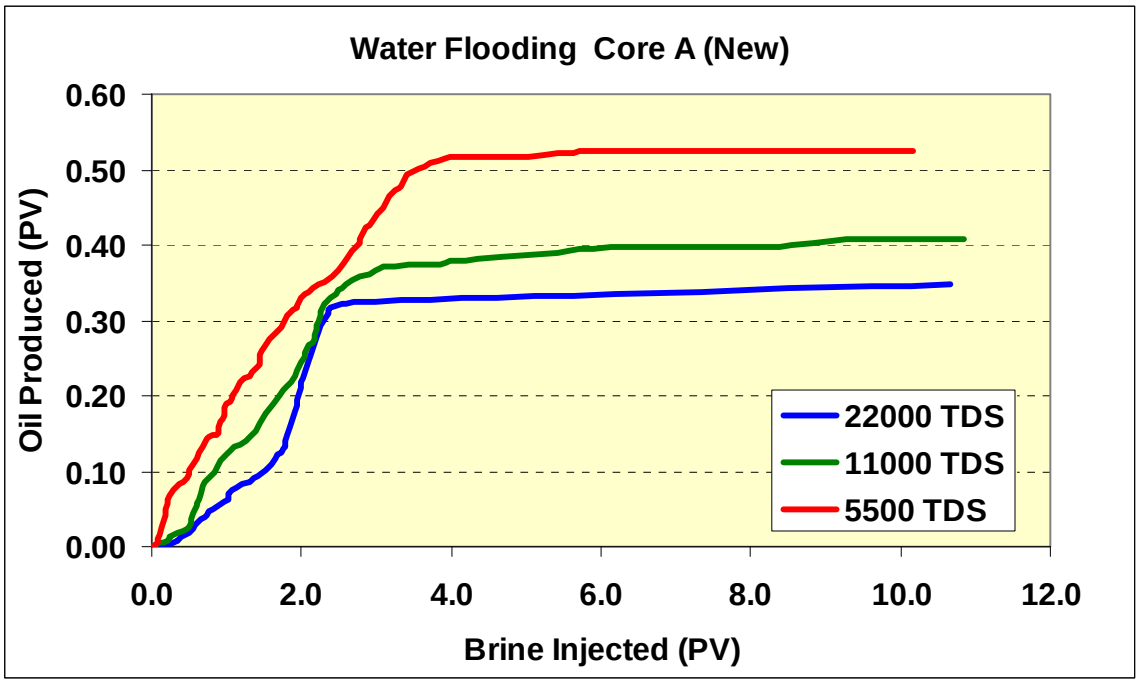

Figure 8.11: Oil Recovery Profile for New Core A.

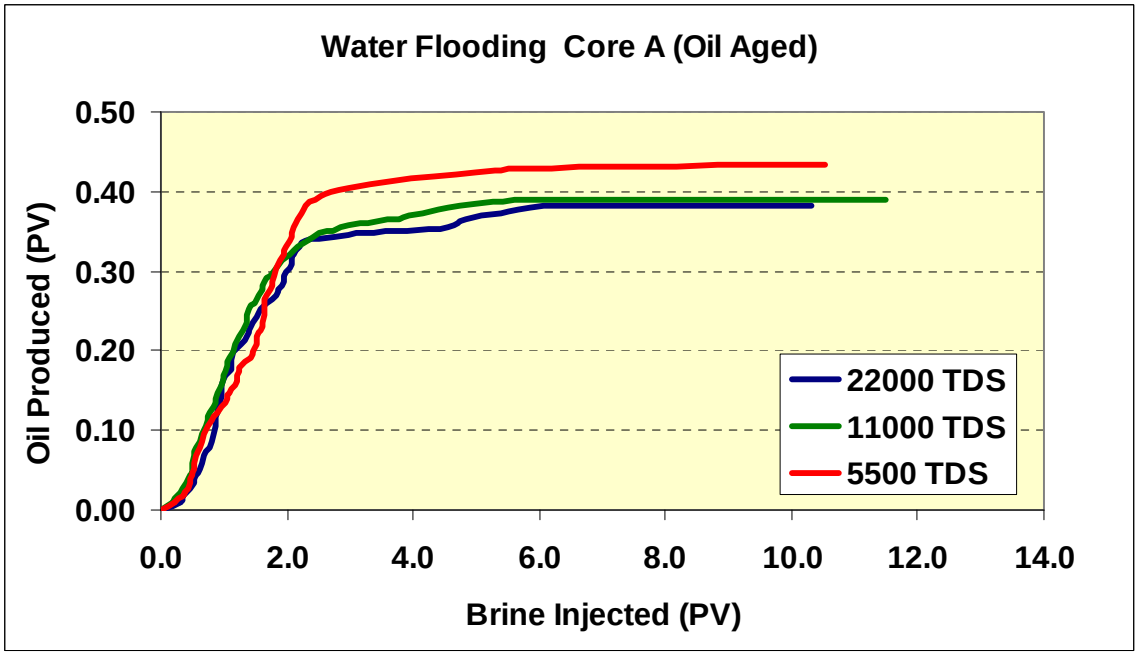

Figure 8.12: Oil Recovery Profile for Oil Aged Core A.

2) Core B

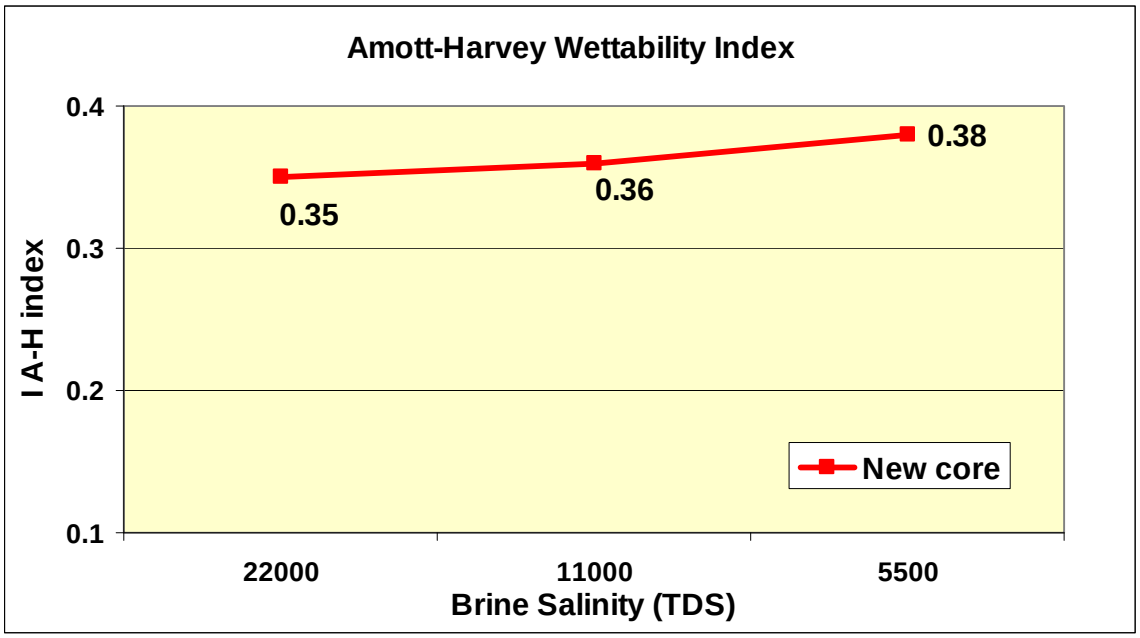

Figure 8.13: Effect of Brine Salinity on Wettability for New Core B.

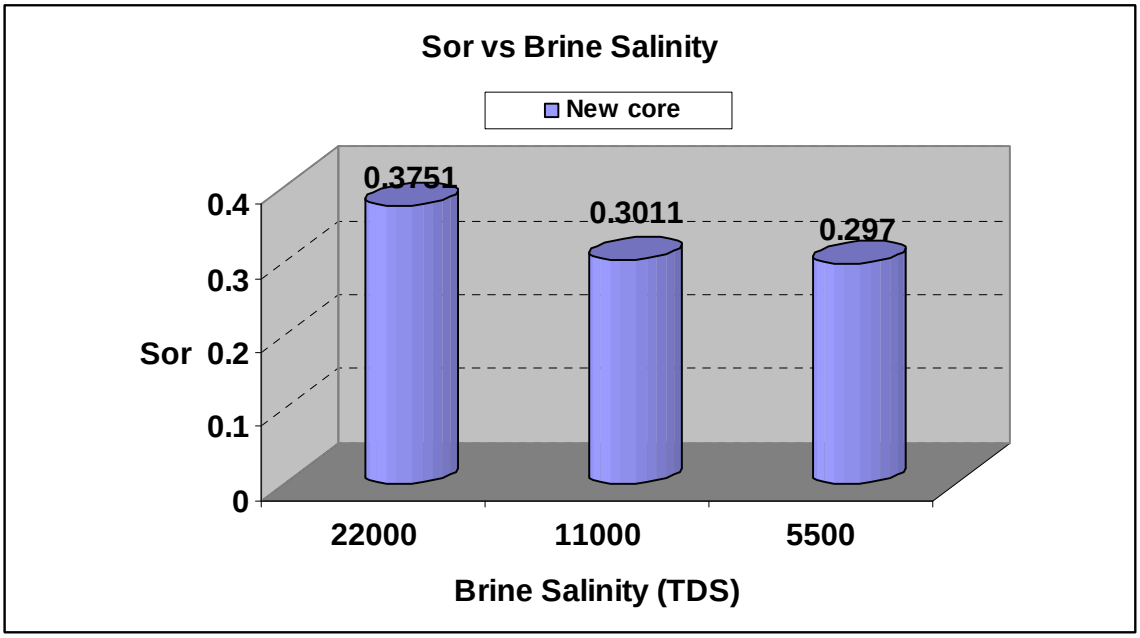

Figure 8.14: Effect of Brine Salinity on Residual Oil Saturation for New Core B.

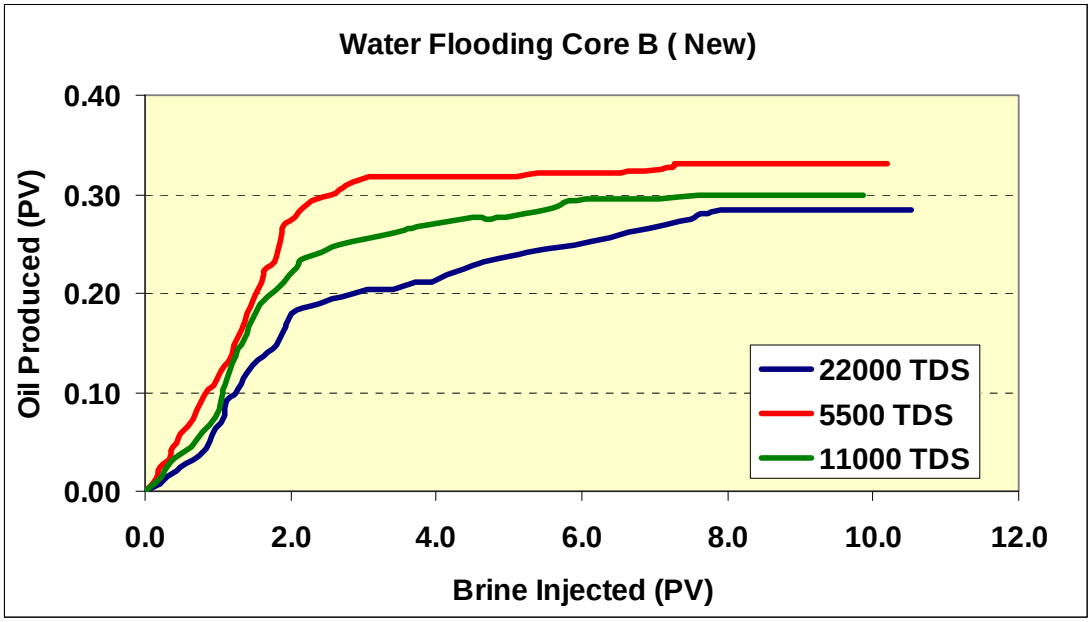

Figure 8.15: Oil Recovery Profile for New Core B.

3) Core C

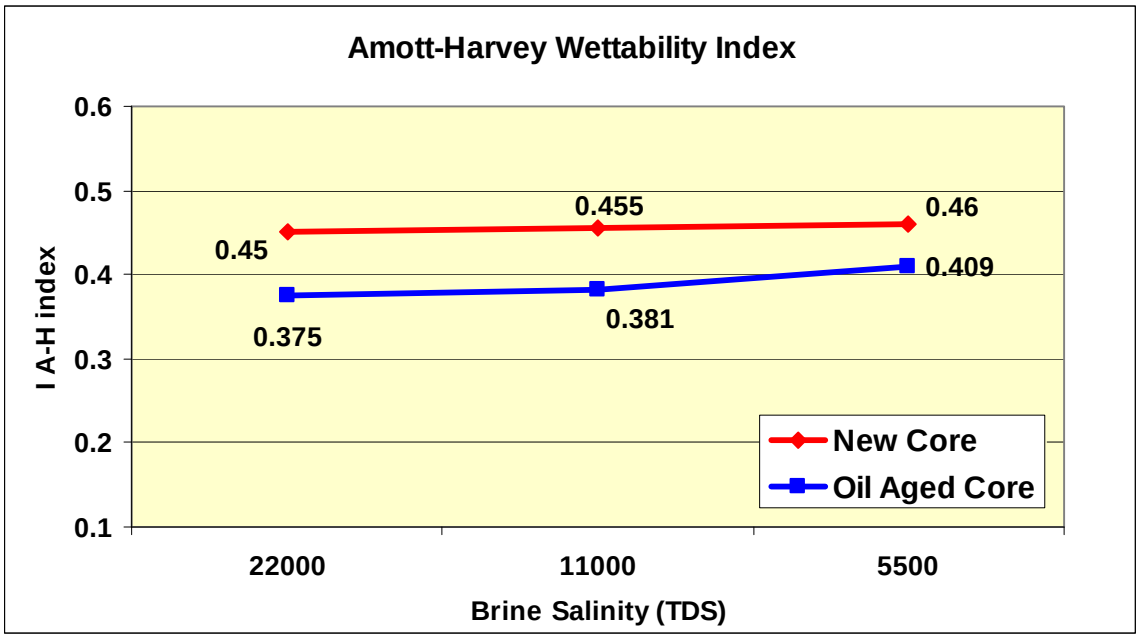

Figure 8.16: Effect of Brine Salinity on Wettability (Core C).

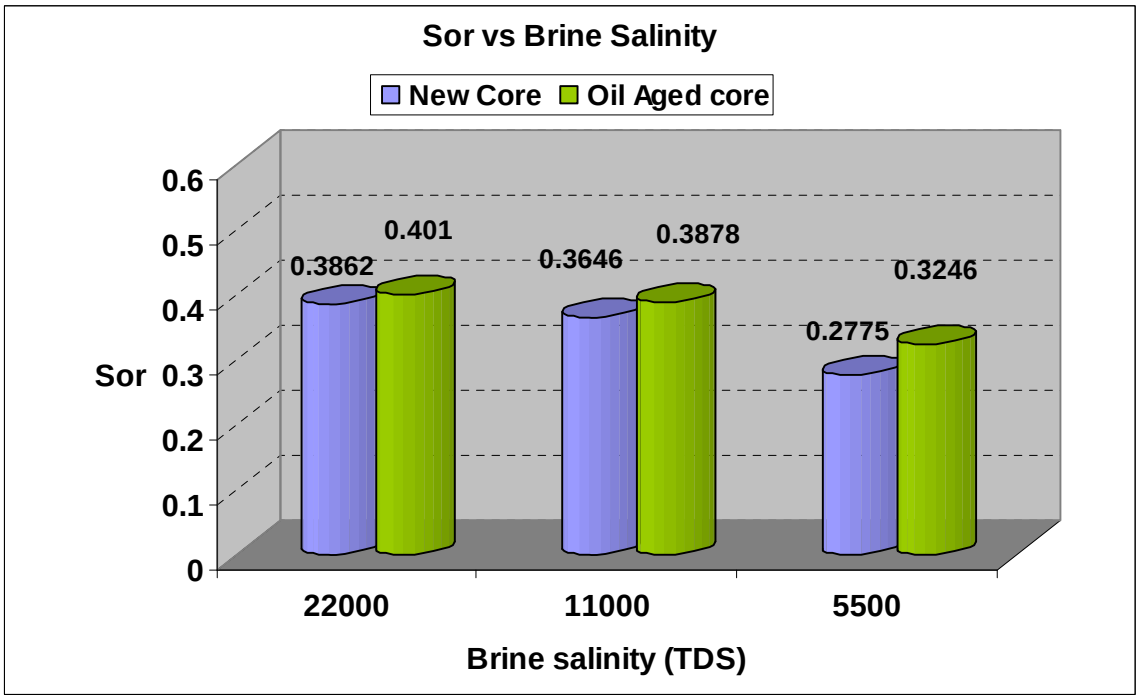

Figure 8.17: Effect of Brine Salinity on Residual Oil Saturation (Core C).

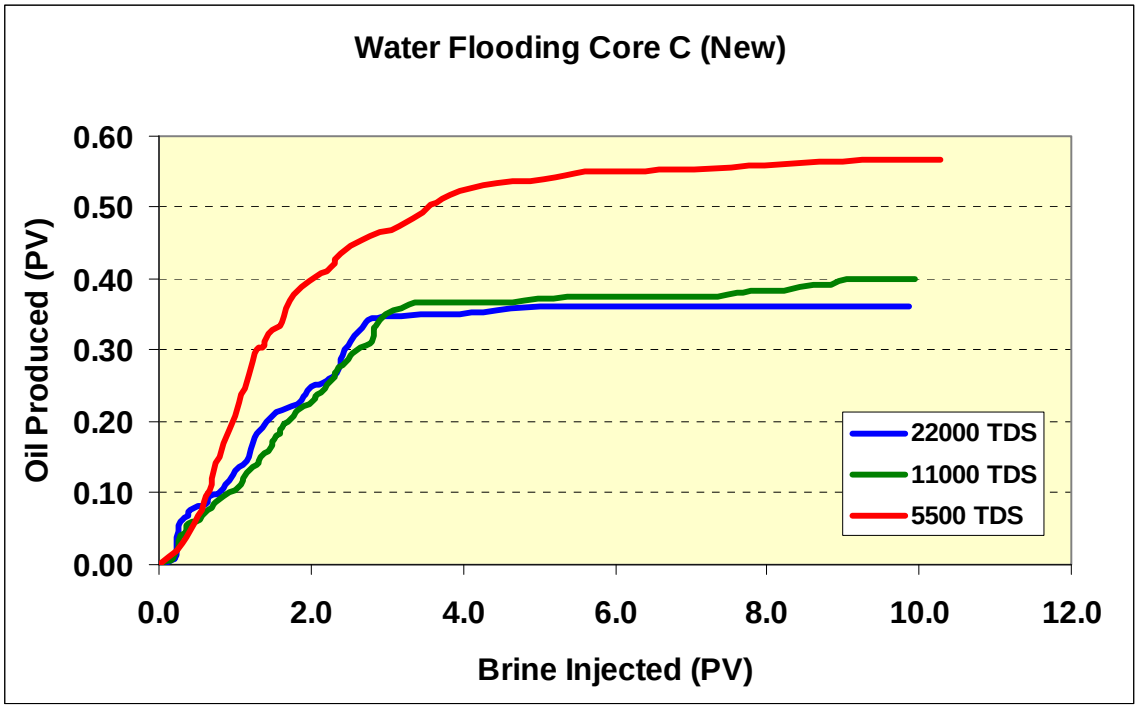

Figure 8.18: Oil Recovery Profile for New Core C.

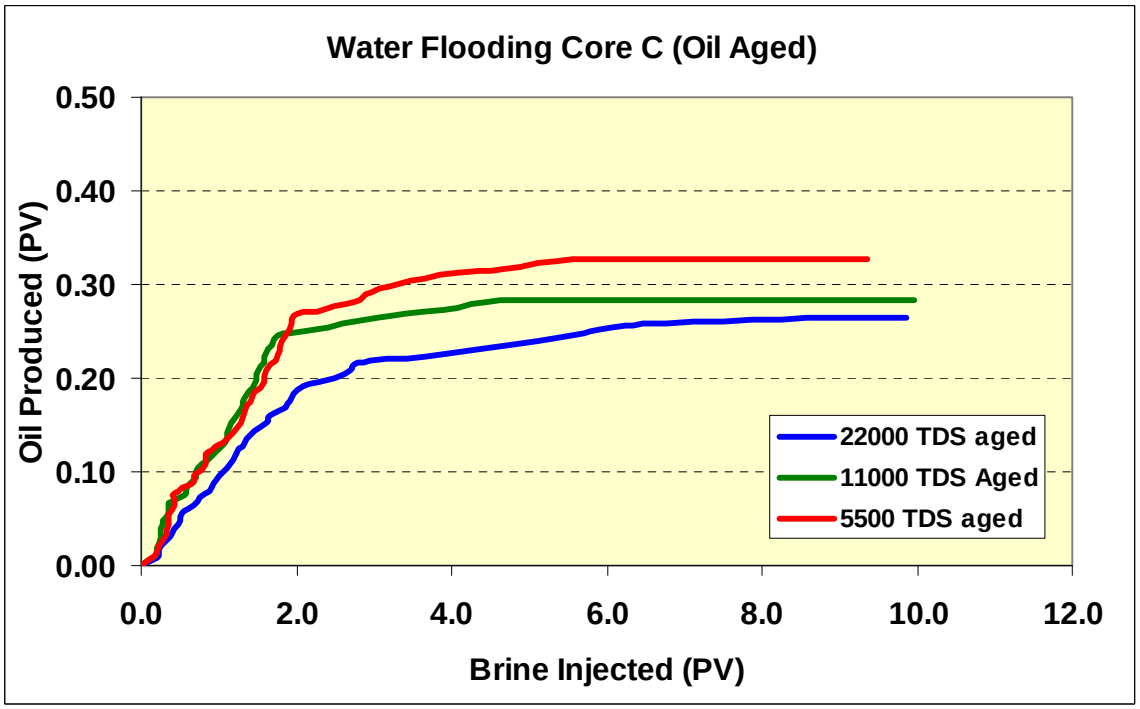

Figure 8.19: Oil Recovery Profile for Oil Aged Core C.

4) Core D

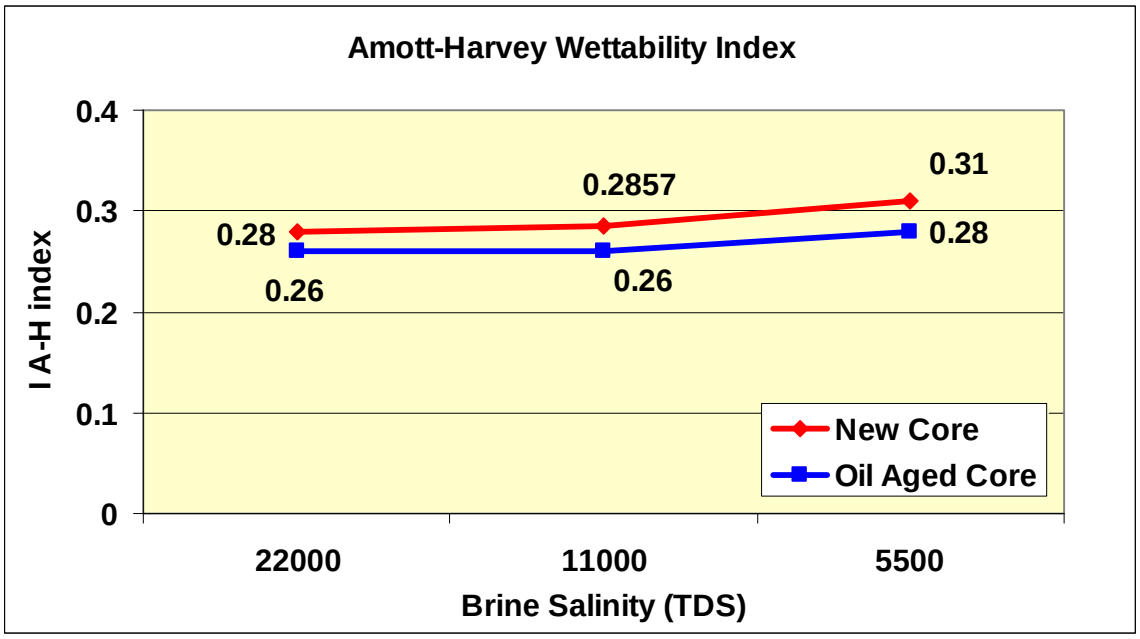

Figure 8.20: Effect of Brine Salinity on Wettability (Core D).

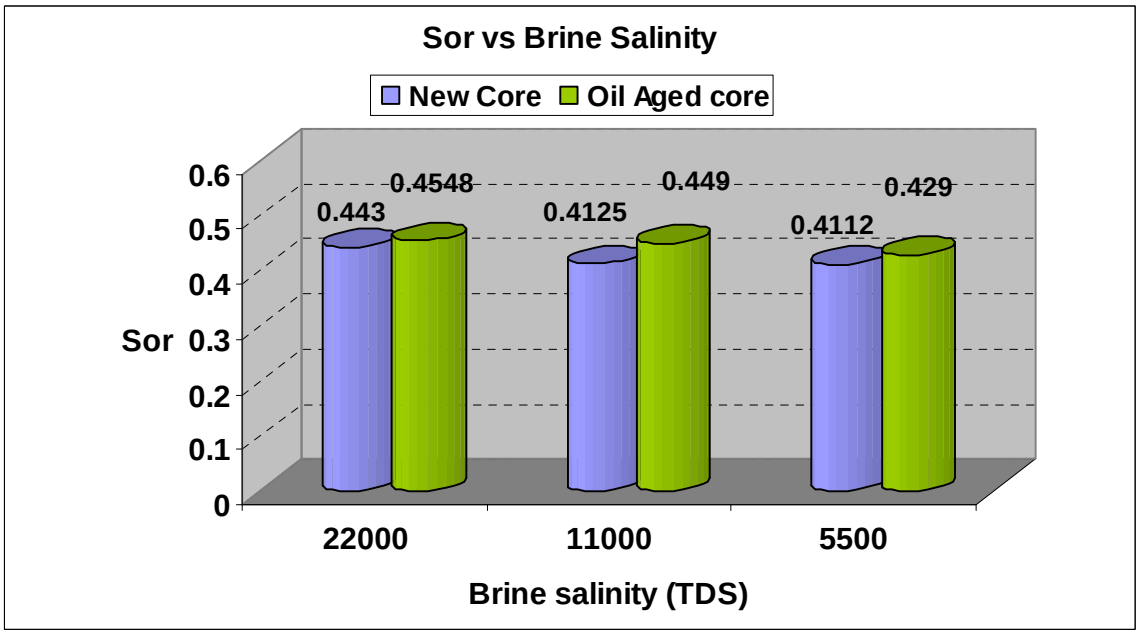

Figure 8.21: Effect of Brine Salinity on Residual Oil Saturation (Core D).

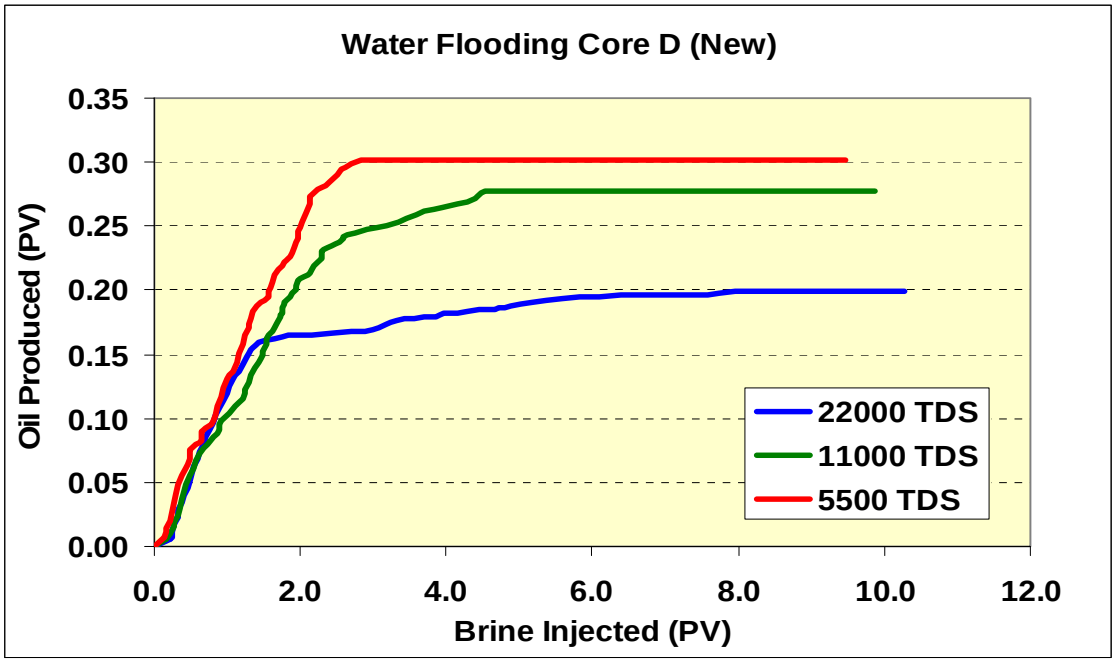

Figure 8.22: Oil Recovery Profile for New Core D.

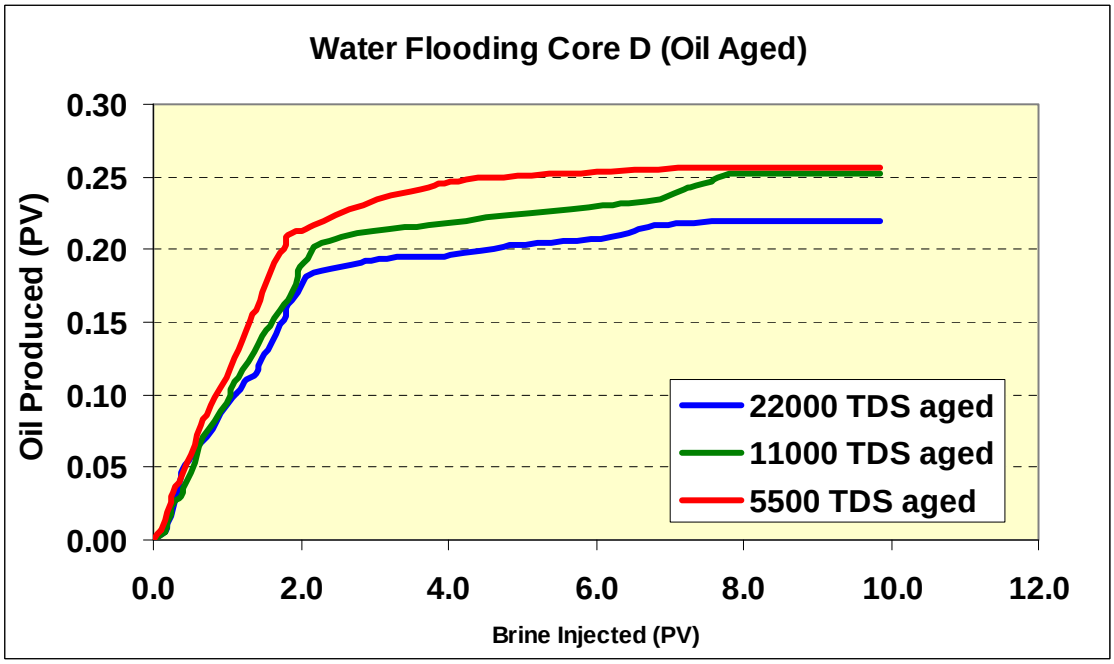

Figure 8.23: Oil Recovery Profile for Oil Aged Core D.

5) Core F

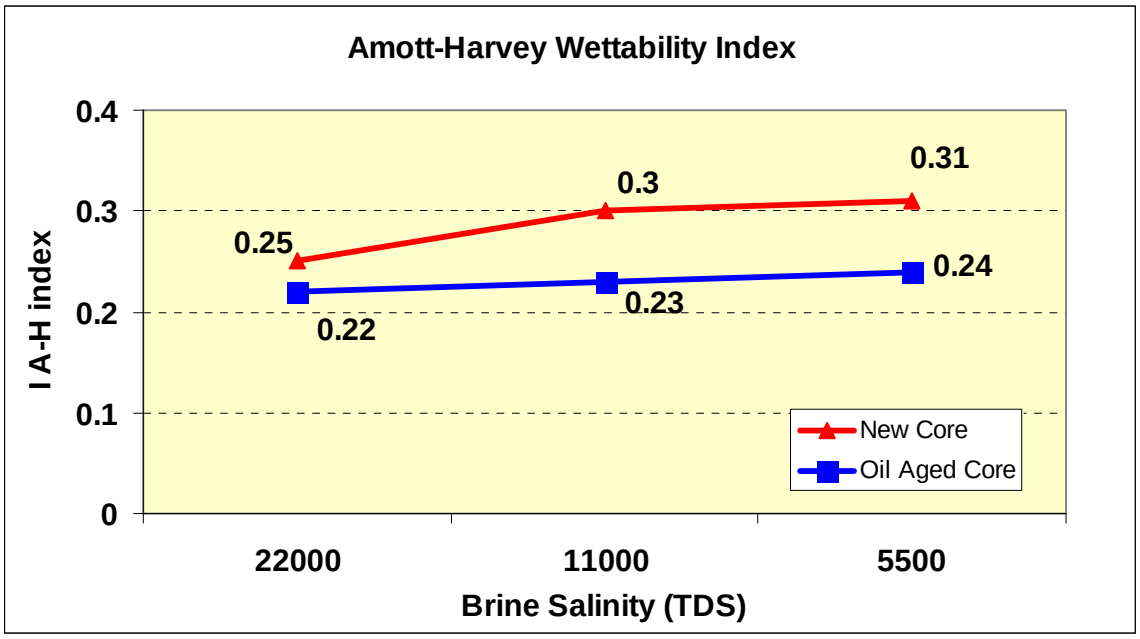

Figure 8.24: Effect of Brine Salinity on Wettability (Core F).

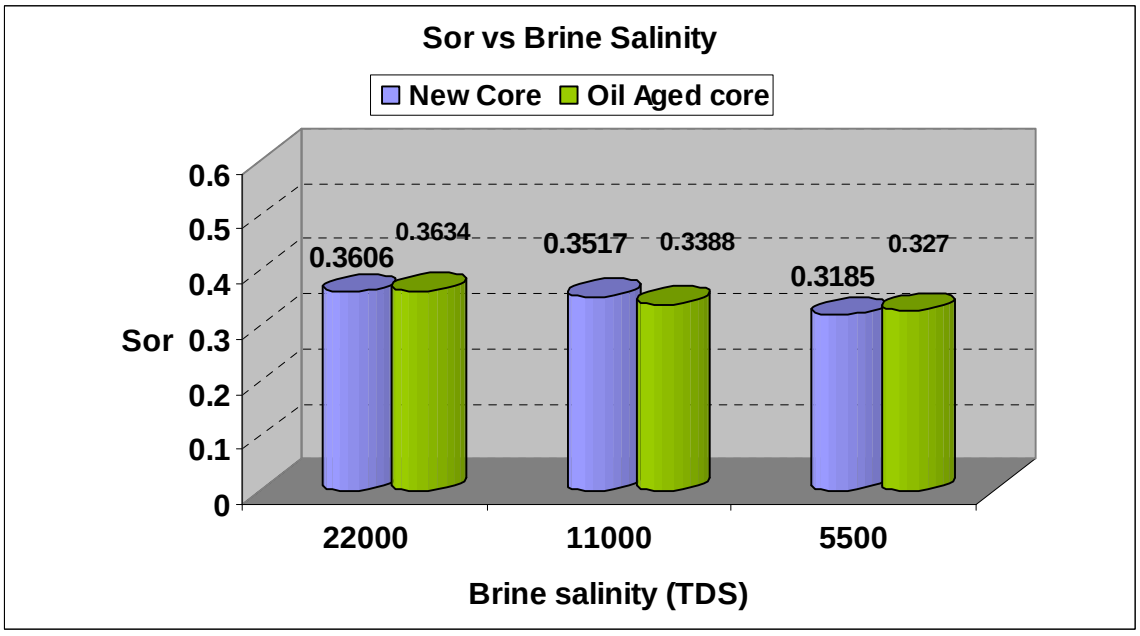

Figure 8.25: Effect of Brine Salinity on Residual Oil Saturation (Core F).

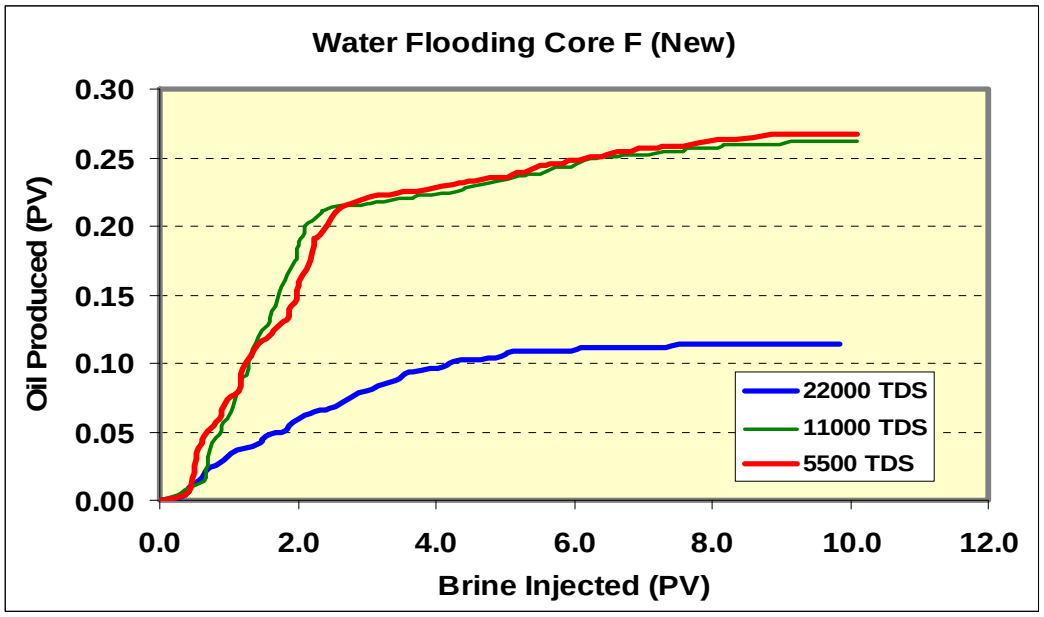

Figure 8.26: Oil Recovery Profile for New Core F.

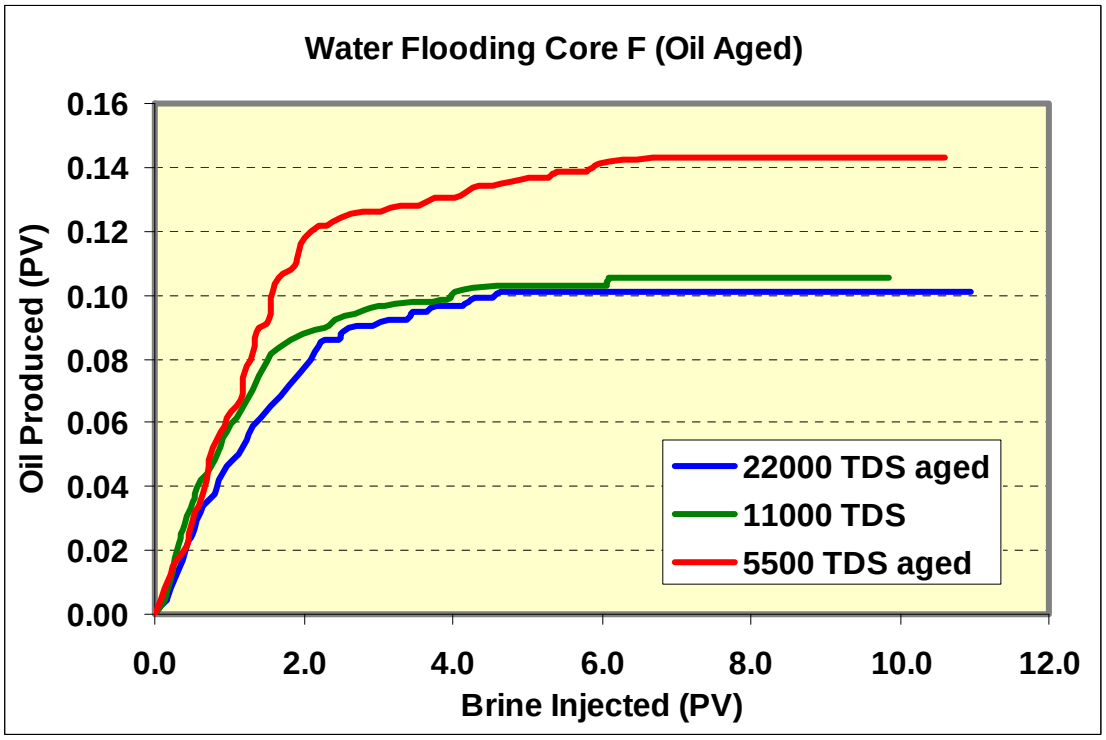

Figure 8.27: Oil Recovery Profile for Oil Aged Core F.

6) Core G

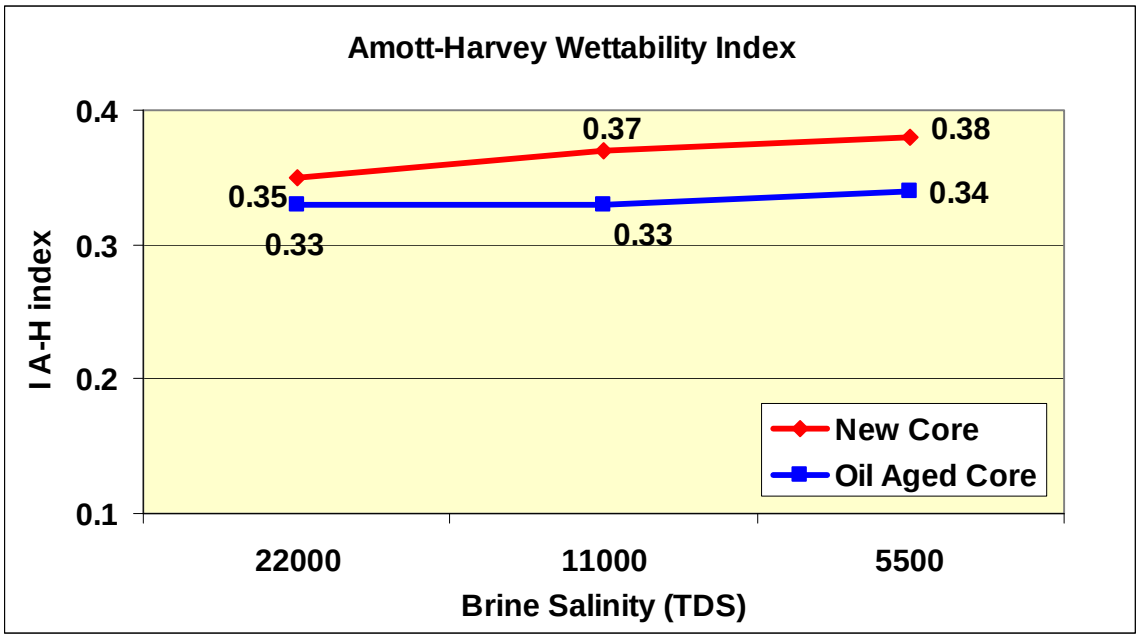

Figure 8.28: Effect of Brine Salinity on Wettability (Core G).

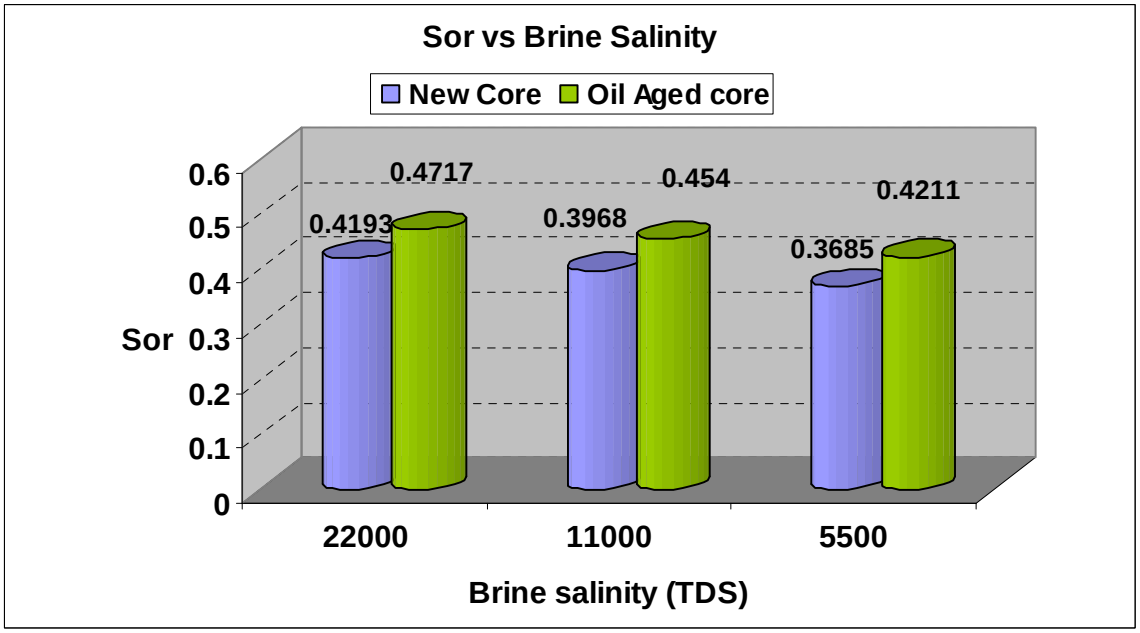

Figure 8.29: Effect of Brine Salinity on Residual Oil Saturation (Core G)

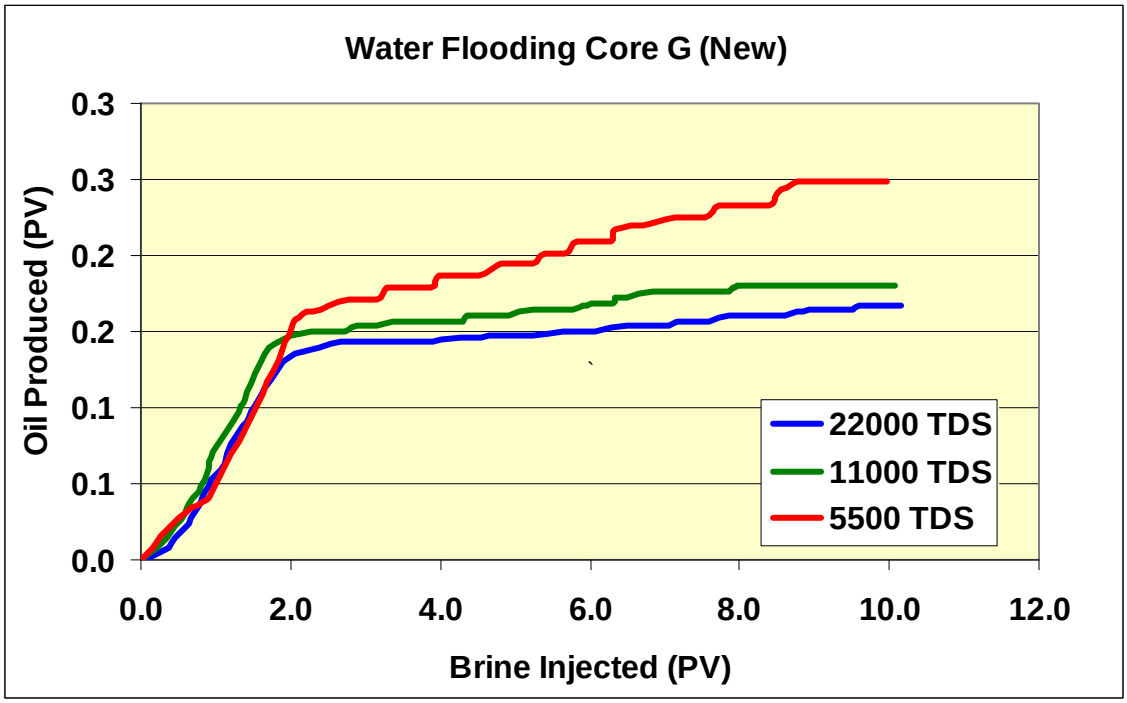

Figure 8.30: Oil Recovery Profile for New Core G.

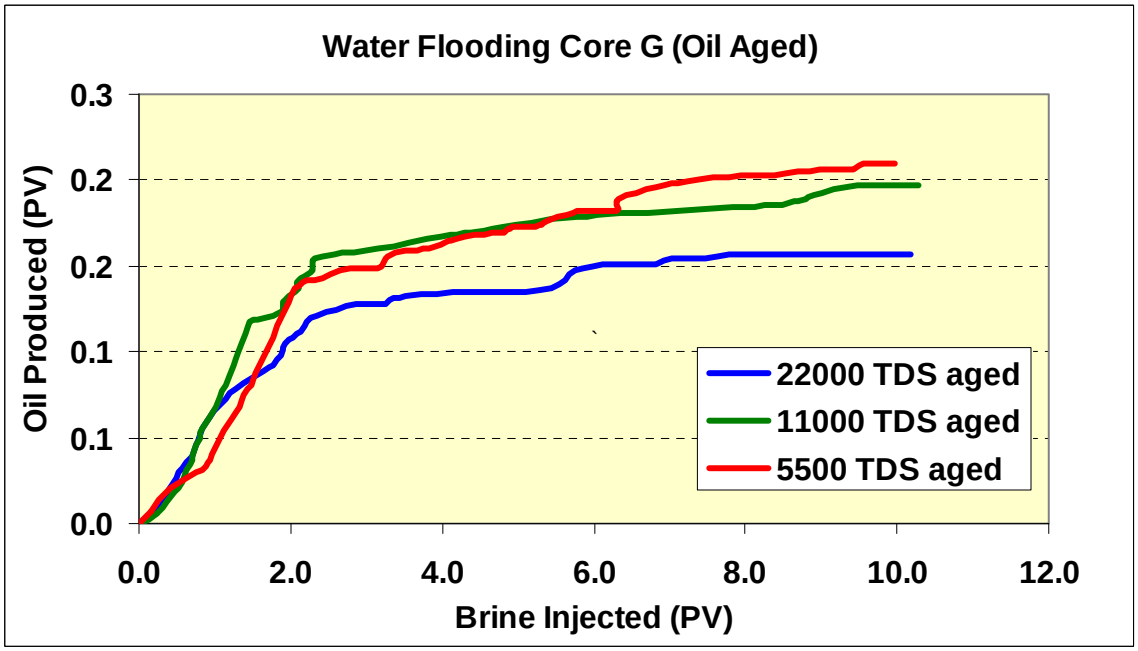

Figure 8.31: Oil Recovery Profile for Oil Aged Core G.

7) Core I

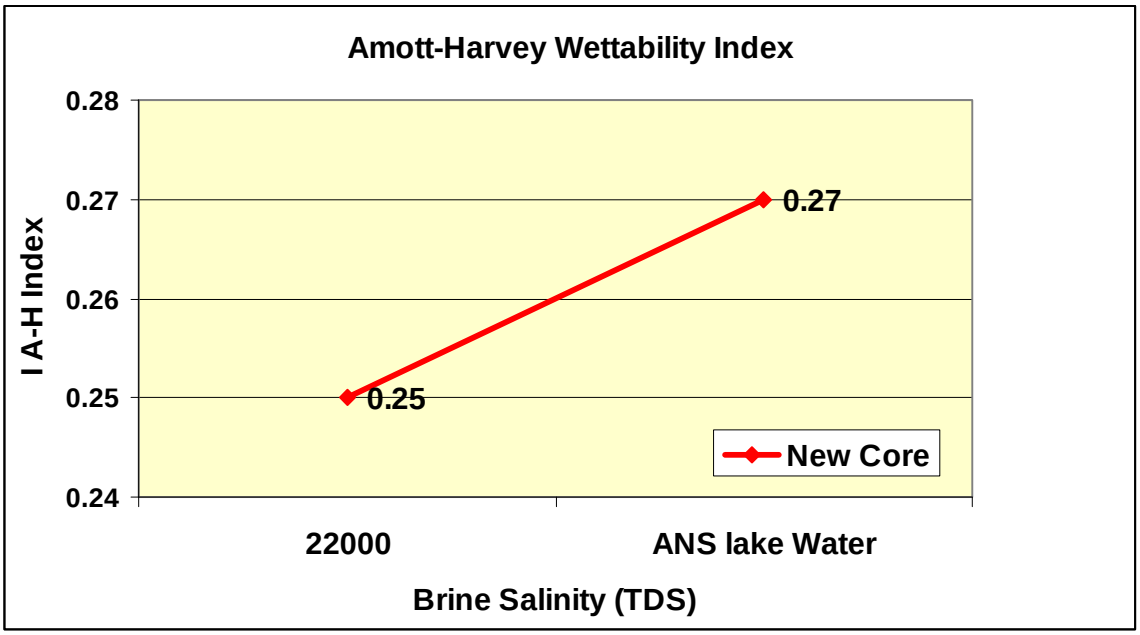

Figure 8.32: Effect of Brine Salinity on Wettability for New Core I.

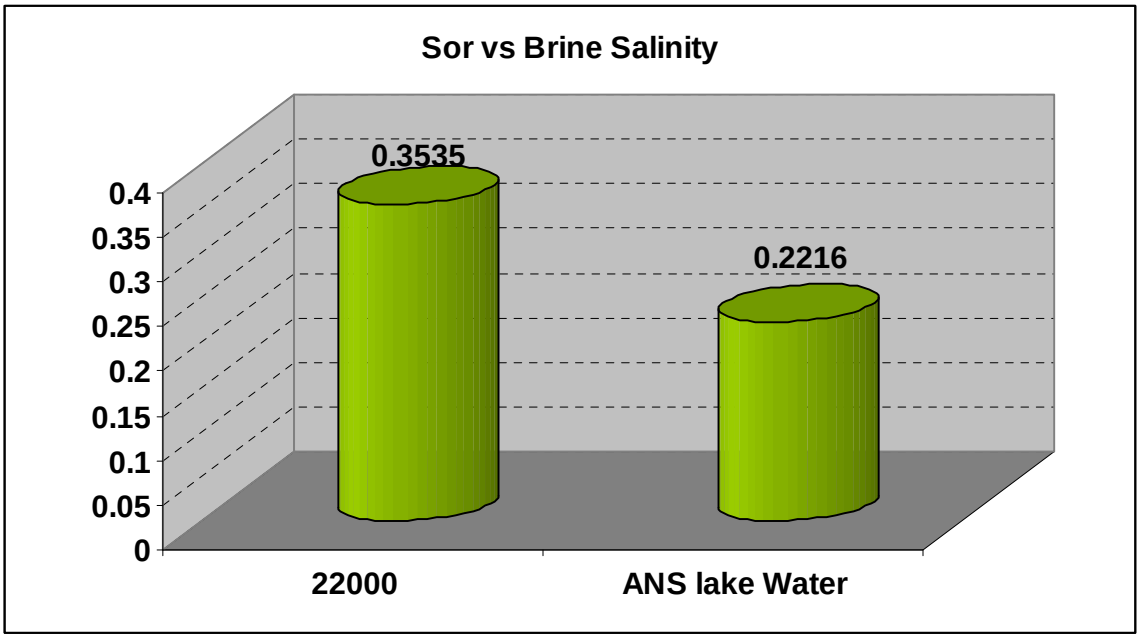

Figure 8.33: Effect of Brine Salinity on Residual Oil Saturation for New Core I.

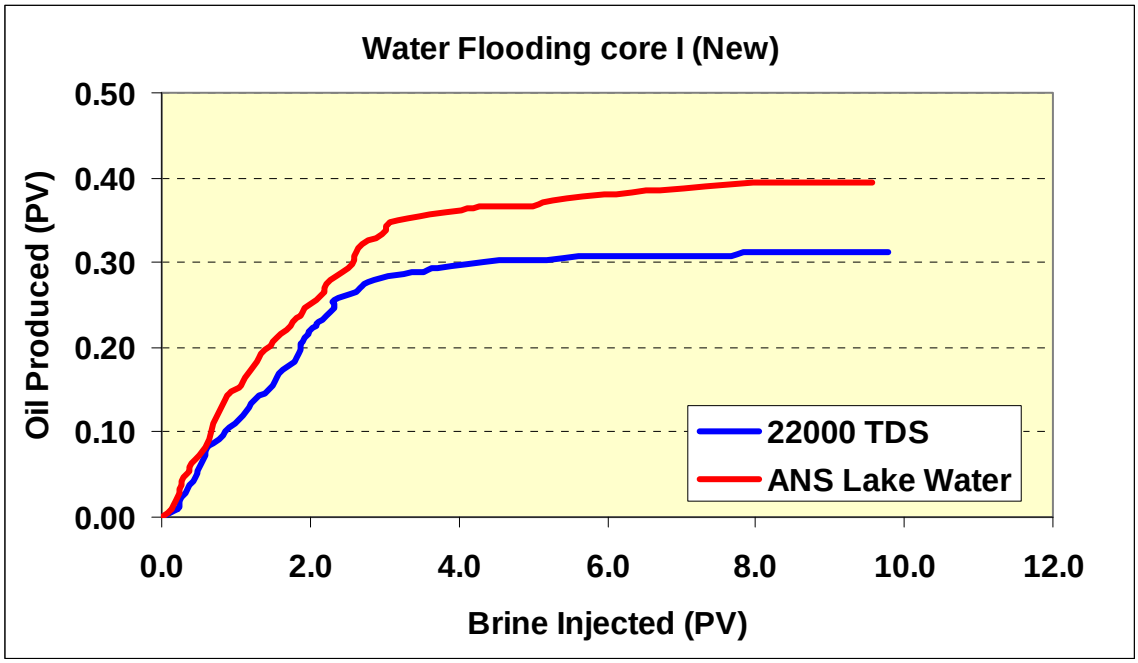

Figure 8.34: Oil Recovery Profile for New Core I.

8) Core J

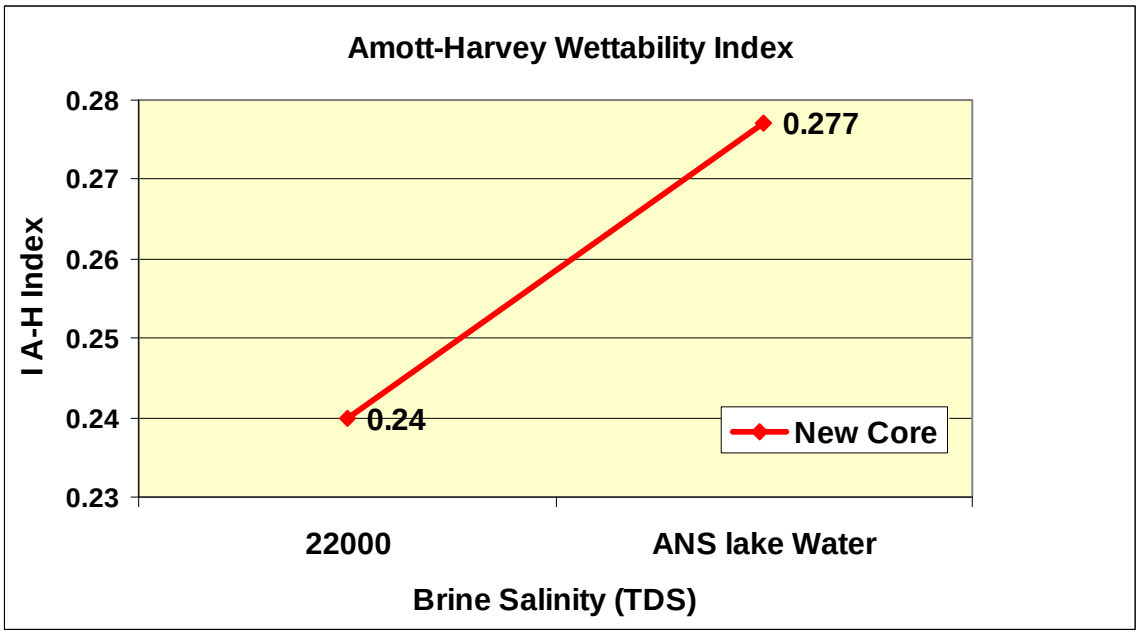

Figure 8.35: Effect of Brine Salinity on Wettability for New Core J.

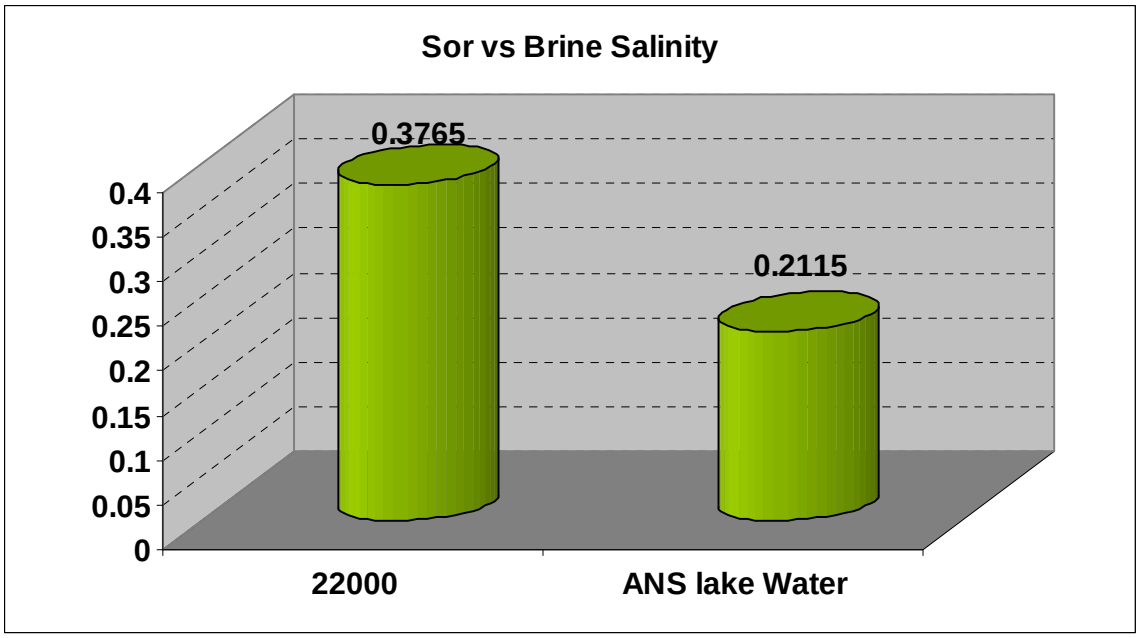

Figure 8.36: Effect of Brine Salinity on Residual Oil Saturation for New Core J.

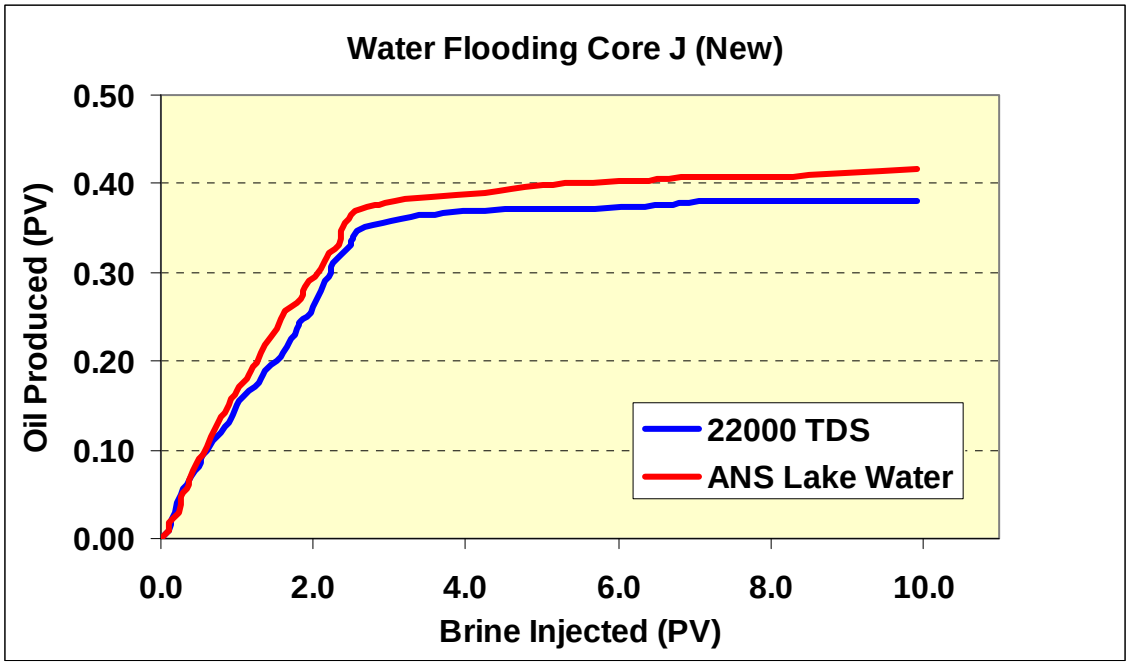

Figure 8.37: Oil Recovery Profile for New Core J.

CHAPTER 9: Cyclic Water Injection (Within-Scope Expansion)

9.1 Introduction

All waterfloods that have been conducted so far on several core samples have indicated that residual oil saturation is substantially reduced by lowering the salinity of the injection brine. However, continuous injection of water (conventional waterflood) may cause fingering/channeling of water, causing an early breakthrough of water and thus reducing oil recovery. On the other hand, in cyclic water injection, the injection of water is not continuous; it is switched on and off using a timing device in the pumping system. In these types of experiments, during the off period, spontaneous fluid spreading is observed, leading to smoother and stable displacement fronts as compared with continuous injection.

One of the major benefits in cyclic water injection is the fact that residual oil saturation is reached relatively earlier than the continuous injection mode—obviously something that is very attractive for field applications. For example, for recovering 60% of the oil, in continuous water injection you may end up injecting 1.5 PVs of water, whereas in cyclic water injection one may need only 1 PV of water—essentially more oil recovered for the same amount of water injected. This is demonstrated in the work of Ivanov (SPE 99678; paper presented at Tulsa IOR meeting in April 2006). Ivanov's team conducted experiments using two-phase, immiscible, flow-through homogeneous-packed glass bead cells. Cyclic and continuous water injection was performed. Ivanov observed a smoother displacement of oil by water in cyclic when compared with conventional waterflooding. Though final oil recovery was more or less the same in both conditions, intermediate oil recovery was higher in cyclic than continuous injection, suggesting an early achievement of residual oil saturation and thereby less expense of water. Less water is required to recover the same amount of oil in cyclic injection. The experiments also concluded that lesser flow rates and shorter time intervals of pulse injection resulted in better recovery. Cyclic water injection has also been applied successfully in some reservoirs in the USA, Russia, and China.

This additional work is to experimentally test if cyclic rather than continuous water injection and/or the cyclic low-salinity water injection instead of continuous injection is successful in reducing the residual oil saturation early enough.

9.2 Experimental Description and Setup

The setup used for low-salinity waterflooding of representative cores was used with minor modifications. Water injection is performed at a lesser flow rate for a fixed time. The flow is then stopped or some idle time is provided so that the already flooded water can spread within the pores to displace oil out of the core. The flow is started again, and this sequence continues. This method can be related to a flow switch on-off mechanism. The ISCO pump is programmed to deliver this type of cyclic or pulse injection with a constant flow rate, alternating the idle flow period. The ISCO pump can be programmed to deliver cyclic injection by varying the flow rate as well as the time intervals of the pulse.

Cores used were representative cores. Some of them were new and the rest were the ones that were used for continuous water injection. The same dead-oil sample used with representative cores was used for the cyclic runs too. Brines of 22,000, 11,000, and 5,500 were reconstituted in the lab, and ANS lake water was procured from Kuparuk Deadarm Lake-5 (thanks to Michael Lilly and Dr. Horacio Toniolo). All the runs were conducted at atmospheric temperature and overburden pressure conditions.

Three sets of experiments were performed:

1. Cyclic injection of lab-reconstituted brines of 22,000, 11,000, and 5,500 TDS salinity on low-salinity continuous waterflooded representative cores (3 in number) saturated with dead oil
2. Cyclic injection of lab-reconstituted brine of 22,000 TDS salinity and ANS lake water on low-salinity continuous waterflooded representative cores (3 in number) saturated with dead oil
3. Cyclic injection of lab-reconstituted brine of 22,000 TDS salinity on new representative cores (5 in number) saturated with dead oil by varying the time intervals of the pulse (through the ISCO pump).

9.3 Results

The effect of low-salinity brine injection was consistently pronounced in the results of all three sets of experiments. This confirms the results obtained through low-salinity continuous waterflooding. For all three sets, an attempt was made to commence all coreflood experiments at the similar initial condition; that is, the cores were at initial oil saturation (S_{oi}) and interstitial/connate water saturation (S_{wi}). The connate water salinity of all sets of experiments was kept constant at a "high" salinity of 22,000 TDS in order to simulate the reservoir saturation conditions.

For the first and second sets of experiments, cyclic injection aided in slight increase of oil recovery as compared to continuous injection. The residual oil saturation values also were considerably reduced. Within cyclic injection as the salinity of the brine was lowered, increased oil recovery and reduced residual oil saturation was a very consistent trend. Oil recovery, residual oil saturation, and Amott-Harvey wettability index were calculated after every run. Most of the runs confirmed the shift of the wettability index towards water-wet condition after a lowered salinity run. The best case was with ANS lake water with maximum oil recovery. It was also observed that oil was being produced even during the idle time of injection. This suggests that the water, which is flooded at a lower flow rate, takes its time to spread into pore capillaries during the flow time and displaces oil during the idle time.

For the third set, experiments were conducted on new (clean) core samples. As stated earlier, waterfloods were carried out using 22,000 TDS salinity brine. A constant flow rate of 30 cc/hr was used. Two time intervals of the pulse were used: 1 min and 0.3 min. The results showed a clear reduction in the residual oil saturation with 0.3-min and then 1-min pulse intervals. There was a slight increase in oil recovery with the lesser time interval pulse.

All the results are displayed in graphs and tables.

9.3.1 First Set (Used Cores with 3 Salinities)

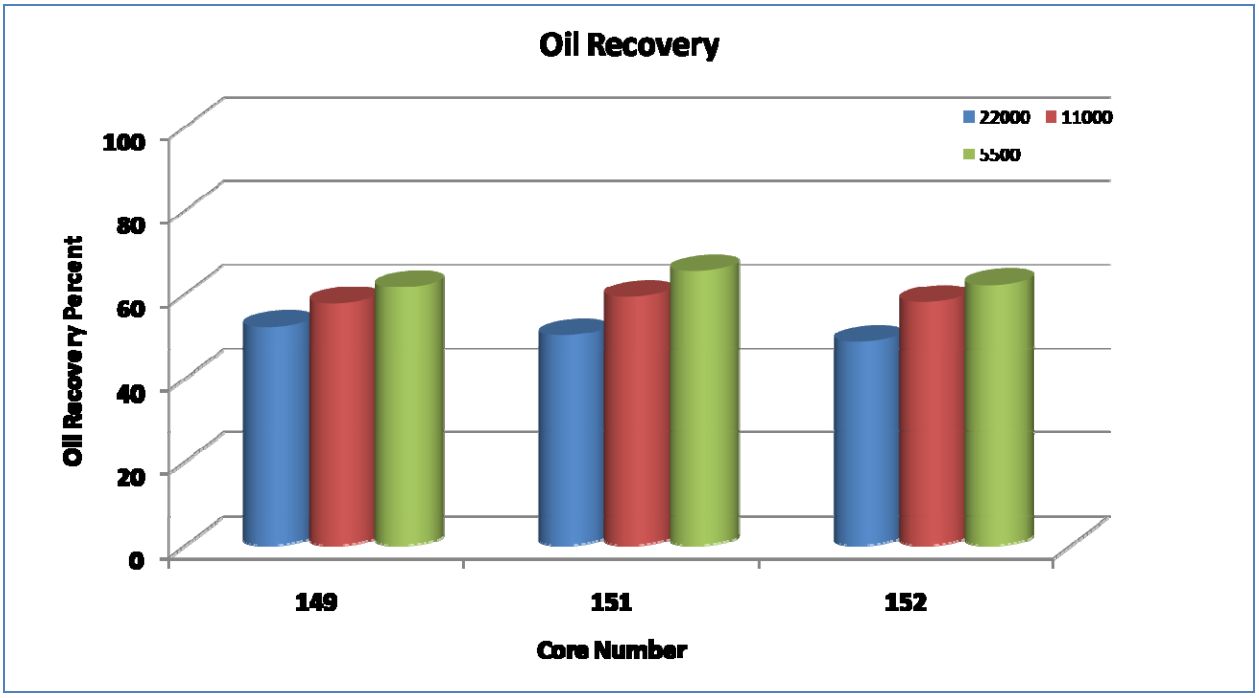

Figure 9.1: Oil Recovery (3 Salinities)

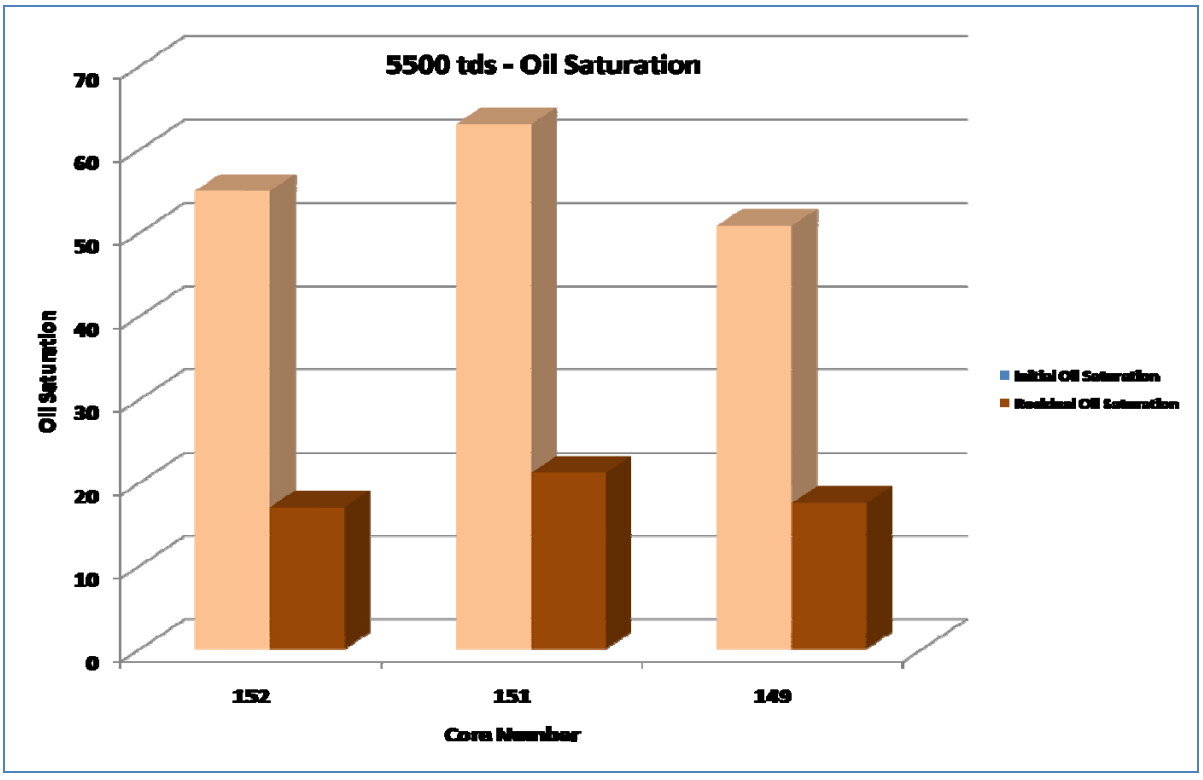

Figure 9.2: Initial vs. Residual Oil Saturation (5,500 TDS, 3 Salinities)

Core 149

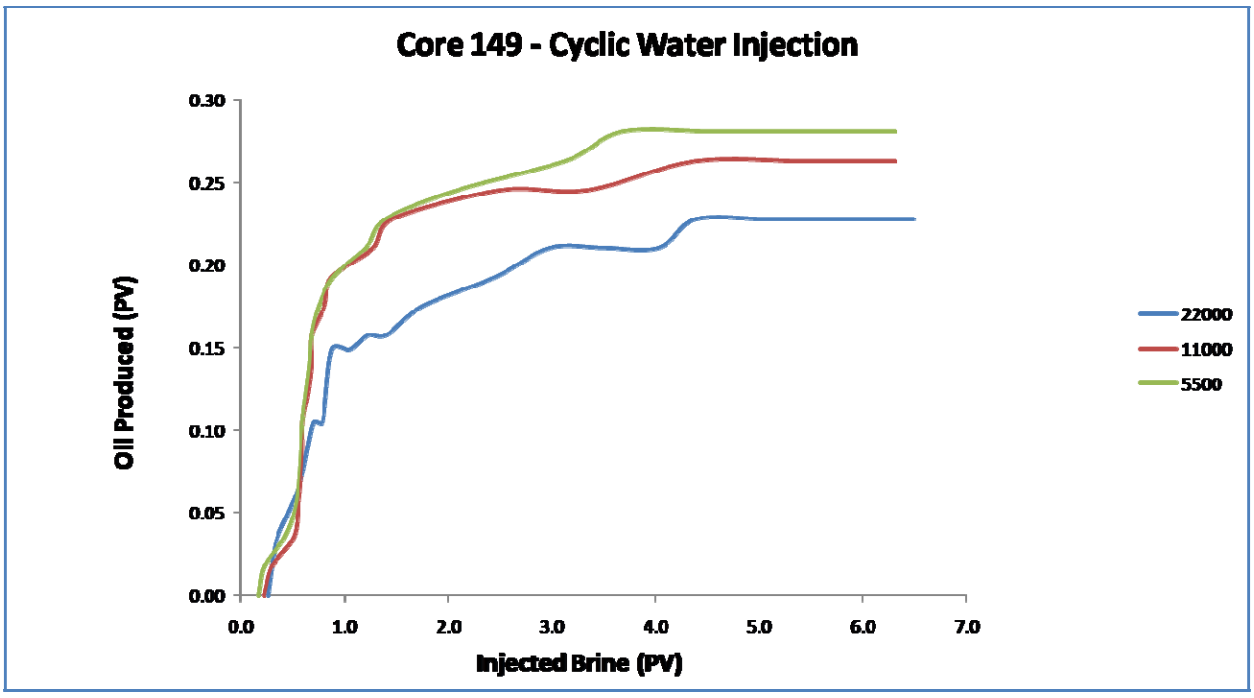

Figure 9.3: Injected Brine vs. Oil Produced (Core 149)

Core 151

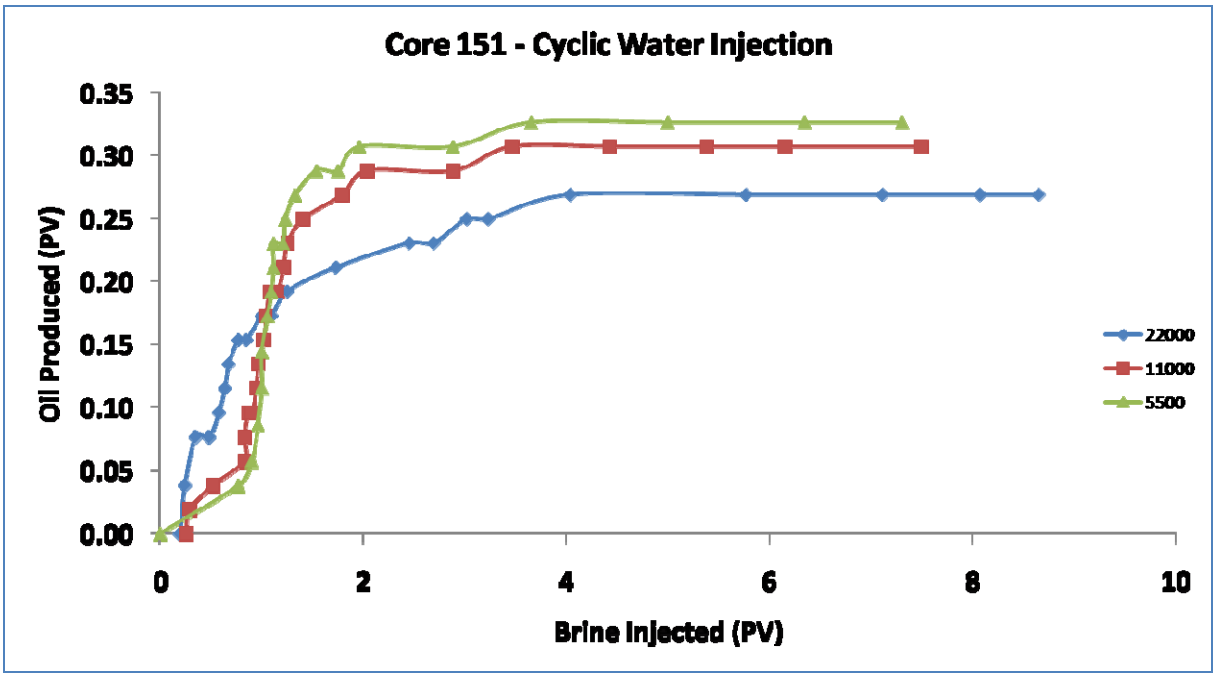

Figure 9.4: Injected Brine vs. Oil Produced (Core 151)

Core 152

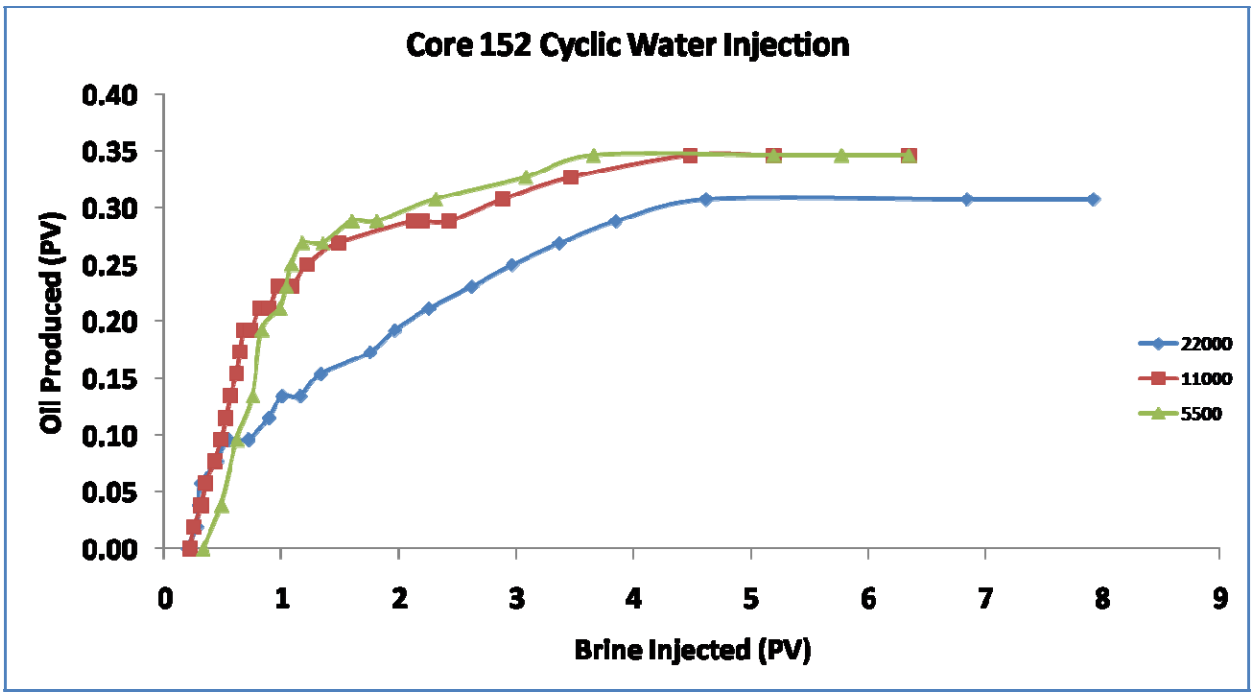

Figure 9.5: Injected Brine vs. Oil Produced (Core 152)

Table 9.1: Results (Cyclic)

Oil Recovery

Core No./ Salinity-TDS	22000	11000	5500
149	21.03	19.2	17.5
151	26.90	21.10	17.30
152	32.6	25	21.1

Residual Oil Saturation

Core No./ Salinity-TDS	22000	11000	5500
149	52.00	57.69	61.53
151	50.00	59.25	65.38
152	48.48	58.06	62.06

Amott-Harvey Index

Core No./ Salinity-TDS	22000	11000	5500
149	0.23	0.263	0.23
151	0.31	0.33	0.357
152	0.42	0.375	0.307

9.3.2 Second Set (Used Cores with 22,000 TDS and ANS Lake Water)

Core 43

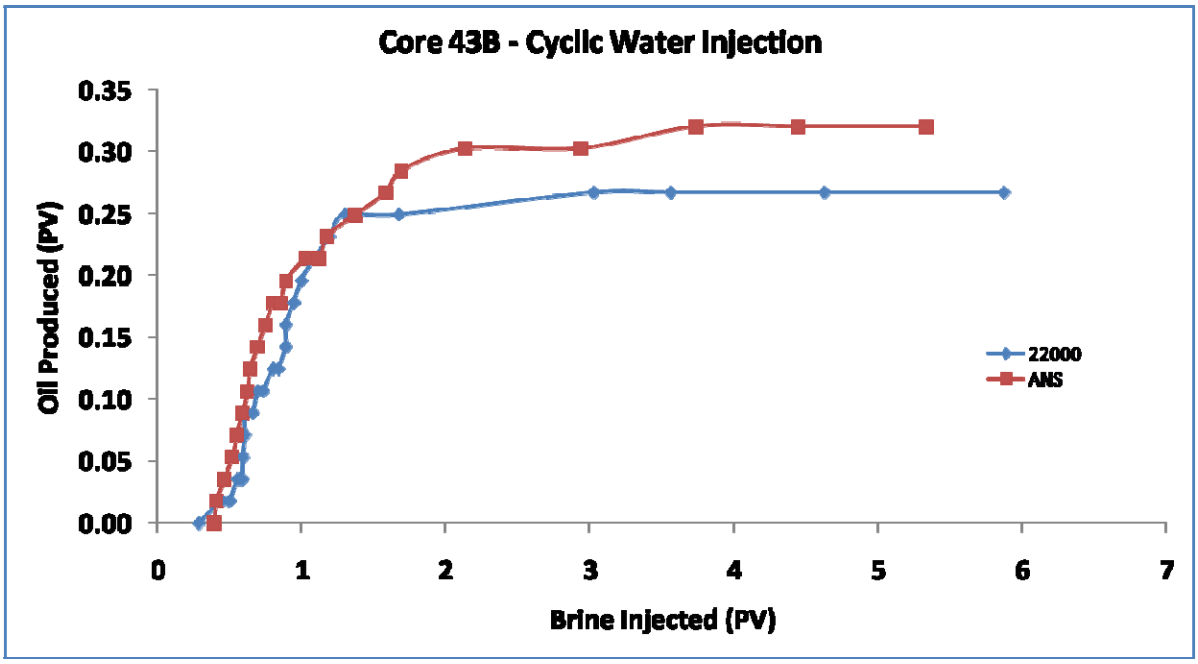

Figure 9.6: Injected Brine vs. Oil Produced (Core 43)

Core 45

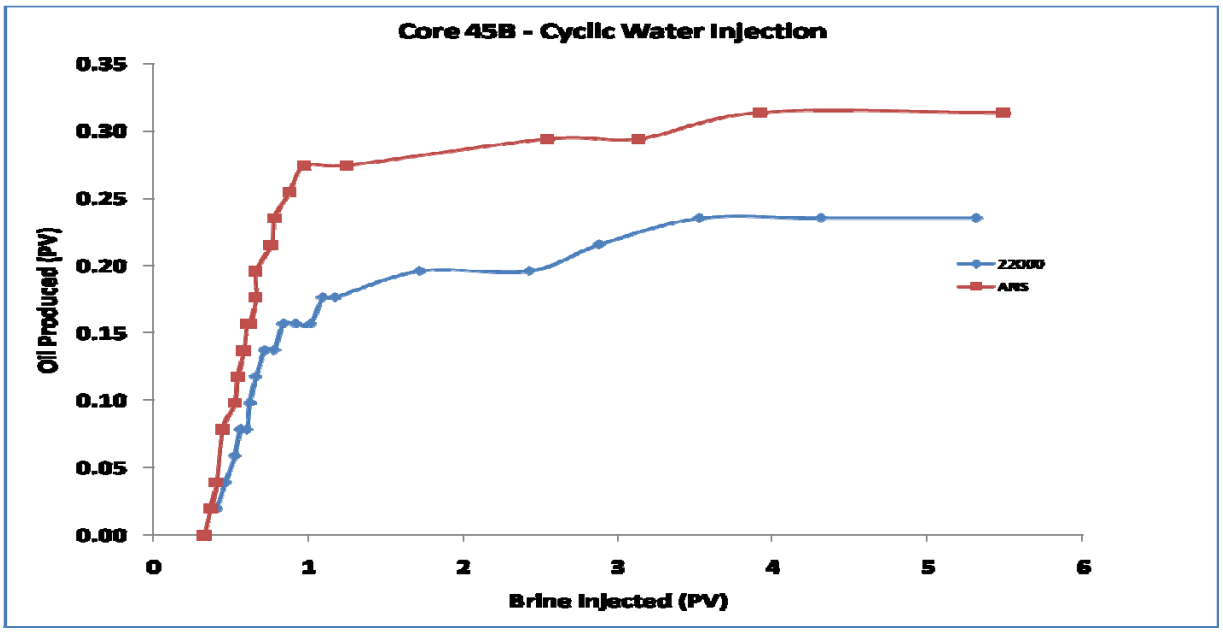

Figure 9.7: Injected Brine vs. Oil Produced (Core 45)

Core 46

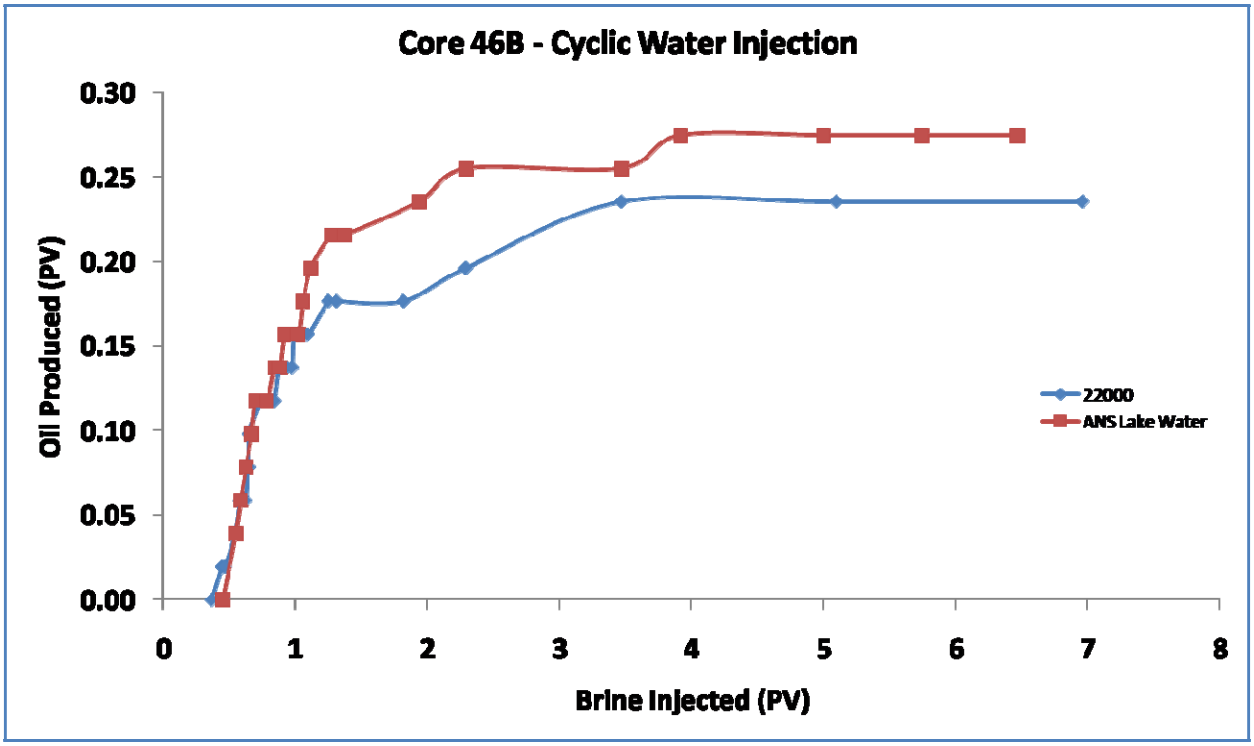

Figure 9.8: Injected Brine vs. Oil Produced (Core 46)

9.3.3 Third Set (New Cores with 22,000 TDS and Different Time Intervals)

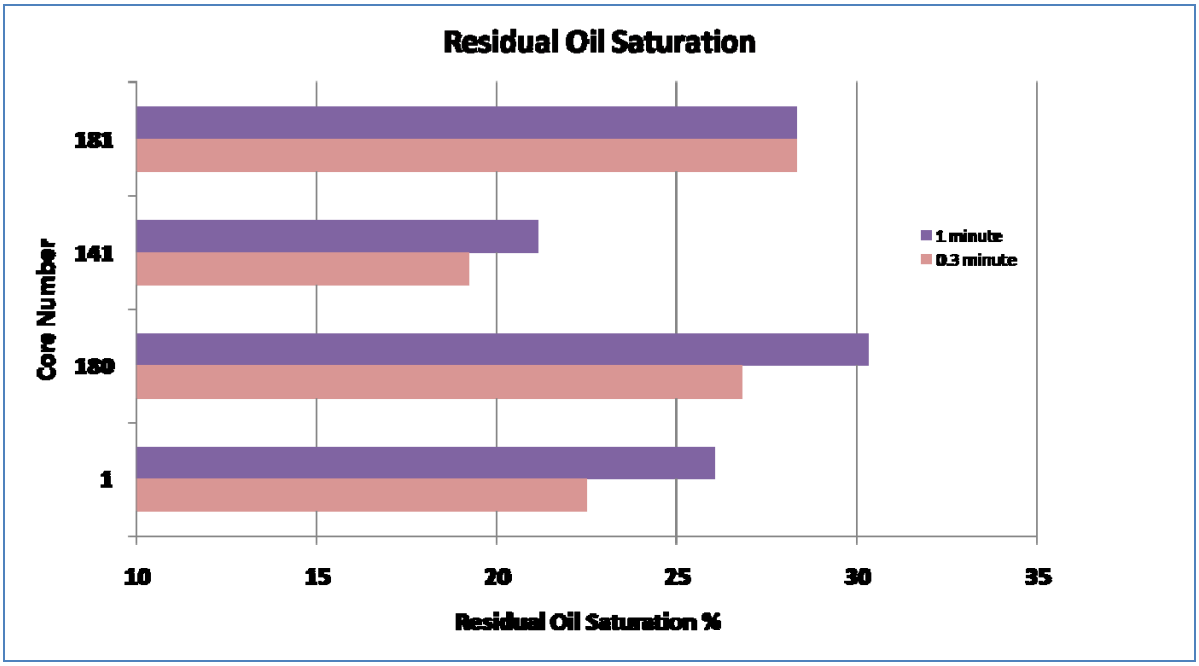

Figure 9.9: Residual Oil Saturation (Varying Time Intervals)

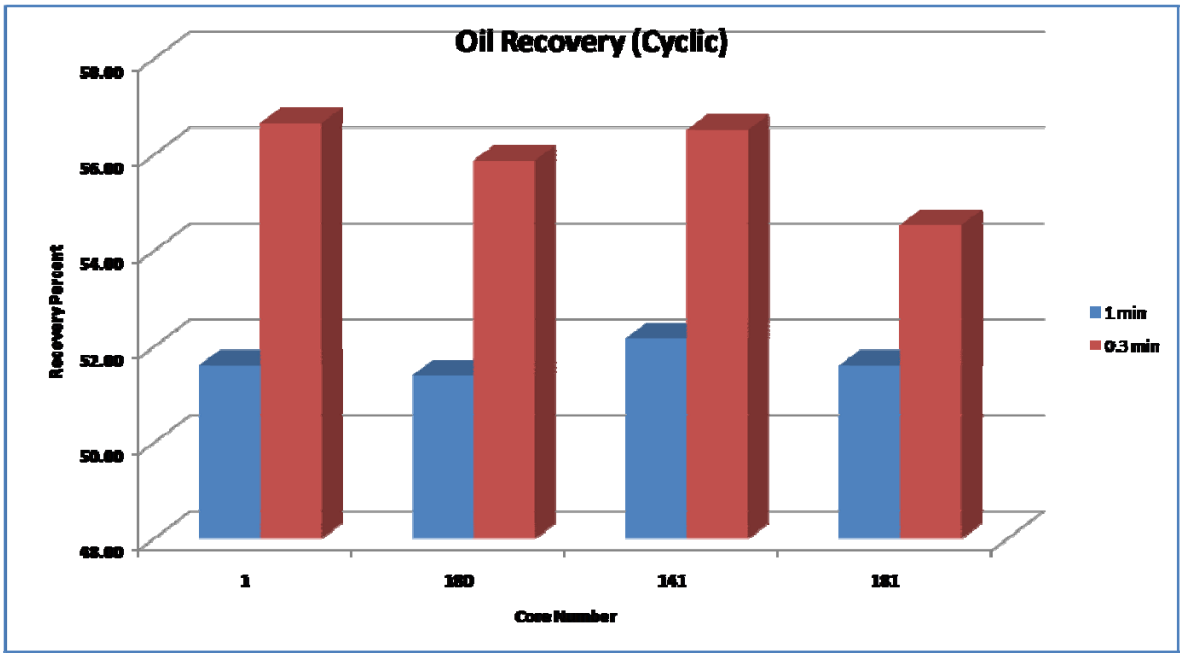

Figure 9.10: Oil Recovery (Varying Time Intervals)

Core 1

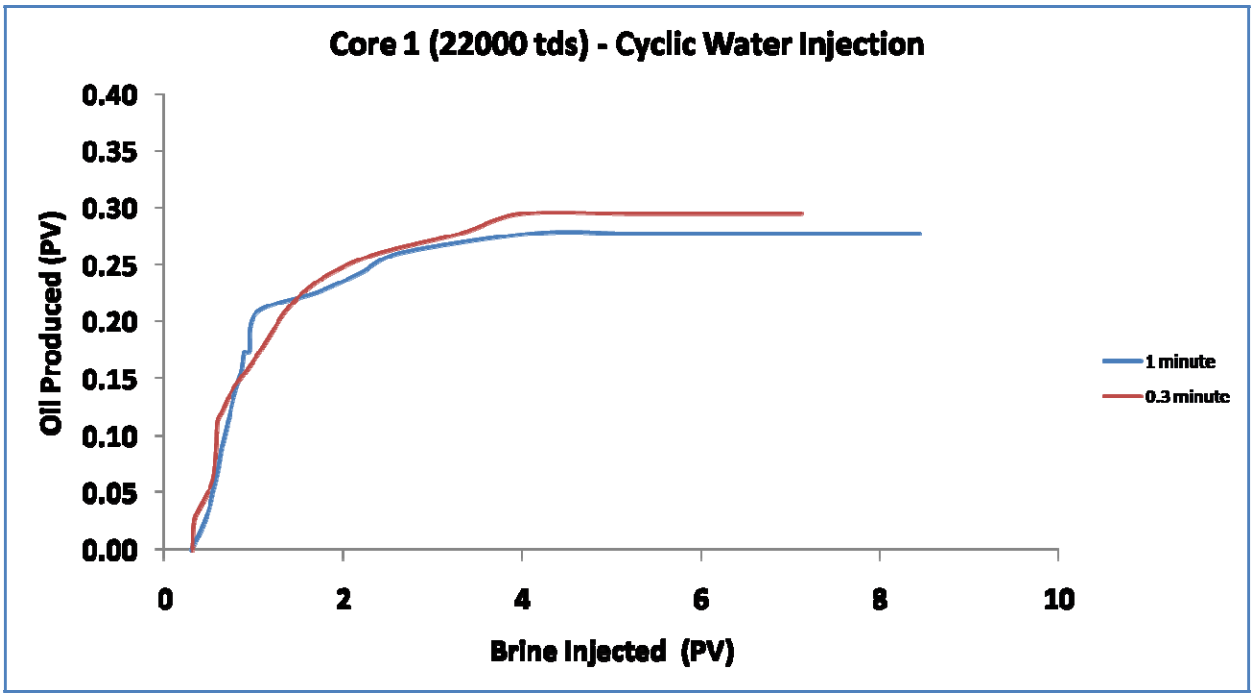

Figure 9.11: Injected Brine vs. Oil Recovered (Core 1)

Core 141

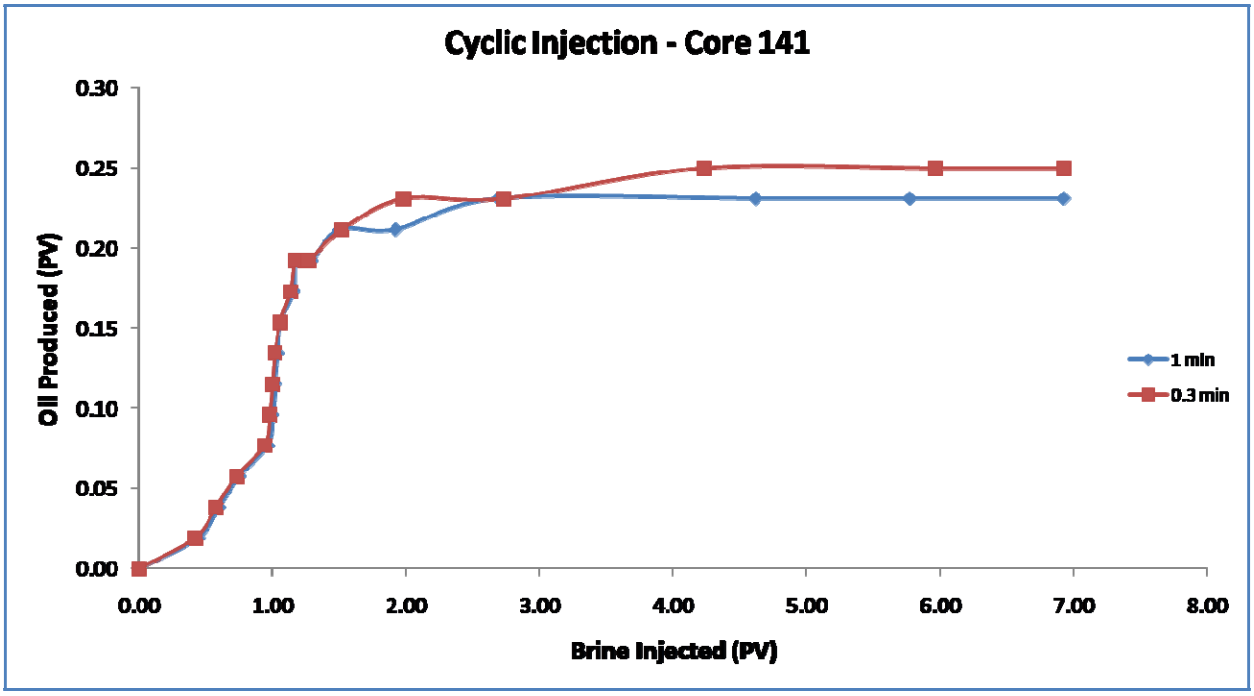

Figure 9.12: Injected Brine vs. Oil Recovered (Core 141)

Core 180

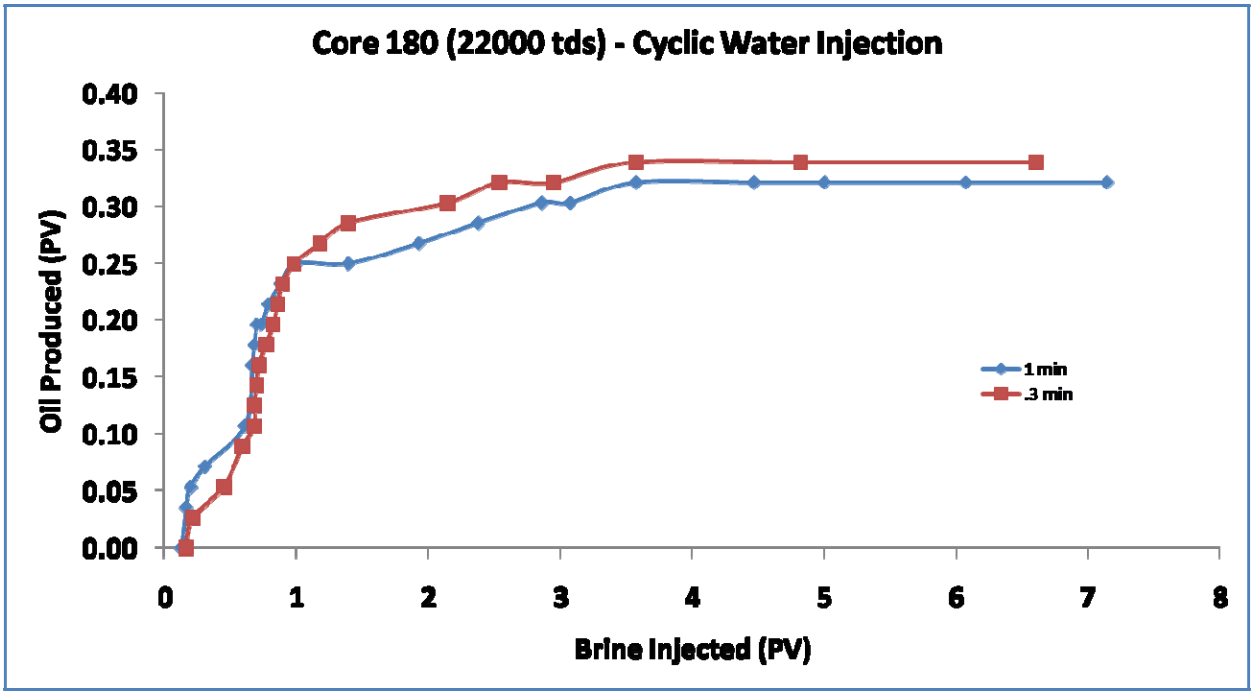

Figure 9.13: Injected Brine vs. Oil Recovered (Core 180)

Core 181

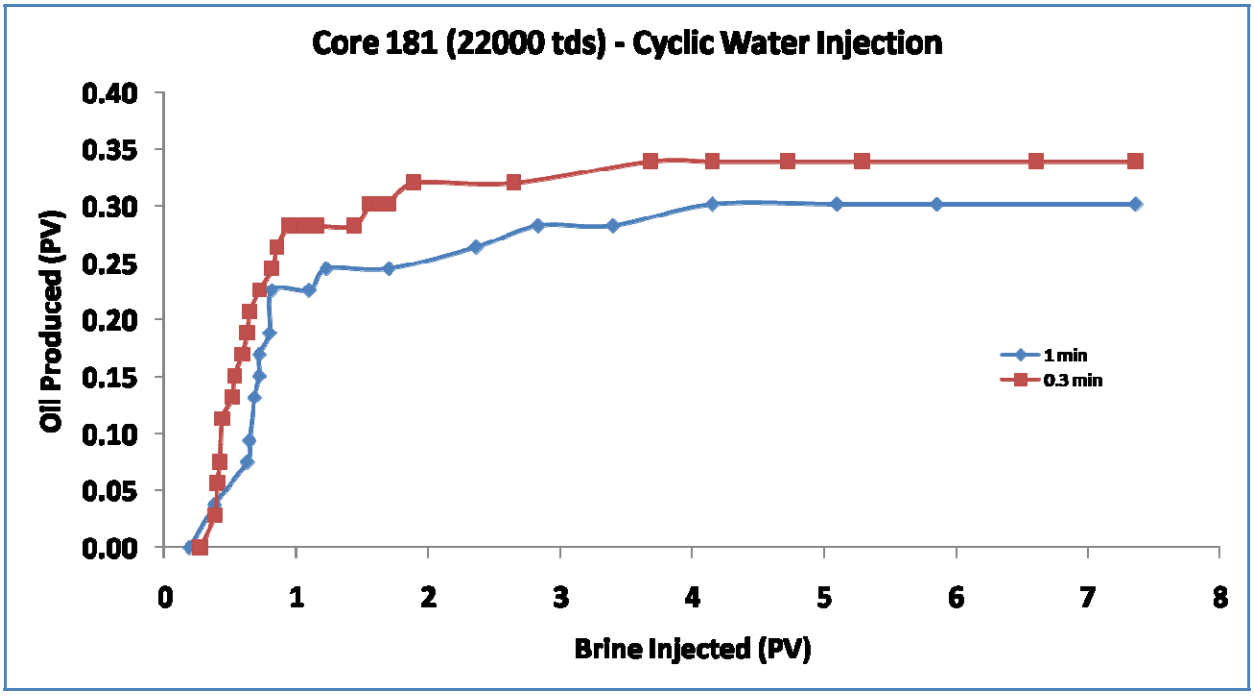

Figure 9.14: Injected Brine vs. Oil Recovered (Core 181)

Table 9.2: Results (Varying Time Intervals)

Oil Recovery

	Time	
Core #	**1 min**	**0.3 min**
1	51.61	56.66
180	51.40	55.88
141	52.17	56.52
181	51.61	54.54

Residual Oil Saturation

	Time	
Core #	**1 min**	**0.3 min**
1	26.04	22.50
180	30.30	26.78
141	21.10	19.20
181	28.30	28.30

CHAPTER 10: Conclusions and Recommendations

10.1 Conclusions

1. Extensive literature review on the effect of wettability on oil recovery has been done and presented. Reported cases of improved oil recovery for water-wet, intermediate-wet, mixed-wet, and oil-wet conditions have been reported. While there is no consensus on the wetting state for optimal oil recovery, more research findings seem to indicate that some form of intermediate wetting condition leads to optimal oil recovery. It is pertinent to note that characterizing a mixed-wet state using the Amott-Harvey method results in an index value that is typically classified as intermediate-wet.
2. The coreflood rig used for the all coreflood studies was developed indigenously. The development process ranged from baseline design on paper, to equipment ordering, to interfacing different parts of the equipment from different manufacturers and finally running the coreflood rig. The rig performed as anticipated and all operational issues that arose while running the rig were addressed.
3. Low-salinity waterfloods performed on two different types of core samples and oil samples (TAPS crude oil and decane) showed improvement in waterflood characteristics with observed reduction in residual oil saturation and improvement in the oil recovery efficiency. Incremental oil was recovered when the salinity of the brine was reduced from 4% to 2% to 1%.
4. Low-salinity waterfloods have the potential for improved oil recovery for either the tertiary recovery or secondary recovery process. When low-salinity brine is used for the tertiary oil recovery, simultaneous production of oil and water is observed. The tertiary process was carried out by injecting the high-salinity brine followed immediately by the low-salinity brines. For the secondary recovery process, production of only the oil phase was observed until water breakthrough with no further oil production observed after the breakthrough of water. For the secondary recovery process, all the corefloods commenced at the same initial condition where the core is at the connate water saturation. The observed increase in recovery with low-salinity corefloods is consistent with experimental results reported by other researchers. However, some researchers have

reported that no improved oil recovery was observed for low-salinity waterflood in the secondary recovery process.

5. When the injected brine was heated, it is observed that more oil is recovered compared to injecting brine of similar salinity at ambient temperature. It is suspected that, in addition to other mechanisms, the improved recovery of oil at elevated temperature may be due to viscosity reduction of the TAPS crude oil. Published research studies on the effect of change in oil viscosity in mobilization of the trapped-oil phase during waterflooding indicate that some reduction in residual oil saturation was observed.
6. The injection of low-salinity brine (at ambient and elevated temperature), for the decane/DNR core system resulted in an increase in the Amott-Harvey index and thus water-wetness of the core samples. This observed trend in wettability variation with reduction in brine salinity agreed with some of the published results of similar experimental studies, but is incongruent with other published results that indicated a decrease in water-wetness. Currently, published reports that explain the mechanism of COBR interaction that results in increase in water-wetness of core samples with decrease in brine salinity are few. One such report has indicated the influence of brine pH in wettability change, with high pH brine resulting in a more water-wet condition and lower pH brine resulting in a less water-wet condition.
7. Results from this study indicate that there is potential for increasing ANS oil production and thus increasing the throughput of TAPS by improving oil recovery in matured ANS oil reservoirs through low-salinity brine injection. Currently waterflooding at ANS is done using formation water and formation water typically has high salinity. Research suggests that a cost-effective means of achieving low-salinity brine injection is by *diluting* the formation water by mixing with seawater. However, further research has indicated no benefits in terms of incremental oil recovery based on mixing formation brine and seawater. Two plausible options for ANS would be to use the low-salinity water reservoir, Prince Creek reservoir, located at the ANS or to set up a brine desalination plant.
8. The injection of low-salinity brine at reservoir temperature, for the ANS crude oil/ANS new (clean) core system resulted in an increase in the Amott-Harvey wettability index and thus water-wetness of the core samples. This observed trend in wettability variation

with reduction in brine salinity agreed with some of the published results of similar experimental studies.

9. The low-salinity waterflood also resulted in an increase in the water-wetting state of ANS crude oil/oil aged ANS core system.
10. The water-wetness of the ANS core samples decreased when the cores were aged with ANS crude oil. Thus, the Amott-Harvey wettability index (I_{AH}) shifted from strongly water-wet to slightly water-wet condition. However, the injection of low-salinity brine resulted in a slight increase in the water-wetness of the cores.
11. The low-salinity waterflood resulted in a reduction in residual oil saturation (S_{or}) as the brine salinity decreased (from 22,000 TDS to 11,000 TDS and 5,500 TDS) for new (clean) as well as oil aged ANS core samples. Thus, more pore volumes of oil are recovered when brine of lower salinity is injected.
12. Experiments performed using ANS lake water (50–60 TDS), which serves the purpose of less salinity brine, resulted in an increase of oil recovery. Hence, ANS lake water could be considered as a potential option of water supply for the waterflooding process employed on North Slope. Alternatively, ANS lake water can be considered for dilution of the high-salinity ANS reservoir brine.
13. Low-salinity waterfloods have the potential for improved oil recovery in the secondary recovery process. This could be concluded on the basis of experimental results obtained from three sets of low-salinity waterflood experiments (partial as well as complete reservoir condition corefloods), performed on ANS core samples, carried out as part of the present study.
14. Cyclic water injection contributes to further reduction of residual oil saturation and this has been consistently proved by all the runs conducted on both used and new representative cores.
15. Significant increase in oil recovery is also observed in cyclic injection as compared to continuous waterflooding and this can be groomed as a potential option for EOR.
16. Oil is produced even during the idle time of the injection and thus more oil has been recovered with less usage of water. Lesser flow rates and lesser time pulse intervals is an interesting option for secondary oil recovery.

10.2 Recommendations

1. There is need to conduct detailed economic evaluation of the logistics of transporting and storing low-salinity brine from the Prince Creek formation to some of the distant ANS fields, as well as the option of desalination of formation water. It is believed that the gains as a result of improved oil recovery may more than offset the cost of transportation and storage of the low-salinity brine or the desalination of the formation water.
2. Imaging technology such as X-ray, CT scanning could be considered for detailed visualization of the pore space, especially at the residual oil saturation condition to determine the location of remaining oil. This will also help in better understanding of the relationship between wettability and residual oil saturation as much information can be obtained by visualization of the pore space.
3. Since low-salinity ANS lake water floods showed promising results in terms of significantly reduced residual oil saturation, this water can be considered as a potential source for either direct injection or dilution of high-salinity reservoir water to reap the benefits of low-salinity waterfloods. However, a detailed study on the economics of these two options is worth considering for future work.

REFERENCES

[1] Buckley, S.E. and Leverett, M.C.: "Mechanism of Fluid Displacement in Sands," *Trans.*, AIME (1942) **146**, 187–196.

[2] Rathmell, J.J., Braun, P.H. and Perkins, T.K.: "Reservoir Waterflood Residual Oil Saturation from Laboratory Tests," *JPT* (February1973) **25**, 175–185.

[3] Jerauld, G.R. and Rathmell, J.J.: "Wettability and Relative Permeability of Prudhoe Bay: A Case Study in Mixed-Wet Reservoirs," paper SPE 28576 presented at the 1994 SPE Annual Technical Conference and Exhibition, New Orleans, Louisiana, 25–28 September.

[4] Morrow N.R., Cram, P.J. and McCaffrey, F.G.: "Displacement Studies in Dolomite with Wettability Control by Octanoic Acid," *SPEJ* (August 1973); *Trans.*, AIME, **255**, 221–232.

[5] Anderson, W.G.: "Wettability Literature Survey-Part 6: The Effects of Wettability on Waterflooding," *JPT* (December 1987) **39**, 1605–1622.

[6] Li K. and Firoozabadi, A.: "Experimental Study of Wettability Alteration to Preferential Gas-Wetness in Porous Media and it Effects," *SPEREE* (April 2000) 139–149.

[7] Morrow N.R.: "Wettability and Its Effect on Oil Recovery," JPT (December 1990) 1476–1484.

[8] Denekas, M.O, Mattax, C.C. and Davis, G.T.: "Effect of Crude Oil Components on Rock Wettability," *JPT* (November 1959); *Trans.*, AIME, **216**, 330–333.

[9] Brown, R.J. and Fatt, I.: "Measurements of Fractional Wettability of Oilfield Rocks by Nuclear Magnetic Relaxation Method," *Trans.*, AIME (1956) **207**, 262–264.

[10] Jones, S.C. and Roszelle, W.O.: "Graphical Techniques for Determining Relative Permeability from Displacement Experiments," *JPT* (May 1978) 807–817.

[11] Owens, W.W. and Archer, D.L.: "The Effect of Rock Wettability on Oil-Water Relative Permeability Relationships," *JPT* (July 1971); *Trans.*, AIME, **251**, 873–878.

[12] Anderson, W.G.: "Wettability Literature Survey – Part 2: Wettability measurement," *JPT* (Nov 1987), 1246–1262.

[13] Treiber, L.E., Archer, D.L. and Owens, W.W.: "A Laboratory Evaluation of the Wettability of Fifty Oil-Producing Reservoirs," *SPEJ* (December 1972); *Trans*., AIME, **253**, 531–540.

[14] Amott, E.: "Observations Relating to the Wettability of Porous Rock," *Trans*., AIME (1959) **216**, 156-192.

[15] Cuiec, L.E.: "Wettability and Oil Reservoirs," *Proc*., North Sea Oil and Gas Reservoirs Seminar, Trondheim, Norway, (December 1985), Graham and Trotman (eds.), London, 193–207.

[16] Boneau, D.F. and Clampitt, R.L.: "A Surfactant System for the Oil-Wet Sandstone of the North Burbank Unit," *JPT* (May1977) 501–506.

[17] Robin, M.: "Interfacial Phenomena: Reservoir Wettability in Oil Recovery," *Oil and Gas J.* (2001) **56**, No. 1, 55–62.

[18] Cuiec, L.E.: "Rock/Crude Oil Interactions and Wettability: An Attempt to Understand Their Interrelation," paper SPE 13211 presented at the 1984 SPE Annual Technical Conference and Exhibition, Houston, Texas, September 16–19.

[19] Adamson, A.W.: *Physical Chemistry of Surfaces*, Fourth Edition, John Wiley and Sons Inc., New York City (1982) 332–368.

[20] Melrose J.C.: "Wettability as Related to Capillary Action in Porous Media," *SPEJ* (September 1965) 259–271.

[21] Morrow, N.R.: "Capillary Pressure Correlations for Uniformly Wetted Porous Media," *J. Cdn. Pet Tech.* (October-December 1976) **15**, No. 4, 49–69.

[22] Donaldson, E.C., Thomas, R.D. and Lorenz, P.B.: "Wettability Determination and its Effect on Recovery Efficiency," *SPEJ* (March 1969) 13–20.

[23] Leverett, M.C.: "Capillary Behavior in Porous Solids," *Trans*., AIME (1941) **142**, 152–169.

[24] Morrow, N.R.: "Physics and Thermodynamics of Capillary Action in Porous Media," *Ind. Eng. Chem.* (June 1970) **62**, No. 6, 32–56.

[25] Morrow, N.R., Lim, H.T. and Ward, J.S.: "Effect of Crude-Oil-Induced Wettability Changes on Oil Recovery," paper SPE 13215; *SPEFE*, (February 1986), 89–103.

[26] Sharma, M.M. and Wunderlich, R.W.: "The Alteration of Rock Properties due to Interactions with Drilling Fluid Components," paper SPE 14302 presented at the 1985 SPE Annual Technical Conference and Exhibition, Las Vegas, Nevada, September 22–25.

[27] Ma, S.M., Zhang, X., Morrow, N.R and Zhou, X.: "Characterization of Wettability from Spontaneous Imbibition Measurements*," J. Cdn. Pet. Tech.* (1999) **38**, No. 13, 1 – 8.

[28] Basu S. and Sharma, M.M.: "Characterization of Mixed-Wettability States in Oil Reservoirs by Atomic Force Microscopy," *SPEJ* (December 1997) **2**, 427–435.

[29] Strand, S., Standnes, D.C. and Austad, T.: "New Wettability Test for Chalk," paper presented at the 2004, 8th International Symposium on Reservoir Wettability and its Effect on Oil Recovery, Houston, Texas, 16–18 May.

[30] Looyestijn, W. and Hofman, J.: "Wettability Index Determination by Nuclear Magnetic Resonance," paper SPE 93624 presented at the 2005, 14th SPE Middle East Oil and Gas Show and Conference, Bahrain, 12–15 March.

[31] Li, K. and Horne, R.N.: "A Wettability Evaluation Method for Both Gas-Liquid-Rock and Liquid-Liquid-Rock Systems," paper SPE 80233 presented at the 2003 SPE International Symposium on Oilfield Chemistry, Houston, Texas, February 5–8.

[32] Li, K. and Horne, R.N.: "Wettability of Steam-Water-Rock Systems," *Proc.* Seventh International Symposium on Reservoir Wettability, Freycinet, Tasmania, Australia, (March 12–15, 2002).

[33] Kyte, J.R., Naumann, V.O. and Mattax, C.C.: "Effect of Reservoir Environment on Water-Oil Displacements," *JPT* (June 1961) 579–582.

[34] Cuiec, L.: in *Interfacial Phenomena in Petroleum Recovery*, N. Morrow (ed.) Marcel Dekker, New York, New York (1991).

[35] Schmid C.: "The Wettability of Petroleum Rocks and the Results of Experiments to Study Effects of Variations in Wettability of Core Samples," *Erdoel Kohle* (August 1964) **17**, No. 8, 605–609.

[36] Holbrook, O.C. and Bernard, G.C.: "Determination of Wettability by Dye Adsorption," *Trans*. AIME (1955) **204**, 86–91.

[37] Iwankow, E.N.: "A Correlation of Interstitial Water Saturation and Heterogeneous Wettability," *Prod. Monthly* (October 1960) **24**, 18.

[38] Salathiel, R.A.: "Oil Recovery by Surface Film Drainage in Mixed-Wettability Rocks," *JPT* (October 1973) 1216–1224.

[39] Trantham, J.C and Clampitt, R.L.: "Determination of Oil Saturation after Waterflooding in an Oil-Wet Reservoir – The North Burbank Unit Track 97 Project," *JPT* (May 1977) 491–500.

[40] Reisberg, J. and Doscher, T. M.: "Interfacial Phenomena in Crude-Oil-Water Systems," *Prod. Monthly* (Nov. 1956) **20**, 43–50.

[41] Johansen, R.T. and Dunning, H.N.: "Relative Wetting Tendencies of Crude Oils by Capillarimetric Method," *Prod Monthly* (September 1959) **23**, 20.

[42] Mungan, N.: "Relative Permeability Measurements Using Reservoir Fluids," *SPEJ* (October 1972) 398–402.

[43] Hirasaki, G.J.: "Wettability: Fundamentals and Surface Forces," *SPEFE* (1991) **6**, 217–226.

[44] Kaminsky, R. and Radke C.J.: "Water Films, Asphaltenes, and Wettability Alteration," paper SPE 39087 presented at the 1998 SPE/DOE Symposium on IOR, Tulsa, Oklahoma, 19–22 April.

[45] Bobek, J.E., Mattax, C.C. and Denekas, M.O.: "Reservoir Rock Wettability – Its Significance and Evaluation," *Trans*. AIME (1958) **213**, 155–160.

[46] Wunderlich, R.W.: "Obtaining Samples with Preserved Wettability," *Interfacial Phenomena in Oil Recovery*, N.R. Morrow (ed.), Marcell Dekker, New York City (1990), 289–318.

[47] Morgan, J.T. and Gordon, G.T.: "Influence of Pore Geometry on Water-Oil Relative Permeability," *JPT* (October 1970), 199–208.

[48] Craig, F.F., Jr.: *The Reservoir Engineering Aspects of Waterflooding*, Monograph Series 3, SPE-AIME, Dallas, Texas (1971).

[49] Raza, S.H., Treiber, L.E. and Archer, D.L.: "Wettability of Reservoir Rocks and its Evaluation," *Prod. Monthly* (April 1968) **32**, No. 4, 2–7.

[50] Donaldson, E.C., Chilingarian, G.V. and Yen, T.F.: "Enhanced Oil Recovery, I–Fundamentals and Analyses," Developments in Petroleum Science, 17A, Elsevier 1985.

[51] Donaldson, E.C. and Thomas, R.D.: "Microscopic Observations of Oil Displacement in Water-Wet and Oil-Wet Systems," paper SPE 3555 Presented at the 1971 SPE Annual Meeting, New Orleans, Louisiana.

[52] Anderson, W.G.: "Wettability Literature Survey – Part 5: The Effects of Wettability on Relative Permeability," *JPT* (November 1987) 1453–1468.

[53] Mungan, N.: "Interfacial Effects in Immiscible Liquid-Liquid Displacement in Porous Media," *SPEJ* (September 1966); *Trans*., AIME, **237**, 247–253.

[54] McCaffery, F.G.: "The Effect of Wettability on Relative Permeability and Imbibition in Porous Media," PhD dissertation, U. of Calgary, Calgary, Alberta (1973).

[55] McCaffery, F.G. and Bennion, D.W.: "The Effect of Wettability on Two-Phase Relative Permeabilities," *J Cdn. Pet. Tech.* (October–December 1974) **13**, No. 4, 42-53.

[56] Morrow N.R. and Mungan, N.: "Wettability and Capillarity in Porous Media," Report RR-7, Petroleum Recovery Research Institute, Calgary, Alberta (January 1971).

[57] Morrow N.R. and McCaffery, F.G.: *Displacement Performance in Uniformly Wetted Porous Media*, Wetting, Spreading, and Adhesion, G.F. Padday (ed.) Academic Press, New York City (1978).

[58] Morgan, J.T. and Gordon, D.T.: "Influence of Pore Geometry on Water-Oil Relative Permeabilities," *JPT* (Oct. 1970) 1199–1208.

[59] Caudle, B.H., Slobod, R.L. and Brownscombe, E.R.: "Further Developments in the Laboratory Determination of Relative Permeability," *Trans*., AIME (1951) **192**, 145–150.

[60] Willhite, G.P.: *Waterflooding*, SPE Textbook Series, Richardson, TX (1996) **3**.

[61] Wang F.H.L.: "Effect of Wettability Variation on Water/Oil Relative Permeability, Dispersion, and Flowable Saturation in Porous Media," paper SPE 15019 presented at the 1986 Permian Basin Oil and Gas Recovery Conference of the SPE, Midland, Texas, 13–14 March.

[62] Braun, E.M. and Blackwell, R.J.: "A Steady-State Technique for Measuring Oil-Water Relative Permeability Curves at Reservoir Conditions," paper SPE 10155 presented at the 56th Annual Fall Technical Conference and Exhibition of the SPE AIME, San Antonio, Texas, (1981), October 5–7.

[63] Richardson, J.G., Perkins, F.M., and Osoba, J.S.: "Differences in the Behavior of Fresh and Aged East Texas Woodbine Cores," *Trans.*, AIME (1955) **204**, 86–91.

[64] Singhal, A.K., Mukherjee, D.P., and Somerton, W.H.: "Effect of Heterogeneous Wettability on Flow of Fluids through Porous Media," *J. Cdn. Pet. Tech.* (July–September 1976) **15**, No. 3, 63–70.

[65] Fatt, I. and Klikoff, W.A.: "Effect of Fractional Wettability on Multiphase Flow through Porous Media," *Trans.*, AIME (1959) **216**, 426–432.

[66] Moore, T.F. and Slobod, R.L.: "The Effect of Viscosity and Capillarity on the Displacement of Oil by Water," *Prod. Monthly* (August 1956) 20–30.

[67] Kennedy, H.T., Burja, E.O. and Boykin, R.S.: "An Investigation of the Effects of Wettability on the Recovery of Oil by Water Flooding," *J. Phys. Chem.* (1955) **59**, 867.

[68] Li, K., Lenormand, R., Robin, M. and Codreanu, B.D.: "Numerical Evaluation of the Combined Effect of Wettability and Heterogeneity on Waterflood Performance," P*roc.* Ninth European Symposium on Improved Oil Recovery, EAGE, Hague, Netherland, (1997) October 20–22.

[69] Jadhunandan, P.P. and Morrow, N.R.: "Effect of Wettability on Waterflood Recovery for Crude-Oil/Brine/Rock Systems," paper SPE 22597, presented at the 66th Annual Technical Conference and Exhibition, Dallas, Texas, (1991) October 6-9.

[70] Tweheyo, M.T., Holt, T. and Torsæter, O.: "An Experimental Study of the Relationship between Wettability and Oil Production Characteristics," *J. Cdn. Pet. Tech.* (1999) **24**, 179–188.

[71] Kinney, P.T. and Nielsen, R.F.: "Wettability in Oil Recovery," *World Oil* (April, 1951) **145**.

[72] Coley, L.H., Marsden, S.S. and Calhoun, J.C., Jr.: "A Study of the Effect of Wettability on the Behavior of Fluids in Synthetic Porous Media," *Prod. Monthly* (June 1956) **20**, 29–45.

[73] Newcombe, J., McGhee, J. and Rzasa, M.J.: "Wettability Versus Displacement in Water Flooding in Unconsolidated Sand Columns," *Trans*., AIME (1955) **204**, 227–232.

[74] Kyte, J.R., Naumann, V.O. and Mattax, C.C.: "Effect of Reservoir Environment on Water-Oil Displacement," *SPEJ* (July 1961); *Trans*., AIME, **222**, 579–582

[75] Mungan, N.: "Interfacial Effects in Immiscible Liquid-Liquid Displacement in Porous Media," SPEJ (September 1966); *Trans*., AIME, **137**, 247–253.

[76] Zhang, P. and Austad, T.: "The Relative Effects of Acid Number and Temperature on Chalk Wettability," paper SPE 92999 presented at the 2005 SPE International Symposium on Oilfield Chemistry, Houston, Texas, 2–4 February.

[77] Tang, G.Q. and Firoozabadi, A.: "Effect of Viscous Force and Initial Water Saturation on Water Injection in Water-Wet and Mixed-Wet Fractured Porous Media" paper SPE 59291 presented at the 2000 SPE/DOE Improved Oil Recovery Symposium, Tulsa, Oklahoma, 3–5 April.

[78] Høgnesen, E.J., Strand, S. and Austad, T.: "Waterflooding of Preferential Oil-Wet Carbonates: Oil Recover Related to Reservoir Temperature and Brine Composition," paper SPE 94166 presented at the 2005 SPE Europe/EAGE Annual Conference, Madrid, Spain, 13–16 June.

[79] Zhang, P. and Austad, T.: "Waterflooding in Chalk: Relationship Between Oil Recovery, New Wettability Index, Brine Composition and Cationic Wettability Modifier," paper SPE 94209 presented at the 2005 SPE Europe/EAGE Annual Conference, Madrid, Spain, 13–16 June.

[80] Al-Hadhrami, H.S. and Blunt, M.J.: "Thermally Induced Wettability Alteration to Improve Oil Recovery in Fractured Reservoirs," paper SPE 71866, presented at the 2000 SPE/DOE Improved Oil Recovery Symposium, Tulsa, Oklahoma, 3–5 April.

[81] Graue, A. and Bognø T.: "Wettability Effects on Oil Recovery Mechanisms in Fractured Reservoirs," paper SPE 56672, presented at the 1999 SPE Annual Technical Conference and Exhibition, Houston, Texas, 3–6 October.

[82] Dixit, A.B., McDougall, S.R., Sorbie, K.S. and Buckley, J.S.: "Pore-Scale Modeling of Wettability Effects and Their Influence on Oil Recovery," paper SPE 54454; *SPEREE* (February 1999) 25–36.

[83] Wood A.R., Wilco, T.C., MacDonald, D.G., Flynn, J.J. and Angert, P.F.: "Determining Effective Residual Oil Saturation for Mixed Wettability Reservoirs: Endicott Field, Alaska," paper SPE 22903 presented at the 1991 Annual Technical Conference and Exhibition of SPE, Dallas, Texas, 6–9 October.

[84] Huang,Y., Ringrose, P.S., Sorbie, K.S. and Larter, S.R.: "The Effects of Heterogeneity and Wettability on Oil Recovery from Laminated Sedimentary Structures," paper SPE 30781 presented at the 1995 SPE Annual Technical Conference and Exhibition, Dallas, Texas, 22–25 October.

[85] Talash, A.W. and Crawford, P.B.: "Experimental Flooding Characteristics of 75% Water-Wet Sands," *Prod. Monthly* (February 1961) **25**, No. 2, 24–26.

[86] Buckley, J.S. and Morrow, N.R.: *An Overview of Crude Oil Adhesion Phenomena*, Physical Chemistry of Colloids and Interfaces in Oil Production, H.Toulhout, J. Lecourtier (Editors), Editions Technip, Paris (1991).

[87] Tang, G. and Morrow, N.R.: "Influence of Brine Composition and Fines Migration on Crude Oil/Brine/Rock Interactions on Oil Recovery," *Proc.* 5th International Symposium on Evaluation of Reservoir Wettability and Its Effects on Oil Recovery, Trondheim, Norway, (June 1998).

[88] Buckley, J.S., Liu, Y. and Monsterlee, S.: "Mechanism of Wettability Alteration by Crude Oils," *SPEJ* (March 1998), **3**, 54–61.

[89] Tang, G. and Morrow, N.R.: "Oil Recovery by Waterflooding and Imbibition–Invading Brine Cation Valency and Salinity," *Proc*. International Symposium of the Society of Core Analysts, Golden, Colorado, August 1999.

[90] Tang, G. and Morrow, N.R.: "Salinity, Temperature, Oil Composition, and Oil Recovery by Waterflooding," paper SPE 36680 presented at the 1996 SPE Annual Technical Conference and Exhibition, Denver, Colorado, 6–9 October.

[91] Sharma, M.M. and Filoco, P.R.: "Effect of Brine Salinity and Crude-Oil Properties on Oil Recovery and Residual Oil Saturations," *SPEJ* (September 2000) **5**, No 3, 293–300.

[92] Filoco, P.R. and Sharma, M.M.: "Effect of Brine Salinity and Crude-Oil Properties on Relative Permeabilities and Residual Saturations," paper SPE 49320 presented at the 1998 SPE Annual Meeting, New Orleans, Louisiana, 27–30 September.

[93] McGuire, P.L., Chatham, J.R., Paskvan, F.K., Sommer, D.M. and Carini, F.H.: "Low Salinity Oil Recovery: An Exciting EOR Opportunity for Alaska's North Slope," paper SPE 93903 presented at the 2005 SPE Western Regional Meeting, Irvine, California, 30 March–1 April.

[94] Webb, K.J., Black, C.J.J. and Al-Ajeel, H.: "Low Salinity Oil Recovery – Log-Inject-Log," paper SPE 89379, 2004 SPE/DOE Fourteenth Symposium on Improved Oil Recovery, Tulsa, Oklahoma, 17–21 April.

[95] Webb, K.J., Black, C.J.J. and Edmonds, I.J.: "Low Salinity Oil Recovery: The Role of Reservoir Condition Corefloods," 13th European Symposium on Improved Oil Recovery, Budapest, Hungary, (2005) 25–27 April.

[96] http://www.temco.com/tempstuff/cfr10.htm.

[97] Melrose, J.C.: "Interpretation of Mixed Wettability States in Reservoir Rocks," paper SPE 10971 presented at the 1982 SPE Annual Technical Conference and Exhibition, New Orleans, Louisiana, 26–29 September.

[98] Hall, A.C., Collins, S.H. and Melrose, J.C.: "Stability of Aqueous Wetting Films in Athabasca Tar Sands," paper SPE 10626 presented at the 1982 SPE Int'l Symposium on Oilfield and Geothermal Chemistry, Dallas, Texas, 25–27 January.

[99] Verwey, E.J.W. and Overbeek, J.T.G.: *Theory of the Stability of Lyophobic Colloids*, Elsevier Scientific Publishing Co. Inc., New York City (1948) 66–105, 135–163.

[100] Sharma, A.: "Phase Behavior Analysis of Gas-To-Liquid (GTL) Products for Transportation through Trans-Alaskan Pipeline System," MS Thesis, University of Alaska Fairbanks, Alaska (August 2003).

[101] Mohanty, K.K., Davis, H.T. and Scriven, L.E.: "Physics of Oil Entrapment in Water-Wet Rock," SPERE (February 1987) 113–128.

[102] Taber J.J: "Dynamic and Static Forces Required to Remove a Discontinuous Oil Phase From Porous Media Containing Both Oil and Water," SPEJ (March 1969) 3–12.

[103] Stegemeier, G.L.: *Mechanism of Entrapment and Mobilization of Oil in Porous Media*, Improved Oil Recovery by Surfactant and Polymer Flooding, Academic Press, New York City (1977) 55–91.

[104] Saripalli, K. P., H. Kim, PSC Rao and M. D. Annable, 1997. "Use of Interfacial Tracers to Measure Immiscible Fluid Interfacial Areas in Porous Media", *Env. Sci. and Tech.*, 31(3): 932-936.

[105] Vijapurapu, S. and R. Dandina. Effect of brine dilution and surfactant concentration on spreading and wettability, SPE 80273.

NOMENCLATURE

1. V_{osp} – Volume of spontaneous oil displacement
2. V_{ofd} – Volume of forced oil displacement
3. V_{wsp} – Volume of spontaneous water displacement
4. V_{wfd} – Volume of forced water displacement
5. I_w – Displacement by water ratio
6. I_o – Displacement by oil ratio
7. EOR – Enhanced Oil Recovery
8. ANS – Alaska North Slope
9. IOR – Improved Oil Recovery
10. AETDL – Arctic Energy Technology Development Laboratory
11. DNR – Department of Natural Resources
12. KR – Kuparuk River
13. IWS – Interstitial Water Saturation
14. PV – Pore Volume
15. ROS, S_{OR} – Residual Oil Saturation
16. OOIP – Original Oil in Place
17. ppm – Parts per million
18. PFS – Produced Fluid Separator
19. DP – Differential Pressure
20. TDS – Total Dissolved Solids
21. DI – de-ionized
22. S_{wc} – Connate Water Saturation
23. IFT – Interfacial tension
24. OWC – Oil/Water Contact
25. I_{AH} – Amott Harvey Wettability Index

APPENDIX

Citations of papers published based on the work conducted in this project:

1. Agbalaka, C.C., Dandekar, A.Y., Patil, S.L., Khataniar, S. and Hemsath, J.R.: Coreflooding Studies To Evaluate The Impact Of Salinity And Wettability On Oil Recovery Efficiency. *Transport in Porous Media*; ***DOI 10.1007/s11242-008-9235-7, web release May 6, 2008***. (Corresponding Author)
2. Patil, S.B., Dandekar, A.Y., Patil, S.L., Khataniar, S.: "Low Salinity Brine Injection for EOR on Alaska North Slope (ANS)". Accepted for presentation at the *International Petroleum technology Conference*, 3-5 December 2008, Kuala Lumpur, Malaysia.
3. Agbalaka, C.C., Dandekar, A.Y., Patil, S.L., Khataniar, S. and Hemsath, J.R.: "The Effect of Wettability on Oil Recovery: A Review". Accepted for presentation as alternate paper or poster at the *SPE Asia Pacific Oil & Gas Conference and Exhibition (APOGCE)*, October 2008 in Perth, Australia.
4. Kulathu, S., Dandekar, A., Patil, S., Khataniar, S. and Chukwu, G.A.: "Low salinity cyclic water floods for enhanced oil recovery in Alaska North Slope". Presented at the 2008 Arctic Science Conference, September 2008.

National Energy Technology Laboratory

626 Cochrans Mill Road
P.O. Box 10940
Pittsburgh, PA 15236-0940

3610 Collins Ferry Road
P.O. Box 880
Morgantown, WV 26507-0880

One West Third Street, Suite 1400
Tulsa, OK 74103-3519

1450 Queen Avenue SW
Albany, OR 97321-2198

539 Duckering Bldg./UAF Campus
P.O. Box 750172
Fairbanks, AK 99775-0172

Visit the NETL website at:
www.netl.doe.gov

Customer Service:
1-800-553-7681